



CHALMERS
UNIVERSITY OF TECHNOLOGY



The 200 m timber tower

A study on the possibilities of constructing a 200 meter tall timber building

Master's thesis in Structural Engineering and Building Technology

SEBASTIAN GYLLENSTEN
AXEL MODIG

DEPARTMENT OF ARCHITECTURE AND CIVIL ENGINEERING

CHALMERS UNIVERSITY OF TECHNOLOGY
Gothenburg, Sweden 2020
www.chalmers.se

MASTER'S THESIS ACEX30

The 200 m timber tower

A study on the possibilities of constructing a 200 meter tall timber building

Master's Thesis in Structural Engineering and Building Technology

SEBASTIAN GYLLENSTEN

AXEL MODIG

Department of Architecture and Civil Engineering

Division of Structural Engineering

Research Group for Lightweight Structures

CHALMERS UNIVERSITY OF TECHNOLOGY

Göteborg, Sweden 2020

The 200 m timber tower
A study on the possibilities of constructing a 200 meter tall timber building
Master's Thesis in Structural Engineering
SEBASTIAN GYLLENSTEN
AXEL MODIG

© SEBASTIAN GYLLENSTEN & AXEL MODIG, 2020

Examensarbete ACEX30
Institutionen för arkitektur och samhällsbyggnadsteknik
Chalmers tekniska högskola, 2020

Department of Architecture and Civil Engineering
Division of Structural Engineering and Building Technology
Research Group for Lightweight Structures
Chalmers University of Technology
SE-412 96 Göteborg
Sweden
Telephone: + 46 (0)31-772 1000

Cover: Illustration of the proposed 200 m timber tower.

Department of Architecture and Civil Engineering
Göteborg, Sweden, 2020

The 200 m timber tower

A study on the possibilities of constructing a 200 meter tall timber building

Master's Thesis in Structural Engineering and Building Technology

SEBASTIAN GYLLENSTEN

AXEL MODIG

Department of Architecture and Civil Engineering

Division of Structural Engineering

Research Group for Lightweight Structures

Chalmers University of Technology

ABSTRACT

As the interest in timber buildings is increasing, more attention is pointed towards high-rise timber buildings. Partly because it is one of the main areas pushing the development within the field of timber structures. As the current tallest timber building, *Mjöstornet* in *Brumunddal* is approximately 10 times shorter than the world's tallest building, *Burj Khalifa*, the intuition says that there is room for major improvements regarding tall timber structures. The aim of this thesis is therefore to investigate the possibilities to build a 200 m tall timber tower while still fulfilling the requirements for strength, stability and dynamics. In order to anchor the project in reality, the assumed building location is *Gothenburg* with the ground conditions of solid rock.

Early in the study it was concluded that in order to push the height limits, the building design had to be improved compared to the existing timber buildings. The main geometries of interest turned out to be the circular shape thanks to its aerodynamical benefits. This base shape was applied in various ways, generating five different concepts ready for evaluation.

Each of the five concepts were modelled and preliminary sized using *Grasshopper* and *Karamba 3D*, whereafter they were evaluated based on their dynamic performance, global stiffness, and a few other evaluation criteria. The evaluation was primarily made with structural performance in mind and secondary with regard to comfort, quality and economical aspects.

The results show that one of the concepts have great potential of reaching 200 m despite the uncertainties regarding joint stiffness and structural damping. Also, a few of the other concepts might be able to reach 200 m if subject to some structural and dynamical improvements.

Key words: Acceleration, Aerodynamics, Burj Khalifa, Dynamics, Mjöstornet, Tall timber structure, Timber, Wind load.

Contents

ABSTRACT	I
CONTENTS	III
PREFACE	VII
1 INTRODUCTION	1
1.1 Background	1
1.2 Aim	1
1.3 Limitations	1
1.4 Problem specification	2
1.5 Method	2
2 THEORETICAL FRAMEWORK	3
2.1 What is a timber building?	3
2.2 Timber as a structural material	4
2.2.1 Material properties	4
2.2.2 Orthotropic behaviour	4
2.2.3 Weight of timber	5
2.2.4 Influence of moisture	5
2.2.5 Creep	7
2.3 Wood products suitable for tall buildings	9
2.3.1 Sawn timber	9
2.3.2 Glulam	9
2.3.3 CLT – Cross laminated timber	9
2.3.4 LVL – Laminated veneer lumber	10
2.4 Connections in timber structures	11
2.4.1 Dowel joints	11
2.4.2 Glued-in rods	13
2.4.3 Glued-in steel plates	13
2.4.4 CLT connections	13
2.4.5 Connection failure behaviour	14
2.4.6 Importance of stiff connections	15
2.5 Timber in high-rise buildings	16
2.6 Tallness and slenderness for high-rise buildings	17
2.7 Structural systems for tall buildings	18
2.7.1 Frame system	18
2.7.2 Shear-wall systems	18
2.7.3 Tube systems	19
2.7.4 Outrigger systems	21
2.7.5 Buttressed core system	22
2.7.6 Hyperboloid truss system	23

2.8	Existing high-rise buildings made of timber	24
2.8.1	Mjöstornet	24
2.8.2	Hoho – Vienna	25
2.8.3	Origine – Québec	26
2.9	General design considerations	27
2.9.1	Fire safety	27
2.9.2	Sound and vibration	31
2.9.3	Elevators	31
2.9.4	Daylight	31
2.9.5	Economy	34
2.9.6	The construction phases	35
2.10	Time dependent effects on tall buildings	36
2.11	Design of high-rise buildings	37
2.11.1	Conceptual design	37
2.11.2	Scheme design	37
2.11.3	Detailed design phase	37
2.12	Loads on tall structures	38
2.12.1	Design situations	38
2.12.2	Load combinations	38
2.12.3	Self-weight	40
2.12.4	Imposed load	40
2.12.5	Wind loads	41
2.12.6	Snow load	46
2.12.7	Seismic loads	47
2.12.8	Accidental loads	47
2.12.9	Temporary loads during construction	47
2.13	Shape coefficients for non-rectangular buildings	48
2.13.1	Shape coefficients for circular buildings	48
2.13.2	Shape coefficients for hyperboloid shaped buildings	51
2.13.3	Shape coefficients for Y-shaped buildings	52
3	STRUCTURAL DESIGN	53
3.1	Building and component design - ULS	53
3.1.1	Ways to enhance the ULS performance	53
3.2	Design of building components – SLS	54
3.2.1	Ways to enhance the SLS performance	54
3.3	Global design – SLS	55
3.3.1	Ways to improve the global SLS performance	56
3.4	Global design for dynamic behaviour	57
3.4.1	Design according to Eurocode and ISO-standards	57
3.4.2	Evaluation of wind-induced vibrations – ISO 10137	57
3.4.3	Peak acceleration	58
3.4.4	Ways to improve the dynamic behaviour	59
4	CONCEPTUAL DESIGN	61

4.1	General description of the finite element models	63
4.1.1	Material	63
4.1.2	Support conditions	64
4.1.3	Joints	64
4.1.4	Loads	64
4.1.5	Verification of the finite element model	64
4.1.6	Mesh	65
4.2	Stabilizing core study	66
4.3	Stabilizing truss study	72
4.4	Hyperboloid shape study	76
4.5	Proposals for a 200 m timber tower	78
4.5.1	Mega truss and core system with perimeter columns	78
4.5.2	Mega truss and internal truss-based core system	81
4.5.3	Mega truss with internal truss and hollow center	84
4.5.4	Hyperboloid with continuous perimeter elements and a CLT core	87
4.5.5	Hyperboloid perimeter truss-frame system with stabilizing core	90
5	EVALUATION	94
5.1.1	Rentable area	94
5.1.2	Mass timber per area of rentable space	94
5.1.3	Used ground area	95
5.1.4	Daylight	96
5.1.5	Number of joints	97
5.1.6	Vertical deformations	97
5.1.7	Horizontal deformations	98
5.1.8	Foundation moment due to wind	99
5.1.9	Dynamic performance	100
5.1.10	Result summary	101
5.2	The 200 m timber tower	105
6	DISCUSSION	107
6.1	The 200 m timber tower	107
6.1.1	Possible and needed improvements	108
6.1.2	Potential error sources	109
6.1.3	Assumptions and building codes	110
6.1.4	Questioning the rules to build higher?	111
6.2	Utilized software	112
7	CONCLUSIONS	113
7.1	Future research	115
8	REFERENCES	116
	APPENDIX	120

Appendix I	121
Appendix II	125
Appendix III	133
Appendix IV	140
Appendix V	153
Appendix VI	155
Appendix VII	156
Appendix VIII	157
Appendix IX	162
Appendix X	168

Preface

This report has been made as the final work during the master's programme *Structural Engineering and Building Technology*. It is conducted in order to investigate the possibilities to build a 200 m tall timber tower satisfying all requirements needed for humans comfortably and safely occupying the building. The project has been carried out during spring term 2020 at the Department for Architecture and Civil Engineering under the Division of Structural Engineering, group for Lightweight Structures, Chalmers University of Technology, Sweden. Initiator of the project is *VBK* who came up with the project idea and has contributed with valuable reflections and supervision along the entire project.

Most of the work has been done at *VBK's* office in *Gothenburg*. They have also contributed with material in terms of computers and software needed for the project. However, due to the unique situation with Covid-19, the last two months of work have been carried out from home.

We would especially like to thank our supervisors from *VBK*, Andreas Lindelöf and Johan Örnborg for their guidance during the project. Also, thanks to examiner Robert Jockwer at the Department of Structural Engineering for his continuous response during the project.

Gothenburg, June 2020

Sebastian Gyllensten and Axel Modig

1 Introduction

In recent years the demand for timber-based structures has increased. This is in part due to factors such as the growing environmental awareness and its highly appreciated properties from an architectural standpoint. A natural progression from this is high-rise buildings made of timber. Timber as a material has numbers of significant benefits but its drawbacks are the ones that needs special attention when producing high-rise buildings.

This thesis covers the structural aspects of high-rise buildings made from timber. How the material specific properties can be managed to allow for maximum building height and how the building geometry can be optimized to further increase the possibility to build as high as possible.

1.1 Background

The current tallest timber building in the world – *Mjøstornet* is located in Norway, *Brumunddal* and is 85 m high. The difference between this and the highest concrete building, *Burj Khalifa* in *Dubai*, is approximately a factor of 10. Intuitively, the overall geometry of *Mjøstornet* does not seem to be optimized for a high-rise building and therefore, it should be possible to build even higher structures in timber.

The demand for timber structures has increased in recent years and the knowledge in the field is growing fast. Therefore, it is time to push the current limitations and utilize the advantages of timber in a wider area of applications. Construction company *VBK* is therefore interested in evaluating whether it is possible to design a 200 m tall building with timber as the main structural material.

1.2 Aim

The aim of the thesis is to evaluate the impact of the façade geometry, structural geometry and structural system, and find out how these factors can be managed to optimize building height for a timber structure. The main goal is therefore to find a structural system for a 200 m tall building that fulfills the demands on stiffness and strength as well as accelerations, constructability and cost.

1.3 Limitations

The project is limited to the structural parts and behavior of the building above the ground; therefore, no extensive evaluation of the foundation will be made.

Assumptions regarding the building, its location and surroundings:

- *Gothenburg* region.
- Reference wind speed: 25 m/s (Boverket, 2019a), p.54.
- The foundation is anchored in solid rock. No consideration is taken for the foundation work, the lowest considered point is the connection between timber elements and the foundation.
- The entire building will be used for offices.
- Commercially available slab elements are used to limit the design work while fulfilling serviceability limit state requirements.
- Long term effects will only be discussed briefly.

1.4 Problem specification

- What are the limitations for timber structures, high-rise buildings and the combination of them?
- What kind of structural geometry is preferable to maximize the building height?
- Is it realistic to build a 200 m tall building from timber? What is required to build such a building?

1.5 Method

The work has covered the following steps:

1. First, a literature study was carried out. This to map out about critical factors when building tall buildings in general and timber structures in particular.
2. Second, three sub-studies were made where stabilizing systems such as cores and trusses of two different shapes were evaluated individually. This was done using the program *Rhino 3D* with its extensions *Grasshopper* and *Karamba 3D*.
3. Thereafter, five proposals were developed. The basis for these proposals were the literature study, the previously made sub-studies and inspiration from existing high-rise buildings. All proposals were made with a relatively similar rentable area to enhance comparability.
4. Results were then extracted for each proposal whereafter they were compared, evaluated and a winning concept was chosen.
5. Finally, the final solution was presented, and a discussion was made regarding possible improvements for the winning proposal and the project as whole.

Following this workflow, gave the technical base needed for the project already in an early stage. Thereafter, critical factors could be detected, assessed and improved in the subsequent steps.

2 Theoretical framework

As support for the critical choices regarding the design of the 200 m high timber tower a literature study is made. The study includes information about timber as a material, high structures, structural elements, loads, the design process and other relevant design considerations.

2.1 What is a timber building?

The Council of Tall Buildings and Urban Habitat (CTBUH) states that a timber structure might still have connections using other materials. The important limitation is that the non-timber connection materials are localized within the structure. Timber structures might also include other materials such as concrete, for example as concrete slabs, as long as they are not included in the primary load bearing system. This means that, if necessary, with regard to building requirements, additional concrete parts might be added to the timber tower if needed to improve its global behavior. Using concrete in the primary load bearing system would re-categorize the building to either a mixed-structure or a composite structure depending on how the materials are combined (Council on Tall Buildings and Urban Habitat, n.d.).

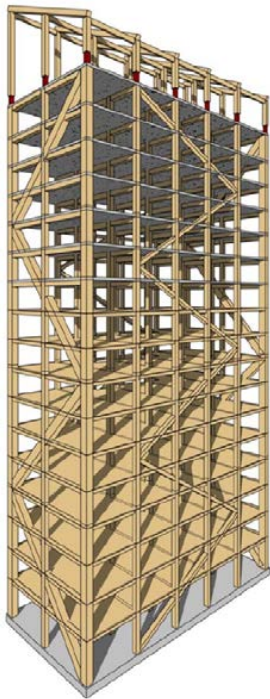


Figure 1: Structural system of Mjöstornet, the current tallest timber building with floors 12-18 made of concrete to increase the building mass (Abrahamsen, 2018).

2.2 Timber as a structural material

The timber material has been used for tools and structures long before the modern civilizations. During different time periods and in various locations, the utilization has varied. However, it has always been there as one of the main construction materials. In recent years, as environmental consciousness and rational building procedures has got a more central role in the construction industry, the interest in timber buildings has increased substantially. Considering the modern building industry, the material itself has several advantages, which utilized to its full potential will have a pronounced impact on the future buildings and the building stock (Essays, 2013).

Timber structures has beneficial properties such as: Non-toxic material, renewable, little energy needed in production, lightweight and possible pre-fabrication. Combining these factors with material suited construction types, the material can be used as a worthy competitor to the traditional steel and concrete structures in a wide array of applications (Essays, 2013).

2.2.1 Material properties

Structurally, timber has a relatively high capacity compared to its density (Crocetti, Johansson, Lidelöw, et al., 2015). It also shows an orthotropic behavior which has to be especially considered in design when determining on the layout of vertical load bearing system and bracing systems. Whether the systems should be integrated or separated for best material utilization and overall behavior. Also, wood is a hygroscopic material leading to changes in volume and overall properties when subjected to water (vapor or liquid). This property stands for some of the big challenges when building using timber as the construction material. Furthermore, timber will have creep deformations when subject to long term loading which is another factor important to consider in design (Yipintsoi, 1976).

2.2.2 Orthotropic behaviour

As the structure of timber is based on fibers running along the tree and an annual division into growth rings within the cross-section, the material has different properties in different directions. These directions are commonly referred to as longitudinal, tangential and radial directions. In practice, this orthotropic behavior is mostly simplified to two main directions – parallel to the grain or perpendicular to the grain. As the material responds different in bending, compression and tension, there is a substantial number of material parameters to account for in design (Domone & Illston, 2010). Since the strength and stiffness differs significantly depending on the directions a special consideration has to be made when designing each of the structural elements (Crocetti, Johansson, Lidelöw, et al., 2015).

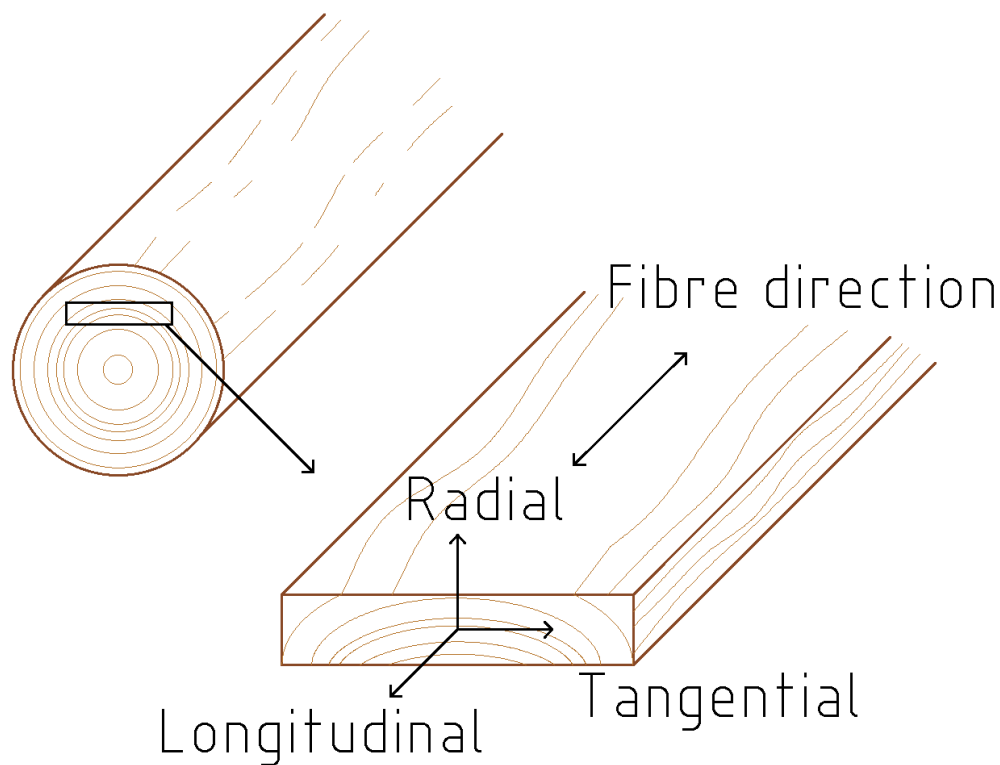


Figure 2: Illustration of the three idealized directions of timber giving the base for orthotropic behavior

2.2.3 Weight of timber

In general, the density of timber from different wood species ranges between 170 and 1 200 kg/m³ (Domone & Illston, 2010) while for concrete, it is usually around 2 400 kg/m³. The Nordic timber products usually remain within 300-500 kg/m³ which means an approximate weight difference of a factor six for a similar volume of concrete and timber. The low weight allows for easier transportation, construction and in some instances reduced foundation work. However, a lower mass reduces the inertia of the building which might have consequences for the overall behavior of the building when considering dynamic effects (Crocetti, Johansson, Lidelöw, et al., 2015).

2.2.4 Influence of moisture

Timber is a hygroscopic material, constantly seeking for a new equilibrium state with the surrounding atmosphere. Depending on the relative humidity in the surroundings and the moisture content within the material either adsorption or desorption will occur to some extent (Domone & Illston, 2010).

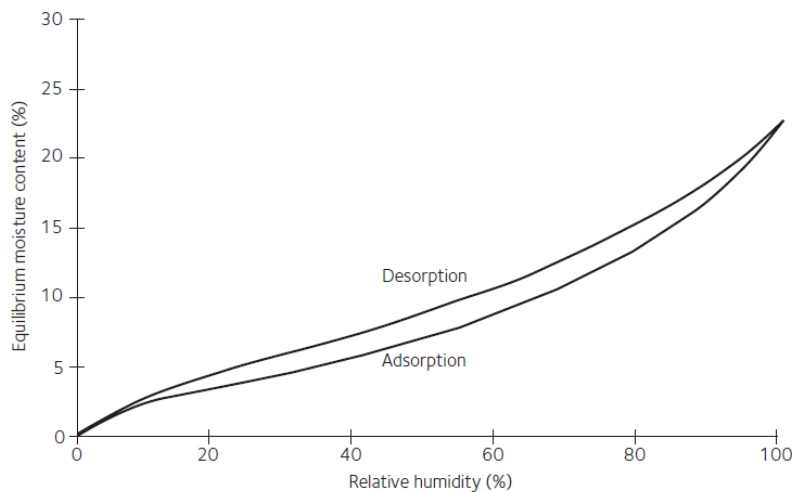


Figure 3: Principal relation between relative humidity and equilibrium moisture content for wood during absorption and desorption (Crocetti, Johansson, et al., 2016).

Processed timber products usually approach a water content around 12 % when stored in unheated indoor climate. This value is aimed for to minimize the difference between the timber product and the expected conditions at its intended use. It has also been shown that the strength of timber increases as the material is drying out. Therefore, it is of advantage to dry the material as much as possible before usage but also to keep it as dry as possible when in service. The strength difference between a moisture level around the fiber saturation point and a completely dried out specimen is almost of a factor three. However, it is not reasonable to dry out the material completely, this is one reason why 12 % moisture content has been chosen as a compromise between material performance and rational production. The adsorption and desorption isotherms show that a normal indoor climate will result in a moisture content around 12 % (Domone & Illston, 2010).

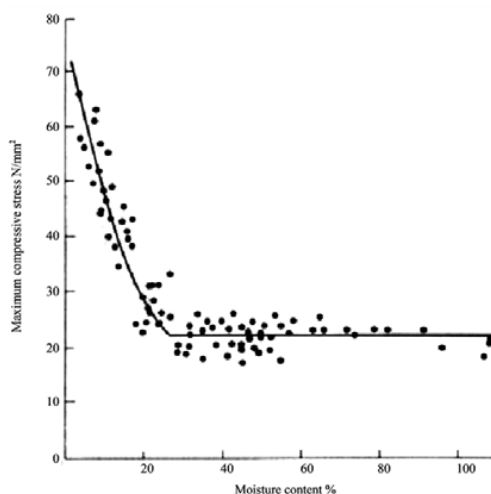


Figure 4: Relation between compressive strength in longitudinal direction and moisture content in wood (Platts, 2014)

As the fresh timber dries from the fiber saturation point, it shrinks. This size change happens according to the orthotropic principles mentioned above and results in a change of dimensional ratios. However, since modern day timber products are already dried during production, this shrinkage is of minor importance during construction. Apart

from this, varying conditions will always affect the timber in some way. The usual response to annual changes in moisture conditions is of small magnitude and can in most instances be neglected. Also, due to the slow diffusion of water through the timber material, these effects are further reduced, especially for elements with large cross-sections. Furthermore, treating the material surface can further improve the resistance to moisture and reduce the dimensional changes (Domone & Illston, 2010).

Similarly to the material strength, timber stiffness varies with the moisture content. Studies have shown an almost linear relationship between modulus of elasticity and moisture content for ranges below the fiber saturation point where a lower moisture content opens for a higher stiffness (Domone & Illston, 2010).

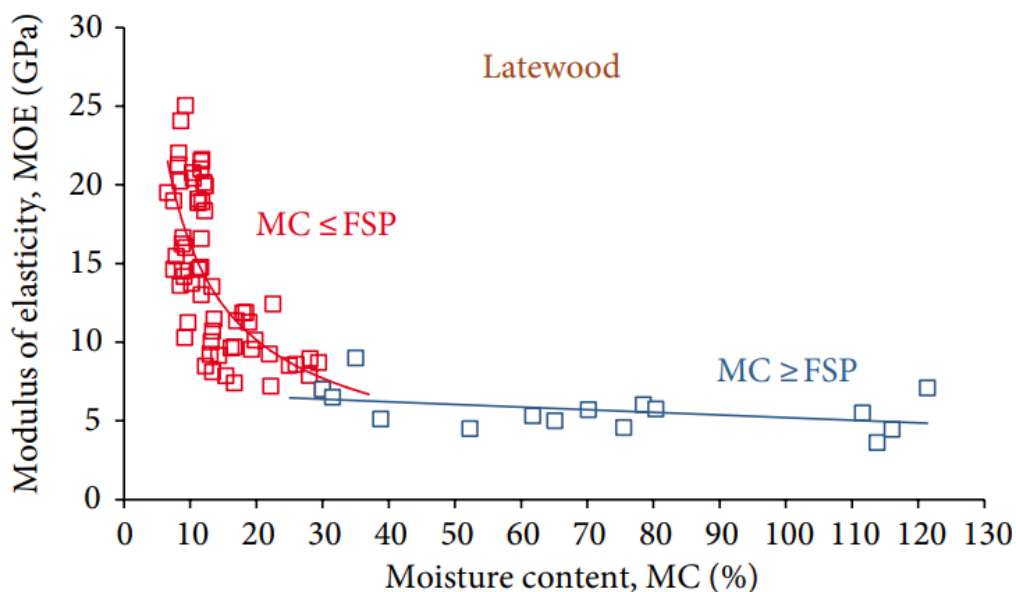


Figure 5: Relation between moisture content and modulus of elasticity in the longitudinal-radial plane in Sitka spruce (Roszyk, 2014).

An important consideration for tall buildings is that even small variations can have a significant impact over longer distances. Therefore, changes due to varying moisture conditions must be regarded early in design. With a well-developed moisture safe design, the impact of moisture can be kept small and the structure will not be affected negatively.

2.2.5 Creep

As a load is applied to a timber structure, instantaneous elastic deformations will occur. However, with time, the deformations will grow due to creep in the material. These time dependent deformations consist of two parts. The first one acts as a delayed elastic deformation which after removal of the load will gradually vanish. The second part is irreversible and will therefore remain after unloading. These irreversible deformations are a consequence of viscous flow within the material (Domone & Illston, 2010).

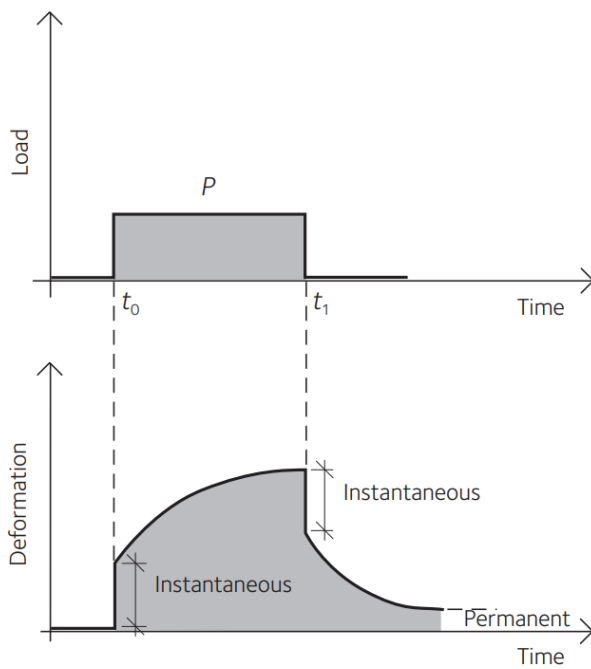


Figure 6: Schematic relation between loading, time and creep deformations (Crocetti, Johansson, et al., 2016).

Considering the effect of creep for high rise structures, it is mainly relevant in service state, when determining final deflections. However, for a structural system unevenly loaded, the creep deformations might be concentrated to certain structural elements. This could result in load redistribution and unexpected load paths if not considered in design.

2.3 Wood products suitable for tall buildings

Apart from regular sawn timber, there are numerous options when it comes to wood-based building materials. As tall structures usually are subject to higher loads resulting in large element sizes, wood products available in large dimensions are of special interest.

2.3.1 Sawn timber

Sawn timber is a traditional wood product where the dimension limitations are depending on the available tree sizes. To ensure sufficient material properties for the intended use, it is strength graded during production. The common strength grades in Sweden ranges from C14 to C35 where the number indicates the bending capacity parallel to the grain, i.e. C14 has 14 MPa bending capacity (*Konstruktionsvirke - TräGuiden*, 2017). In Sweden, the maximum dimension available are made with a height of 245 mm and a total length of 5.5 m (Crocetti, Johansson, Lidelöv, et al., 2015).

2.3.2 Glulam

The oldest engineered wood product is glulam, it is made from multiple smaller lamellas, glued together and connected using finger joints. The fibers within all lamellas runs in the same direction, the axial direction of the glulam beam. Studies have shown a lower variability in capacity for glulam compared to plain sawn timber. This can be explained by the structure. Since glulam consists of multiple strength graded lamellas, the probability of significant defects within on specific area of the material is heavily reduced. However, for the average capacity the difference between glulam and sawn timber is relatively small. Due to the gluing process, glulam can be made in much larger dimensions than ordinary sawn timber (Crocetti, Johansson, Lidelöv, et al., 2015).

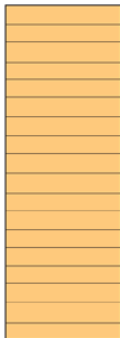


Figure 7: Principal sketch of a glulam beam section (Crocetti, Johansson, Kliger, et al., 2015).

The available dimensions for glulam are up to 2 x 2 m and lengths of 30 m according to F. Morell (personal communication, 24 February 2020) at *Moelven*. When producing large glulam elements multiple small ones are usually joined using glue. This was pointed out by R. Jockwer (personal communication, 12 May 2020) at Chalmers.

2.3.3 CLT – Cross laminated timber

CLT is a relatively new wood product made from boards glued together into solid timber elements, often used in the structural system as stabilizing walls or as slab elements. Commonly, every other board layer is placed perpendicular to the previous one. This gives overall high stiffness and load bearing capacity, especially suitable for the load bearing systems within buildings. It is also possible to manufacture relatively

large elements of CLT which is an advantage when constructing tall buildings (*Introduktion - TräGuiden*, 2017).

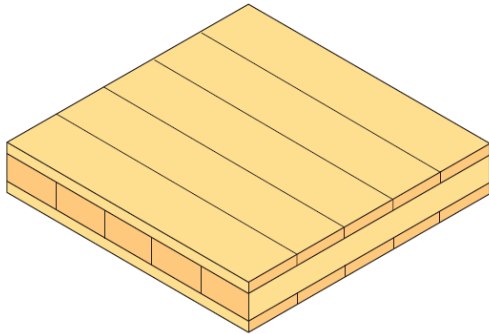


Figure 8: Principal illustration of a CLT slab with three layers (Crocetti, Johansson, Kliger, et al., 2015).

Available dimensions for CLT are up to 3.45 x 16 m with a standard thickness up to 320 mm according to J. Szyber (personal communication, 17 March 2020) at *Stora Enso*. However, according to *Svenskt trä* thicknesses up to 500 mm are available (Svenskt Trä, 2017b).

2.3.4 LVL – Laminated veneer lumber

LVL is basically a number of veneer layers glued together, either alternately in the perpendicular direction, all layers in the same direction or any combination in between. The production process leads to even lower variability in the material than for example glulam, simply by further distribution potential weaknesses throughout the element. Overall, the stiffness and capacity of LVL are high. However, significant reductions for these values can be observed for large elements and this must be considered in design (*Träbaserade kompositprodukter av faner - TräGuiden*, 2017).

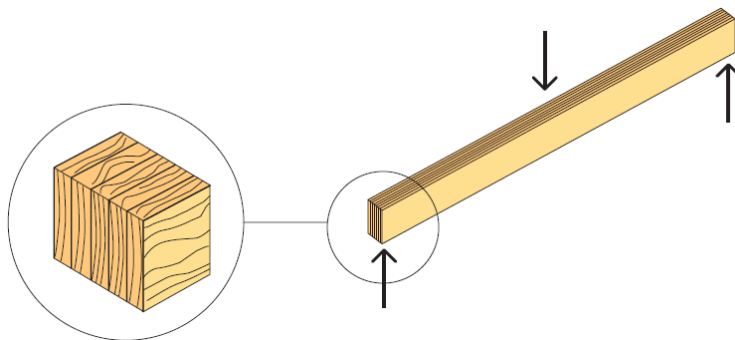


Figure 9: Principal illustration of an LVL-beam with all layers in the same direction (Crocetti, Johansson, Kliger, et al., 2015).

Available dimensions for LVL from *Stora enso* are up to 2.5 x 2.5 m and 24 m long (StoraEnso, n.d.) High strength LVL from *Pollmeier* can be manufactured in dimension up to 1.36 x 0.3 m with lengths up to 18 m (Pollmeier, n.d.). Similarly, to the glulam elements large elements can only be obtained by joining multiple elements to each other (personal communication R. Jockwer, 12 May 2020).

2.4 Connections in timber structures

Traditionally, the junctions were handmade using puzzle-like connections created through shaping of the timber. Also, dowels were used, often based on a stronger timber species than the surrounding material in the joint. However, the making of these joints is labor intensive and they are performing rather poor when it comes to tensile loads. Therefore, in modern buildings, the area of utilization for these joints are limited to restoration objects, buildings with short spans etc. Modern timber connections often utilize steel or glue which allows for better performance when it comes to the weaknesses of the old connections (Crocetti, Johansson, Kliger, et al., 2015).

A connection must fulfill the intended requirements on stiffness, fire safety, ductility, rational building and more. Therefore, not only a sufficient connection has to be chosen, but also a well thought through application for the connection design. After all, the connection capacity should preferably be equal or higher than for the rest of the structure (Crocetti, Johansson, Kliger, et al., 2015).

Even though there are numerous variations of timber connections on the market. The strict demands on tall structures leaves mainly two connection concepts suitable for the task, dowel-based joints and joints with glued-in rods (Crocetti, Johansson, Kliger, et al., 2015).

2.4.1 Dowel joints

The main load transfer mechanism for dowel based joints is shear (Crocetti, Johansson, Kliger, et al., 2015). This also means that the joint requires some kind of overlap within the connection. In practice, this can be made either by overlapping the timber elements or by using a slotted-in steel plate, fixed to the timber members using dowels. In most cases it is advantageous to arrange the connection in a symmetrical way, it is also of great benefit to increase the number of shear planes within the connection. An increased number of shear planes leads to more distributed stresses acting on the dowels (Rodd & Leijten, 2003).

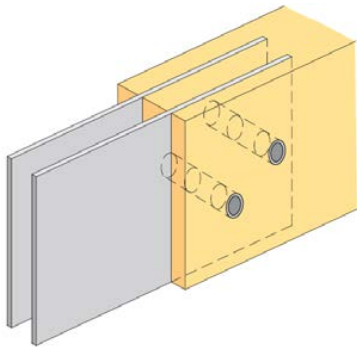


Figure 10: Principal sketch of two slotted in steel plates fixed to the timber member using dowels (Crocetti, Johansson, Kliger, et al., 2015).

A necessary but disadvantageous part of dowel joints is the need for grooves or holes in the timber elements. This reduces the cross-section which might weaken the structure. Also, when transferring moment, the efficiency of the connection increases as the dowels are moved further away from the connection centroid. Important though is that the dowels are not located too close to the element surface which could lead to local failure. Also, moment transferring connections often results in forces at an angle

to the grain which has to be accounted for considering the strongly orthotropic behavior of timber (Rodd & Leijten, 2003).

Johansen's yield theory shows the capacity for a doweled timber connection depending on its possible failure modes. Observing the failure modes in Figure 11, it can be noted that the capacity of a dowel connection can basically be related to its geometrical shape and the material strengths of the included parts. Therefore, these are the factors to consider if looking for improvements (SIS, 2009). Tests has showed that reinforcing layers glued to the timber at the shear planes can have a significant effect on the embedment strength of timber. Available materials for such reinforcement are for example densified veneer wood, plywood or thin steel plates. Also, various kinds of fiber fabrics can be utilized. The main purpose of these reinforcements is to improve the material strength in the otherwise weak directions. Therefore, a properly made reinforcement can bring the embedment strength to such levels that the connection manages the same loads as the structural elements themselves. Furthermore, maximum connections stiffness can be obtained using either resin injected dowels or hollow tube dowels expanded for perfect fit using a hydraulic jack. At the same time, ductility must be ensured, similarly it can be reached using hollow tubes dowels or by utilization of many small dowels which is proven to show larger deformations than the equivalent of few large dowels (Rodd & Leijten, 2003).

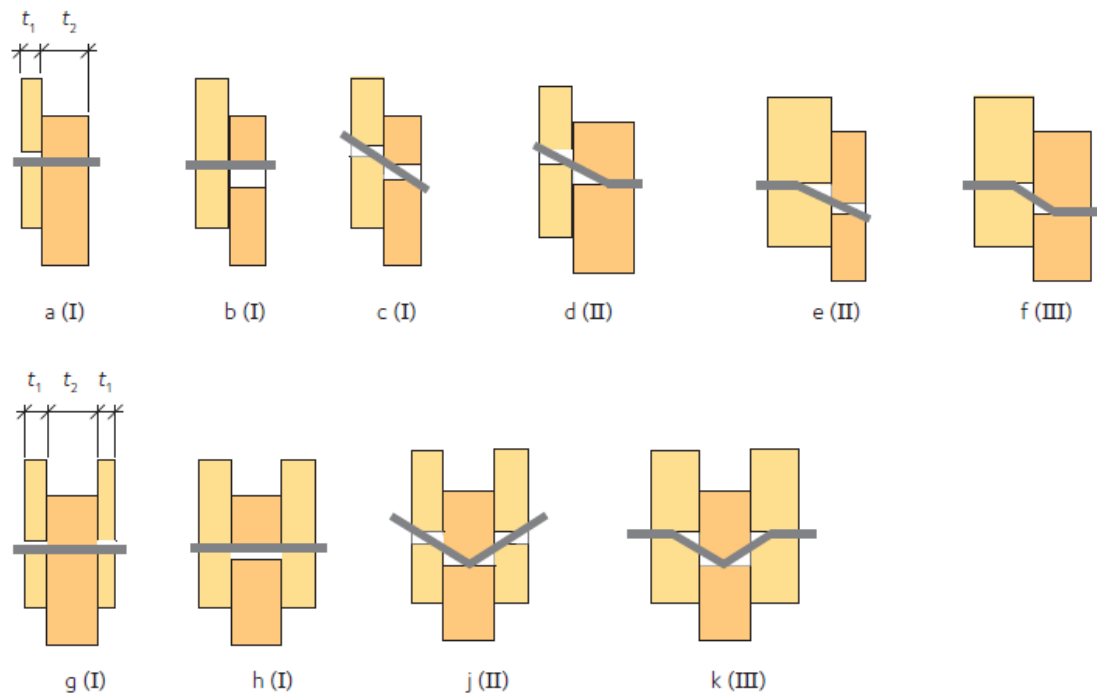


Figure 11: Illustration of possible failure modes according to Johansen's yield theory (Crocetti, Johansson, Kliger, et al., 2015).

The currently highest performing dowel joints regarding both stiffness and strength are reinforced with densified veneer wood and connected with either many small resin injected dowels or hollow tube dowels (Rodd & Leijten, 2003).

2.4.2 Glued-in rods

The timber is pre-drilled whereafter most commonly, threaded steel rods are inserted and glued to the element. This type of connection can for example be used when transferring loads between a concrete slab and a load bearing column. It has the advantage of being almost completely enclosed by the timber element, often preferable from an aesthetical standpoint but especially favorable with regard to fire safety. Its main weakness is the need for special experts when gluing in-situ. Also, it is somewhat sensitive to dynamic loading and must be used in an area with stable conditions (climate class 1 or 2) to avoid potential problems with cracking (14.3.2 *Fast inspänd pelarfot - TräGuiden*, 2017).

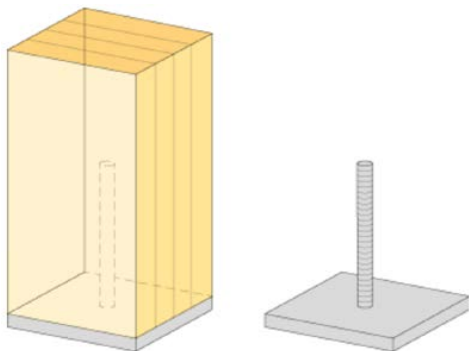


Figure 12: Principal sketch of an application of glued in rods, a column connection (14.3.1 *Ledad pelarfot - TräGuiden*, 2017).

Glued-in rods can individually carry relatively large loads, especially in pure tension or compression. What has to be considered though, is the restrictions when it comes to rod spacings and distances between rods and the timber element edge which might lead to few glued-in rods within a cross-section. Combined with high-capacity timber species, this type of connection can however be used successfully although, at the moment, the widespread experience of dowel joints with slotted in steel plates is higher, mostly resulting in use of doweled connections instead (Crocetti, 2016).

2.4.3 Glued-in steel plates

This connection type has large similarities with both the dowel joints and the glued-in rods. Axially loaded, a glued-in steel plate can provide up to 40 % higher strength and 300 % higher stiffness than a corresponding dowel joint. As for all timber connections, glue-in steel plates must be designed for ductile failure. Steel plates might also allow for a larger force transferring area since they can be made with a relatively large cross-sectional area compared to for example threaded rods which have a limitation in cross-sectional area to circumference ratio (Cepelka, 2017).

2.4.4 CLT connections

Most CLT connections are based on various steel plates to transfer loads. In some cases, self-tapping screws and overlaps of the CLT elements is used. However, this is mostly in smaller structures with relatively small forces (Cepelka, 2017).

The steel plate connections are of mainly two types. Externally mounted or slotted in plates. The slotted in plates are either of dowel connection type, as glued-in steel plates or a glued dowel connection (Cepelka, 2017). Compared to other timber materials,

dowel-type connections are especially well suited for CLT elements. This is since every other layer is arranged in the perpendicular direction to the previous layer and rigidity is provided against splitting in both main directions. As for other connection types, externally placed connections might be beneficial in the production stage and provide good possibilities for inspection. However, they need special care when it comes to fire safety. Slotted in plates are more labor intensive but are automatically provided with some fire protection, are more aesthetically appealing and will not risk interference with for example installations (Azumi et al., 2018).

2.4.5 Connection failure behaviour

When considering the material aspect in failure of a structural member, the failure can occur either in tension, compression or shear, in any direction relative to the grain. The design goal is always to load the structural member in its strong direction, which for timber is parallel to the grain (Azumi et al., 2018). Considering tension failure for timber, it shows a linear elastic behavior until the failure load is reached. The failure load corresponds with deformations of about 1 % whereafter rupture occurs. This failure mode shows no ductility and must be avoided on a structural level (Pirinen, 2014).

The behavior in compression is significantly different. As the compressive load capacity is reached, the cell walls start to buckle. This leads to a gradual softening of the material as the deformations increases. When considering pure timber without any imperfections, the tensile capacity is much larger than the compressive strength. This means that theoretically, the compressive zone would be governing when it comes to bending, and therefore a ductile failure would occur. However, in reality, the imperfections are hard to control and therefore compressive failure cannot be assumed in design (Pirinen, 2014).

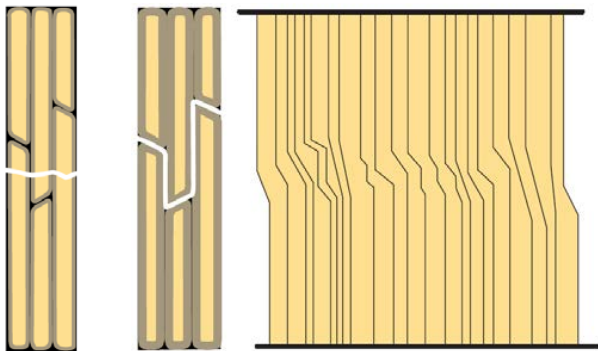


Figure 13: Principal tension (two to the left) and compression (right) failure of timber loaded parallel to the grain (Crocetti, Johansson, Kliger, et al., 2015).

The shear capacity is directly dependent on the loading direction of the timber and the fact whether the shear plane occurs across the fibers or between the fibers. The shear capacity across the fibers is rather high and can usually be disregarded in design. For the cases with shear parallel to the grain, the failure is often concentrated to a lignin layer resulting in brittle failure (Pirinen, 2014).

In practice this means that timber can in many cases have a ductile behavior during failure. However, this cannot be assumed reliably, and design is therefore made based on brittle failure. Therefore, the connections are designed to provide ductility to the structure. By designing a dowel connection so that failure occurs either by compression

failure in the wood or by yielding of the dowels, this is acquired. For a glued connection (either glued-in rods or glued-in plates), the design must ensure ductile failure in the connector piece (Pirinen, 2014).

2.4.6 Importance of stiff connections

Specifically, for tall timber structures is their dependency on the connection quality since accumulated joint deformations might lead to significant displacements at the top of the building (Ramage et al., 2017). For a tall structure with multiple connections this effect on the global stiffness might lead to displacements several times higher than the elastic deformations assuming fully rigid connections. Increasing the stiffness of structural elements does not have any significant impact on the global behavior if the connection stiffness is not sufficient. Also, if the global stiffness is too low, the movement related requirements for the upper floors will not be fulfilled. Apart from global deflections and accelerations, the stiffness will also influence the eigenfrequencies of the building (Malo et al., 2016).

The slip between two shear wall elements attached using dowel joints might reduce the stiffness for lateral deflections to only 30 % of the equivalent stiffness for a single shear wall element without connections. To counteract this, one solution is to attach steel ties along the CLT elements for the full height of the building. These solutions were not used in the project *Haut*, instead a timber concrete composite structure was used. However, the method is anticipated to have potential and might very well be used in future projects (Verhaegh et al., 2018).

To minimize connection slip, the most efficient way is to utilize glue for the joints. When completely filling the voids, the slip is nearly eliminated which means high interaction and a more rigid structure (Cepelka, 2017).

Based on the available information regarding timber joints, if wanting to maximize the global stiffness of a building, glued or resin injected connections should be used. However, due to the labor intensity this would increase overall cost drastically. Therefore, if economy is a major concern, critical joints must be detected, and the gluing concentrated to these. This will maximize the global structural efficiency for a specific economical limitation.

2.5 Timber in high-rise buildings

Since the governing behavior for high-rise timber buildings is usually connection dependent and small deflections in joints near the ground can have big influence on global displacement, the design of such building will mainly be with regard to lateral stability. The best solution would be if the self-weight of the building managed to resist the overturning due to wind loads, but it is complicated with the typical slender high-rise buildings. Due to the high slenderness ratio, it is important to transfer vertical loads into the lateral load system, preferably close to the façade, to create resistance against horizontal wind loads. Also, higher building mass will create more resistance to the wind loads. This is hard to achieve for timber structures since the material is much lighter than steel and concrete (Ramage et al., 2017).

An investigation regarding a 300 m tall timber building have once been carried out. There, the chosen design was based on a geometry, moving step-wise upwards in a spiral shape with diagonal bracing systems. The suggested columns were up to 2.5 m by 2.5 m, sizes which have not been used in any building so far. Therefore, before building such structure, elements of that size need to be tested and potentially new production systems have to be developed. Problems regarding transportation due to the massive element sizes have also been detected, and it is suggested that the largest elements are assembled on site (Ramage et al., 2017).



Figure 14: Design of a super tall timber structure reaching 300 m above the ground from the project Oakwood Tower (PLP Architecture - PLP Labs, n.d.).

2.6 Tallness and slenderness for high-rise buildings

The tallness of a building is a somewhat subjective topic, but guideline definitions have been determined by CTBUH based on building height only. The statement is that *Tall buildings* ranges within the span 50-300 m, *Supertall buildings* within 300-600 m and *Megatall buildings* above 600 m. Considering the aimed building height for this particular timber tower, 200 m, it will fall into the category of *Tall buildings*. However, the impression of a building depends on way more factors than their raw height. Location, surroundings, slenderness and global response are a number of factors influencing this impression (Council on Tall Buildings and Urban Habitat, n.d.).

In order to obtain a reasonable starting point regarding the slenderness of this timber tower it is of value to study existing structures. Skyscrapers with a slenderness higher than 1:10 can be viewed as 'slender' (Hayes, 2018). Rough measurements for the tallest existing timber buildings shows a slenderness below 1:5.2 for the narrowest side of the structures (Abrahamsen, 2018). Since most of these buildings have a rectangular floor plan, the slenderness in the other direction is usually even lower.

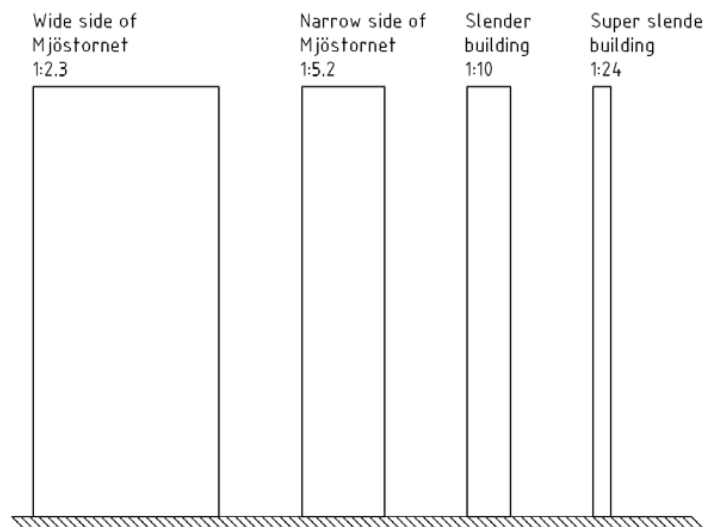


Figure 15: Examples of slenderness ratios.

Reviewing these slenderness ratios, the high values, common in skyscrapers, seems out of reach for a timber building constructed with today's technology. Instead a start value in approximate of the current tallest timber building might give the project a more realistic chance for success.

Note that in order to be called a building, at least 50 % of the height must be occupiable (Council on Tall Buildings and Urban Habitat, n.d.).

2.7 Structural systems for tall buildings

Designing a high-rise building is a complex process with a lot of things to consider both during construction and for the finished building. Normally high-rise buildings rely on a central core in the building. The core is usually located at the geometrical center. However, for unsymmetrical buildings or buildings with an irregular shear wall pattern. An offset position might be preferable targeting the torsional center of the building instead. There are many different systems that are used when building up a structure, some are more advantageous for taller buildings (Truby et al., 2014). Specific structural elements can be read about in Appendix I.

2.7.1 Frame system

One of the most common and simple structural systems is the frame system. It is usually built up by frames made of columns and beams. The connections are often rigid, and a flat slab is the most common slab choice. If using pinned connections, the horizontal loads must be transferred in another way. The most common alternatives here are stabilizing trusses or diaphragm action using various sheet materials. Depending on the building size, frames can be used both along the façade and internally (Truby et al., 2014). The frame system can be seen in Figure 16.

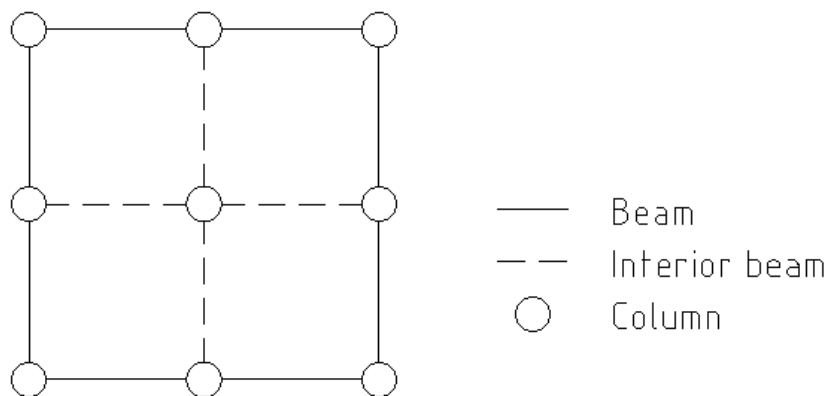


Figure 16: Frame system.

2.7.2 Shear-wall systems

Shear-wall system, which also can be called core-system, is one type of systems which is built up with shear walls to take care of the lateral loads. The most common way is to have shear walls in two directions, sometimes placed as a core in the middle of the building. The purpose of the shear walls is to work as vertical cantilevers, taking care of the all lateral loads and some vertical loads while letting the other columns in the building take care of only vertical loads. It is common to have more than one core, for example with elevators facing each other and then connect the cores with beams in between (Truby et al., 2014). The shear-wall system is shown in Figure 17.

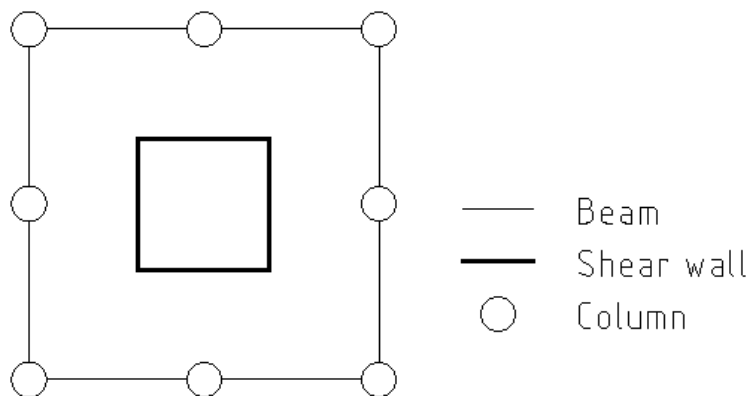


Figure 17: Shear-wall system.

A combination of the frame system and shear-wall system is also possible. With this combination, it is hard to utilize the frame action due to the typical low heights in the rooms. The core and the frames would have different deflections if they were separate, but when they are combined, they are restrained by each other and will create a different, stiffer, deflection profile (Truby et al., 2014). The combined system of shear-walls and frame can be seen in Figure 18.

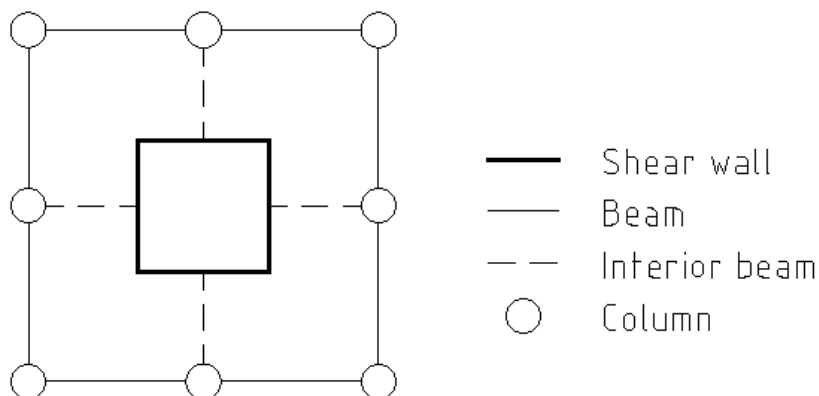


Figure 18: Combination of shear-wall and frame-system.

2.7.3 Tube systems

One system that was introduced by Fazlur R. Khan was the framed-tube system, which has also been a big factor in developing skyscrapers. There are different kinds of framed-tube systems, it can be hollow, have a tube inside, be bundled, having diagonal bracing at the façade or be outrigger-braced for example. For the original hollow form, columns are placed closed to each other along the façade and connected by beams. The building will act like a stiff cantilever with the possibility to have columns inside to sustain vertical loads (Truby et al., 2014). The frame-tube system is shown in Figure 19.

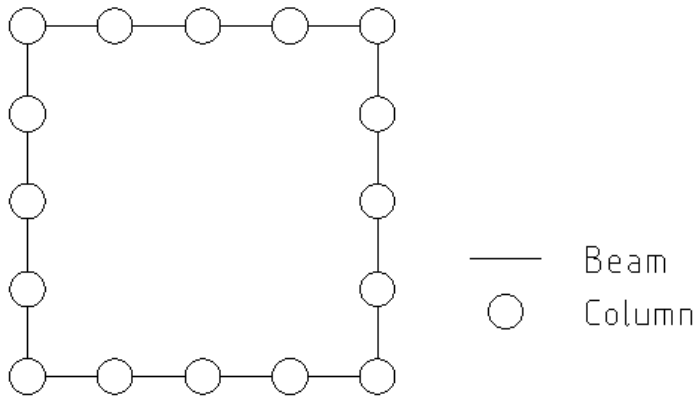


Figure 19: Framed-tube system.

The tube-in-tube system is similar to the system with shear wall – frame system, but it has one external and one internal tube. The combination of outer and inner tubes will create a more stable structure towards the lateral loads (Truby et al., 2014). The tube-in-tube system can be seen in Figure 20.

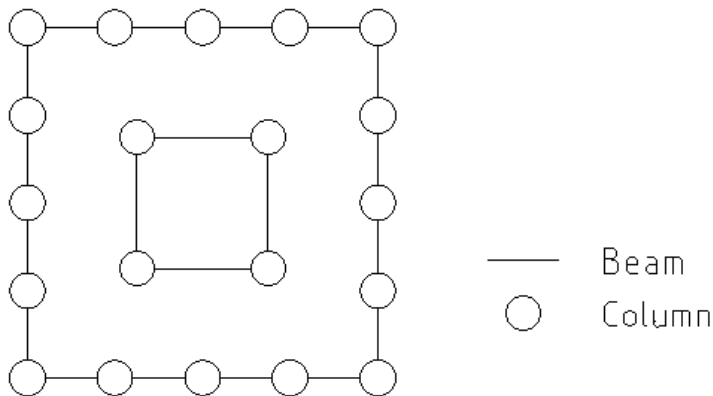


Figure 20: Tube-in-tube system.

The bundled-tube or modular-tube system can be seen as a combination of framed-tube system with internal frames, which creates a number of sections inside. The small modules in the building will make it more robust at the same time as it reduces possible shear lag effects (Truby et al., 2014). The bundled-tube or modular-tube system is shown in Figure 21.

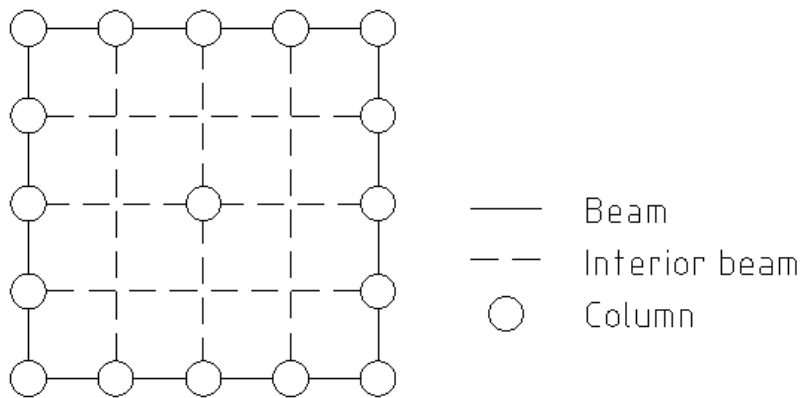


Figure 21: Bundled-tube or modular-tube system.

There is a braced-tube system which has diagonal bracing frames along the façade to create extra stiffness against lateral loads. These diagonal elements will also help distributing the vertical loads and create a more redundant structure (Truby et al., 2014). The braced-tube system can be seen in Figure 22.

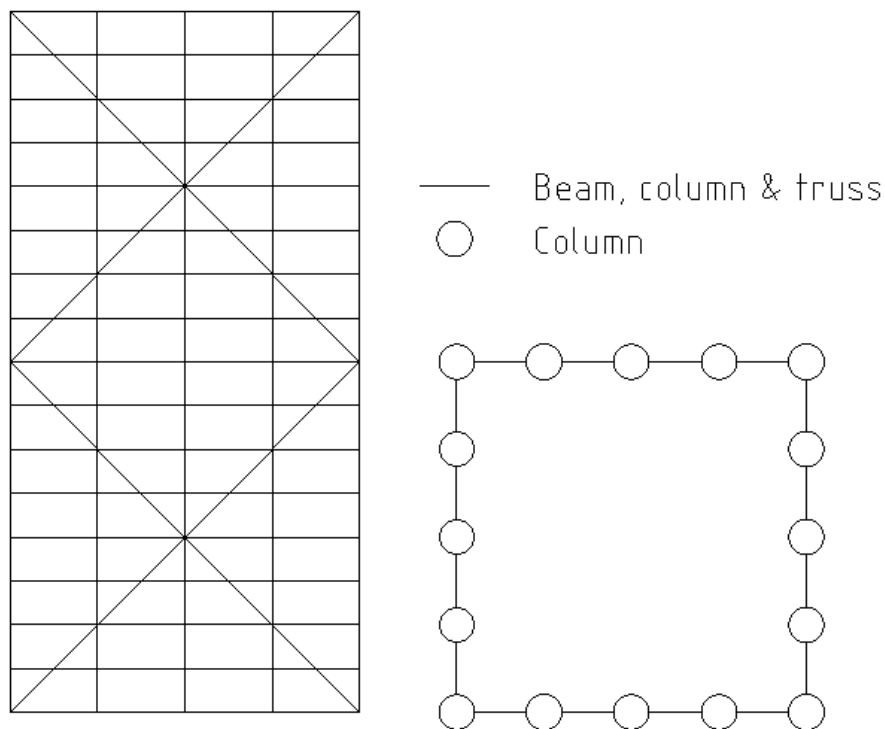


Figure 22: Braced-tube system side (left) and top (right) view.

2.7.4 Outrigger systems

The outrigger-braced system is built up with one extra-large core in the middle and a perimeter tube at the edges. At certain heights of the building, the perimeter columns and the core are connected by outrigger elements, which usually are trusses. These particular levels usually have either trusses or solid walls as façade to redistribute forces from above (Truby et al., 2014). The outrigger-braced system is shown in Figure 23.

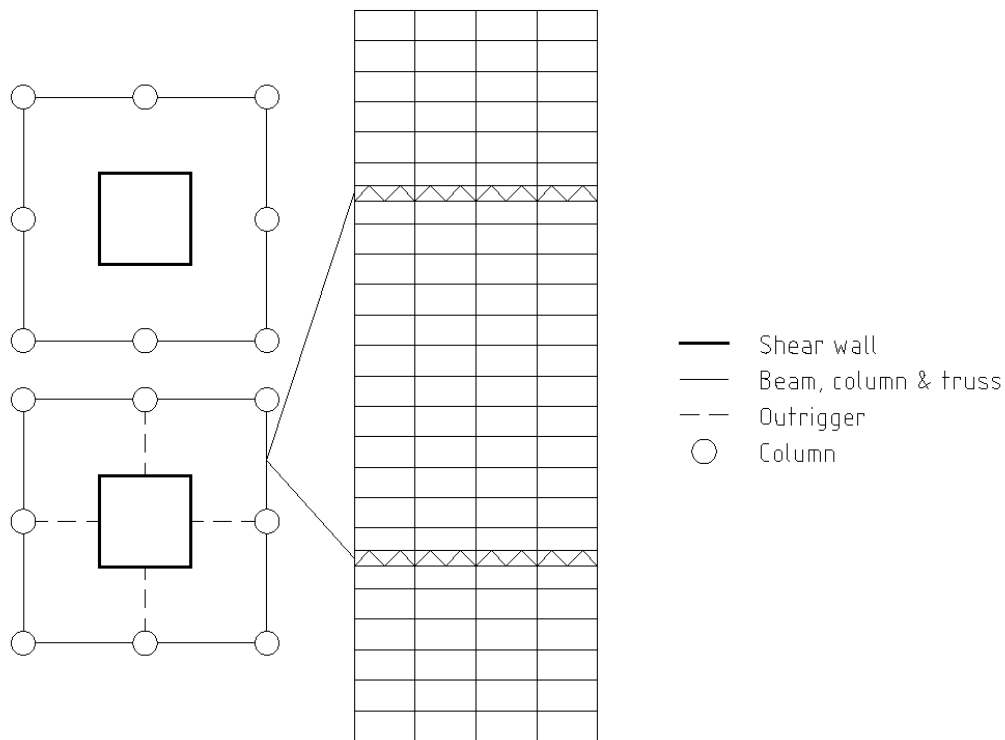


Figure 23: Outrigger-braced system.

2.7.5 Buttressed core system

The basic concept of the buttressed core system is its Y-shape acting like a tripod for the structure. Each wing is attached to a hexagonal central core leading to a highly stable system where each wing is buttressed by the two other wings. The intention with the structure is that the hexagonal core should give torsional rigidity while the wings provides the structure with shear resistance and larger inertia for global moment action. *Tower Palace III* in Seoul, completed in 2004, was the first building based on this system. It showed high performance both regarding structural behavior and wind response. Even though this structure was not near the height of modern day skyscrapers, it showed the great potential of the structural system and building layout (Baker & Pawlikowski, 2012).

Spreading the walls within each wing might create higher torsional stability but it also requires more openings and results in less light in the central parts of each wing. It is therefore of advantage to construct the floor layout in a way that avoids these problems (Baker & Pawlikowski, 2012). An example of a simplistic section for a buttressed core system can be seen in Figure 24.

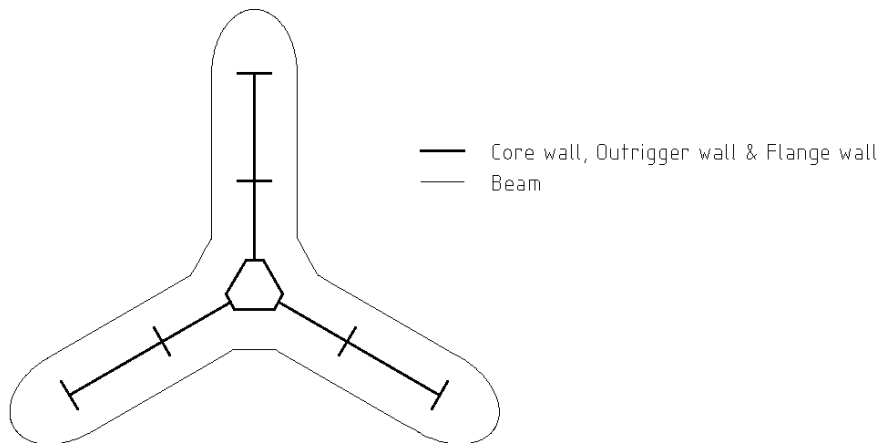


Figure 24: Typical section for a building with the buttressed core system.

2.7.6 Hyperboloid truss system

Two main properties of hyperboloid structures are aesthetics and efficiency. Since the shape is curved in two directions, it is much more resistant to buckling than an ordinary cylinder. There is also a special case of the hyperboloid system with the advantage that it can be composed entirely of straight continuous elements spanning from the foundation to the roof. Currently, hyperboloid structures are most common in various towers, partly due to the possibility of low material consumption (Debney, n.d.).

In practice the hyperboloid truss system is often combined with stiffening rings to allow for better force distribution through the system. Also, due to the nature of the shape, a waist is formed in the structure. This is essential for the vertical curvature to take place. However, if it is made too distinct, it might result in a weakness in the structure (Debney, n.d.).

A dynamical advantage of the shape is that it might allow for larger floors in the upper third, making it possible to concentrate mass where it is mostly needed in dynamic design. A property which might be especially beneficial for a timber structure.



Figure 25: Principal illustration of a hyperboloid.

2.8 Existing high-rise buildings made of timber

When trying to push the limits regarding building height for a certain material it is of great importance to study existing structures of such type. Therefore, in this section, some of the current tallest timber buildings are described.

2.8.1 Mjöstornet

Mjöstornet is with its 85.4 m the current highest timber building in the world. It consists of 18 floors, including offices, apartments, hotel rooms and more. The building was completed in 2019 and is located in *Brumunddal*, Norway. The idea to build the world's highest timber building in this particular place came from an investor named *Arthur Buchardt*, who grew up in the area. He had a vision to create this building by using local and sustainable resources and production (Abrahamsen, 2018).



Figure 26: *Mjöstornet*, the current tallest timber building reaching 85.4 m above the ground (Abrahamsen, 2018).

One of the governing factors when designing high buildings are the horizontal accelerations created by wind loads. Therefore, measuring equipment were installed both during construction and when the building was finished to see the building's behavior and structural damping ratio (Abrahamsen, 2018).

2.8.1.1 Structural system

The skeleton of the structure is built up by glulam beams, columns and trusses along the edges. The trusses are there to increase the stiffness of the building and transfer horizontal as well as vertical loads to the ground. The staircases and walls around elevators are made of CLT and are mainly for secondary load bearing and not to transfer horizontal loads. The building stands on a concrete slab which is supported by piles that can take both compression and tension forces. The first ten floors above the ground are made of timber decks while the seven top floors have concrete slabs. These slabs will give the building a higher mass in the top which will contribute to make the building more comfortable for the users in the top floors (Abrahamsen, 2017). The pergola on the top of the building is made of glulam and the balconies are made of CLT. There is also 120 tons of steel components included in the building (Abrahamsen, 2018). The volumes of the structural components can be seen in Table 1.

Table 1: Volume of structural members in Mjöstornet.

Glulam	1 400 m ³
CLT	450 m ³
Timber floors	650 m ³
Concrete slabs	1 100 m ³
Pergola glulam	100 m ³
CLT balconies	85 m ³

The building is designed for high fire safety. It is supposed to manage at least 120 minutes of fire for the load bearing parts and 90 minutes for the floors. The building is also designed to be ductile enough to lose one floor. No wind tunnel tests were made for this building since the geometry is clearly defined by shape coefficients in the Eurocode (Abrahamsen, 2017).

2.8.2 Hoho – Vienna

Hoho is the second tallest building with wood as its main construction material. The height is 84 m (*Development | HoHo Wien, n.d.*) and it was finished in 2019. The building accommodates apartments, hotel, business areas and a wellness center (*Das Holzhochhaus | HoHo Wien, n.d.*) divided on the 24 floors of the building (*Facts & Figures | HoHo Wien, n.d.*).

The structure is stabilized with a concrete core while timber stands for the major volume of the structure through the timber columns, solid timber exterior walls and timber concrete composite floor elements (*Technology | HoHo Wien, n.d.*). All of the timber components are prefabricated. In total, 76 % of the total structural element volume is made from timber (*HoHo, Vienna Nearing Completion - Timber Architecture, n.d.*).



Figure 27: Hoho in Vienna, a timber building with a stabilizing concrete core (*Medien | HoHo Wien, n.d.*).

2.8.3 Origine – Québec

As part of a Canadian project to increase the utilization of local grow wood products, building of *Origine* in Québec was initiated. The structure consists of 12 floors of timber and a bottom floor constructed as a concrete podium for the rest of the structure (CCE - Canadian Consulting Engineer, 2017). The timber structure is mainly composed from load bearing walls made of CLT, but glulam is also used as columns and beams complementing the structure. It is used as a residential building (*Origine* | *Think Wood*, n.d.).

When the project first started, the *Quebec Construction Code* limited timber buildings to four floors. If wanting to build taller than that, the designer had to prove that the construction fulfills the demands regarding fire resistance. Therefore, parallel to the rest of the project extensive testing and researching were executed in order to fulfill these requirements (*Origine* | *Think Wood*, n.d.).



Figure 28: *Origine* in Québec. A timber building standing on a podium of concrete (*Origine* | *Think Wood*, n.d.).

2.9 General design considerations

When developing a building design, a wide range of factors must be considered. The pure performance can be coupled to the structural elements and the structural system. However, in order to fulfill all requirements on a building, the design must include fire management, sound and vibrations, daylight, installations and more.

2.9.1 Fire safety

When designing for fire, two important things to consider are the escaping possibilities and the time a building can resist fire. Regarding the escape, it is important to have enough stairs, exits and possibly systems such as smoke control provisions and sprinkler systems. The building elements are usually designed to hold for 90 minutes of fire, but more important elements might have a resistance time of 120 minutes or more (Truby et al., 2014).

Design for fire resistance should be done according to SS-EN1995-1-2 and SS-EN-1991-1-2.

Fire is regarded as an accidental load of which three main controls has to be made. These controls are for burn time, load resistance and material temperature. However, for timber the material temperature verification is of marginal importance (SIS, 2005).

$$t_{fi,d} \geq t_{fi,requ} \quad (1)$$

$$R_{fi,d,t} \geq E_{fi,d,t} \quad (2)$$

$$\theta_d \geq \theta_{cr,d} \quad (3)$$

$t_{fi,d}$	<i>Design fire resistance time.</i>
$t_{fi,requ}$	<i>Required fire resistance time.</i>
$R_{fi,d,t}$	<i>Design resistance for a member at time t.</i>
$E_{fi,d,t}$	<i>Design value for load on a burning member at time t.</i>
θ_d	<i>Design value of material temperature.</i>
$\theta_{cr,d}$	<i>Design value of the critical material temperature.</i>

The structure must be verified to ensure sufficient capacity and structural redundancy in case of fire. This can be verified either through a global analysis, analysis of sub-structures or single elements (SIS, 2004).

In fire design, adjusted values for material resistance and stiffness should be used. These should be based on the 20 percent fractile value for a material subject to normal temperatures (SIS, 2009):

$$f_{d,fi} = k_{mod,fi} \frac{f_{20}}{\gamma_{M,fi}} \quad (4)$$

$$S_{d,fi} = k_{mod,fi} \frac{S_{20}}{\gamma_{M,fi}} \quad (5)$$

$f_{d,fi}$	<i>Design resistance in case of fire.</i>
f_{20}	<i>Characteristic resistance for the 20 percent fractile at normal temperatures.</i>
$S_{d,fi}$	<i>Design value for stiffness in case of fire.</i>
S_{20}	<i>Characteristic stiffness for the 20 percent fractile at normal temperatures. Represents either Young's modulus or the shear modulus.</i>
$k_{mod,fi}$	<i>Load duration and moisture factor accounting for reduction in strength and stiffness due to elevated temperatures in case of fire.</i>
$\gamma_{M,fi}$	<i>= 1.0, partial coefficient for material properties in case of fire.</i>

Table 2: Characteristic resistances and stiffnesses for various timber materials for the 20 percent fractile at normal temperatures. Based on table 2.1 in SS-EN 1995 (SIS, 2009) and p.137 in KL-trähandboken (Svenskt Trä, 2017a).

	f_{20}	S_{20}
Sawn timber	$1.25 f_k$	$1.25 S_{05}$
Glulam	$1.15 f_k$	$1.15 S_{05}$
LVL	$1.10 f_k$	$1.10 S_{05}$
CLT	$1.15 f_k$	$1.15 S_{05}$

f_k	<i>Characteristic resistance for the material.</i>
S_{05}	<i>Characteristic stiffness for the 5 percent fractile at normal temperatures. Represents either Young's modulus or the shear modulus.</i>

There are different methods available for design with regard to fire resistance. One method that might be used to verify the resistance of structural components is by utilization of a reduced cross-section. Basically, the original cross-section is reduced with the estimated charring depth and a transition zone inside the charred wood that will not contribute to the strength and stiffness. This reduction is done for all sides subject to fire. The effective charring depth d_{ef} consisting of both the charred and the weakened timber (SIS, 2009), as shows in Figure 29 can be determined as follows:

$$d_{ef} = d_{char} + k_0 d_0 \quad (6)$$

d_{ef}	<i>Effective charring depth.</i>
d_{char}	<i>Notional charring depth.</i>
$k_0 d_0$	<i>Weakened timber thickness.</i>

Table 3: Thickness of non-charred weakened timber for a cross-section subject to fire. Obtained from table 4.1 in SS-EN 1995 (SIS, 2009).

	$k_0 d_0$ [mm]
$t < 20$ minutes	$\frac{7}{20}t$
$t \geq 20$ minutes	7

CLT elements will not be subject to sectional weakening due to rounded corners. Therefore, it will char as shown in Figure 30 resulting in a slower charring rate (SIS, 2009).

Table 4: Notional charring depths for various timber materials. Based on table 3.1 in SS-EN 1995-1-2 (SIS, 2009) and p.138 in KL-trähandboken (Svenskt Trä, 2017a).

	$d_{char} = \beta t$ [mm]
Sawn timber: Softwood and beech, $\rho_k \geq 290 \text{ kg/m}^3$	0.70 t
Glulam: Softwood and beech, $\rho_k \geq 290 \text{ kg/m}^3$	0.80 t
Sawn timber or glulam: Hardwood, $\rho_k = 290 \text{ kg/m}^3$	0.70 t
Sawn timber or glulam: Hardwood, $\rho_k \geq 290 \text{ kg/m}^3$	0.55 t
LVL: $\rho_k \geq 480 \text{ kg/m}^3$	0.70 t
CLT	0.65 t

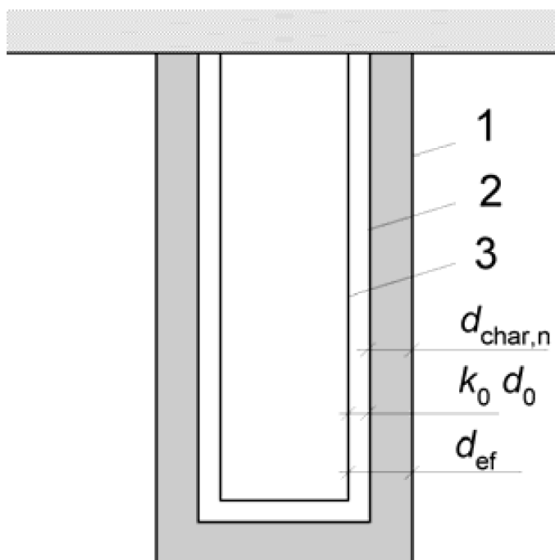


Figure 29: General illustration and definition of remaining area and cross-sectional reduction due to charring of the wood. Figure 4.1 in SS-EN 1995 (SIS, 2009).

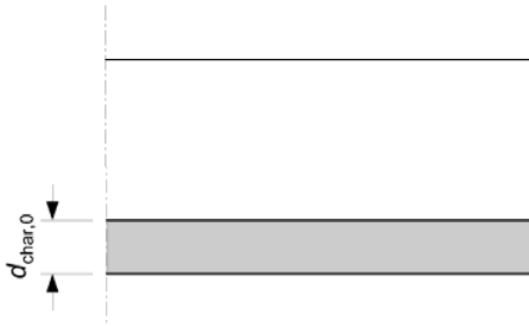


Figure 30: Illustration of the charring depth for a wide section. Figure 3.1 in SS-EN 1995 (SIS, 2009).

The reduced cross-section method assumes that the core material remains unaffected by the fire and will therefore not lose any of its capacity. Based on a chosen fire exposure, a reduced cross-section can be determined, and the capacity verified (SIS, 2009).

Timber has a fairly constant burning rate. Also, the char layer has insulating properties. This saves the construction from reaching high temperatures. Even during long exposure to fire, the core temperature of a large timber element remains nearly unaffected (Svenskt Trä, 2017a).

The fire resistance time is depending on a range of factors. In *Mjöstornet* resistance times of 90 minutes was chosen for the secondary load bearing elements and 120 minutes for the primary load bearing system. Considering the occupancy classes with offices, apartments, hotel, cafeteria, restaurant and more. Coupled with the tallness of the building, high fire requirements are a necessity (Abrahamsen, 2017).

The *200 m timber tower* will only consist of offices and therefore an occupancy class with lower demands. However, it will be more than twice the height of *Mjöstornet*. Therefore, similar standards are chosen for a rough estimation of the structural fire resistance. 90 minutes for local load bearing components and 120 minutes for elements critical to the global stability of the structure.

Table 5: Fire resistance time values chosen for rough fire design.

Structural component	Fire resistance time [minutes]
Beams	90
Slabs	90
Shear walls	120
Columns	120
Truss	120

When designing *Mjöstornet* several investigations were done regarding fire. One conclusion they made is that large timber elements will self-extinguish if a proper fire design is done (Abrahamsen, 2017).

Apart from proper fire design, preventing phenomena such as chimney effect and fire spreading along the façade, other possible measures might be of advantage in critical areas. A few examples of such measures are fire retardant paintings, plaster board covers, sprinklers, fire stops in the façade and insulating covers over joints.

2.9.2 Sound and vibration

Due to the low mass of timber floors, they are prone to transfer sound quite easily. This is one major concern when designing timber floors. However, when utilizing commercially available slab elements, the designs are made to fulfill all requirements.

2.9.3 Elevators

At least one of the elevators in a Swedish building must fit a person in a wheelchair and an assistant. For buildings with more than 10 floors an additional elevator must be added to the building. For buildings with a floor area larger than 900 m² at least two rescue elevators must exist with the size of 1.1 x 2.1 m each (Boverket, 2011). With that interior size of an elevator a shaft of approximately 1.6 x 2.5 m is needed (KONE, n.d.-a). The Turning Torso, which is an office and residential building in Sweden, is just below 200 meters tall and has 5 elevators (KONE, n.d.-b).

2.9.4 Daylight

According to *the National Board of Housing*, there are daylight requirements on areas where people stay longer than temporarily. A simple rule of thumb when designing a building is that the window area should be at least 10 % of the floor area in a room (Boverket, 2019b). Through history, an array of different simple daylight rules has been used. However, most of them consider a maximum room depth or a limiting window height to room depth ratio. Summarizing these guidelines while assuming adequate window area and standard ceiling height, full daylight can be expected within 5 m from the window and some daylight will reach as deep as 10 m, deeper rooms than that should be avoided (Ibrahim & Hayman, 2005).

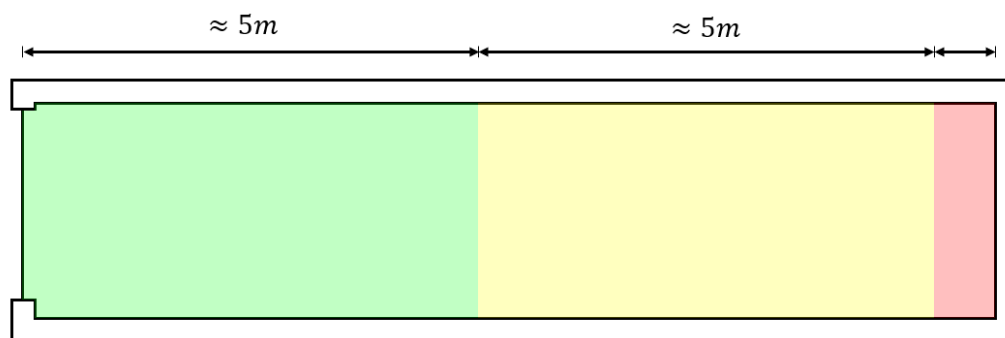


Figure 31: Illustration of maximum room depths to acquire sufficient daylight in a room with standard ceiling height and adequate window area.

Following are some illustrations of variation in daylight for various shapes following the rule of thumb described above.

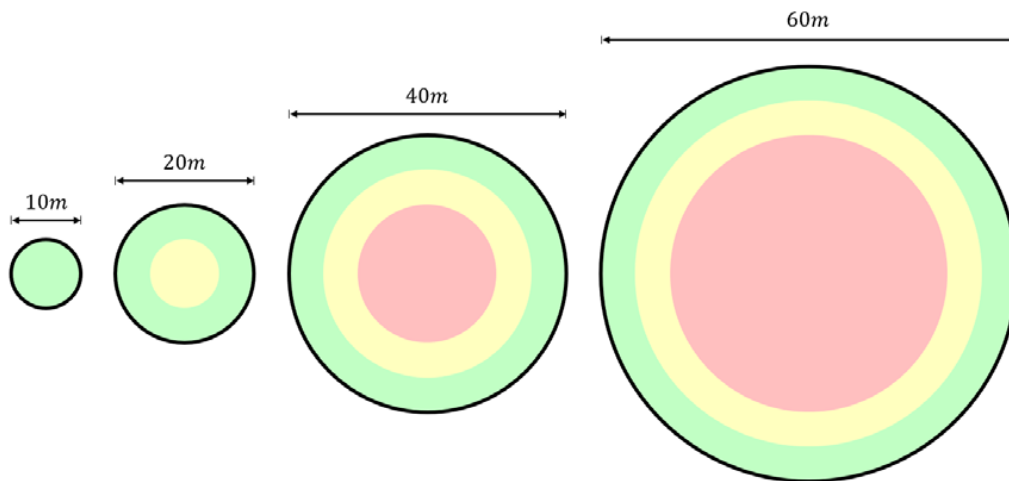


Figure 32: Illustration of good (green), acceptable (yellow) and poor (red) daylight conditions for a few circular sections.

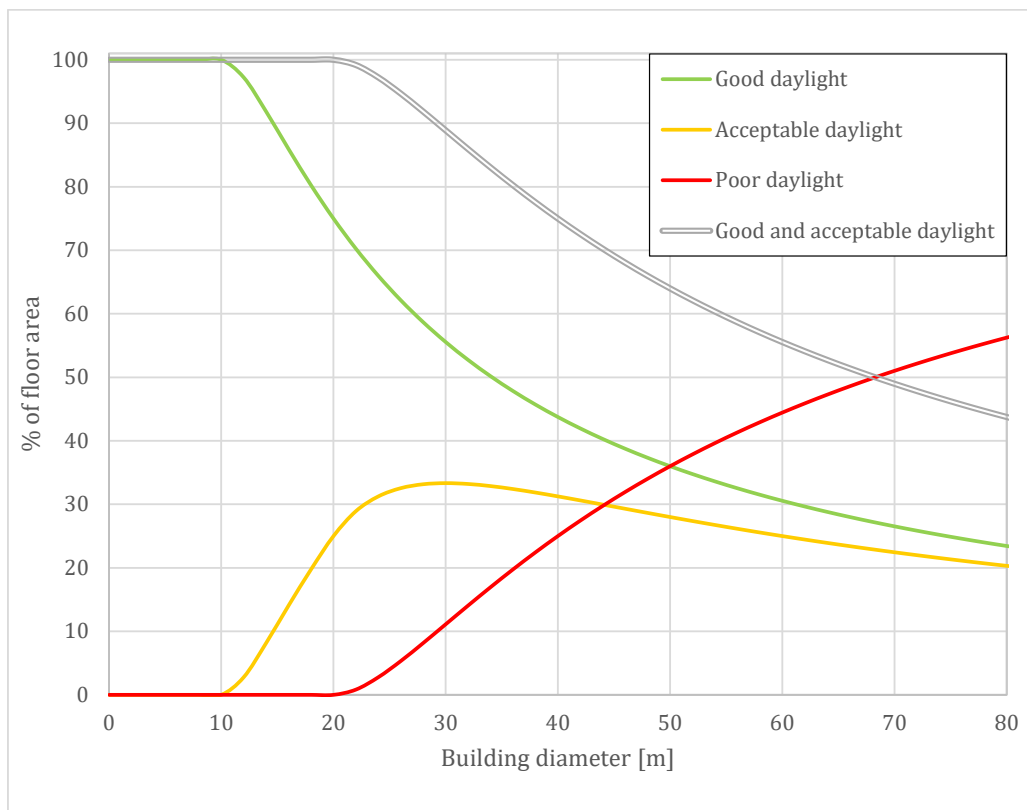


Figure 33: Floor area ratios for daylight in a circular building based on the rule of thumb, 5 m for good daylight and 10 m for acceptable daylight.

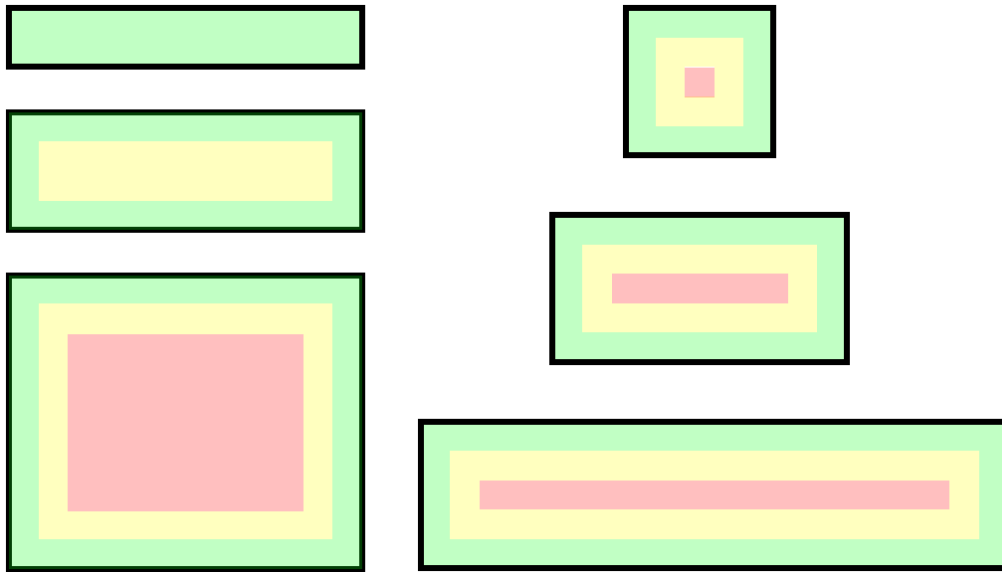


Figure 34: Illustration of good (green), acceptable (yellow) and poor (red) daylight conditions for various rectangular floor shapes.

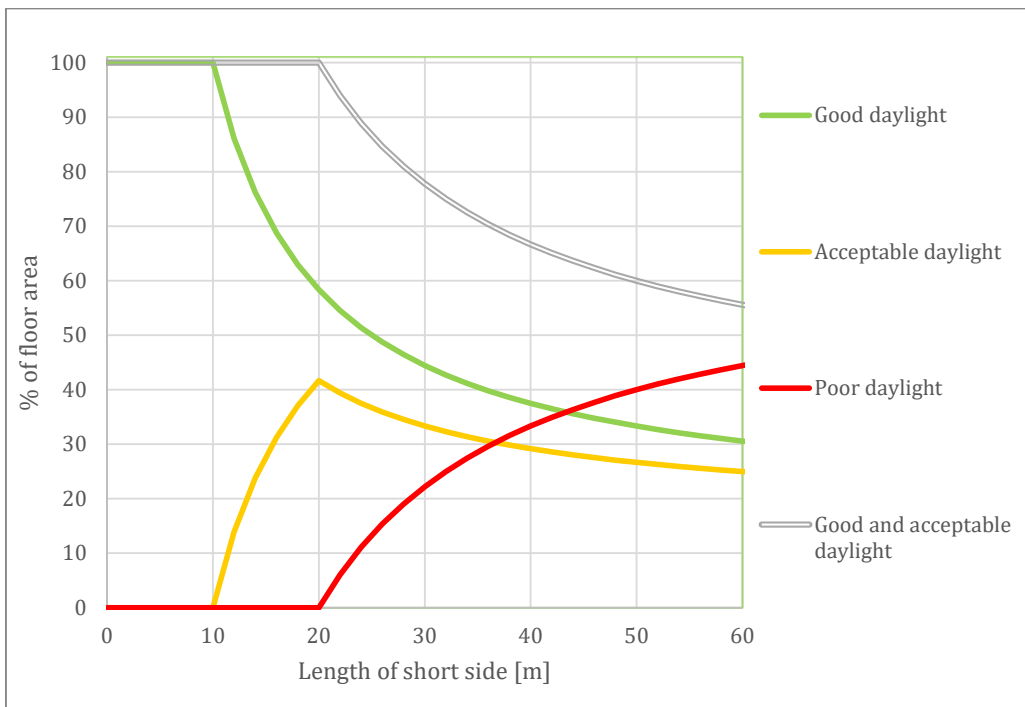


Figure 35: Floor area ratios for daylight in a rectangular building with a 60 m long side and a varying short side. Based on the rule of thumb, 5 m for good daylight and 10 m for acceptable daylight.

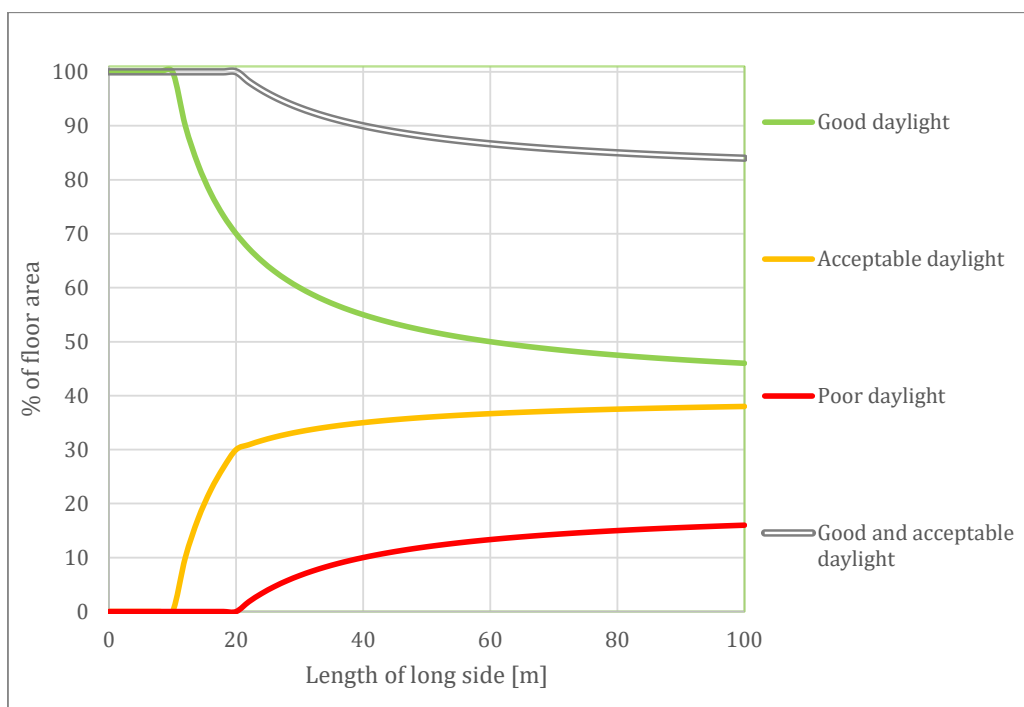


Figure 36: Floor area ratios for daylight in a rectangular building with a 25 m short side and varying long side. Based on the rule of thumb, 5 m for good daylight and 10 m for acceptable daylight.

With an opening in the center of a building, the daylight conditions can be significantly improved while still utilizing a less slender structure. By increasing the inner radius along with the outer radius, poor daylight conditions can mostly be eliminated.

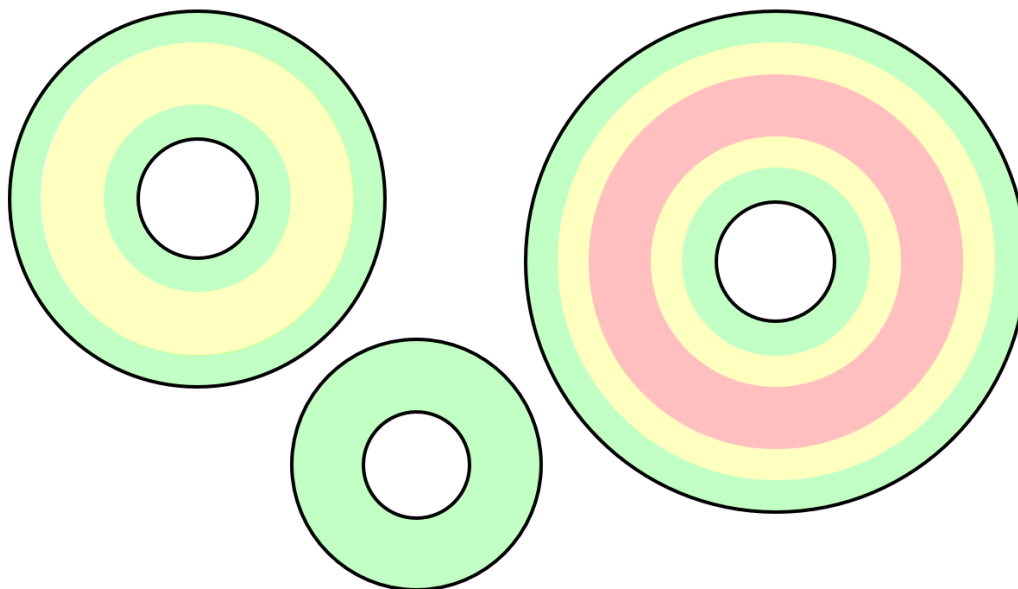


Figure 37: Illustration of good (green), acceptable (yellow) and poor (red) daylight conditions for a few circular floors with open sections in the middle.

2.9.5 Economy

Depending on the building purpose, the economical aspect will be of varying importance. For general residential buildings, offices or student apartments, low costs

are of highest priority. However, when trying to build a landmark building, larger expenses can often be motivated.

2.9.5.1 Economically justifiable building height

The economically defensible approximate top height for a few common structural systems are listed in Table 6 (Truby et al., 2014). Worth to notice is that these heights are for general tall buildings and not timber buildings in particular.

Table 6: Common structural systems and their approximate suitable upper height.

Structural system	Suitable height [m]
Frame	75
Shear wall	120
Shear wall – Frame	160
Framed tube	160
Tube in tube	190
Bundled tube or modular tube	225
Bracing	300
Outrigger-braced	350

2.9.5.2 Economy of timber joints

Joints within a timber structure is one of the most important areas from an economic standpoint. Since they require special attention in all stages of the design and production process, the joint cost can stand for a significant portion of the overall building cost. Therefore, in general timber building design, simple joints are highly appreciated. However, when trying to maximize stiffness performance, glued or resin injected joints are the only choices. This drives the cost further due factors such as increased work during assembly, additional quality controls, environmental control during gluing and delays due to curing time.

2.9.6 The construction phases

There are lots of things to consider when planning the construction of a building. For example order of construction, how the cranes are going to work, the logistics and storage of elements. In these types of buildings, floors are usually repeated and therefore it is favorable to have a standardized construction process for the floors. If the core is built up first and is stable enough, it is common to have the cranes progressing upwards together with it. Otherwise it is possible to connect the crane to the slabs and move it upwards from there. If the core is the main stabilizing elements of the building, it is usual that it is growing upwards first and then the rest of the elements are mounted and attached to it. To protect the workers on site and people around the building it is necessary to have the working space enclosed (Truby et al., 2014).

2.10 Time dependent effects on tall buildings

A high-rise building will deform both horizontally and vertically during its lifetime. This can be due to for example elastic deformation, eccentric loading, shrinkage and creep. When a column, wall or core is loaded in compression it will undergo elastic, axial deformation of which the magnitude depends on the load level and the material properties. Since the stresses usually are different for walls, columns and core the axial shortening might differ between elements on a certain storey. This difference might also vary over different stories. Asymmetry and eccentricity may also lead to diversity in vertical deformation. The biggest differences in high-rise buildings are usually around the levels at 70 % of the building height (Truby et al., 2014).

The movements and deformations can be predicted and planned for already in the design phase. There are multiple ways to design for movements. One way is to design for the target height directly at construction and therefore allowing long-term shortening. Another way would be to increase the building height slightly to counteract the expected shortening. It is important to design such that non-structural members are not loaded when deformations occur for the structural system. For advanced structures such as high-rise buildings FE-analyses are often made regarding time-dependents effects (Truby et al., 2014).

During construction, sensors are often placed to measure and monitor movements and deformations. This gives a possibility to compare real values with the predicted once whereafter modifications can be done if needed. It is common to select a few walls and columns to measure as well as the total building deformation. Sometimes the sensors are used for long term monitoring exceeding the time of the construction phase (Truby et al., 2014).

2.11 Design of high-rise buildings

Design of a high-rise structure can be divided into three different phases, concept, scheme and detailed design. The conceptual design is mainly to obtain an appropriate design of the structure with basic assumptions. The scheme design phase is to verify the design by analyzing and doing tests. The detailed design phase is a more elaborated and calculated version of the scheme design phase to confirm that the requirements are achieved. There are some extra important things to consider when designing a high-rise building, for example the dynamic wind loads as well as the comfort for the people using the building. The differences in vertical deformation between the components is also significant for high-rise buildings as well as the column restraint and capacity of the foundation (Truby et al., 2014).

2.11.1 Conceptual design

The first two things to be decided when designing a high-rise building are the height of the building and the number of levels. After that the stabilizing system is chosen to then decide the type, positions and shapes of structural elements in the building. There are lots of essentials to consider when doing the conceptual design, for example effects of openings in the structure, lateral restraint of walls and torsion stiffness of the building. The targets from the structural engineer is to make the building efficient and stable. This is done by for example changing masses and leading the forces through the right structural elements. An early analysis should be made in this face, either by software or hand calculations, this to find out the structural behavior and other important effects (Truby et al., 2014).

2.11.2 Scheme design

The first thing to do is to finalize the size and location of all significant structural elements, this is done with a more complex model. Then scheme-phase drawings and a description of the system should be produced as well as predicted amount of material to be used. Further investigations regarding the essentials are done, for example if the wind loads from the code are sufficient or if wind tunnel tests are necessary. It is up to the engineer to check if the elements are economical or if there are possibilities to make the building more efficient and also design for the movement limits between the levels. In this phase a dynamic study regarding the wind loads are done, checking if the stiffness and mass are enough. Investigations regarding a potential damper and its placements are done in this phase (Truby et al., 2014).

2.11.3 Detailed design phase

In this phase complete drawings with legitimate calculations and a list of all materials and workmanship needed are done. Plenty of checks are done in this phase, for example strength of the elements, movements and comfort for the occupants. Joints and details are chosen and designed in the building. Temporary loads and openings are considered as well as tolerances during construction (Truby et al., 2014).

2.12 Loads on tall structures

The loads acting on any structure can mainly be categorized in three groups. Permanent loads, variable loads and accidental loads. For a particular load, the characteristic value should be chosen as the most representative value. A combination of these loads must be used in design to make sure sufficient behaviour is obtained (SIS, 2004).

The building must sustain the worst load combination of vertical and horizontal loads. Especially for tall structures, the vertical loads will be large. However, the horizontal loads will be more vulnerable to these types of buildings. In early design, it is of importance to have some sense on the magnitudes of the anticipated design (Truby et al., 2014).

2.12.1 Design situations

The structure must be able to withstand a wide range of load situations (SIS, 2004), examples of these are:

- Sustained loading due to normal use.
- Temporary loading caused during construction or reparation.
- Exceptional design situations such as fire, explosion, collision or local failure of elements.
- Seismic design situations.

These scenarios should also be combined in such way that all reasonably occurring situations are managed in design. However, loads that cannot physically occur at the same time should not be used in the same load combination (SIS, 2004).

2.12.2 Load combinations

When designing a structure, for each critical case of loading, a load combination should be determined. If present, this load combination must have one main variable load or one accidental load (SIS, 2004).

General expression for load combinations:

$$E_d = E \{ \gamma_{G,j} G_{k,j} ; \gamma_P P ; \gamma_{Q,1} Q_{k,1} ; \gamma_{Q,i} \psi_{0,i} Q_{k,i} \}, \quad j \geq 1 ; i > 1 \quad (7)$$

Can also be viewed as:

$$E_d = \sum_{j \geq 1} \gamma_{G,j} G_{k,j} + \gamma_P P + \gamma_{Q,1} Q_{k,1} + \sum_{i > 1} \gamma_{Q,i} \psi_{0,i} Q_{k,i} \quad (8)$$

E_d	<i>Design load effect</i>
$\gamma_{G,j}$	<i>Partial coefficient for distributed self-weight j.</i>
$G_{k,j}$	<i>Characteristic load value for distributed self-weight j.</i>
γ_P	<i>Partial coefficient for prestressing actions.</i>
P	<i>Relevant representative load value due to prestressing.</i>
$\gamma_{Q,1}$	<i>Partial coefficient for the main variable load.</i>
$Q_{k,1}$	<i>Characteristic load value for the main variable load.</i>

$\gamma_{Q,i}$	<i>Partial coefficient for secondary variable load i.</i>
$\psi_{0,i}$	<i>Combination value for secondary variable load i.</i>
$Q_{k,i}$	<i>Characteristic load value for secondary variable load i.</i>
" + "	<i>"To combine with".</i>
Σ	<i>"The combined effect of".</i>

The load combination factors must be adjusted depending on the intended use for the load combination. Therefore, three common load combinations for SLS are specified directly in Eurocode (SIS, 2004).

- I. *Characteristic load combination. Mainly used for irreversible limit state calculations.*

$$E_d = \sum_{j \geq 1} G_{k,j} \text{ "+" } P_k \text{ "+" } Q_{k,1} \text{ "+" } \sum_{i > 1} \psi_{0,i} Q_{k,i}, \quad j \geq 1; i > 1 \quad (9)$$

E_d	<i>Design load effect</i>
$G_{k,j}$	<i>Characteristic load value for distributed self-weight j.</i>
P_k	<i>Characteristic load value due to prestressing.</i>
$Q_{k,1}$	<i>Characteristic load value for the main variable load.</i>
$\psi_{0,i}$	<i>Combination value for secondary variable load i.</i>
$Q_{k,i}$	<i>Characteristic load value for secondary variable load i.</i>

- II. *Frequent load combination. Mainly used for reversible limit state calculations.*

$$E_d = \sum_{j \geq 1} G_{k,j} \text{ "+" } P \text{ "+" } \psi_{1,i} Q_{k,1} \text{ "+" } \sum_{i > 1} \psi_{2,i} Q_{k,i}, \quad j \geq 1; i > 1 \quad (10)$$

E_d	<i>Design load effect</i>
$G_{k,j}$	<i>Characteristic load value for distributed self-weight j.</i>
P	<i>Relevant representative load value due to prestressing.</i>
$\psi_{1,i}$	<i>Combination value for frequent value of a variable load i.</i>
$Q_{k,1}$	<i>Characteristic load value for the main variable load.</i>
$\psi_{2,i}$	<i>Combination value for a quasi-permanent value of a secondary variable load i.</i>
$Q_{k,i}$	<i>Characteristic load value for secondary variable load i.</i>

- III. *Quasi-permanent load combination. Mainly used for calculations regarding long term effects and the appearance of the structure.*

$$E_d = \sum_{j \geq 1} G_{k,j} \text{ "+" } P \text{ "+" } \sum_{i \geq 1} \psi_{2,i} Q_{k,i}, \quad j \geq 1; i \geq 1 \quad (11)$$

E_d	<i>Design load effect</i>
$G_{k,j}$	<i>Characteristic load value for distributed self-weight j.</i>
P	<i>Relevant representative load value due to prestressing.</i>
$\psi_{2,i}$	<i>Combination value for a quasi-permanent value of a variable load i.</i>
$Q_{k,i}$	<i>Characteristic load value for variable load i.</i>

For an accidental load case based on fire, the following load combination must be used (SIS, 2004):

$$E_d = \sum_{j \geq 1} G_{k,j} + P + \psi_{1,1} Q_{k,1} + \sum_{i > 1} \psi_{2,i} Q_{k,i}, \quad j \geq 1; i > 1 \quad (12)$$

E_d	<i>Design load effect</i>
$G_{k,j}$	<i>Characteristic load value for distributed self-weight j.</i>
P	<i>Relevant representative load value due to prestressing.</i>
$\psi_{1,1}$	<i>Combination value for the frequent main variable load.</i>
$Q_{k,1}$	<i>Characteristic load value for the main variable load.</i>
$\psi_{2,i}$	<i>Combination value for a quasi-permanent value of a secondary variable load i.</i>
$Q_{k,i}$	<i>Characteristic load value for secondary variable load.</i>

2.12.3 Self-weight

All components contributing to the self-weight should be summarized and regarded as one single gravitational load when applied in the load combination. To obtain the self-weight of each component, the mass should be determined from nominal element sizes and the corresponding characteristic value for the material density. For a simple case, load bearing components, non-load bearing components and permanent installations are the ones included when determining the self-weight (SIS, 2005).

For cases where the density is not specified in Eurocode or in manufacturers tables, it is calculated as the product between the mean density and the gravitational constant $g \approx 10 \text{ m/s}^2$ (SIS, 2005).

2.12.4 Imposed load

When the building is in use, imposed loads are created. In short, these loads are due to people, movable objects, vehicles and rare situations in utilization leading to load concentration. When applying the imposed load in the calculation model, it is usually done as distributed loads, line loads, point loads or any combination of the mentioned load patterns (SIS, 2005).

The imposed load applied to a specific construction element should be chosen in a realistic but unfavourable way. This means that an element loaded from only one storey should be designed with regard to the worst load placement possible while elements loaded from multiple floors should be designed assuming even load distribution on the floors above. When designing elements loaded from multiple floors, the accumulated load should be used. However, due to low probability of maximum loading on all the

contributing area, the imposed load can sometimes be reduced. For slabs, beams or roofs, the reduction factor α_A can be applied, it depends on the contributing area resulting in loads on the element. For columns or load bearing walls, a load reduction (α_n) can be done depending on the number of floors contributing to the load (SIS, 2005).

Depending on the building use, different load levels can be expected. Table 7 shows guideline levels for imposed loads stated in Eurocode SS-EN 1991-1-1.

Table 7: Imposed loads for a few different building uses (SIS, 2005).

Characteristic values for imposed load	Distributed load [kN/m ²]	Point load [kN]
Residential buildings: Slabs	1.5-2.0	2.0-3.0
Office	2.0-3.0	1.5-4.5
Conference rooms	3.0-4.0	2.5-7.0
Stores	4.0-5.0	3.5-7.0

The reduction factors for imposed loads are determined as follows:

$$\alpha_A = \frac{5}{7}\psi_0 + \frac{A_0}{A} \leq 1.0 \quad (13)$$

$\alpha_A \geq 0.6$ *For conference rooms and store areas.*
 ψ_0 *Factor for combination value for imposed load.*
 $A_0 = 10\text{m}^2$ *Reference area.*
 A *Loaded area.*

$$\alpha_n = \frac{2 + (n - 2)\psi_0}{n} \quad (14)$$

$n > 2$ *Number of floors with the same load category.*
 ψ_0 *Factor for combination value for imposed load.*

2.12.5 Wind loads

Wind acts on a building surface through either pressure or suction depending on factors such as the surface geometry, wind direction, turbulence and more. Due to air leakage in the façade, these effects can be seen both externally on the façade and on the interior side of façade elements. Generally, wind actions are accounted for as pressure or suction perpendicular to the loaded surface. However, in cases with along wind sweeping past large surfaces, tangential friction forces might need consideration (SIS, 2005).

The considered wind load on a structure depends on the wind, building size, shape and dynamic properties.

Table 8: Reference wind speed for a few Swedish cities, chosen according to national annex NA in SS-EN 1991-1-4 (SIS, 2005).

Reference wind speed, v_b	[m/s]
Gothenburg	25
Malmö	26
Stockholm	24

The calculation procedure when determining wind loads are described in Appendix II.

2.12.5.1 Conceptual design regarding wind

Wind might be one of the more complex loads acting on a tall structure. Apart from the geographically unique loading situation, the façade shape will have a significant impact on the load levels. Therefore, wind load must be considered in multiple stages of design in order to create a high performing building.

2.12.5.2 Wind load levels and response scenarios

The wind impact on a building stems from an array of complex factors resulting in a unique situation for every single building. In general, though, the wind behavior close to the earth's surface shows a turbulent irregular flow pattern. However, a greater distance from the surface generally results in a more uniform air flow and wind direction. On the other hand, due to the wind interaction with the earth's surface, the wind speeds are generally lower close to the surface and higher further up in the atmosphere. Practically, this means that the surroundings as well as the actual wind situation together creates a specific wind situation and the wind load for a structure (Gunawardena et al., 2017).

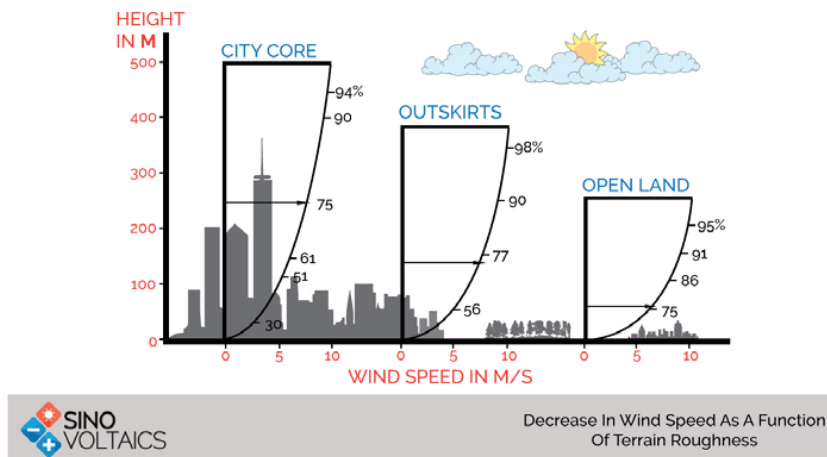


Figure 38: Example of how the wind speed can vary with height depending on obstacles in the area (Sinovoltaics.com, 2019).

Apart from the wind on the location, the external geometry of the structure influences how large portion of the wind that will be caught and therefore generate wind loads. Also, the wind will induce dynamic response in multiple ways. The intuitive mode of motion, along-wind, is one of the critical modes. However, due to the complex behavior of wind, crosswind motion is also present as well as torsional motions. The torsional modes are usually coupled with higher natural frequencies than what is relevant for wind loads. But the phenomenon might need to be considered for some structures,

especially wall dominant constructions with a large eccentricity between the stiffness center and the aerodynamic center (Gunawardena et al., 2017). Illustrations of the various wind deformation modes can be seen in Figure 39.

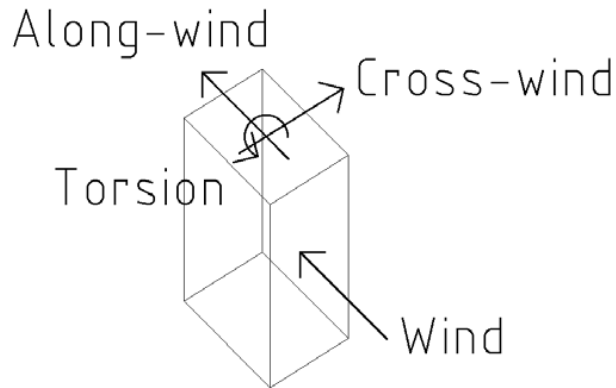


Figure 39: Possible wind deformation modes for a structure.

Overall, there are two main areas in which the wind effects can be managed. Through the structural and the architectural design perspectives, and to obtain the tallest possible buildings, both these areas needs special attention.

2.12.5.3 Building design regarding wind loads

The governing loads for high-rise buildings are typically wind loads and in some cases seismic loads. High-rise buildings usually move horizontally, specially at the top, due to wind loads. There are different limits regarding the movement, for example the horizontal movement from storey to storey can vary between $\frac{h_{storey}}{500}$ to $\frac{h_{storey}}{200}$ while the total maximum movement usually is $\frac{h_{building}}{500}$. When designing this type of buildings, it is important to consider dynamic loads and the natural frequency of the building to not obtain resonance (Truby et al., 2014).

2.12.5.4 Aerodynamics and façade geometry

In general, rectangular or square building shapes catches more wind than round ones. Buildings with a cupped shape might have a streamlined and therefore beneficial behavior for winds in one direction but catches wind extensively when the wind blows in the opposite direction. This means that it is necessary to consider the main wind directions when orienting a building. Doing so will influence the actual wind load acting on the building (Vikas Kumar Nirmal, 2017). Examples of the wind reaction to various shapes can be seen in Figure 40.

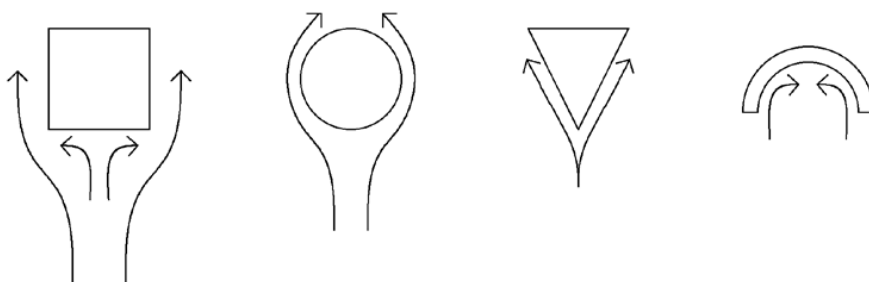


Figure 40: Example of wind reaction to various shapes.

Furthermore, tall buildings subject to whirling winds might result in development of vortices around the building. For the world's current tallest building, *Burj Khalifa*, this phenomenon has been prevented by its wide base and its irregular narrowing of the plans which disturbs buildup of vortices (Vikas Kumar Nirmal, 2017).

From an architectural standpoint, the global and local wind actions are often considered through macro- and micro-aerodynamic modifications. In practice, the macro perspective refers to geometrical measures used to improve the aerodynamics for the whole building (Alaghmandan et al., 2016). Typical examples of this is global tapering, stepping or twisting of the building or to include openings in the structure. The micro perspective on the other hand refers to general rounding or chamfering of the façade corners, utilization of recessions, fins, etc. in the structure (Sharma et al., 2018).

Even though aerodynamics is an important part in development of a building, it cannot be used as the only considered measure in design. It must be weighed against other design aspects and a suitable compromise has to be found.

2.12.5.5 Corner modifications

In the design of *Taipei 101 tower*, the relation between global cross-sectional shape and design wind loads was investigated through wind tunnel testing. The initial design suggested a square cross-section for the tower, but through the wind tunnel testing, a more efficient corner design could be developed. The final choice was a double recession corner which resulted in 25 % reduced wind loads for the building. A rule of thumb when rounding or chamfering the corners is that the modification should be performed to at least 10 % of the building width. Otherwise, the improvement might not be of satisfying magnitude (Xie, 2014). Examples of different corner modifications are shown in Figure 41.

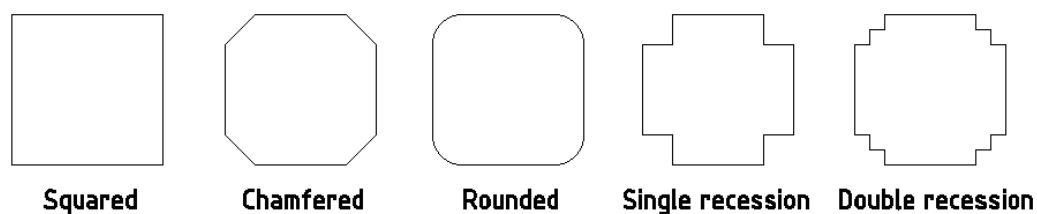


Figure 41: Examples corner modification that can be used in management.

2.12.5.6 Twisting

Twisting can also have a significant impact on the wind forces acting on a building. Generally, the force acting on a building gets reduced with increased twisting angle. For the first 180 degrees, there is an approximately linear relationship between force and twisting. After that the relation changes and it seems to converge towards a maximum reduction value. One could argue for wind-motivated twisting up to 360 degrees but more than that would be for architectural purposes. A twist in the building will though reduce the effectiveness of directional optimization (Xie, 2014). An example of a twisted building can be seen in Figure 42.

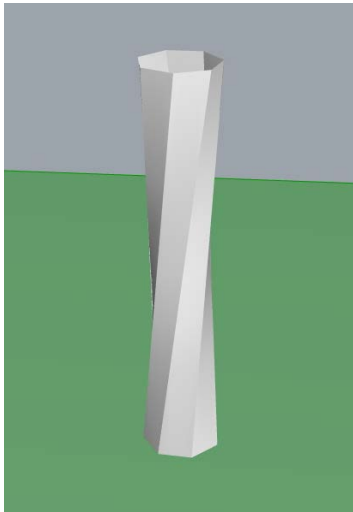


Figure 42: Example of twisting applied to a tower with heptagon shape.

2.12.5.7 Tapering

A taper in a building will create a large reduction of the peak response. A clearly beneficial change in many design cases. Important to note though, is that the peak response is not eliminated. Instead, the tapering seems to spread out the peak of the frequency-response curve to a larger region, especially above the frequency of the peak for a corresponding uniform structure. This means that the effect of tapering must be considered together with the natural frequency of the structure as the resonance response due to wind might be shifted to a higher frequency. In general, the effect due to tapering can be summarized as follows: Including tapering will drastically decrease the buildings peak response due to wind. However, it will slightly increase the building response for frequencies above the peak value. Therefore, tapering can be considered as beneficial in the ultimate limit state but slightly negative in service limit state when it comes to the buildings wind induced response (Xie, 2014). An example of tapering applied to a tower with heptagon shape can be seen in Figure 43.

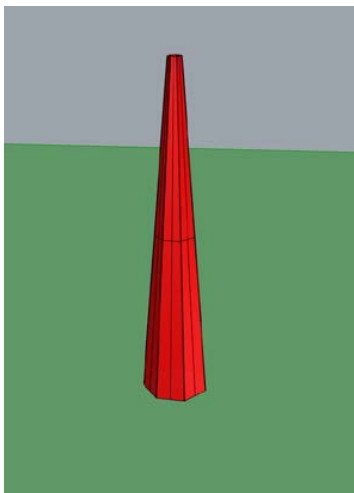


Figure 43: Example of tapering applied to a tower with heptagon shape.

2.12.5.8 Along-wind and cross-wind design

As shown in Figure 39, a single wind direction might introduce various motions in a building. All of which must be considered in design of high-rise structures. When designing with regard to cross-wind response the most effective measures are smoothening of the building corner, tapering and twisting of the building. For along-wind response, smoothening of the corners is still of large benefit. Also, utilization of openings in the structure and building orientation optimization are worth considerations during design (Xie, 2014).

2.12.5.9 Wind tunnel test to obtain case specific values for the wind load

General guidelines for design do not apply well to unconventional building geometries when it comes to wind loads. In order to obtain more realistic values and possibly increase the potential for building of tall structures, an analysis of the actual situation must be performed. This can be done mainly in two ways, by performing a traditional wind tunnel test or through virtual wind tunnel analysis based on computational fluid dynamics (Gunawardena et al., 2017).

Even though some studies have shown a high correlation between actual wind tunnel tests and its virtual equivalent, the old way might still be more reliable.

To know if wind tunnel test is necessary for a building one could examine a few geometrical and structural aspects. For example, if the slenderness ratio h/d is greater than 5 a wind tunnel test could be necessary. Also, it is possible to look at the structural frequencies. If the first eigenfrequency is smaller than $46/h$ or if the first vibration modes looks very three-dimensional it might be beneficial to do a wind tunnel test. One could also watch the surroundings, in case there are more high-rise buildings around, which protects the building from some of the wind, this might be another reason to conduct a wind tunnel study (Truby et al., 2014).

When creating the model for a wind tunnel test it is common to have a scale between 1:200 and 1:500. The area around the building within 500 meters is usually built up, as well as influencing buildings outside the area, to get accurate results of the wind behavior. It is also of interest to do a scenario including future planned buildings in the area (Truby et al., 2014).

2.12.6 Snow load

The snow load acting on a structure depends on the characteristic snow load value for the geographical location, exposure to wind, thermal conditions and surrounding structures (SIS, 2003).

2.12.6.1 Calculation procedure to determine snow load on a structure or structural component, SS-EN 1991-1-3:2004.

$$s = \mu_i C_e C_t s_k \quad (15)$$

s *Snow load on a roof.*
 μ_i $= 0.8$, *shape factor for snow load on a flat roof.*

- C_e = 0.8, exposure factor for an area with high degree of wind exposure.
 C_t = 1.0, thermal coefficient assuming no reduction of snow load due to heat transfer through the surface.
 s_k Characteristic snow load value on the ground for the geographical location.

Table 9: Characteristic snow load values for a few Swedish cities, obtained from table NB:1, SS-EN 1991-1-3 (SIS, 2003) and snow loads for a flat roof with high degree of wind exposure.

Snow load values	Characteristic snow load, s_k [kN/m ²]	Snow load on a roof, s [kN/m ²]
Gothenburg	1.5	<u>0.96</u>
Malmö	1	0.64
Stockholm	2	1.28

2.12.7 Seismic loads

For Swedish conditions, seismic loads are of such minor magnitudes that they have been regarded as irrelevant for the national design regulations. Therefore, there are no seismic zones defined and seismic loads can be neglected in design (SIS, 2016).

2.12.8 Accidental loads

A high-rise building should be designed to avoid collapse in case of accidental loads such as explosions or impact loads. Since the consequence of failure in a high-rise building usually is high, a risk analysis should be considered and evaluated carefully. There are different levels of design against accidental loads. Examples could be design with regard to attacks on the building as well as design for cases when an element is removed, for example due to an explosion load or ongoing refurbishment work. Ductility and robustness in the structure is important in this sense, both regarding the economical and safety aspects (Truby et al., 2014).

2.12.9 Temporary loads during construction

Loads during construction can be higher than the maximum loads during the lifetime of a building, particularly in the beginning of the constructing phase. One of the extra loads during construction work of high-rise buildings are the tower cranes and it is important with experience from old buildings when designing for this, to decide whether the cranes should be attached to the core or slab for example. Also, other equipment and temporary structures may create extra loads (Truby et al., 2014).

2.13 Shape coefficients for non-rectangular buildings

As indicated in section 2.12.5.1, it is of advantage to strive for circular buildings when trying to reduce the wind loads acting on the structure. This reduces the wind load and increases the possibility to maintain slenderness of the building which is necessary to avoid unwanted depth in the floor plan and poor light conditions. Sufficient light conditions can though be obtained in other ways. When designing *Burj Khalifa*, they managed the combination of wind load, stiffness and daylight in another way. By utilizing the Y-shaped floor, the stiffness could be drastically increased while still providing the wanted indoor light conditions. This compensates for the increased wind loads appearing when the wind direction coincides with any of the concave sides of the building.

In order to maximize building height, the base geometries of interest are therefore limited to circular buildings and one Y-shaped building. Façade geometries with both vertical and hyperboloid surfaces are considered.

2.13.1 Shape coefficients for circular buildings

Eurocode specifies shape coefficients for both circular cylinders and cross-sections with regular polygon shapes. Due to practical reasons, it might in some cases be of advantage to design a building as a polygon rather than a pure cylindrical shape. Also, as the number of corners in the polygon increases, the overall shape approaches a pure circle.

A description for determination of shape coefficient for a regular polygon can be found in Appendix II.

2.13.1.1 Shape factor for force on a circular cylinder

SS-EN 1991-1-4 states the shape factor used to determine force on a long circular cylinder like building with ratios $\frac{h}{d} > 5$.

$$c_f = c_{f,0} \psi_\lambda \quad (16)$$

c_f	<i>Shape factor for force on a circular cylinder-shaped building.</i>
$c_{f,0}$	<i>Shape factor for force on structure disregarding end effects.</i>
ψ_λ	<i>Reduction factor for force coefficient regarding end effects. Determined according to Figure 91.</i>

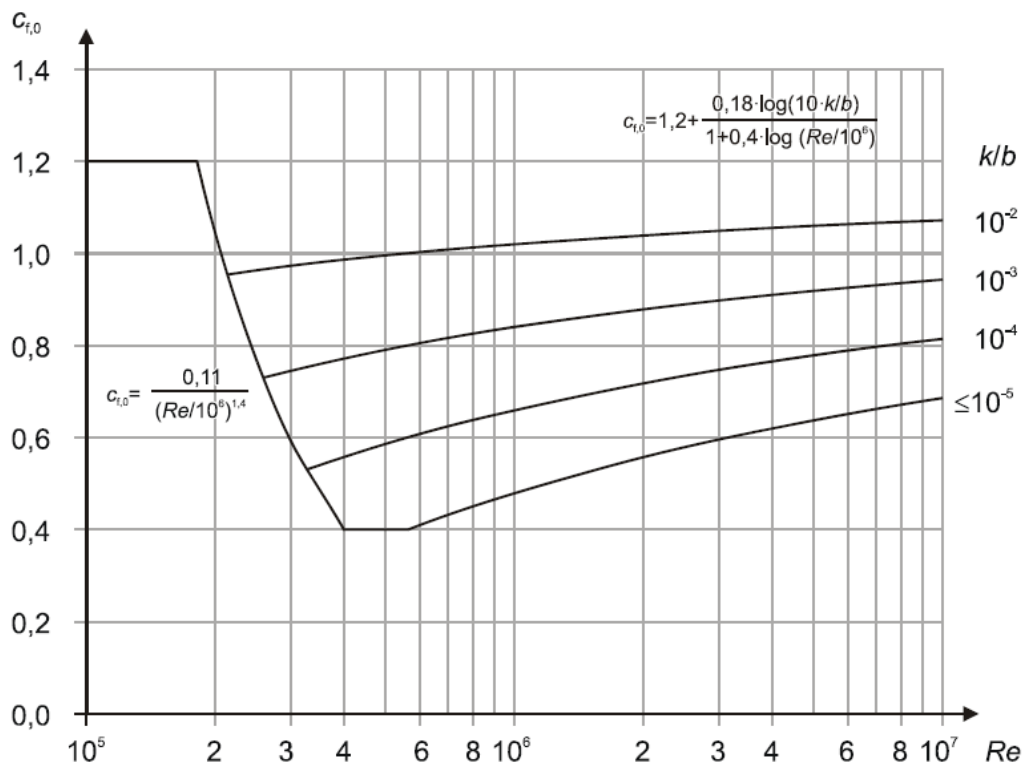


Figure 44: Shape factor for force on a circular cylindrical structure disregarding end effects. Figure 7.28 in SS-EN 1991-1-4 (SIS, 2005).

- $c_{f,0}$ Shape factor for force on structure disregarding end effects.
 Re Reynolds number. See equation (25) in Appendix II.
 k Relative surface roughness.
 b Width of the structure.

Table 10: Equivalent surface roughness, k for a few common materials. Obtained from table 7.13 in SS-EN 1991-1-4 (SIS, 2005).

Surface material	Equivalent surface roughness, k [mm]
Glass	0.0015
Thin layer of paint	0.0060
Even concrete	0.2000
Planed timber	0.5000
Uneven concrete	1.0000
Sawn timber	2.0000
Masonry	3.0000

2.13.1.2 Shape factor for pressure on a circular cylinder

The shape factor for wind pressure on a circular cylinder can according to SS-EN 1991-1-4 be determined as:

$$c_{pe} = c_{p,0} \psi_{\lambda\alpha} \quad (17)$$

c_{pe}	Shape factor for external wind load on a circular cylinder.
$c_{p,0}$	Shape factor for external wind load on a circular cylinder disregarding end effects.
$\psi_{\lambda\alpha}$	Reduction factor for shape coefficient regarding end effects for circular cylinders.

When determining $c_{p,0}$, the wind angle of incidence (α) must be accounted for as well as Reynold's number. This results in a continuously varying pressure coefficient around the structure (SIS, 2005).

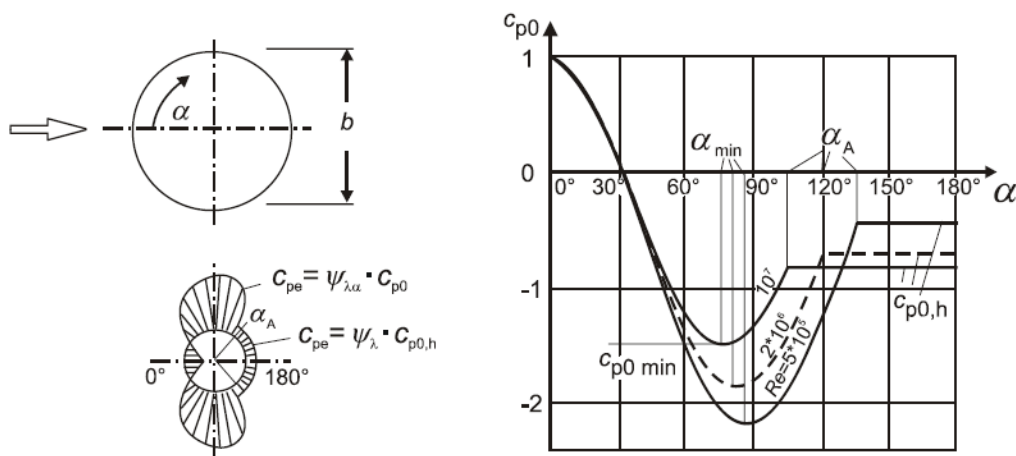


Figure 45: Shape factor for external wind load on a circular cylinder disregarding wind effects. Figure 7.27 in SS-EN 1991-1-4 (SIS, 2005).

Re	Reynolds number. See equation (25) in Appendix II.
α	Angle between façade section and wind direction, $\alpha \leq 180^\circ$.
α_{min}	Angle between façade section and wind direction that corresponds with the lowest $c_{p,0}$.
α_A	Angle between façade section and wind direction whereafter $c_{p,0}$ is constant.

For structures with a high Reynold's number, the relation between the shape factor $c_{p,0}$ and the wind angle of incidence α approaches a bilinear curve. This curve drops linearly from 1 to -1 in the range $0 < \alpha < 60^\circ$ whereafter it has a constant value around -1 . For this special case $\alpha_{min} = \alpha_A = 60^\circ$.

$$\psi_{\lambda\alpha} = 1 \quad 0 \leq \alpha \leq \alpha_{min} \quad (18)$$

$$\psi_{\lambda\alpha} = \psi_\lambda + (1 - \psi_\lambda) \cos\left(\frac{\pi}{2} \left(\frac{\alpha - \alpha_{min}}{\alpha_A - \alpha_{min}}\right)\right) \quad \alpha_{min} < \alpha < \alpha_A \quad (19)$$

$$\psi_{\lambda\alpha} = \psi_\lambda \quad \alpha_A \leq \alpha \leq 180^\circ \quad (20)$$

$\psi_{\lambda\alpha}$	<i>Reduction factor for shape coefficient regarding end effects for circular cylinders.</i>
ψ_{λ}	<i>Reduction factor for shape coefficient regarding end effects. Determined according to Figure 91.</i>
α	<i>Angle between façade section and wind direction, $\alpha \leq 180^\circ$.</i>
α_{min}	<i>Angle between façade section and wind direction that corresponds with the lowest $c_{p,0}$.</i>
α_A	<i>Angle between façade section and wind direction whereafter $c_{p,0}$ is constant.</i>

2.13.2 Shape coefficients for hyperboloid shaped buildings

When it comes to hyperboloid shaped buildings, the literature is limited. Eurocode specifies how to calculate the wind loads for a circular cylinder, but not for buildings with a curvature along the vertical direction.

One approach to utilize known calculation methods for this unconventional shape would be to discretize the hyperboloid into multiple small cylinders. Since both geometries has a circular plan shape, their wind response can be anticipated to coincide to some extent. However, a curvature in the vertical direction will result in vertical force components as a result of the wind. This aspect will be neglected if using a calculation model completely based on discretized cylinders. However, one could argue that a curvature in the vertical direction would increase the aerodynamic performance which means that discretized circular cylinders as a representation for the wind load might be a conservative and therefore acceptable choice.

An even more realistic approach, although conservative might be to determine the wind load magnitudes according to the discretized cylinder model but apply the force vectors perpendicular to the façade. This would probably capture both load magnitudes, load directions and global response in a better way.

To get as representative wind load values as possible, a wind tunnel study would be preferable.

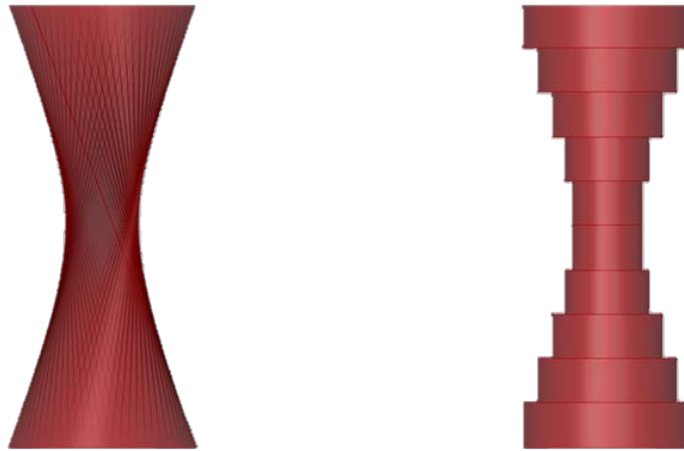


Figure 46: Principal example of a discretization of a hyperboloid shaped building into circular cylinders.

2.13.3 Shape coefficients for Y-shaped buildings

Since the buttressed core system is an interesting concept for high-rise buildings made of timber, wind loads for such structure have been investigated. However, due the complexity for parametric modelling such structure, it had to be disregarded from the final proposals. The findings regarding shape coefficients on Y-shaped structures are summarized in Appendix III.

3 Structural design

Design of a building and its components should be made with regard to both *ultimate limit state* (ULS) and *service limit state* (SLS) as long as one of the cases cannot alone show the performance needed to fulfill the requirements of the other case. The design in any reasonable case must be verified for the particular loads, material properties, product properties and geometrical measures (SIS, 2004).

3.1 Building and component design - ULS

Ultimate limit state performance is a relatively straight forward application of the rules in Eurocode and EKS11. Full design procedure regarding ULS can be seen in Appendix IV.

3.1.1 Ways to enhance the ULS performance

Considering the ULS design verifications described above, the performance can be described by load magnitudes, load distribution through the structure, material capacities, geometrical element properties, support conditions and local stability. Therefore, the following measures can be taken to increase capacity or optimize structural behaviour:

- Reduce loads on the structure.
- Improve the geometry to allow for more even load distribution through the structure.
- Choose stronger materials or materials better suited for each element.
- Optimize sectional geometries.
- Choose support and element combinations that allows optimal utilization of the element properties.
- Stabilize elements from buckling if advantageous in order to increase utilization ratios.

3.2 Design of building components – SLS

The deformation of any loaded structural part must be managed in order to avoid damages on different material surfaces and to fulfill functional requirements as well as aesthetical requirements. Both instantaneous deflections u_{inst} and long-term deflections u_{fin} must be managed. u_{inst} should be calculated based on the characteristic load combination and mean values for the material stiffnesses while u_{fin} should be determined using the quasi-permanent load combination (SIS, 2009). Full design procedure for elements in SLS can be read about in Appendix V.

3.2.1 Ways to enhance the SLS performance

Concluding the element design regarding local SLS performance a few main areas can be determined. In order to improve the performance in these aspects the following measures can be taken:

- Reduce the element loads.
- Improve geometrical stiffness.
- Use stiffer materials.
- Use materials less prone to creep deformations.
- Provide stable conditions and constant moisture content in the elements.

3.3 Global design – SLS

SS-EN 1990 specifies deformations that need consideration in SLS design. In short, these are summarized as vertical deflections of structural components, horizontal deformations of a single floor and horizontal deformation for the entire building. The vertical deflections for slabs and beams must fulfill the stated requirements to ensure comfortable use of the building. The global deformations are also crucial in design. However, they are more directed towards durability and long-term effects on the building such as differentiation in shortening between various structural components (SIS, 2004).

In global SLS design, horizontal deformations are critical. However, the literature shows little information about limiting values. Commonly, the demands are specified by the client and therefore chosen according to the particular building or material specific limits in for elastic deformations. A recurring value when searching the area is though $\frac{L}{500}$ as a guiding limit for the maximum horizontal deformation of a building (Svenskt Trä, 2017a).

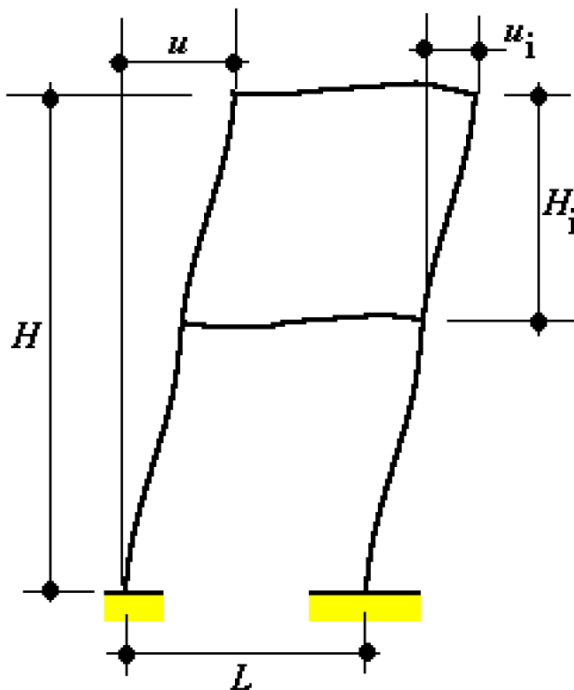


Figure 47: Schematic illustration of floor displacement u_i and maximum displacement of a structure u . Figure A1.2 in SS-EN 1990.

For a 200 m tall building, this means a maximum horizontal deformation of 400 mm:

$$\frac{200m}{500} = 400mm$$

Applying the same criterion to a single storey of a 200 m tall building with 60 storeys, gives a deformation limit of 6.67 mm:

$$\frac{3.33m}{500} \approx 6.67mm$$

In *KL-trähandboken* they state that the total horizontal deformation of a CLT shear wall can be expressed as the sum of bending, shear and joint deformations.

$$\delta_{tot} = \delta_{shear} + \delta_{bending} + \delta_{joint} \quad (21)$$

It is also mentioned that CLT elements has a high stiffness and a significant portion of the deformations are concentrated to the joints.

3.3.1 Ways to improve the global SLS performance

In order to improve the global resistance against horizontal deflections, all of the terms in equation (21) must be considered. Therefore, to optimize the structure, shear and bending stiffnesses must be improved. This can be done either through utilization of higher-grade material or optimization of the geometry. The same applies to the joints where tighter connections with little or no slip will provide the structure with highest maximum possibility to attain low deformations. Note that if the joint stiffness is low, stiffer material will not have any significant effect on the global behaviour. Therefore, the joints must be prioritized when trying to improve overall stiffness.

Apart from the various stiffnesses, the wind load stands for the remaining aspect when it comes to horizontal deflections. By improving the aerodynamics of the building, the wind loads can be reduced and thus the deformations as well.

3.4 Global design for dynamic behaviour

Especially for high-rise buildings, the dynamic behaviour is of high importance. Therefore, the structure must be verified to fulfill requirements for human comfort for wind-induced vibrations.

3.4.1 Design according to Eurocode and ISO-standards

The dynamic actions on a structure should be calculated according to ISO 4354 or *EKS11* and *SS-EN 1991-1-4* while *SS-ISO 10137* states the guidelines for human response regarding wind-induced motions. The older standard *ISO 6897* has slightly different limits which might be an interesting comparison when verifying the dynamic behavior. The guidelines from *ISO 10137* can be read about in the following section while *ISO 6897* can be read about in Appendix VI.

3.4.2 Evaluation of wind-induced vibrations – ISO 10137

To make sure the service limit state conditions for wind induced vibrations are fulfilled, general guidelines for eigenfrequencies and peak accelerations of a structure are determined (SIS, 2008).

The basic concept is that motions and accelerations with a one-year return period should be used when evaluating a structure. However, if required due to local conditions, multiplication factors could be used to further tighten the guidelines (SIS, 2008).

The evaluation curves are made through measurements of existing buildings as well as probabilistic evaluations regarding human discomfort. This also means that the requirement for residential areas are harder to fulfill than for a similar office area (SIS, 2008).

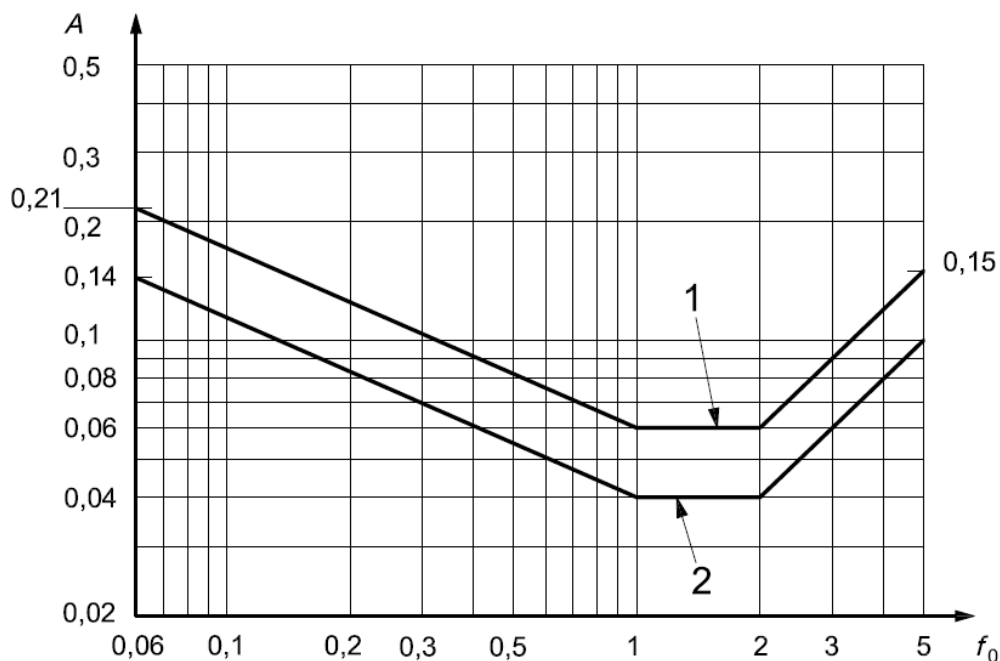


Figure 48: Evaluation curves for 1-Office and 2-Residential areas according to figure D.1 (SIS, 2008).

- f_0 First natural frequency in a structural direction of the building and in torsion.
 A Peak acceleration of the target floor.

Any torsional peak acceleration should be expressed as an equivalent translational acceleration.

$$A_t = r \cdot A_\theta \quad (22)$$

- A_t Torsional peak acceleration expressed as equivalent translational acceleration.
 r Distance between torsional center and the critical point.
 A_θ Torsional (angular) peak acceleration.

Wind velocity for a 1 year return period can based on EKS11 be determined as follows:

$$v_{b,1year} = 0.75 v_{b,50years} \sqrt{1 - 0.2 \ln \left(-\ln \left(1 - \frac{1}{T_a} \right) \right)} \quad (23)$$

- $v_{b,1year}$ Reference wind speed with 1 year reoccurrence time.
 $v_{b,50year}$ Reference wind speed with 50 years reoccurrence time.
 T_a = 1 year, number of years for the reoccurrence.

3.4.3 Peak acceleration

EKS11 and SS-EN 1991-1-4 describes the calculation procedure to obtain the peak acceleration of a structure. The equations are based on the assumption that the structure has a cantilever-like action and constant mass along the main axel of the structure.

$$\ddot{X}_{max}(z) = k_p \sigma_{\ddot{X}}(z) \quad (24)$$

- $\ddot{X}_{max}(z)$ Peak acceleration.
 k_p Peak factor. Determined according to equation (2) in Appendix II.
 $\sigma_{\ddot{X}}(z)$ Standard deviation of the acceleration.

$$\sigma_{\ddot{X}}(z) = \frac{3 I_v(h) R q_m(h) b c_f \Phi_{1,x}}{m} \quad (25)$$

- $\sigma_{\ddot{X}}(z)$ Standard deviation of the acceleration.
 $I_v(h)$ Wind turbulence intensity at height h . Determined according to equation (14) or (15) in Appendix II.
 R Factor for resonance response. Determine from equation (5) in Appendix II.
 $q_m(h)$ Wind velocity pressure at height h .
 h Height of the structure.

b	<i>Building width.</i>
c_f	<i>Shape factor for force on the structure. Determine according to section 2.13.</i>
$\Phi_{1,x}$	<i>First mode shape.</i>
m	<i>Building mass per meter length.</i>

$$q_m(h) = \frac{1}{2} \rho v_m^2(h) \quad (26)$$

$q_m(h)$	<i>Wind velocity pressure at height h.</i>
ρ	<i>$= 1.25 \text{ kg/m}^3$, air density.</i>
$v_m(h)$	<i>Mean wind speed at height h. Determined according to equation (9) in Appendix II.</i>
h	<i>Height of the structure.</i>

$$\Phi_{1,x} = \left(\frac{z}{h}\right)^\zeta \quad (27)$$

$\Phi_{1,x}$	<i>First mode shape.</i>
z	<i>Height for uppermost occupied floor.</i>
h	<i>Building height.</i>
ζ	<i>Exponent for mode shape for structures fixed to the ground.</i> <i>$= 1.0$ for structures with stiff core and perimeter columns.</i> <i>$= 1.0$ for large columns combined with shear walls.</i> <i>$= 1.5$ for slender structures with cantilever action.</i> <i>$= 1.5$ for buildings with a concrete core.</i>

3.4.4 Ways to improve the dynamic behaviour

Observing the equations used to determine \ddot{X}_{max} , one can see what parameters that are affecting the dynamic behavior. The factors vary from building specific values such as equivalent mass, stiffness, damping, aerodynamical properties (shape factor) to more place specific measures such as wind load and the surrounding terrain.

The main modifications that can be done when improving dynamic response is through the building specific properties. Increasing the mass, denoted as 1 in Figure 49, will decrease both the natural frequency and the peak acceleration of the building (Edskär, 2018). Due to the slope of the limiting curve, increased mass is the most efficient change for buildings with an eigenfrequency below 1 Hz. Increasing the stiffness will increase the first eigenfrequency but reduce the peak acceleration, indicated as 3 in Figure 49. This means that increasing the stiffness is most efficient in frequency ranges above 2 Hz.

Increasing the stiffness can be done in multiple ways. Either by utilizing stiffer material with higher E- and G-modulus or by working on the geometrical stiffness using thicker elements or a more efficient structural system. Another way to increase the stiffness is by reducing or eliminating joint slip to as large extent as possible.

Increasing the damping of a structure shown as 2 in Figure 49, will not influence the natural frequency. However, the peak acceleration values will be reduced (Edskär, 2018). This is beneficial in all frequency ranges although most efficient if the eigenfrequency is between 1 Hz and 2 Hz. A difficulty with damping is that it cannot be reliably estimated for tall timber structures. An assumption can be made in design, but the true damping can only be determined through measures on the finished building.

When it comes to joints, their stiffness will influence both the damping and the stiffness of a structure. Therefore, both parameters must be considered in design. For high frequency ranges, increased joint stiffness is clearly beneficial. However, in ranges below 2 Hz, there is a large uncertainty regarding the joint slip and its impact on mechanical damping and global stiffness.

Similar to the damping, aerodynamical performance will not affect the natural frequency of a building. It will though impact the force magnitudes acting on the structure. Therefore, aerodynamical performance, similarly, to damping, is beneficial through all frequency ranges.

Concluding rules of thumb for dynamic design:

- Maximize damping.
- Optimize aerodynamic performance.
- If $f_0 < 1$ Hz, increase the mass.
- If $f_0 > 2$ Hz, increase the stiffness.

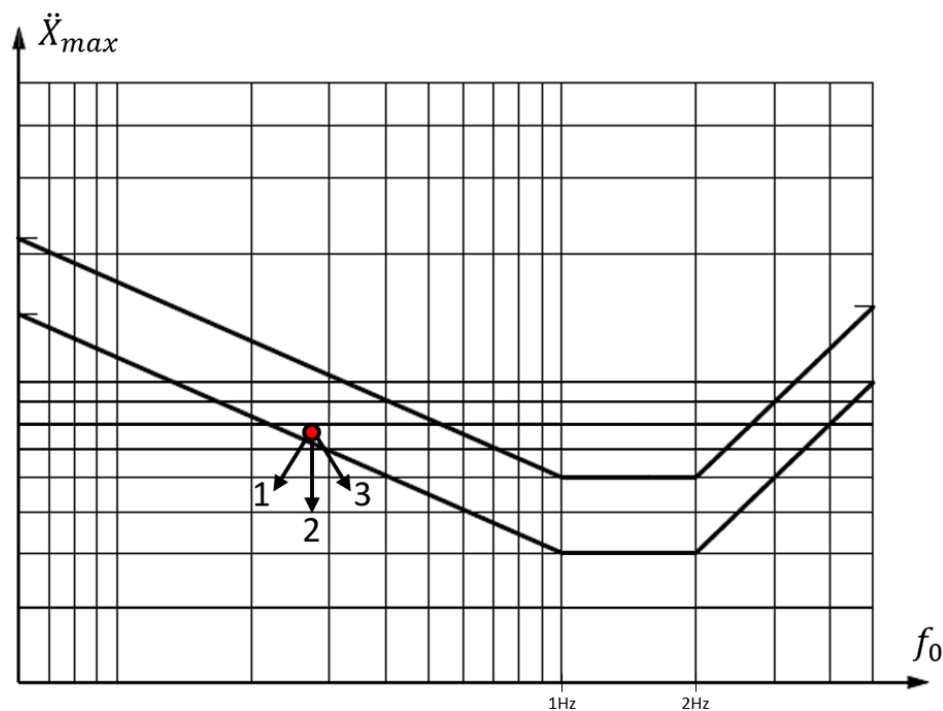


Figure 49: General illustration of change in peak acceleration and lowest frequency due to variation of dynamical properties. 1 = increased mass, 2 = increased damping or improved aerodynamics, 3 = increased stiffness.

4 Conceptual design

The conceptual design will start with three different phases where stabilizing parts are separately designed, evaluated and optimized whereafter they are used for the proposals. These phases are as follows:

- Stabilizing core study.
- Stabilizing truss study.
- Hyperboloid shape study.

Making the proposals in this way will not necessarily result in completely optimized structures. However, multiple proposals can be generated relatively easy based on the knowledge obtained through each analysis. Also, as the proposals have been compared, the winning alternative can always be further developed searching for the best possible structure for the chosen structural system.

Design frames

In order to frame the possibilities for the proposals and limit the design work, the following boundaries have been chosen:

- Each proposal should have 60 stories.
- All circular shapes are discretized into semi-circular shapes in terms of regular polygons with 30 corners, also called triacontagons.
- The floor layouts should allow for reasonably high daylight based on the rule of thumb in section 2.9.4.
- To make the proposals comparable, an equal rentable area is aimed for when developing all of the proposals.
- The total ground footprint is allowed to be large since the 200 m timber tower will be considered as a landmark.
- To avoid vortex shedding, slenderness ratios lower than 1:5 are chosen for the concepts with uniform façade shape. However, verifications regarding the phenomenon have been done and they are shown in Appendix VII.
- The preliminary sizing is made based on ultimate limit state design with the load combination specified below. This choice is made after testing all combinations of favourable and unfavourable loads for one structure:
 - o Self-weight – Unfavourable.
 - o Wind load – Unfavourable.
 - o Imposed load – Unfavourable.
- The tensile stresses are later verified for the following load case:
 - o Self-weight – Favourable.
 - o Wind load – Unfavourable.
 - o Imposed load – Favourable.

Also, the rules specified in the limitations are applied.

Assumptions and input values for the proposals

When modelling the proposals in *Grasshopper*, *Karamba 3D*, a number of choices and input values has been used, these are specified in the list below:

- To eliminate outrigger effect from the slabs, their thicknesses are reduced to 5 cm in all models while the load due to material density for the slab elements was raised to 33.7 kN/m³. This value is chosen since it represents the weight of the *TRÄ8* slabs from *Moelven*. These slab elements are described in Appendix I.

- The slabs are not designed for ULS or SLS. Design of the slabs and eventual supporting structures are assumed as a stage needed in detailed design.
- The following choice is made for the imposed load: $\alpha_n = \alpha_a = 0.5$. Since most floor areas are large and the building has many stories, the probability of maximum loading in all areas is small, and the reduction values approaches their minimum values.
- The wind load is calculated based on wind pressure coefficients.
- The mass for the top third of the building is calculated for the 21 top slabs as well as all other elements within this area. Additional mass due to imposed load is therefore neglected.

4.1 General description of the finite element models

Rhino is a 3D graphics and CAD software which bases geometries on math. In this project *Rhino* is mainly used to visualize the structures as well as confirming that the models are working. The main program used is the *Rhino* extension program called *Grasshopper 3D* which is a visual programming software. Inputs and outputs from different premade components are connected to each other. This graphical modelling is used to generate models that are visualized in *Rhino*. Geometries and dimensions within the models are easy to change by just dragging the input data sliders, so called parametric modelling. Examples for this input data can be building height, bottom diameter and element sizes.

Manual python scripting is also available and have been implemented in some cases when the premade components in *Grasshopper* did not manage the intended task in a satisfiable way.

The models are based on lines and surfaces converted into beam and shell elements using the extension program *Karamba 3D*. This extension is also used to implement material properties as well as assign cross-sections and support to the model. Furthermore, *Karamba 3D* both runs the analysis and gives the available output values.

4.1.1 Material

The different materials and their properties are implemented through a *Karamba 3D* component. Trusses, columns and beams are made of GL30c while the shear walls are made of CLT C30 in all the models. Apart from these elements, slabs are included as well. However, they are mostly used to generate and distribute vertical loads, therefore, they are modelled using different material properties throughout the project.

Material properties used used can be seen in Table 11. The parameter indices show which direction the parameter is for, where 1 is the main direction and 2 is the secondary direction.

Since timber does not yield, the material values chosen for f_{y1} and f_{y2} are of little significance. Instead, they are chosen high enough to avoid yielding in the model. This will make preliminary sizing easier since plastic load redistribution is avoided.

Table 11: Material properties obtained from Swedish wood (Crocetti, Johansson, Lidelöw, et al., 2015) and *KL-trähandboken* (Svenskt Trä, 2017a) used in models.

Material:	GL30c	CLT C30
E_1 [MPa]	13 000	6 840
E_2 [MPa]	13 000	5 560
G [MPa]	650	750
ν_{12} [-]	0.5	0.5
γ [kg/m ³]	430	460
α [1/C°]	$5 \cdot 10^{-6}$	$5 \cdot 10^{-6}$

4.1.2 Support conditions

To simulate a global fixed connection between the building and the ground, all ground level elements are locked from translational movements in x-, y- and z-directions. However, they are free to rotate in all directions.

4.1.3 Joints

The intention when using trusses is to minimize bending and maximize the axial portion of the loads. Therefore, pinned joints would be preferable. However, due to difficulties trying to make the large models work as intended, fixed joints have been used for all the models.

However, based on initial comparisons between truss-frames with fixed and pinned connections, it could be concluded that the difference in most cases are relatively small. Therefore, fixed joints have been used in the models, but the joints have been considered as fixed in preliminary design.

4.1.4 Loads

There are three different loads applied in the models. These are gravity load, wind load and imposed loads. When doing the preliminary sizing for the models these three loads are combined according to the ULS load combination. Later during deformation analysis and dynamic analysis, the SLS combination is used.

In the core and truss analysis, the loads are limited to a single point load acting at the top of the building.

4.1.4.1 Gravity load

The gravity load exists as a component in *Karamba 3D* and is based on the size of the elements as well as their density. However, the mass differs a little bit compared to real mass depending on the element connections and how the elements are extruded from their center lines. One can imagine a connection between a wall and a floor as two connected lines. However, these are then extruded in all directions resulting in 3D slabs and walls. Therefore, there will be small duplicated masses at all element connections.

4.1.4.2 Wind load

The wind loads are calculated as described in Appendix II and applied as point loads acting directly at the façade nodes. Therefore, the wind is acting perpendicular to the façade surface both horizontally and vertically. The point loads are calculated as resultants for the distributed wind pressure on the surrounding surfaces. The wind pressures for each model is determined using a manually made Python-script.

4.1.4.3 Imposed load

The imposed loads are applied as point loads distributed over the slabs according to 2.12.4. Similar to the wind loads these point loads are a sum of the distributed loads on the nearby surfaces on the slabs.

4.1.5 Verification of the finite element model

Some hand calculations are carried out to check whether the model results are reasonable. For example, the mass is calculated from the geometry and density of the building parts and then compared with the values obtained from the model. Also, the

horizontal deformations are hand-calculated for a simple cantilever beam and compared with values obtained from a similar model, this is further described in Appendix VIII.

4.1.6 Mesh

Every surface in the model is divided into a mesh, later converted to shell elements. The precision of the results is often connected to the mesh resolution. However, the run time of the model increases significantly when fine meshes are used, therefore it is favourable to do a convergence study, trying to find a compromise between calculation speed and result reliability. A convergence study has been made and suggests a mesh resolution that gives element sizes around 0.7 x 0.7 m. A detailed text about the study can be seen in Appendix VIII.

4.2 Stabilizing core study

To find the best possible stabilizing core for the building, a study with five different core-concepts was done using *Grasshopper* and *Karamba 3D*. Each concept was also evaluated with different configurations to find the optimized geometry of each concept. A choice of at least 8 elevators at the core is done to satisfy transportation demands within the building. This requires a floor area of approximately 8 times the shaft of 1.6 x 2.5 m close to the core which also impacts the dimensions of the core. The five main concepts with their elevator placement can be seen in Figure 50.

As holes in a shear wall affects the stiffness significantly, the influence of doors and slight changes in the core geometry are anticipated to have a similar effect. This is also the main reason why such large number of alternatives are evaluated.

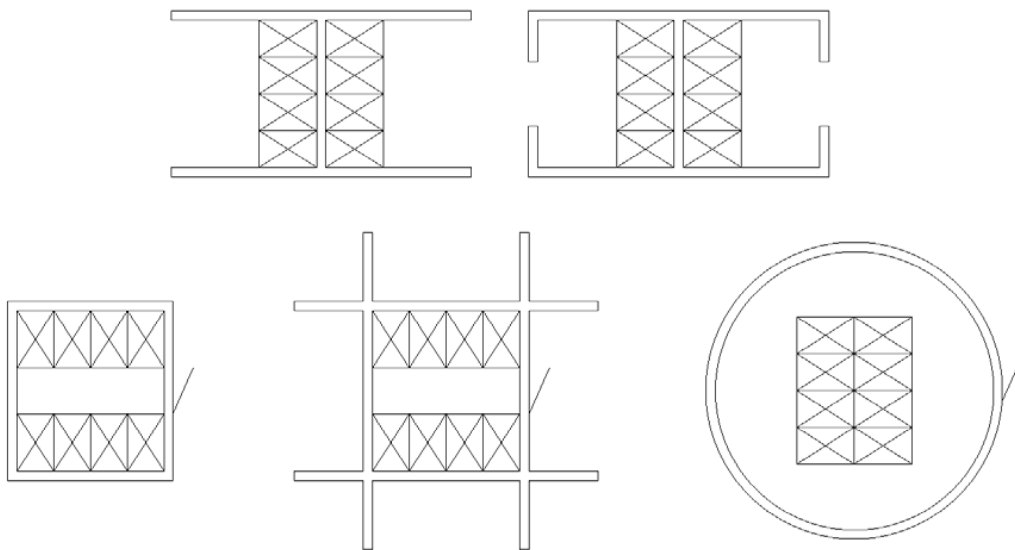


Figure 50: The five main core-concepts.

All the different cores are constructed to fit 8 elevators with at least two meter free space at the openings. For a fair comparison the wall thickness was set to 0.4 m for all cores. To evaluate the results for each concept, models was made in *Grasshopper*, *Karamba 3D* and Point loads were applied at the top of the 200 m tall, 60 storey high structures.

In order to compare the efficiency of the concepts, the flange and web lengths within each section was adjusted so that all concepts obtained the same stiffness and deflection in both main directions.

The first option, a pure H-shape, was straight forward, the web and flanges were adjusted until the deformation in both directions reached a magnitude of 1 cm for the applied load. The final shape and dimensions can be seen in Figure 51.

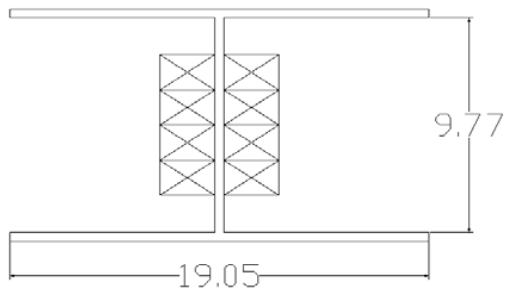


Figure 51: H-shaped core cross-section.

The second concept, H-shape with secondary webs was tested with four different shapes. The secondary webs were set to 0.8, 1.8, 3.8 and 4.165 meters measured from the flanges. Thereafter, the main web and flanges were adjusted to obtain a deformation of 1 cm in each direction. The last option with secondary flanges 4.165 m is designed regarding the minimum opening width of two meters and therefore the maximum length of the extensions is 4.165 m. The different shapes and dimensions can be seen in Figure 52.

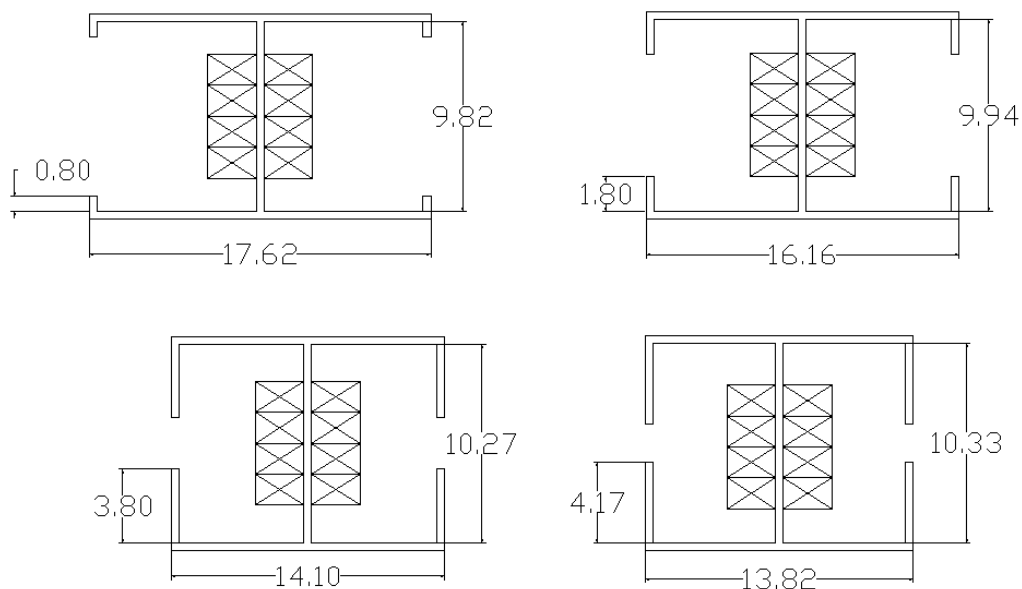


Figure 52: H-shaped cross-sections with extensions.

The closed rectangle concept was tested with five different door configurations. The first one had all openings on the same side. The second option had alternately placed openings on the opposite side for every floor. The third option had openings on two opposite walls at every floor. The fourth configuration had a spiral-like door pattern with one door on each floor. Since this option has openings in different directions on all floors there must be two meter space at all directions inside the core and therefore the elevators are placed in the middle. The openings in this study are 0.9 meter wide and 2.1 meter high which is the same size as the elevator openings. The fifth option had openings in all walls on every storey. All these alternatives can be seen in Figure 53 and Figure 54.

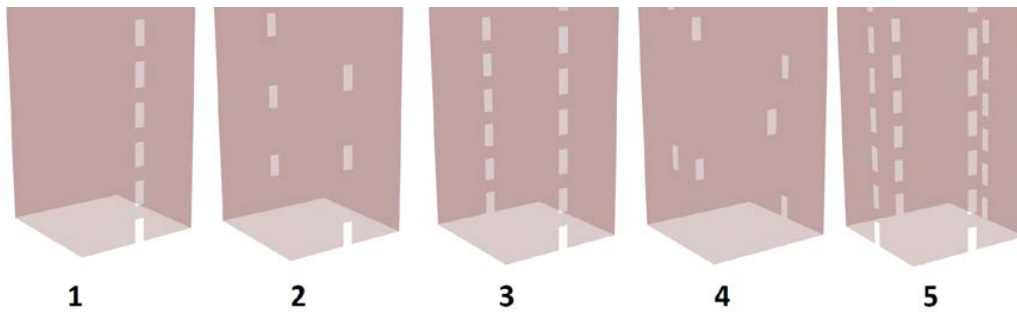


Figure 53: Different opening concepts for the rectangle alternative.

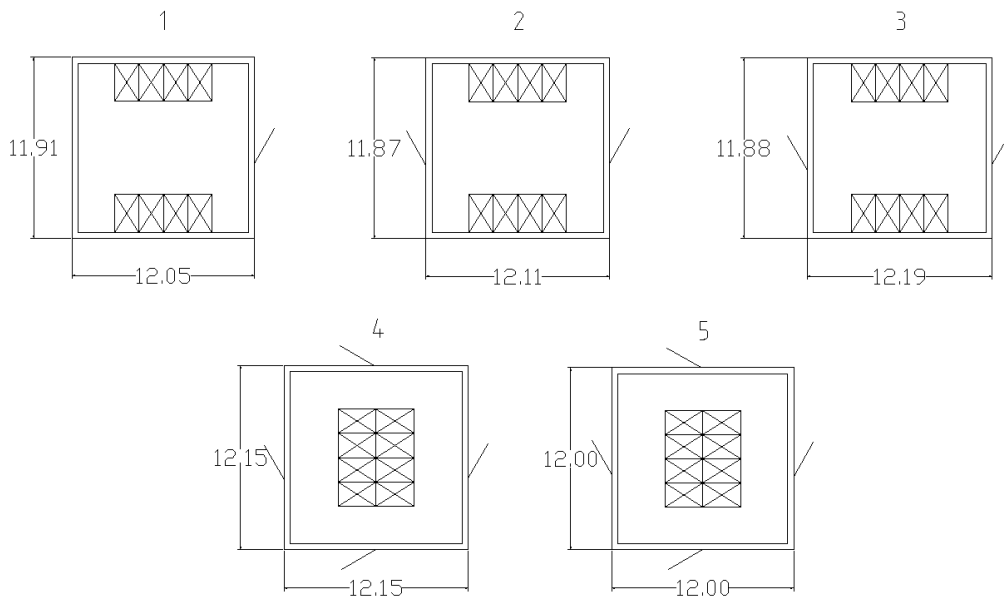


Figure 54: Rectangle cross-section dimensions.

The rectangle concept with extensions was only evaluated for one configuration which is based on the results for the rectangle cores. The openings were therefore located on one side all the way up and the extensions chosen as three meter long. The cross-section and dimensions are shown in Figure 55.

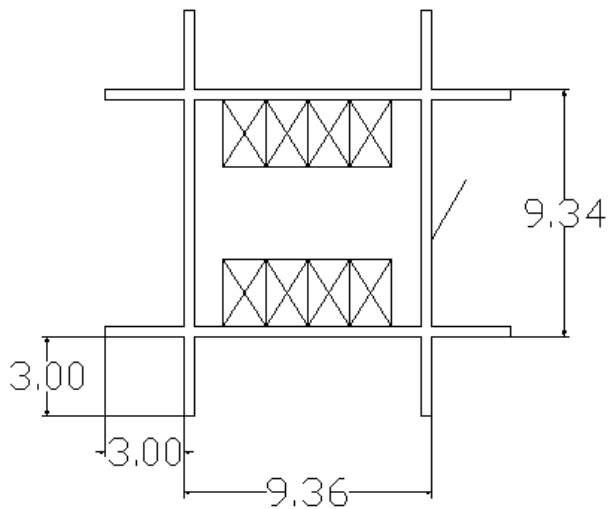


Figure 55: Rectangle cross-section with extensions dimensions.

The last option was a circular core shape, also here the openings were located on one side for all stories. The dimensions and elevator fittings can be seen in Figure 56.

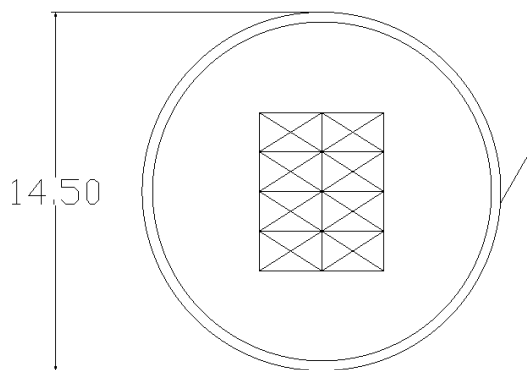


Figure 56: Circular cross-section with opening.

All the concepts were compared and evaluated based on their required interior and exterior floor area, material volume and number of connections. The reason to include both interior and exterior area in the comparison is that parts of the area outside the core might still be usable for other applications. The exterior area is basically a rectangle or circle covering the whole core while the interior area is a polygon covering the outside of the closed shape walls.

The results from the comparison can be seen in Table 12 and Figure 57 where red color indicates a poor result and green indicates a good result. As shown in the table, the H-section is superior regarding the inner area and few connections but demands long walls to reach sufficient stiffness. The H-sections with extensions have poor results for these aspects but have a considerable efficient outer area compared to the normal H-section. All the rectangle options are pretty similar, but rectangle 3 which is the one with openings on two sides and rectangle 1 with openings on one side on every floor are the most efficient once regarding volume and area used. The rectangle option with

extensions is not efficient compared to the other rectangle options regarding volume but has a much smaller inner area which could suit some buildings better. The circular cross-section is the most efficient volume-wise but has a rather big area compared to the rectangular shapes. The connections of the circular shape are chosen to be zero due to the lack of corners, but it is more complicated to construct than the rectangular shapes.

The conclusion of this comparison is that different cores suits different buildings, but for the general case the rectangle with openings on one side all the way up and the circular shape are the best options. The circle saves 160 m³ but demands 21 m² more on every floor which summed up over all floors is 1 260 m². Therefore, the rectangle with openings on one side all the way up is considered the best option for this case.

Also, viewing the results in Table 12 and Figure 57. It is clear that the small differences between many of the alternatives did not make as large difference as anticipated. Therefore, the study could have been carried out with just the base configurations, giving the results needed as a basis for the building proposals.

Table 12: Results from core comparison.

	Mass [kg]	Volume [m3]	Inner area [m2]	Outer area [m2]	Connections in cross-section [-]
H-section	1 770 800	3 850	19	201	2
H-section with small extensions	1 784 900	3 880	187	187	6
H-section with medium extensions	1 828 200	3 974	174	174	6
H-section with big extensions	1 980 100	4 305	156	156	6
H-section with biggest possible extensions	2 014 800	4 380	154	154	6
Rectangle 1	1 651 100	3 589	144	144	4
Rectangle 2	1 652 600	3 593	144	144	4
Rectangle 3	1 650 600	3 588	145	145	4
Rectangle 4	1 650 300	3 588	148	148	4
Rectangle spiral	1 654 000	3 596	144	144	4
Rectangle with extensions	2 137 600	4 647	97	236	4
Circle	1 577 300	3 429	165	165	0

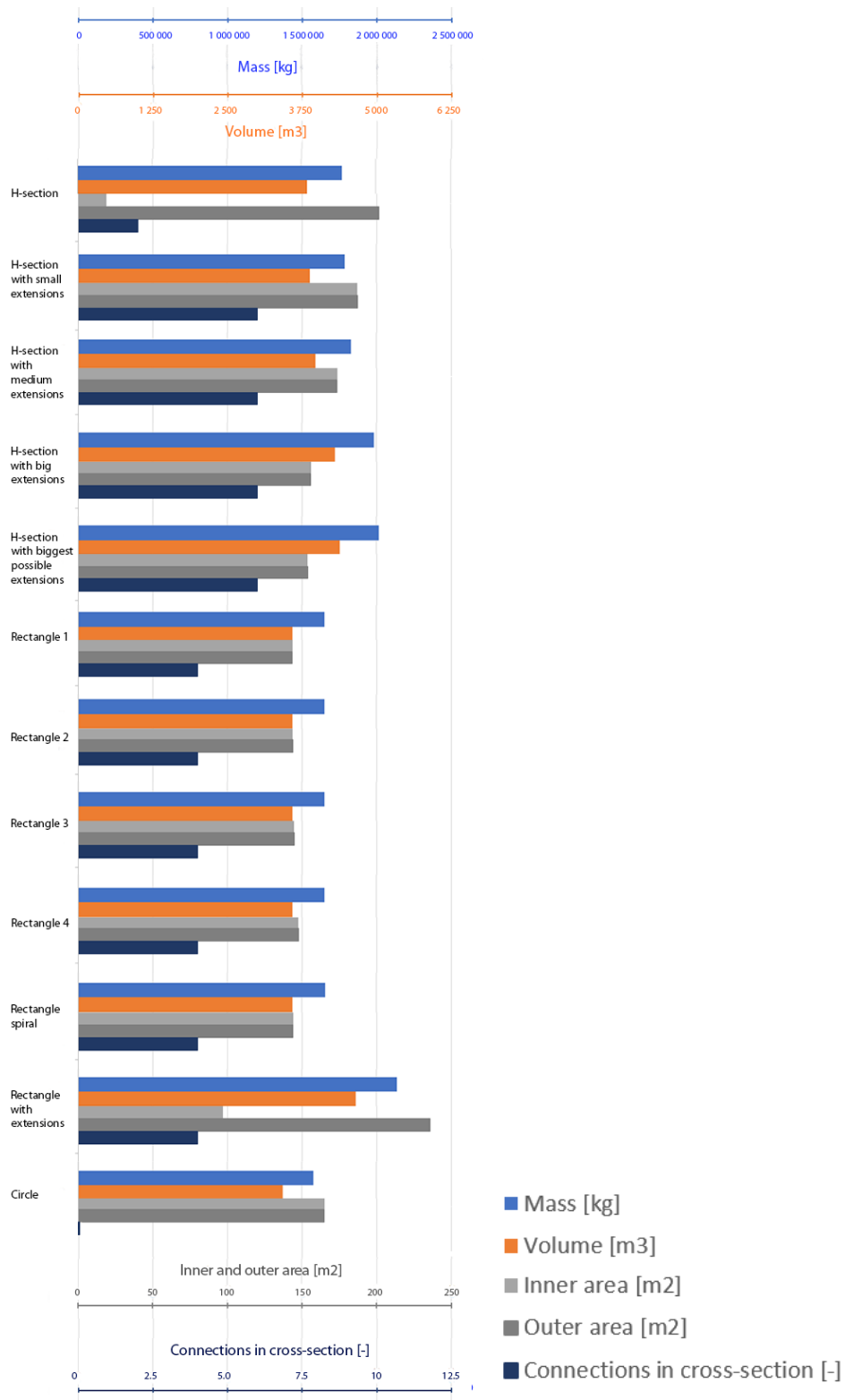


Figure 57: Results from core comparison.

4.3 Stabilizing truss study

When deciding on a truss structure for the buildings, a 200m tall model, based on a triacontagon, was made and analysed in *Grasshopper* and *Karamba 3D*. The model makes it possible to adjustment of the number of floors each truss element should span over. Also, each truss is limited to span until the next corner in line. This to not decrease the usable space inside the building which would have been the case for trusses spanning over two or more corners. Furthermore, the model is made so that the number of trusses height-wise, always equals an integer. The term *truss density* is therefore used to describe *the number of truss elements vertically placed over each other* along the building height. Thus, no partial trusses are used.

A horizontal point load of 100 kN was then applied at the top of the building. Though, in order to distribute this force evenly as well as eliminate local deformations, a slab with neglectable mass and almost infinite stiffness was connected to the top of the structure. Twelve different truss densities were tested and evaluated based on their required mass of timber and horizontal deformation for the applied point load.

The results from the analysis when using only truss can be seen in Figure 58. Surprisingly the densest truss has the second largest deformations. Also, the relation between mass and deformation is different for each case. This might be due to varying influence of shear deformations. However, the exact reason is hard to determine.

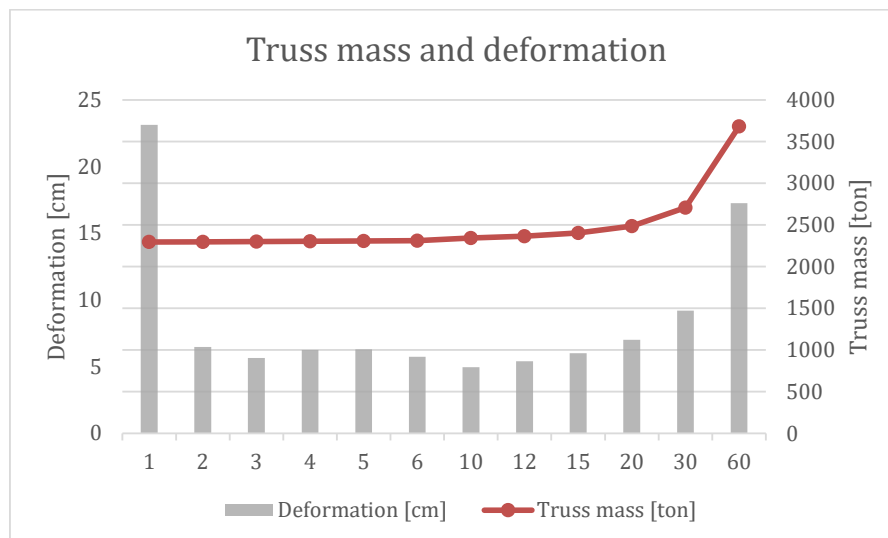


Figure 58: Truss mass and deformation of different truss densities (shown on the x-axis).

Deformation modes for a few truss densities are shown in Figure 59.

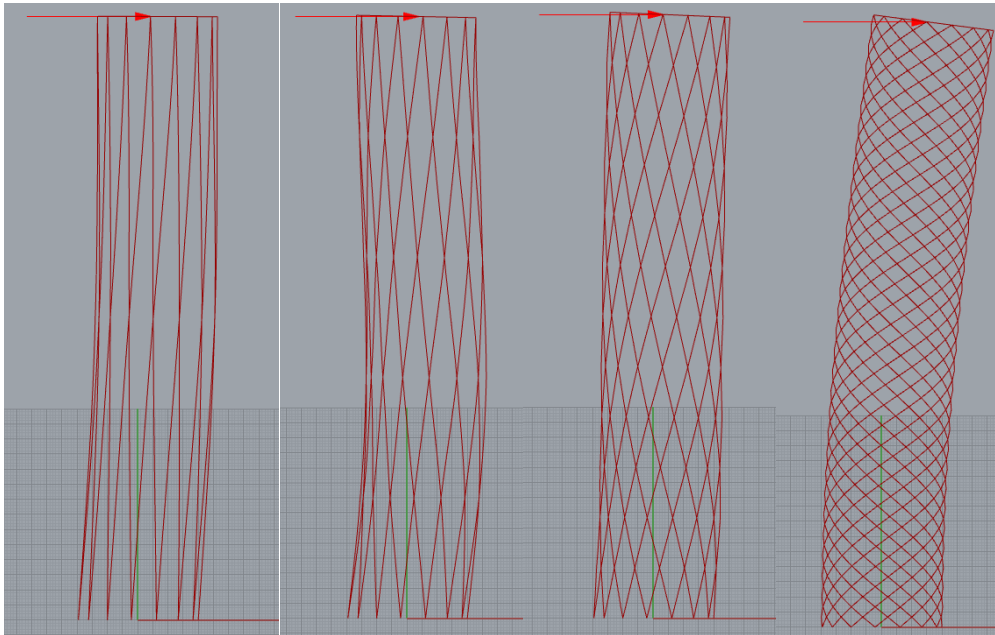


Figure 59: Shear deformation on a few trusses with different truss densities, from the left: Truss density 2, 5, 12 and 60. Displayed using a scale factor of 100.

Since the result was not quite as expected, more elements were added to the model to see how the truss system works in a more complete building. The first idea was to have a simple skeleton with columns, beams and the truss system. As the structural system then would be nearly completed, the Eurocode based wind loads were applied instead of the 100 kN point load. However, this resulted in major local deformations in the model.

Therefore, the slabs were added to increase the structural rigidity and interaction between the truss and frame elements. When the model was tested again there was still significant shear deformations. Therefore, shear walls were added to the model, to get a more balanced ratio between shear and bending deformations.

The structural deformation for the truss system with and without shear walls, can be seen in Figure 60 scaled with a factor of 100. These shear deformations were large when using sparse truss patterns. However, for denser patterns, the phenomenon was strongly reduced.

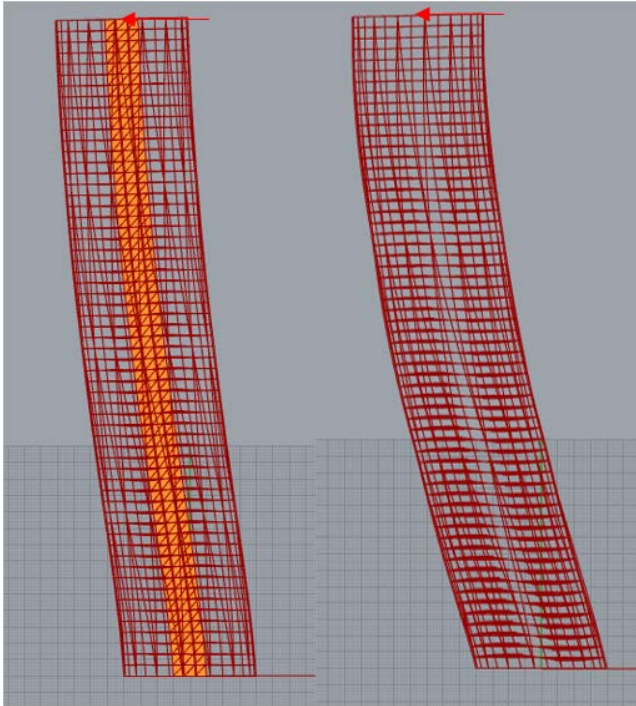


Figure 60: Shear deformation in truss study when using and not using shear walls. Displayed using a scale factor of 100.

The final truss analysis was carried out with wind loads according to Eurocode and varying numbers of trusses along the building height. As measures for the truss performance, the total mass of timber as well as the global deformations due to wind were extracted for each possible truss combination.

The results from this analysis can be seen in Figure 61. When only connecting the trusses between the bottom and top of the building, the truss had a total weight of 2 296 tonnes and a deformation of 33.6 cm. However, when using one truss on every floor a total weight of 3 682 tonnes and a deformation of 7.0 cm was obtained. As visualized in the graph the deformation decreases almost linearly with an increasing number of trusses. However, after 12 trusses along the building height the improvement seems to be leveling out. Worth to notice is that the x-axis in the graph is not linear and that the densest truss pattern has larger deformation than the three sparser truss systems, despite having a lot more mass.

The conclusion of the results is that the mass starts to increase for truss densities of 15 or higher while the deformation approaches the lowest value for a truss density of 10 or above. Ideally a truss with a frequency between 10 and 30 would be used regarding the volume and deformation due to wind.

Choosing a truss density of 15 truss elements along the building height gives an optimal truss angle just below 60°. This angle is therefore used as a guideline when choosing trusses for the proposals.

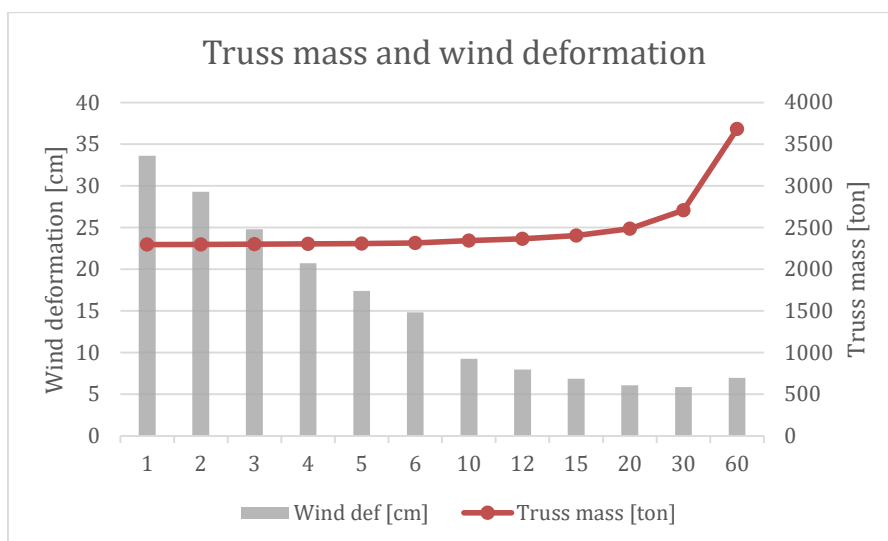


Figure 61: Truss mass and deformation of different truss densities (shown on the x-axis) when the entire structure is included.

4.4 Hyperboloid shape study

As described in section 2.7.6, the hyperboloid shape has a number of benefits when it comes to structural performance. Especially if using a hyperboloid shape with continuous elements, efficiency can be obtained both structurally and material-wise. With this in mind, parametric study has been carried out in order to determine the most efficient structure.

The following steps have been carried out in *Grasshopper* trying to find the optimal hyperboloid shape for this project:

- Create a bottom circle with a radius within the range 25 to 40 m.
- Create a top circle with a radius within the range 5 to 20 m.
- Discretize the top and bottom circles into triacontagons.
- Connect the nodes in the top and bottom ring facing the same radial direction.
- Twist the top nodes around their center point.

Following this procedure generates different hyperboloid shapes depending on the bottom radius, top radius and degree of twisting for the upper nodes.

The parametric study was therefore carried out using the three critical values as input data. Furthermore, the waist was limited to remain outside the internal core determined in section 4.2, which has the size 10 x 10 m. As the evaluation criterion when searching for the optimized hyperboloid shape, the global horizontal deformation due to wind load was used. All of these data were used together with the *Grasshopper* module *Galapagos*, which conducts a generative analysis based on its in- and output values. The determined and optimized shape is shown in Figure 62.

The overall impression from the generative analysis could be summarized as follows, maximize the bottom diameter, the top diameter and the twisting.

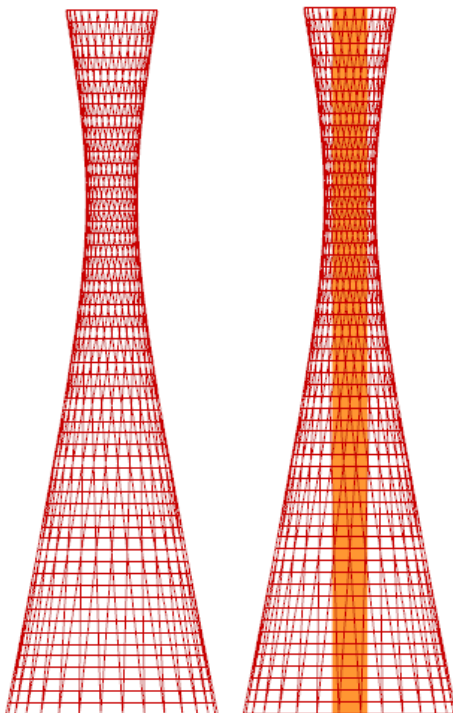


Figure 62: Illustration of the optimized hyperboloid shape with and without limiting internal core.

In order to obtain a rentable area in a similar range as the other proposals, this shape did however need to be enlarged. Doing so was carried out using a scale factor applied to the bottom and top radius on the building. Bottom and top dimensions of the two hyperboloids as well as the scale factor used and the final twisting are shown in Table 13. Also, the scaled hyperboloid compared to the optimized one is shown in Figure 63.

Table 13: Comparison between the basic measures for the optimized and the scaled hyperboloid.

	Bottom radius [m]	Top radius [m]	Scale factor [-]	Twisting [°]
Optimized hyperboloid	30.0	13.0	1.0000	132
Scaled hyperboloid	37.1	16.1	1.2369	

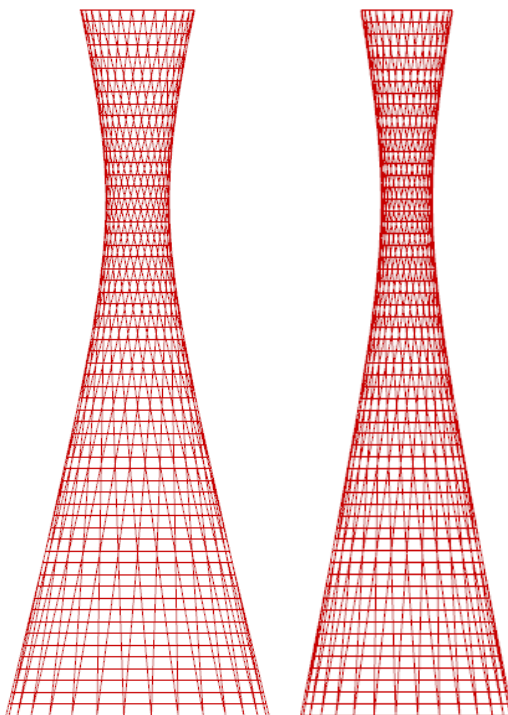


Figure 63: Comparison between the scaled hyperboloid (to the left) and the optimized hyperboloid shape (to the right).

Note that the enlargement of the shape might have made the structure somewhat unoptimized. However, the difference in performance is anticipated as small and the scaled shape is therefore used for the proposals. Also, the shape obtained in this section is used for two of the proposals. One made completely according to the design procedure described in this section and one truss frame model, only based on the global shape.

Since vortex shedding mainly is a problem for uniformly thick buildings, the hyperboloid shape is assumed as enough to disregard vortex shedding in preliminary design. A quick check of the critical wind speeds for each concept has also been made to ensure vortex shedding will not be of importance in this design stage, this verification is shown in Appendix VII.

4.5 Proposals for a 200 m timber tower

To reduce wind loads as much as possible, nearly round structures are aimed for. Inspiration is also taken from other tall building projects; these are briefly described in Appendix IX.

To limit excessive material consumption in areas with lower loads, the structures are divided into five sections along the building height. Each section ranging the following distances above the ground: S1 = 0-40 m, S2 = 40-80 m, S3 = 80-120 m, S4 = 120-160 m, S5 = 160-200 m. The elements are dimensioned for the worst loads in its section. Thus, all elements of the same type within each section are of the same size.

Based on the results from the three previous studies, five different proposals are generated. These are all combinations of a square CLT core, a square truss frame, cylindrical truss frames, a hyperboloid truss and a hyperboloid truss frame. The proposals described in the following subchapters are chosen since they are assumed to represent a large variability among the possible concepts generatable based on the previous results. Also, these concepts have shapes that allows for decent normalization which is a requirement for a fair evaluation. Notable though is that multiple more concepts could have been analyzed. However, five concepts have been chosen to limit the extent of this project.

An additional benefit of the concepts based on a circular shape is the possibility to generate parametric models relatively easy. The buttressed core system on the other hand is based on an array of different shapes. This makes it incredibly difficult to generate a parametrically adjustable model. One model for the buttressed core system have been made, however, since it has to be completely remade in order to fulfill the requirements needed for comparability, it had to be discarded from the study. This, even though the shape itself is of interest for a potential 200m tall timber building.

Observing the element sizes obtained through preliminary design, many of the proposals shown in the following subchapters have large beams. This is a consequence of the simple preliminary design. In an eventual detailed design, a proper support structure for the slabs must be developed.

4.5.1 Mega truss and core system with perimeter columns

Globally, this tower is shaped as a cylinder discretized into a triacontagon with a radius of 20.5 meters. There is one column at each of the perimeter corners, resulting in a pattern with 30 columns around the building equally spaced approximately 4.3 m from each other. For every floor, horizontal beams are placed along the perimeter between each of the columns. The perimeter frame system is also braced by diagonal truss elements. The truss density is determined in accordance with section 4.3, resulting in a truss-ground angle around 58 degrees. In other words, two floors between each truss node. Illustrations of the structure and its horizontal section can be seen in Figure 64.

In the center, a 10 x 10 m square CLT core is placed. The core size and its door configuration are determined in section 4.2. Furthermore, the slabs are supported by the core and the perimeter beams. However, this results in a maximum span length of about 15.5 meters. The pre-fabricated slab elements from *Moelven*, mentioned in Appendix

III can only handle spans up to 8 m. Therefore, in detailed design, further consideration must be made regarding the slab configuration and its ULS and SLS performance. A possible solution might be to use radial beams supporting the slab elements. Notable though is that the weight of the Trä8 slabs has been used in the model to obtain realistic load values in preliminary design.

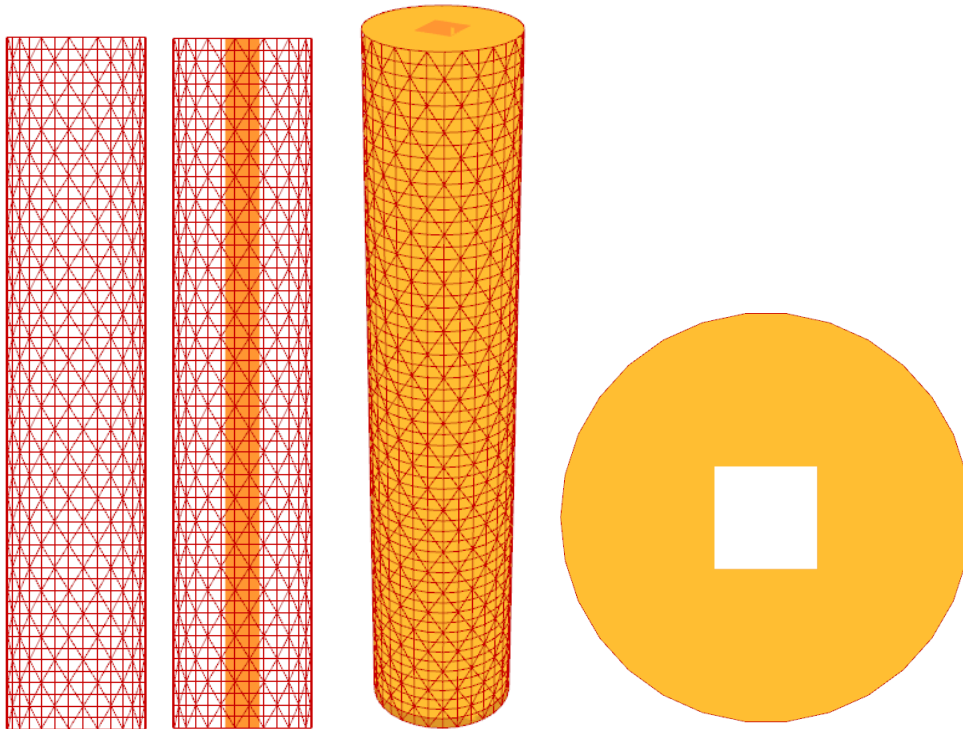


Figure 64: Illustration of the model, from the left: Frame truss from side view, whole structure from side view, whole structure in 3D view, section of the building.

Element sizes and mass timber

Preliminary sizing resulted in element dimensions and mass of timber needed for the structural system as shown in Table 14 and Table 15.

Table 14: Element sizes needed according to ULS design.

<i>Dimensions [mm]</i>	S1	S2	S3	S4	S5
Columns [h x b]	600 x 600	500 x 500	350 x 350	250 x 250	200 x 200
Beams [h x b]	800 x 700				
Truss [h x b]	750 x 750				
Core [t]	850	600	450	450	450

Summarizing the material volume and material densities gives the following timber consumption for each element type, section and the total building.

Table 15: Mass of timber required for the various parts of the structural system. Determined using element dimensions shown in Table 14, element lengths from the grasshopper model and mean densities for glulam (430 kg/m³) and CLT (460 kg/m³).

Mass	S1 [10 ³ kg]	S2 [10 ³ kg]	S3 [10 ³ kg]	S4 [10 ³ kg]	S5 [10 ³ kg]	Total [10 ³ kg]	Part of total mass
Columns	182.2	126.5	62.0	31.6	20.2	422.5	2.3%
Beams	370.5	370.5	370.5	370.5	370.5	1 852.5	10.1%
Truss	338.5	338.5	338.5	338.5	338.5	1 692.5	9.2%
Core	604.8	426.9	320.2	320.2	320.2	1 992.3	10.8%
Slab	2 488.7	2 488.7	2 488.7	2 488.7	2 488.7	12 443.5	67.6%
Total	3 984.7	3 751.1	3 579.9	3 549.5	3 538.1	18 403.3	

Dynamic performance

Calculating the top floor acceleration according to EKS 11 and SS-EN 1991-1-4 and comparing it to the requirements given in ISO 10137 shows that the preliminary sized mega truss with perimeter columns and a CLT core fulfills the requirement for both offices and residential buildings. The first mode's eigenfrequency for this concept is 0.30 Hz.

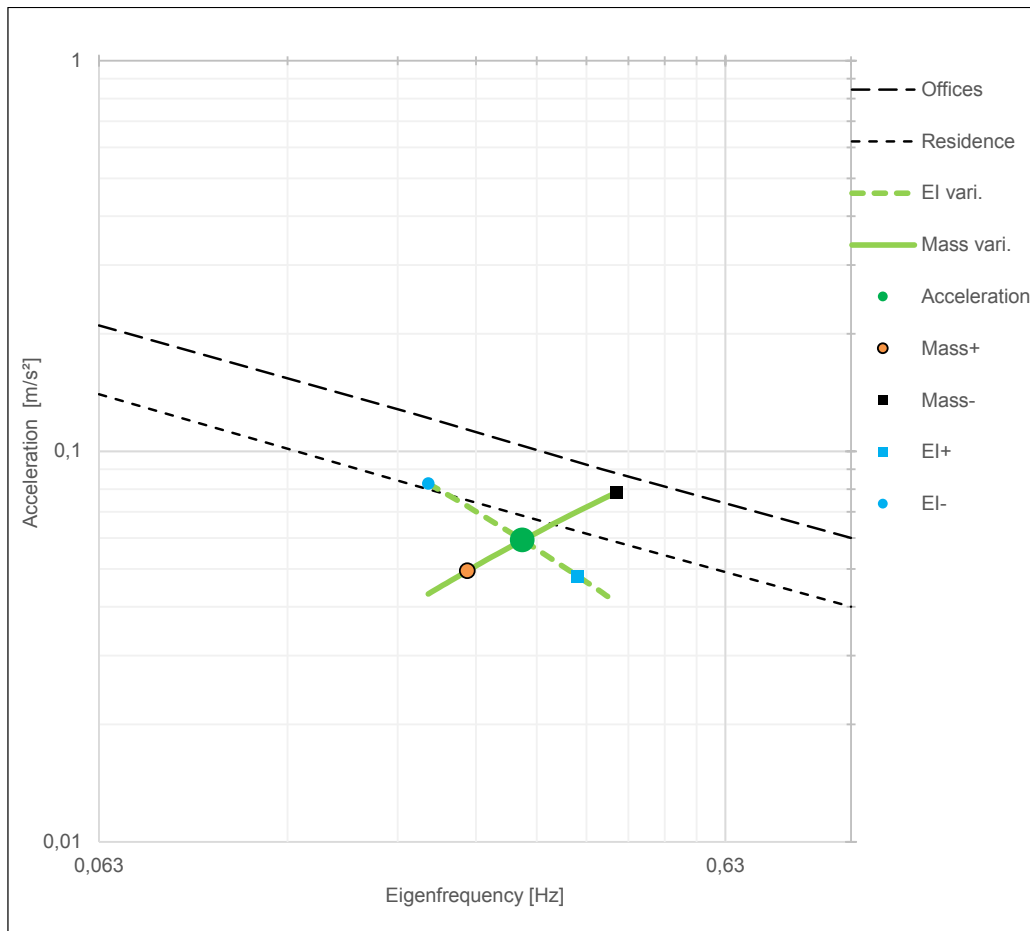


Figure 65: The top floor acceleration compared to the ISO 10137 limits for residential buildings and office buildings. Anticipated trend lines for acceleration change due to increased or decreased stiffness and mass are also shown by the dashed and solid green lines. The calculation is made for a mechanical logarithmic decrement of 10 %.

4.5.2 Mega truss and internal truss-based core system

This structure is mostly the same as the one described in section 4.5.1. The main difference is the core choice where a 10 x 10 m square truss frame core is used. The inner truss frame consists of vertical columns at the four corners. The space between each corner is spanned by internal beams carrying the distributed loads to the columns. Diagonal bracings are chosen to span over five floors resulting in a truss-ground angle around 60 degrees. Since the core carries large vertical loads, this relatively steep truss angle is chosen to relieve the column loads somewhat. Also, similar to the previous concept, due to the long spans between core and perimeter, extra care must be taken for the slabs and its support structure in detailed design. Illustrations of the trusses, section and building as whole can be seen in Figure 66.

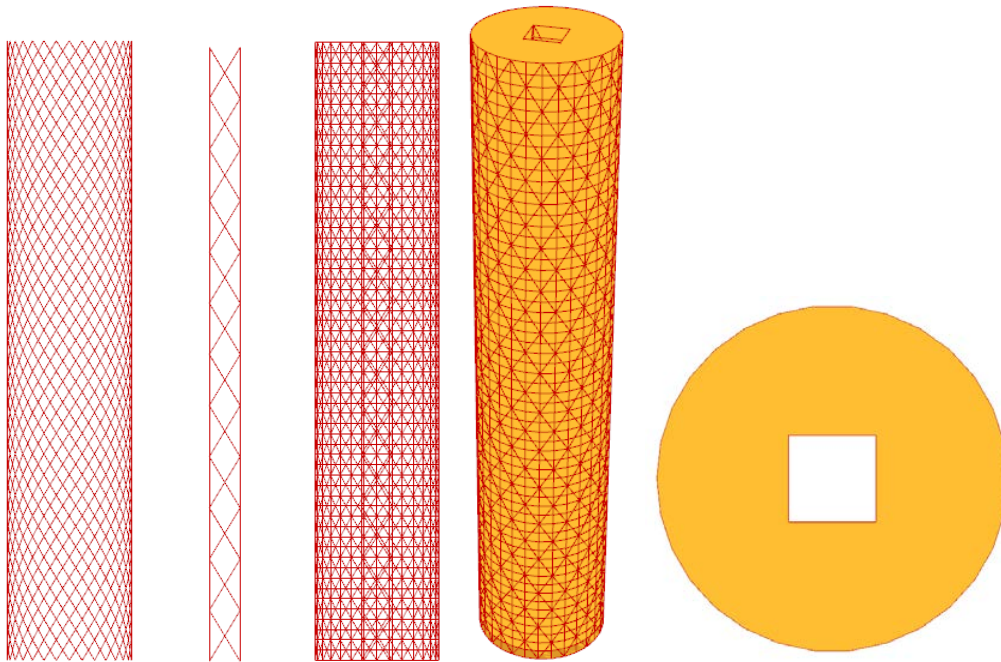


Figure 66: Illustration of the model, from the left: Perimeter truss from side view, inner truss from side view, whole structure from side view, whole structure in 3D view, section of the building.

Element sizes and mass timber

Preliminary sizing resulted in element dimensions and mass of timber needed for the structural system as shown in Table 16 and Table 17.

Table 16: Element sizes needed according to ULS design.

Dimensions [mm]	S1	S2	S3	S4	S5
Perimeter columns [h x b]	650 x 650	500 x 500	400 x 400	250 x 250	200 x 200
Perimeter beams [h x b]	800 x 700				
Perimeter truss [h x b]	750 x 750				
Core columns [h x b]	1300 x 1300	1100 x 1100	900 x 900	600 x 600	350 x 350
Core beams [h x b]	1000 x 800				
Core truss [h x b]	850 x 850				

Table 17: Mass of timber required for the various parts of the structural system. Determined using element dimensions shown in Table 16, element lengths from the grasshopper model and mean densities for glulam (430 kg/m³) and CLT (460 kg/m³).

Mass	S1 [10 ³ kg]	S2 [10 ³ kg]	S3 [10 ³ kg]	S4 [10 ³ kg]	S5 [10 ³ kg]	Total [10 ³ kg]	Part of total mass
Perimeter columns	213.9	126.5	81.0	31.6	20.2	473.2	2.6%
Perimeter beams	370.5	370.5	370.5	370.5	370.5	1 852.5	10.2%
Perimeter truss	338.5	338.5	338.5	338.5	338.5	1 692.5	9.3%
Core columns	114.1	81.7	54.7	24.3	8.3	283.1	1.6%
Core beams	164.7	164.7	164.7	164.7	164.7	823.5	4.5%
Core truss	113.7	113.7	113.7	113.7	113.7	568.5	3.1%
Slab	2 488.7	2 488.7	2 488.7	2 488.7	2 488.7	12 443.5	68.6%
Total	3 804.1	3 684.3	3 611.8	3 532.0	3 504.6	18 136.8	

Dynamic performance

The acceleration for the top floor at the buildings first natural frequency satisfies the ISO 10137 requirement for both offices and residential buildings. Comparing the result for this one and the previous proposal the difference can be concluded as negligible when it comes to dynamic performance. The first mode's eigenfrequency for this concept is 0.31 Hz.

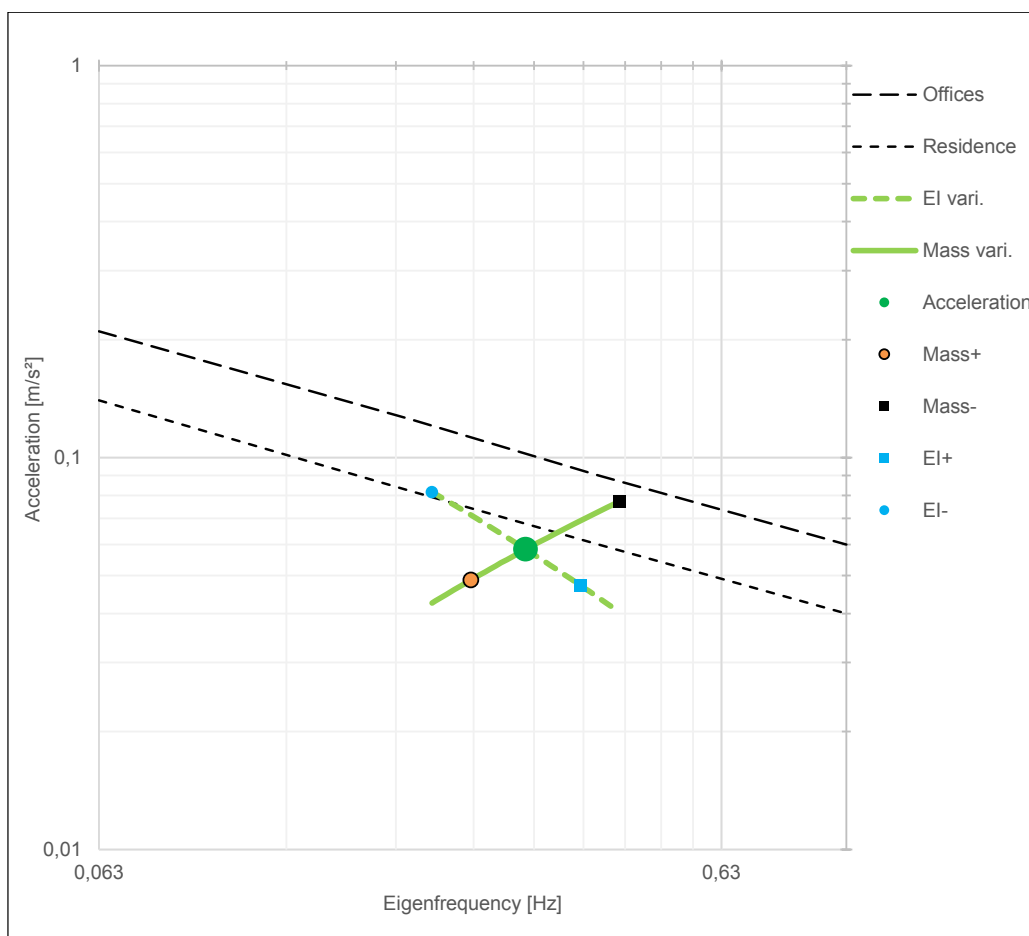


Figure 67: The top floor acceleration compared to the ISO 10137 limits for residential buildings and office buildings. Anticipated trend lines for acceleration change due to increased or decreased stiffness and mass are also shown by the dashed and solid green lines. The calculation is made for a mechanical logarithmic decrement of 10 %.

4.5.3 Mega truss with internal truss and hollow center

This building is based on two mega truss frames. One interior truss frame with a radius of 16 m and an external one with a radius of 26 m. The building is concentrated to the area between these while the center portion inside the internal truss is a complete hollow center allowing for daylight entering the building from the inside as well. Theoretically, since all slab area is clearly within 10 m from the facades the proposal could be assumed to have great light conditions.

Both of the truss frames are circles discretized into triacontagons with columns at each corner. Therefore, there are 30 columns along the perimeter, equally spaced with a distance of approximately 5.4 m and 30 columns along the inner façade placed with a spacing of 3.4 m. There are also beams spanning the gap between each column along both the inner and outer edges of the floors. Furthermore, there are radial beams joining the two truss frames as well as carrying the floors.

The inner truss spans over two floors between each connection. This results in a truss-ground angle around 63°. A slightly lower truss angle is chosen for the outer truss. This requires a sparser pattern where each truss element spans across three floors.

Illustrations of the building, its section and the truss frames can be seen in Figure 68 and Figure 69.

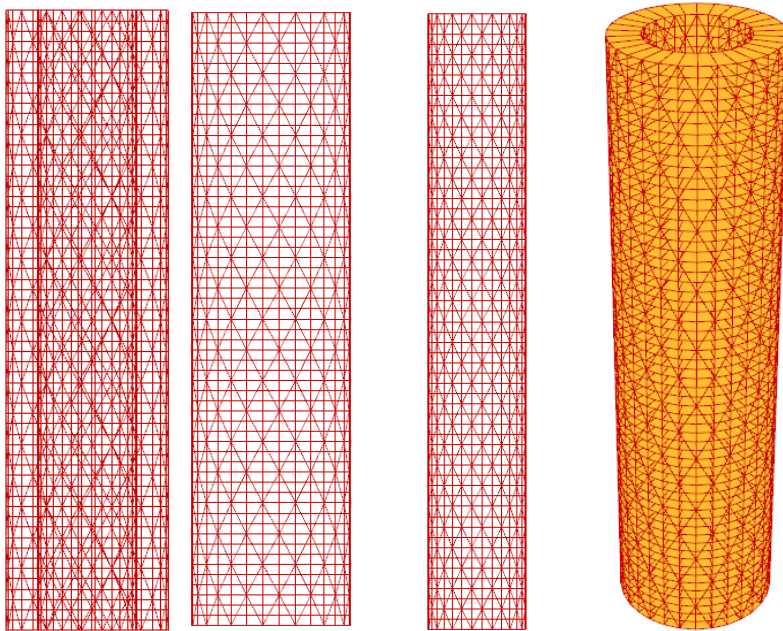


Figure 68: Illustration of the model, from the left: Whole structure from side view, perimeter truss frame from side view, inner truss frame from side view, whole structure in 3D view.

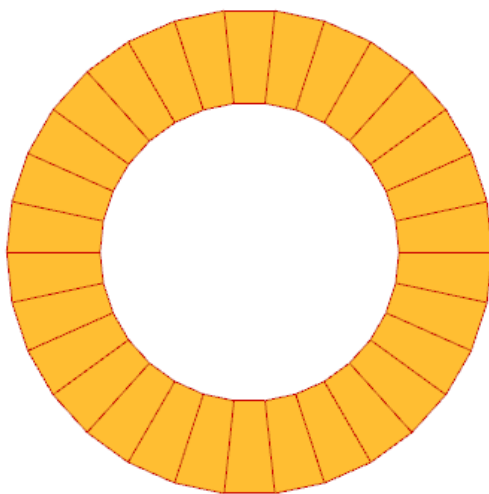


Figure 69: Building section. The radial beams can be seen as the red lines between the inner truss and the outer truss.

Element sizes and mass timber

Preliminary sizing resulted in element dimensions and mass of timber needed for the structural system as shown in Table 18 and Table 19.

Table 18: Element sizes needed according to ULS design.

Dimensions [mm]	S1	S2	S3	S4	S5
Outer columns [h x b]	600 x 600	500 x 500	400 x 400	300 x 300	200 x 200
Outer beams [h x b]	300 x 200				
Outer truss [h x b]	650 x 650				
Inner columns [h x b]	450 x 450	450 x 450	300 x 300	200 x 200	200 x 200
Inner beams [h x b]	300 x 200				
Inner truss [h x b]	650 x 650				
Radial beams [h x b]	500 x 300				

Table 19: Mass of timber required for the various parts of the structural system. Determined using element dimensions shown in Table 18, element lengths from the grasshopper model and mean densities for glulam (430 kg/m³) and CLT (460 kg/m³).

Mass	S1 [10 ³ kg]	S2 [10 ³ kg]	S3 [10 ³ kg]	S4 [10 ³ kg]	S5 [10 ³ kg]	Total [10³ kg]	Part of total mass
Outer columns	182.2	126.5	81.0	45.6	20.2	455.5	2.5%
Outer beams	50.4	50.4	50.4	50.4	50.4	252.0	1.4%
Outer truss	243.4	243.4	243.4	243.4	243.4	1 217.0	6.7%
Inner columns	102.5	102.5	45.6	20.2	20.2	291.0	1.6%
Inner beams	31.0	31.0	31.0	31.0	31.0	155.0	0.9%
Inner truss	239.3	239.3	239.3	239.3	239.3	1 196.5	6.6%
Radial beams	231.6	231.6	231.6	231.6	231.6	1 158.0	6.4%
Slab	2 692.6	2 692.6	2 692.6	2 692.6	2 692.6	13 463.0	74.0%
Total	3 773.0	3 717.3	3 614.9	3 554.1	3 528.7	18 188.0	

Dynamic performance

The acceleration for the top floor at the buildings first natural frequency satisfies the ISO 10137 requirement for both office buildings and residential buildings with a similar margin as the previous proposals. However, the first mode's eigenfrequency for this concept is 0.37 Hz which is higher than for the other proposals.

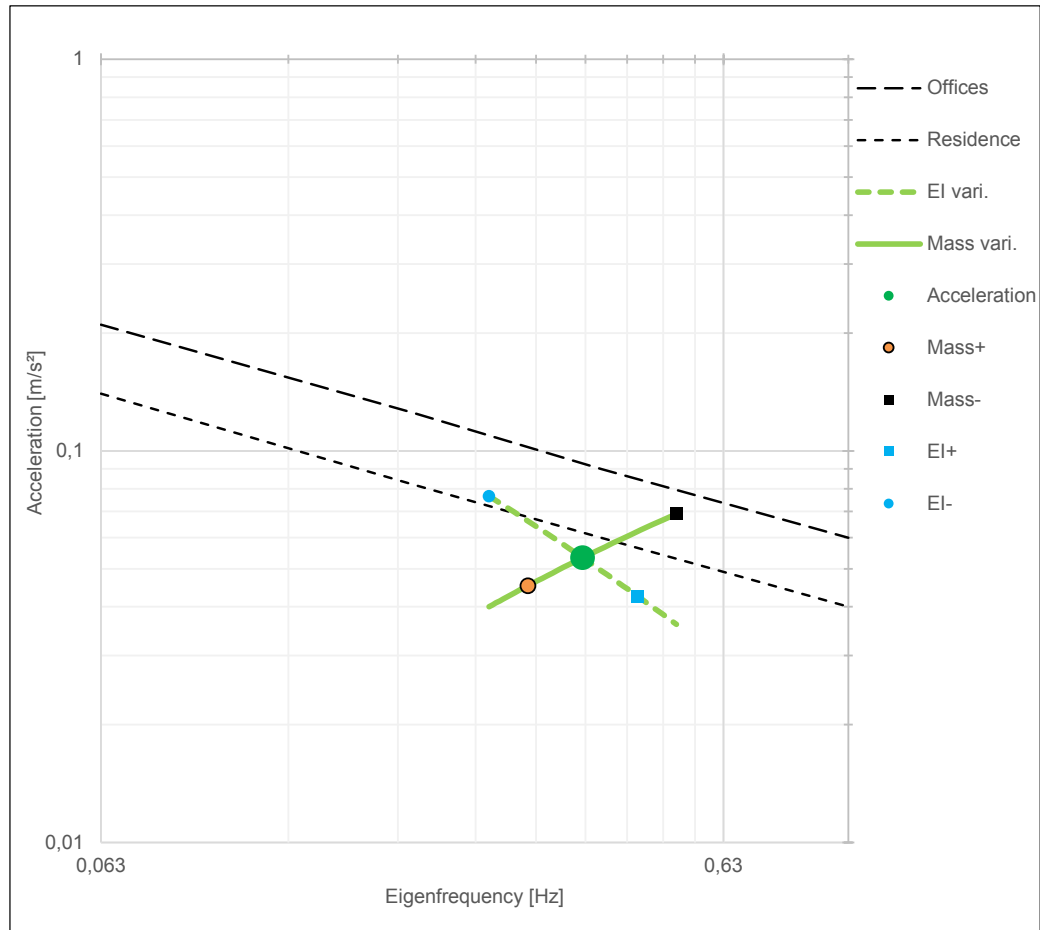


Figure 70: The top floor acceleration compared to the ISO 10137 limits for residential buildings and office buildings. Anticipated trend lines for acceleration change due to increased or decreased stiffness and mass are also shown by the dashed and solid green lines. The calculation is made for a mechanical logarithmic decrement of 10 %.

Compared to the other concepts the radial beams used might be considered as beneficial. The reason why they are included is that the initial model provided much larger spans between the inner and outer truss. However, after adjusting the model with regard to rentable area, the spans decreased significantly and the need for these beams was reduced. Instead they might be somewhat misleading for the results. They are however left in the model since extensive modelling would be required to make such change.

4.5.4 Hyperboloid with continuous perimeter elements and a CLT core

The building facade has the shape of a hyperboloid with a bottom diameter of 74.2 m, a top diameter of 32.2 m and a waist diameter just above 18 m. The waist is located

approximately 145 m above the ground. In the center, a quadratic CLT core is placed, measuring 10 x 10 m. The core design is determined according to section 4.2.

As a consequence of the generative analysis and the geometrical type, the truss has a varying diagrid-like pattern. At the bottom part, there is almost 14 stories between the truss intersections. However, at the waist, the truss pattern approaches a density of one intersection per floor. The buckling length is though much shorter since the truss connects to the perimeter beams and carries the floors. As a result of this, the buckling length is approximately equal to the height of one story, 3.33 m.

Specifically, for this concepts, as the beams along the perimeter are directly connected to the truss system, the beam lengths varies around the perimeter on each floor as well as each story. However, all of these beams are designed section-wise resulting in significantly over-sized beams for the short spans. Illustrations of the truss, core and structure in general can be seen in Figure 71 and Figure 72.

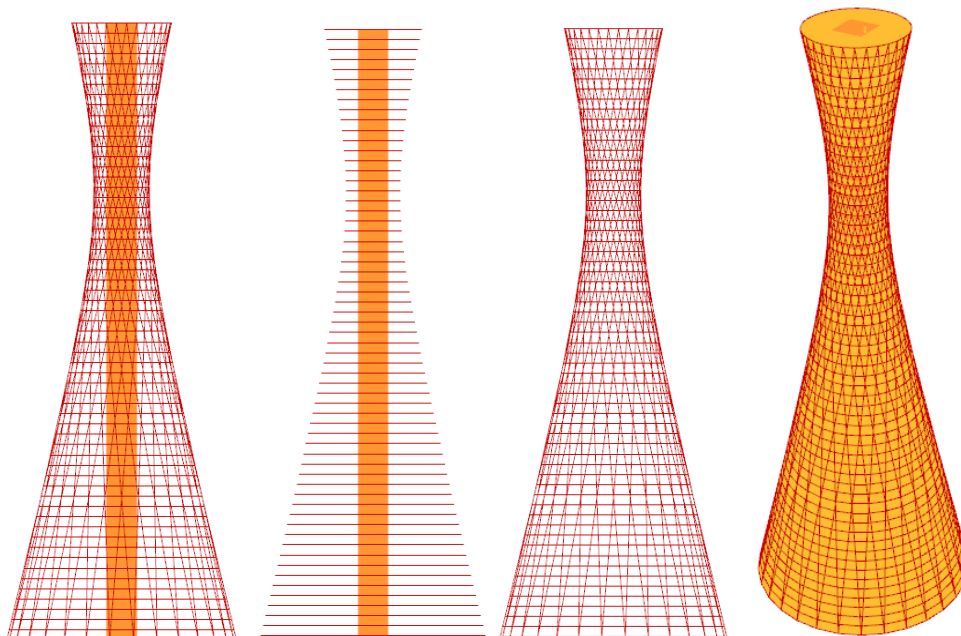


Figure 71: Illustration of the model, from the left: Whole structure from side view, slabs and core from side view, truss and beam system from side view, whole structure in 3D view.

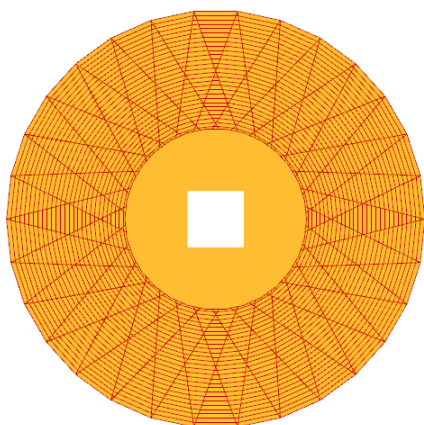


Figure 72: Top view of the building.

Element sizes and mass timber

Preliminary sizing resulted in element dimensions and mass of timber needed for the structural system as shown in Table 20 and Table 21.

Table 20: Element sizes needed according to ULS design.

Dimensions [mm]	S1	S2	S3	S4	S5
Outer beams [h x b]	500 x 400				
Truss [h x b]	550 x 550				
Core [t]	3600	1050	300	250	250

Table 21: Mass of timber required for the various parts of the structural system. Determined using element dimensions shown in Table 20, element lengths from the grasshopper model and mean densities for glulam (430 kg/m³) and CLT (460 kg/m³).

Mass	S1 [10 ³ kg]	S2 [10 ³ kg]	S3 [10 ³ kg]	S4 [10 ³ kg]	S5 [10 ³ kg]	Total [10 ³ kg]	Part of total mass
Outer beams	208.1	148.9	94.6	61.0	86.3	598.9	3.2%
Truss	315.4	315.4	315.4	315.4	315.4	1 577.0	8.5%
Core	2 561.5	747.1	213.5	177.9	177.9	3 877.9	21.0%
Slab	6 627.8	3 312.2	1 232.4	382.9	886.0	12 441.3	67.3%
Total	9 712.8	4 523.6	1 855.9	937.2	1 465.6	18 495.1	

Dynamic performance

The acceleration for the top floor at the buildings first natural frequency satisfies the ISO 10137 requirement for office buildings, but it is a little above the requirements for residential buildings as shown in Figure 73. The first mode's eigenfrequency for this concept however highest among the considered proposals with a value of 0.55 Hz.

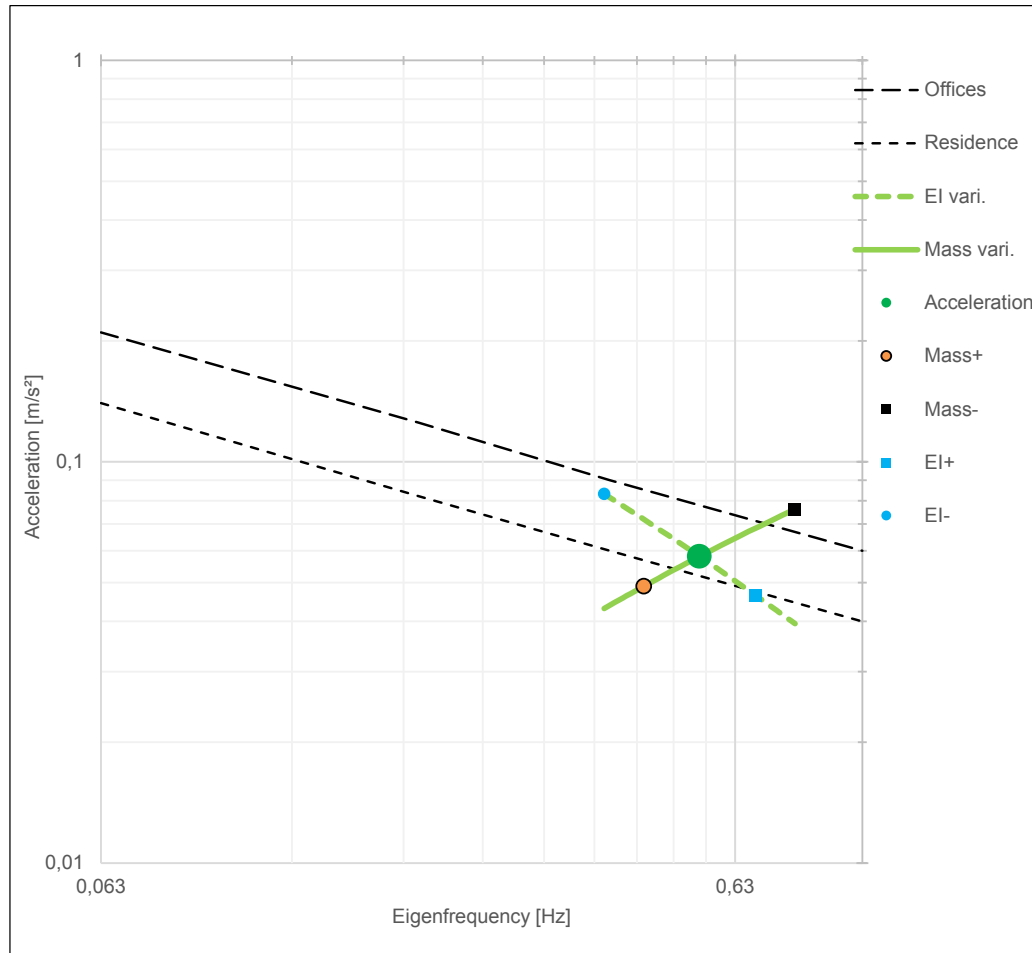


Figure 73: The top floor acceleration compared to the ISO 10137 limits for residential buildings and office buildings. Anticipated trend lines for acceleration change due to increased or decreased stiffness and mass are also shown by the dashed and solid green lines. The calculation is made for a mechanical logarithmic decrement of 10 %.

4.5.5 Hyperboloid perimeter truss-frame system with stabilizing core

The global geometry of this model is exactly the same as for the hyperboloid with continuous elements shown in section 4.5.4. This is obtained by extracting the slab diameters from that model and using it as input values when generating this geometry. By doing so, a comparison can be carried out with two different façade load bearing systems, the one with continuous straight elements ranging from the top rim to the bottom and this one, with a perimeter truss-frame where the elements changes direction at every floor.

On the whole, the structure is similar to the one shown in section 4.5.4. The slabs, core and global geometry are all the same, although sized differently in the preliminary design. The significant difference can be seen in the façade truss frame system. The columns join the corners of each floor and due to the hyperbolic shape, they are not

vertical. Also, a diagrid truss is used to generate stability at the perimeter. Since this model has columns taking care of the major vertical loads along the perimeter, a relatively low truss-ground angle is used with one truss spanning across each storey. However, since the slabs are of varying size, the truss angles are also varying along the building height. This truss density is chosen to provide resistance against horizontal loads, but also since it joins the truss better to the building. A sparser truss pattern would result in trusses outside the facade.

One drawback for this system is the non-vertical columns which might result in additional forces in the slabs. A factor that needs special consideration in detailed design.

Illustrations of the truss frame, core and building as whole can be seen in Figure 74 and Figure 75.

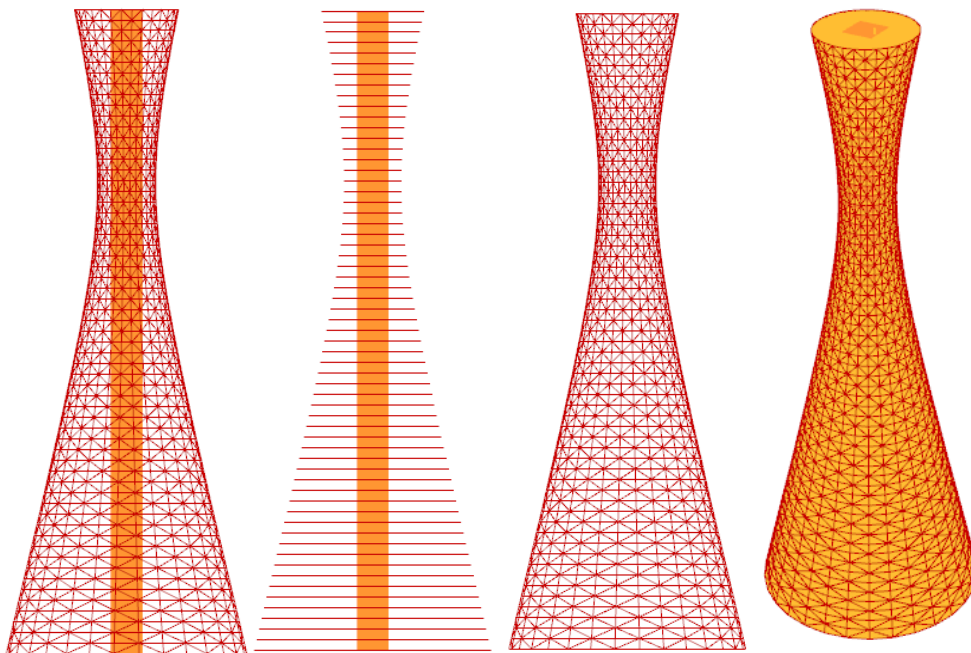


Figure 74: Illustration of the model, from the left: Whole structure from side view, slabs and core from side view, truss frame system from side view, whole structure in 3D view.

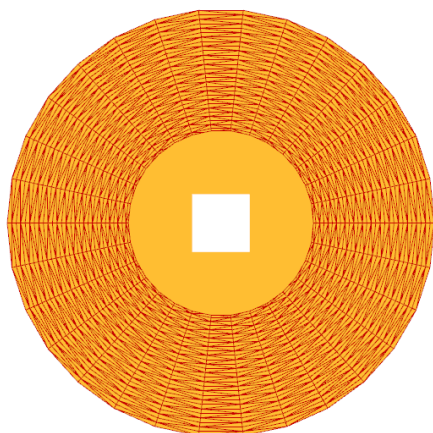


Figure 75: Top view of the building.

Element sizes and mass timber

Preliminary sizing resulted in element dimensions and mass of timber needed for the structural system as shown in Table 22 and Table 23.

Table 22: Element sizes needed according to ULS design.

Dimensions [mm]	S1	S2	S3	S4	S5
Columns [h x b]	750 x 750	500 x 500	350 x 350	200 x 200	200 x 200
Beams [h x b]	500 x 400				
Truss [h x b]	400 x 400				
Core [t]	3550	1100	300	250	250

Summarizing the material volume and material densities gives the following timber consumption for each element type, section and the total building.

Table 23: Mass of timber required for the various parts of the structural system. Determined using element dimensions shown in Table 22, element lengths from the grasshopper model and mean densities for glulam (430 kg/m³) and CLT (460 kg/m³).

Mass	S1 [10 ³ kg]	S2 [10 ³ kg]	S3 [10 ³ kg]	S4 [10 ³ kg]	S5 [10 ³ kg]	Total [10 ³ kg]	Part of total mass
Columns	292.5	129.7	63.1	20.3	20.5	526.1	2.9%
Beams	208.3	149.0	94.8	61.0	86.2	599.3	3.3%
Truss	184.6	143.9	111.2	94.6	104.0	638.3	3.5%
Core	2 525.9	782.7	213.5	177.9	177.9	3 877.9	21.4%
Slab	6 630.7	3 314.5	1 233.5	382.4	883.2	12 444.3	68.8%
Total	9 842.0	4 519.8	1 716.1	736.2	1 271.8	18 085.9	

Dynamic performance

The top floor acceleration at the building's first natural frequency does not satisfy the ISO 10137 requirement for office buildings as shown in Figure 76. Although, it is only marginally above the limit for the chosen mechanical damping of 10%. Therefore, in order to completely reach the levels needed for offices and residential buildings further dynamical improvements are needed. The first mode's eigenfrequency for this concept is 0.42 Hz.

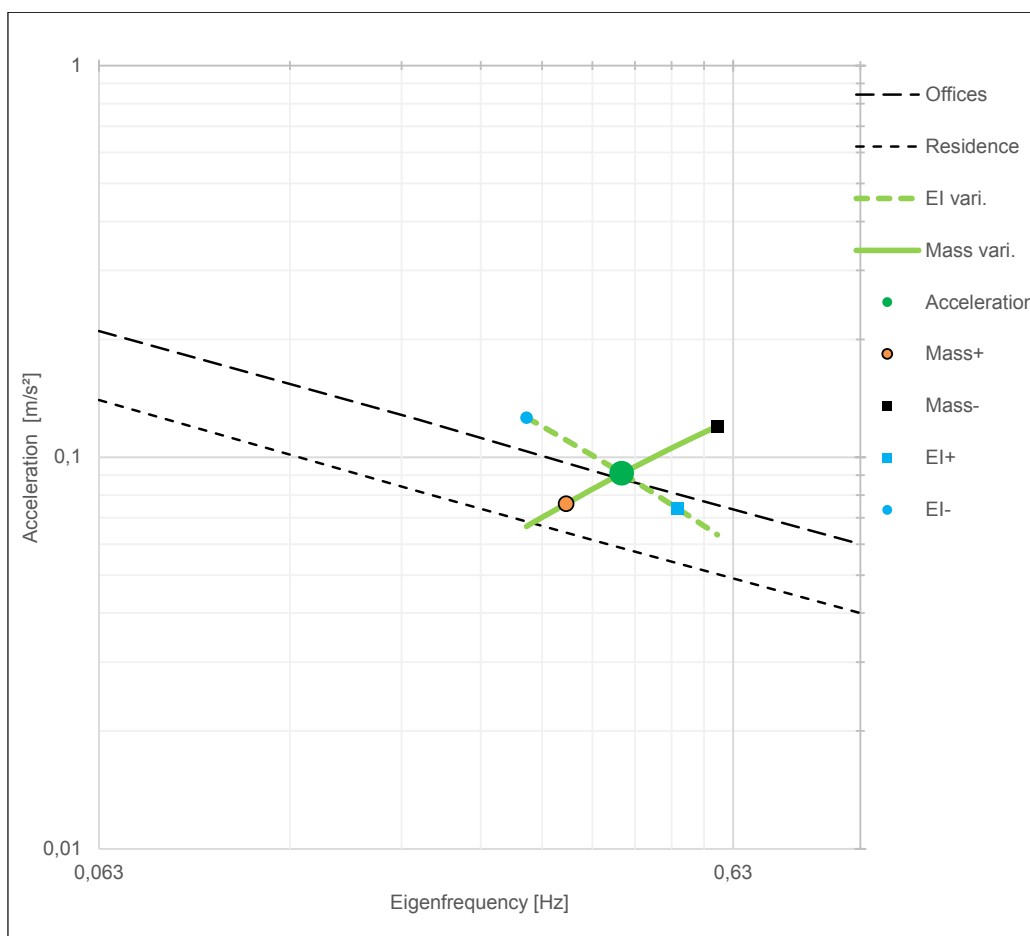


Figure 76: The top floor acceleration compared to the ISO 10137 limits for residential buildings and office buildings. Anticipated trend lines for acceleration change due to increased or decreased stiffness and mass are also shown by the dashed and solid green lines. The calculation is made for a mechanical logarithmic decrement of 10 %.

5 Evaluation

When developing a structure, all hard requirements such as capacities, deflections and accelerations must be fulfilled. Therefore, a pass or fail criterion in any of these properties cannot be used when evaluating and comparing proposals. However, one of these properties can be compared for different buildings. By coupling the hard requirements with other measures, they can be included in the evaluation. Also, the evaluation will be based on other factors which are allowed to vary more while still fulfilling the building code requirements. However, these criteria can be compared for different buildings, showing the overall building performance. Apart, from the criteria connected to structural performance, measures related to cost and constructability are also of importance when choosing a winning concept.

5.1.1 Rentable area

In order to make the proposals comparable a relatively similar rentable area has been aimed for in design. Therefore, comparing the different concepts, a value of approximately 75 000 m² was chosen as the target area.

In Figure 77, the rentable area is shown for each of the proposals. In general, they are of similar magnitude. However, the mega truss with hollow center differs a bit from the others. This is since it requires a certain diameter for the hollow center to be efficient. Also, reducing the outer diameter would make an already thin structure even thinner. The difference is however considered as marginal for the building performance.

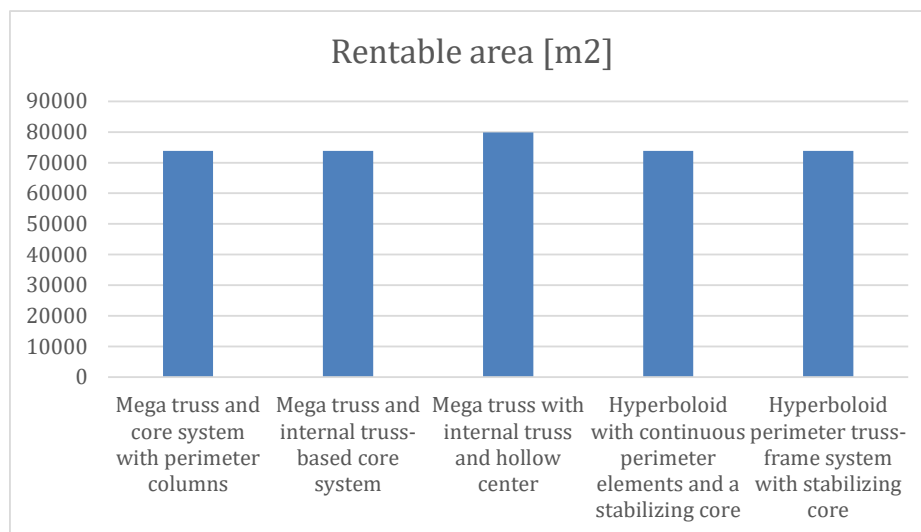


Figure 77: The rentable area for each proposal.

Included in the rentable area is all floor space except for the cores.

5.1.2 Mass timber per area of rentable space

The various concepts will all require different amounts of material for their structural system. One way to quantify the used amount of material is by the total mass of the structural system. A large building will naturally be heavier than a small one, but it might also give larger return. Therefore, it is of interest to normalize the mass and make

it comparable for different buildings. To do this, the mass per rentable floor area is determined.

By comparing the mass per area of rentable space, the buildings can be evaluated on how structurally efficient they are at producing just rentable space. This aspect is of major interest for many commercially produced buildings. However, it does not account for other factors such as daylight and view, two factor that determines the value of the rentable space.

In Figure 78, the mass of timber per area of rentable space can be seen. The result shows that most of the proposals are relatively equal with a timber consumption between 245 and 250 kg/m². The alternative with lowest consumption of timber per rentable area is the mega truss with hollow center, which uses less than 230 kg/m².

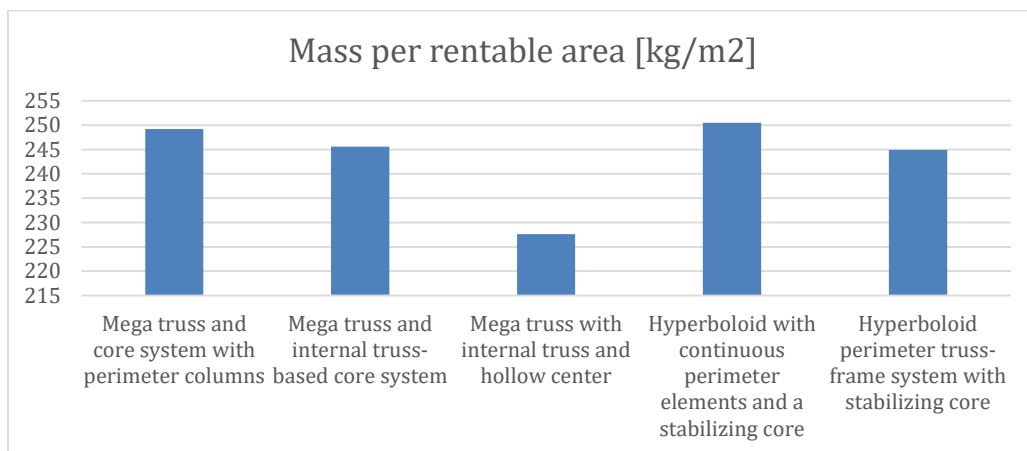


Figure 78: Mass timber per area of rentable space for the investigated concepts.

5.1.3 Used ground area

In many cases it is necessary to occupy as little ground area as possible. Especially when operating in dense urban areas. For these cases it might be of interest to evaluate the concepts by their footprint on the ground. A rough comparison can be made from the occupied ground area as shown in Figure 79.

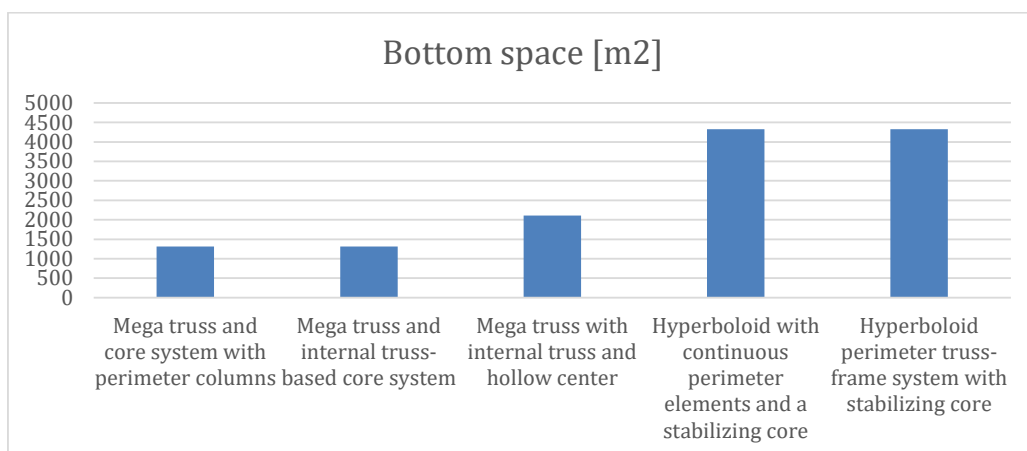


Figure 79: Ground footprint areas for the investigated concepts.

From the figure, the smallest ground footprints are made by the cylindrical mega trusses, second is the hollow core, while the hyperboloids have a ground footprint of more than 3 times the size of the cylindrical mega trusses.

5.1.4 Daylight

If the daylight requirements are not fulfilled, the value of large floor areas is small. Therefore, it is of high importance to maximize the part of the building with enough daylight. By examining the proposals and comparing them to the rule of thumb mentioned in section 2.9.4, the quality of the available floor area can be evaluated daylight wise.

The daylight is evaluated as a ratio between the area with acceptable or good daylight and the total rentable floor area. Results for the different proposals can be seen in Figure 80. Observing the ratios, it can be concluded that most of the proposals are equal with values around 65-80 %. The one unique concept is the mega truss with hollow core in which 100 % of the floor area is within 10 m from the façade.

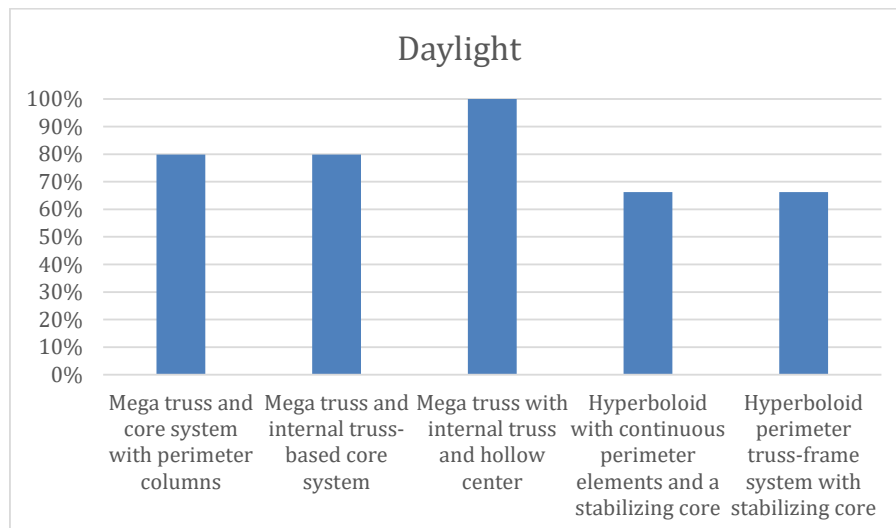


Figure 80: Percentage of rentable floor area with acceptable or good daylight.

Worth mentioning is that these daylight evaluations are made in a simplistic manner, only accounting for the distance between the façade walls and the usable spaces. In reality, the daylight will be influenced by an array of other factors. Especially for these proposals, with relatively large timber elements, the ratio of the façade that is covered by the structural system will have a large influence on the daylight. Also, assuming a similar amount of daylight entering the building from the hollow center as the external façade is clearly optimistic.

In a simple analysis like this, these factors and many others are hard to account for, but they must all be included in a detailed daylight analysis. However, in this thesis, the daylight is mostly used as a property to limit the building dimensions to realistic values.

5.1.5 Number of joints

The number of joints in a structure has a large influence on the building cost. This stems from an array of factors, some of which are detailing work, assembly and cost for the joint components. A low number of joints can therefore be the critical difference when choosing between different equally performing alternatives.

Figure 81 shows the estimated number of joints required for each of the proposals. The best alternatives according to their estimated number of joints are the two cylindrical towers with CLT and truss cores, as well as the hyperboloid with perimeter truss frame. These are all having approximately 4 000 joints. The two remaining concepts do have more than twice the number, being in the range 8 000 and 9 500 joints.

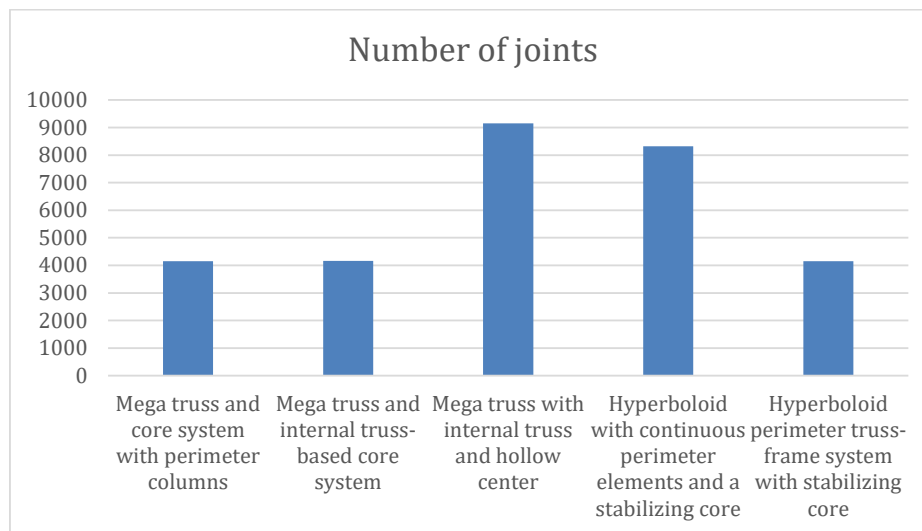


Figure 81: Number of structural joints needed for the different proposals.

The number of joints is calculated manually in the models by looking at the element intersections. Connections between columns, trusses and beams are counted as one joint per intersection while the slab and shear wall have one joint for each edge intersection.

Worth mentioning is that simply supported connections often are simpler to construct than for example connections between 4 truss edges, 2 beam edges and 2 columns which all can be in one joint. In the Hyperboloid with continuous perimeter elements there are also intersection between the trusses themselves which are calculated as joints.

5.1.6 Vertical deformations

In order to evaluate each proposal's structural efficiency regarding vertical loads, the elastic vertical deformations for each concept were determined. For these results, the proposals were modelled with infinitely stiff slabs in order to remove local deformations in the model. The deformations are determined for a combination of self-weight and imposed load.

In Figure 82, the results are displayed. For this evaluation criterion, the hyperboloid structures are highest performing with vertical deformations around 25-40 mm. The cylindrical mega trusses and mega truss with hollow center have higher deformations around 65-80 mm.

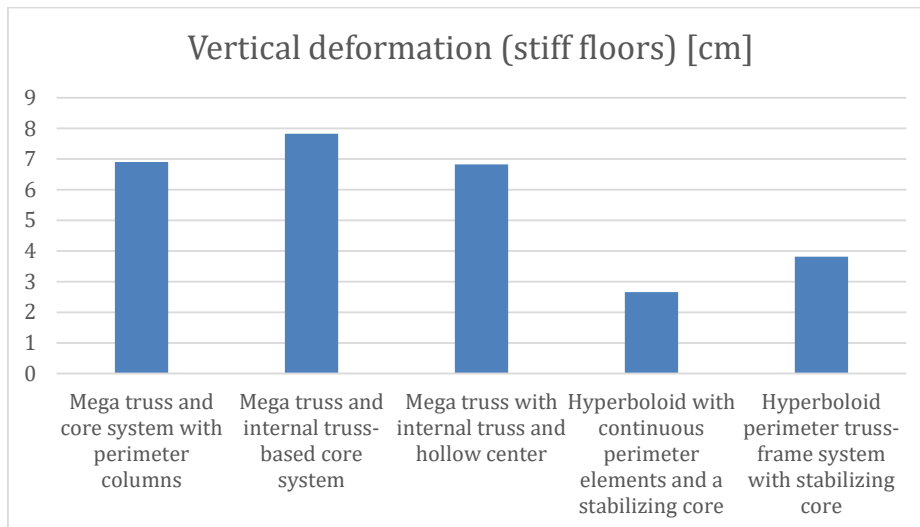


Figure 82: Total instantaneous vertical deformation for the investigated concepts using stiff floors and a combined loading with self-weight and imposed load according to the characteristic load combination in SLS.

When determining the vertical deformations, the loads has been applied according to the characteristic load combination for SLS.

5.1.7 Horizontal deformations

To evaluate the global resistance against horizontal loads, the horizontal deformations has been measured and compared. By doing so, the buildings efficiency at resisting wind loads can be evaluated. A high resistance against wind loads can be accomplished either through high stiffness, an aerodynamic shape or a combination of the two. The best performing buildings must be both stiff and aerodynamically shaped.

Observing the results in Figure 83, there is a relatively small difference between the various concepts. All the proposals have a horizontal deformation of 95-120 mm apart from the hyperboloid with continuous truss elements, which has as low deformation as 48 mm.

The hyperboloid structure with continuous truss elements has a slender upper half, reducing the area subject to critical wind loads significantly. Also, as the truss elements are continuous and straight, they are working in a nearly optimized way, improving the stiffness and strength significantly compared to the other hyperboloid structure. These factors together with the round plan shape result in almost insignificant horizontal deformations.

The mega truss with hollow center has a larger diameter, although it is also circular. The large wall area for the mega truss proposals results in much higher wind loads than for the hyperboloids. However, the horizontal deformations show that these are well managed by the stiff structures.

When determining the horizontal deformations, the characteristic load combination for SLS is used.

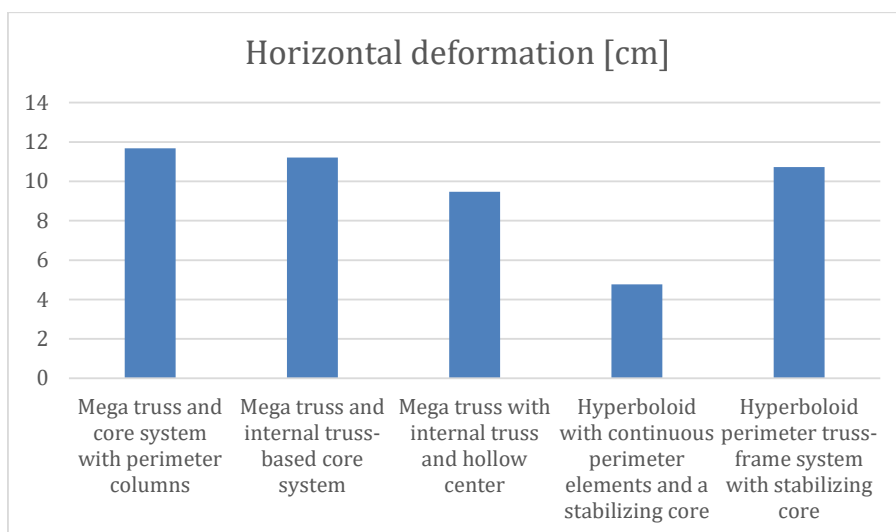


Figure 83: Peak horizontal deformations for the different concepts subject to the characteristic load combinations in SLS.

5.1.8 Foundation moment due to wind

As a measure of the wind load level on the structures, the total global foundation moment due to wind is determined. Comparing the results in Figure 84 to the proposal sizes, there is a clear correlation between the façade area facing the wind, and the foundation moment. Analysing the results for horizontal deflection and foundation moment can therefore give an indication whether the wind resistance is relying more on stiffness or aerodynamics.

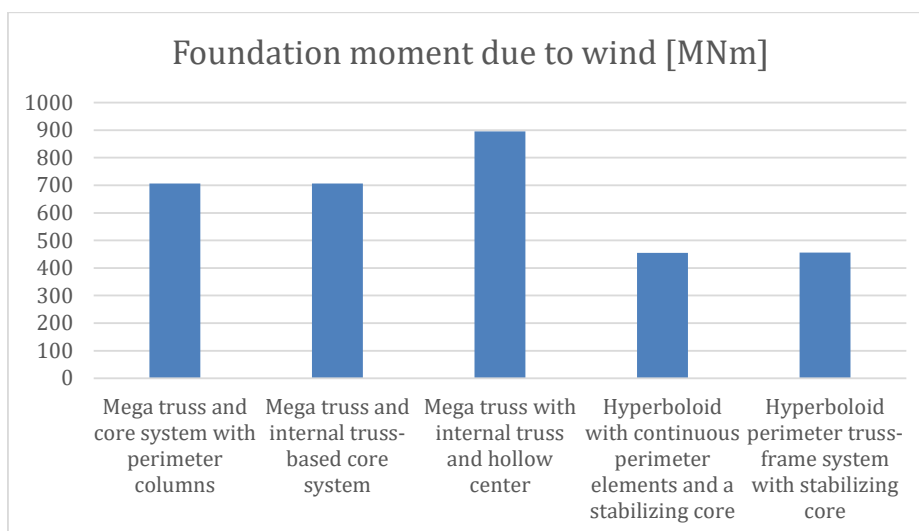


Figure 84: Foundation moment due to wind.

Notable is that the vertical force component from the wind loads are neglected when determining the foundation moment. They are both small to the magnitude, has relatively short lever arms and counteracts each other to some extent. This simplification is only made for the hyperboloids since they are the only concepts modelled with vertical wind force components.

Also, the foundation moment is determined strictly in the along-wind direction. Since the wind load acts symmetrically, elongating the structure in the cross-wind direction, the cross-wind components are not affecting the foundation moment when using this load model. Therefore, the foundation moment is simply calculated as the sum of all along-wind force components multiplied by their lever arm.

The load combination used when obtaining the values is based on ultimate limit state with all loads considered as unfavourable.

5.1.9 Dynamic performance

For tall lightweight structures, the dynamic properties are often crucial in design. Therefore, the investigated concepts have all been evaluated according to EKS11 and SS-EN 1991-1-4 and compared to the requirements given in ISO 10137.

One influencing factor that is hard to predict when determining the peak acceleration of a structure, is the mechanical damping. When reading SS-EN 1991-1-4, approximative logarithmic decrements are specified for various structures. For steel and concrete structures, a common theme can be observed. The logarithmic decrement attains a slightly higher value for buildings than it does for bridges. Also, it is stated that the logarithmic decrement for timber bridges often are in the range 6-12 %. From this, it seems reasonable to assume the mechanical part for a building within the range 5-15 %. However, due to the uncertainties, a value of 10 % has been used when calculating the dynamic performance for each proposal.

Furthermore, since there are no clear guidelines. For the direct dynamic comparison, the top floor acceleration has been determined for various mechanical damping levels. Results and comparison between the proposals, for 0-10 % mechanical logarithmic decrement, are shown in Figure 85.

Important to know about the results is that all joints are assumed as fully rigid and therefore not allowing for any slip. This is not completely realistic although resin injections can provide high joint rigidity. Due to the massive increase of labour needed if gluing all joints, the realistic approach would be to glue the critical joints only. Thus, finding a balance between additional work and loss of stiffness. Since there is a correlation between mechanical damping and joint rigidity, one could argue that loose joints might be beneficial since it allows for higher mechanical damping. However, it would result in lower global stiffness.

Reviewing the results with the assumption on stiffness and mechanical damping in mind, it is clear that most of the structures are close to the limit for office buildings. The hyperboloid with truss frame performs poorly and would most likely not fulfill the requirements for top floor accelerations. On the other side of the spectrum, the circular towers perform good and satisfies the requirements for both offices and residential buildings when using a high mechanical damping. However, with a lower mechanical damping assumed, even the limit for offices is getting close.

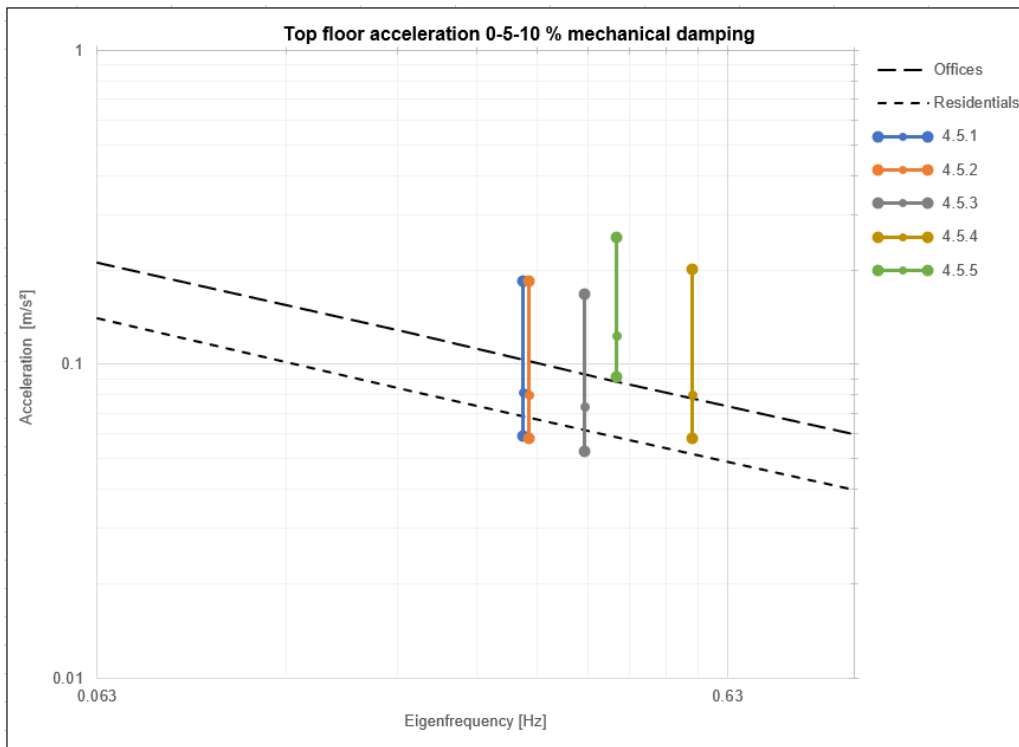


Figure 85: Top floor accelerations for the investigated concepts with 0-5-10 % mechanical damping. The number of each line in the legend is referring to the heading number of the concept in the report.

Important notes on the dynamic calculations is that they are based on the assumption that the structure has a constant mass along its main axle. This is not completely the case for these buildings since two are hyperbolically shaped. Also, all buildings are divided into five sections with different element sizes, resulting in a variation in mass.

Furthermore, the calculation procedure used to determine the top floor acceleration is based on a global cantilever action. All proposals are behaving like this when observing the deformations, but they do have shear deformations as well. Giving room for an additional error margin.

5.1.10 Result summary

From the results above, the proposals can be evaluated from their performance for each of the criteria. Since the aim of this project is to find suitable structure for a 200-meter-tall timber tower, the structural performance is of highest priority. In practise economy is a crucial aspect. However, for this project it is not chosen as the main evaluation criterion. This means that the primary selection will be based on:

- Vertical deformations.
- Horizontal deformations.
- Foundation moment.
- Dynamic performance.

Where the dynamic performance is considered most important. The primary evaluation is therefore based on all these factors; however, high performance dynamically is considered more beneficial than a similar difference for another criteria.

5.1.10.1 Primary evaluation

In order to make a clearer overview for the most interesting evaluation criteria, a summarizing graph has been made and shown in Figure 86. The graph shows the vertical and horizontal deformations as well as the foundation moment due to wind for each concept. Considering the included measures, a high performance is coupled with low values. The lowest horizontal deformations are measured for the hyperboloid with continuous truss elements while both hyperboloids perform well regarding vertical deformations. The cylindrical concepts are all relatively similar deformation-wise. However, the concept with hollow center performs slightly better than the two others regarding horizontal deformations.

Considering the wind load in terms of foundation moment and the horizontal deformations, a comparison can be made. In a simplified way, the horizontal deformations show how well the building can handle wind loads while the foundation moment assigns a value to the actual wind load on the building. Therefore, a generalized comparative evaluation based on the two measures can be made as follows:

- Low horizontal deformation coupled with high foundations moment means high structural stiffness and poor aerodynamics.
- High horizontal deformation coupled with low foundation moment means great aerodynamics but poor structural stiffness.

This way of reasoning means that the two cylindrical towers with CLT core and truss core have average aerodynamics. However, they are comparably weak. The cylindrical tower with hollow center takes the largest wind loads while still deforming comparably little and is thus a stiff structure. The hyperboloids are great aerodynamically. However, the concept with continuous truss elements is also really stiff, resulting in the overall smallest horizontal deformations. In opposite, the hyperboloid with perimeter truss-frame do show relatively large deformations, a result of comparably poor stiffness.

Comparing the two proposals with the lowest horizontal deformation, both handles the wind loads in an efficient way, but the hyperboloid has the best aerodynamical performance.

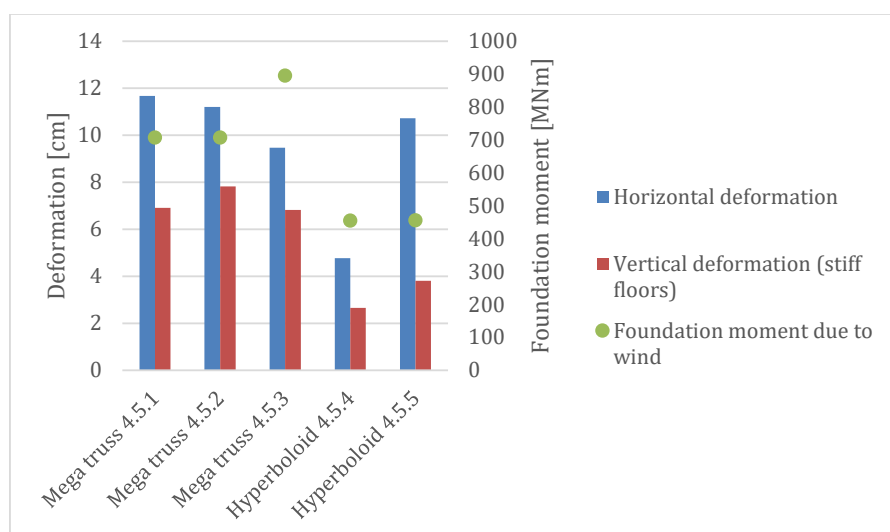


Figure 86: Summarizing graph with horizontal deformations, vertical deformation and mass per rentable area.

Reviewing the dynamic results in Figure 85 shows that the cylindrical buildings are the best alternatives when it comes to dynamic performance. These are both spanning the gap between the requirements for residential buildings and office buildings. The hyperboloid with continuous perimeter elements can reach the requirements for offices provided that a mechanical damping of 6 % can be ensured. However, for the other hyperboloid, the dynamical requirements seem to be out of reach. Anyway, all proposals might still have potential to reach the limits for office buildings with some adjustments and potentially an external damper at the building top.

Considering these results there are two concepts performing better than the others regarding the structural factors. These two concepts are the following ranked in descending order:

- 4.5.3 Cylindrical tower with hollow center.
- 4.5.4 Hyperboloid with continuous truss.

Since the cylindrical tower with hollow core performs superiorly in the dynamic analysis it is considered as the winner when it comes to structural aspects. However, the hyperboloid with continuous truss performs better when it comes to the handling of wind loads as well as global deflections.

5.1.10.2 Secondary evaluation

In order to make a quick comparison of the two remaining concepts for the non-structural properties. A simple ranking system is made for each criterion as shown in Table 24. The ranking is made for each concepts whereafter the number of 1st and 2nd places are counted. The winner is chosen with the largest amount of 1st places.

Table 24: Evaluation matrix for a simple evaluation of the lower prioritized evaluation criteria.

<i>Evaluation matrix</i>	1st	2nd
Mass per Rentable area	Cylindrical tower with hollow center.	Hyperboloid with continuous truss elements
Occupied ground area	Cylindrical tower with hollow center.	Hyperboloid with continuous truss elements
Daylight	Cylindrical tower with hollow center.	Hyperboloid with continuous truss elements
Number of joints	Hyperboloid with continuous truss elements	Cylindrical tower with hollow center.
Cylindrical tower with hollow center.	3	1
Hyperboloid with continuous truss elements	1	3
Result	Cylindrical tower with hollow center.	Hyperboloid with continuous truss elements

Observing the evaluation matrix, one can conclude that it only strengthens the ranking made in the structural evaluation. Therefore, since the cylindrical tower with hollow center performs best, both structurally and for many of the secondary criteria, it is the most promising concept for a potential 200 m tall timber tower.

5.2 The 200 m timber tower

Judging by the evaluation the cylindrical tower with hollow center is the best. As described in section 4.5.3, it consists of a perimeter frame with mega trusses as well as an internal frame with mega trusses. These two stabilizing systems are joined with radial beams and the slabs. The final concept is shown in Figure 87. The material used for the truss frame systems is GL30c while the slabs are chosen as Trä8-elements.



Figure 87: The 200 m timber tower.

The major benefits of this design are that it is a stiff structure and a structural design that allows for a large building diameter. It has comparably good aerodynamics and dynamic performance. Due to its dimensions, it provides a large rentable area with possibilities for good daylight. The mass per rentable area is also good compared to the other proposals.

In total, this building will require relatively large amounts of timber. However, this can be beneficial in one way, since it generates mass necessary for the dynamic performance. Also, building a tower of this size, a large timber consumption cannot be avoided. Furthermore, the large structure with its long truss frames and many slab elements will have a significant number of joints. These will result in additional labour and overall cost in order to ensure high joint quality. Apart from the construction related issues, the building is not really slender. With a diameter of 52 m and height of 200 m, the slenderness ratio will be around 1:4. In other words, a relatively wide building.

Considering the model used in this evaluation, significant simplifications have been made. Therefore, in order to fully determine whether this proposal can be realized, deeper investigations must be made for an array of various factors. A few of these are fire design, detailed daylight analysis, structural long-term effects, geotechnical investigations and foundation work, detailing of technical installations, detailed structural design. Also, since the building is of such height, a wind tunnel study will be of interest in order to study the true behaviour of the structure.

In order to illustrate the properties of this proposal, some technical data of *the 200 m timber tower* are summarized in Table 25 below.

Table 25: Approximate values for technical data of the final concept.

Mass	18 188 tonnes
Rentable area	79 900 m ²
Mass per rentable area	227.6 kg/m ²
Bottom space	2 108 m ²
Foundation moment due to wind	895 MNm
Eigenfrequency	0.37 Hz
Peak acceleration	0.168-0.073-0.053 m/s ²
Horizontal deformation	9.5 cm
Vertical deformation (stiff floors)	6.8 cm
Number of joints	9 150
Daylight	100 %

6 Discussion

Investigating the possibilities to build a 200 m tall timber building is a large topic. In order to get the theoretical framework to base critical choices upon, a substantial amount of work was dedicated to the literature study. However, choosing the right topics to consider when modelling and evaluating was a continuous process, based on a constantly changing knowledge basis. If aiming for the best possible timber building reaching 200 m above the ground, a few changes might have been necessary during the study. However, the time limits significant changes late in the project and the obtained results are all consequences of the earlier made choices. These choices, as well as considered regulations, available knowledge and the software used have all shaped the result for *the 200 m timber tower*.

6.1 The 200 m timber tower

Reviewing the current tallest timber structures, it was obvious that they all, had been made in a somewhat conservative manner. Often based on truss frames with a box shaped global geometry. Therefore, one of the first conclusions during the initial project phase was that, in order to build taller, the building shape needed improvement. Taking inspiration from some of the world's tallest buildings and reading more about building aerodynamics, the circular ones seemed to be the most promising alternatives. The proposal development was therefore based on this shape.

The Y-shape an advantage in the possibility to generate high stiffness without the need of a thick structure. This, by increasing the wing length, resulting in a larger internal lever arm. The drawback is though the concave side catching lots of wind, driving the construction sizes to larger dimensions. Also, it requires massive amounts of materials since it is mostly based on CLT elements.

A disadvantage of the Y-shape applied for the buttressed core system is the complexity of the model. Trying to fully parametrize the buttressed core model would require a massive amount of work, but since it is used for the worlds current tallest building, it is reasonable to assume that a high performance could be expected for a fully optimized buttressed core system. As a result of the project time frame and the geometrical complexity when parametrically modelling a buttressed system, it had to be excluded from the study.

Regarding the circular shape, it has a superior performance when it comes to aerodynamics. However, its thickness is somewhat limited due to the large slabs and small areas within acceptable distance from the windows. At the same time, its stiffness is strongly depending on the building diameter resulting in a situation where stiffness and the building thickness must be compared, judged and weighted against each other. Trying to find the optimal shape, a few different concepts, all based on the circular section were developed. Two basic cylindrical towers mainly used as a base model showing the difference in performance for two different core types. Also, to utilize curvature stiffness, a hyperboloid shape was developed. It was later applied to two different structural systems; one traditional truss frame and one with a truss system based on continuous truss elements only. This to evaluate an eventual benefit of using straight continuous elements spanning from the roof all the way to the foundation.

It turned out that the hyperboloid with perimeter truss frame was a poor solution. Partly since the non-vertical columns induce large forces in the slabs. But also, since the system is significantly weaker than the other hyperboloid.

Using straight continuous elements, the material could be used in a more optimized way resulting in a high performing building. Actually, the concept of a hyperboloid with continuous truss elements is most likely good enough to use for a 200 m tall building after detailed design. During the evaluation, it acquired a clear 2nd place. Also, it has values such as good stiffness and the architectural impression of a landmark building.

The 200 m timber tower, or the cylindrical tower with hollow center, does combine many of the sought for properties. It has a high stiffness, good mass per rentable area and allows daylight to enter the entire structure resulting in a large valuable floor area. It might appear as a bit bulky with its large diameter. However, it performs clearly best structurally while still leaving room for improvements. One critical aspect is to make sure that the structure is rigid enough to not lose its pipe-like shape. To counteract eventual problems in this area, it is possible to include a 3D truss within the hollow center or include a number of shear walls within the building. Any of these changes might be used to stiffen up the structure if needed. Also, in order to fully complete the building, elevator shafts must be included.

Furthermore, there is a number of possible building shapes that have not been investigated. Various types of tapers or setbacks might also be of benefit if applied to any of the circular structures, as well as other diameters for the perimeter and the hollow center. A combination of the two best performing concepts might also make an interesting design, with an external hyperboloid perimeter truss based on straight continuous elements, and an inner circular truss frame, a new possibly even better structure might be within reach.

6.1.1 Possible and needed improvements

In order to make the tower completed there are a number of areas requiring further analysis and improvement. Some examples that might have noticeable impacts on the design are:

- Detailed design regarding wind loads.
- Design for service limit state, both for local elements and global behaviour.
- Fire design. Protection against fire spreading, evacuation routes and sufficient load bearing resistance in case of fire might all require changes in the structural design.
- The foundation design, where the design allows for sufficient loads transfer between the building and the ground.
- All comfort related issues such as installations and daylight design must be carried out since they in some cases might affect the structural composition of the building.

All different aspects must be synchronized in a way that allows for best possible topological optimization. With a well-developed topology, the completed optimized structure can be achieved through continuous element sizing, aiming for high utilization ratios through the entire structure. As shown in Appendix X, the preliminary design in this project resulted in low utilization ratios for many of the elements. This means that there is room for improvement in the area.

As low utilization ratios imply over-consumption of material, optimization might be considered as an ethical aspect. Therefore, in order to build in a sustainable way, both topological optimization and element optimization must be thoroughly considered in any design. However, reducing the material consumption could also reduce the weight of the top third of the building, impacting the dynamic performance. This highlights the complexity in building design, since the change of one parameter might often result in a chain reaction where multiple other areas are affected.

If having a hard time fulfilling the dynamic requirements, there are various dampers available. By introducing such systems to the structure, its dynamics can be improved in multiple ways. For example, by increasing the mass in the top third of the structure. But also, by increasing the damping significantly. By comparing the results with a variation of the logarithmic decrement for mechanical damping, it is clear that an increased damping can have a significant impact on the dynamic response for a building. Also, added mass in a building's top portion can result in major dynamical improvements, especially for structures with eigenfrequencies below 1 Hz. One common way to increase the building mass at the top portion of the building is by using concrete elements, mostly concrete slabs. However, this project has been carried out trying to avoid the use of concrete.

Furthermore, the proposals considered have been designed to avoid outrigger effects. This to not over-estimate the structural stiffness of the concepts. However, using outriggers could be a way to improve the structural behaviour and increase the global stiffness. When discussing the topic of outrigger systems, one could argue whether a discrete approach or a more continuous approach would be preferable. However, this must be determined depending on the specific circumstances for one considered building.

Apart from structure related improvements. Measures can be taken regarding other factors such as technical systems and material choice. Since there are high performing timber elements available on the market, it might be possible to reduce the dimensions of certain elements or redistribute forces using stiffer elements in carefully chosen areas. This widens the possibilities for complex timber structures even more. The element sizes available for these high performing elements are though often limited to small or medium dimension. In order to find large elements, special agreements might be needed between the material producers and design crew.

6.1.2 Potential error sources

Along the work procedure, decisions and simplifications have been unavoidable. Due to the accumulative effect, these might have an impact on the final result. One important factor that has been disregarded in the models is the joint stiffness. Since the joints used in timber structures often allow for slip of various magnitudes. This must be accounted for as it reduces the global stiffness. However, by using high quality, resin injected joints, the slip can pretty much be eliminated. This is though incredibly expensive if applied to all joints within a building. Therefore, modelling a building without slip is in one way realistic, but not economically justifiable. In order to show the true behaviour in the best possible way, specifically assigned joint stiffnesses would have been preferred. Also, since the building is fairly tall, the load paths will be long. With long load paths and multiple joints, the stiffness error in one joint will get

magnified along the building. This coupled with the multiple joints along a load path might impact the stiffness noticeably and is therefore important to consider in design.

Also, with the current knowledge, there is no reliable way to predict the mechanical damping of a building. All known values are based on measures on finished buildings. This introduces an uncertainty in the calculations as the building might be both better or worse than expected. The choice of a logarithmic decrement around 10 % when evaluating the concepts dynamically is therefore done since it represents a mid-range number for the possibly anticipated damping values.

When preliminary sizing the proposals, all load cases were investigated for one structure. There it could be concluded that two of the load combinations represented the worst loads for all elements, these load combinations were mentioned in chapter 4. The choice of limiting the preliminary design to two load cases might be another error source in the project. However, based on the initial comparison, any potential errors are anticipated to be small. Also, wind load on the roofs as well as snow load have been disregarded since they are assumed as small and therefore insignificant in preliminary design.

Lastly, as a project like this grows larger, the risk of miscalculations and human errors increases. Even though continuous verifications have been made, there is always a possibility for mistakes to slip through. The only way to reduce such problems would be by extending the time for development and go through the work multiple times, possibly with peer reviewing as a helpful tool.

6.1.3 Assumptions and building codes

The Eurocode calculations are in many cases specifically made for common buildings with regular shape and height. However, when it comes to unique projects such as tall buildings, the methods used in Eurocode might not be applicable. This is the case for the wind load calculations which are only valid up to 200 m tall buildings. Since the considered building height in this project is just 200 m, the upper limit for wind loads in Eurocode are reached. Therefore, one could discuss whether the reliability of the calculation procedure is waning as the building height approaches 200 m, or if it is the case for heights above 200 m. Anyway, building such heights will be stretching the limits of the Eurocodes. In order to increase the reliability in design, it might be of benefit to apply other methods for determination of wind load. For example, wind tunnel studies, which often are used for tall buildings. This, since it provides the most realistic load values available. In many cases this also means a significant reduction in wind load.

Another case with conditions that are partially fulfilled is when calculating the top floor acceleration in the dynamic analysis. The equations in both Eurocode and EKS11 are based on the assumption of constant mass along the main axis of the structure as well as global cantilever action. All structures analysed in this project do show a global cantilever action although shear deformations are present. Also, the buildings are designed with reduced element sizes higher up in the building. This results in a variation in mass along the main axis of the structure.

In practice, there are few buildings with completely constant mass along their main axis since most structures are at least somewhat structurally optimized with smaller elements in lower loaded areas. Therefore, one could discuss whether constant mass along its main axis actually means constant mass, or just the avoidance of point masses. Anyway, the calculations made are all assuming these requirements as fulfilled.

6.1.4 Questioning the rules to build higher?

The dynamic requirements in the code are based on people's feelings which is a very subjective topic. Some people get sick due to motions while others are not feeling anything at all. Therefore, one could argue that, in order to build even taller buildings, a possibility would be to allow accelerations higher than stated in the requirements for a few top floors. This could then be coupled with information for the users or buyers of these floors and how the users might feel on a windy day. Also, wind tunnel tests could reduce the expected wind loads significantly compared to the values stated in Eurocode. This would also have an impact on the acceleration at the top of the building. Both these factors could be important contributions in the development of even taller timber buildings.

6.2 Utilized software

With a few months' worth of experience, one reoccurring drawback has been noticed with *Rhino 3D* and its extensions. This is the way it generates meshes from surfaces and connects them to each other. For example, when connecting a slab to a wall every slab mesh corner node has to be perfectly aligned with the wall mesh corner nodes. If using two non-synchronized meshes, interaction cannot be obtained. When working with somewhat irregular shapes, ensuring mesh alignment can therefore take up a significant portion of the work. Anyway, there are a couple of options in *Grasshopper* when generating these meshes. However, they are all somewhat inconvenient resulting in either unsymmetrical meshes or significantly more work.

By the use of *Grasshopper* and *Karamba 3D*, models can easily be made, visualized and analysed. The software calculates everything from forces and deformations to eigenfrequencies and total mass. However, one feature that have been sought for but not found, is a way to extract element stresses. For this project, all stresses have therefore been determined manually from the cross-sections and forces, used and obtained from the model. Doing this operation for the beam elements is fairly straight forward. However, the shell elements require significantly more work.

Another feature that could use some improvements is the coupling with other programs. Most of the results are manually extracted from *Grasshopper* and later used in either *Excel* or *Mathcad*. The element sizing was done as manual iterative work, going back and forth between *Karamba 3D* and *Mathcad*. However, this procedure could have been done through Python scripting. Doing so would have reduced the iterative manual work drastically, allowing the program to do the bulk of the work.

Another problem with this software is the possibilities to present the modelling work. Since the programming is graphical, using modules and wires instead of the typical text-programming, large models are usually hard to understand for other people than the programmers themselves. This makes it nearly impossible to present the coding in a clear way. Therefore, only the results, assumptions, choices and pictures are presented from this software. Also, when using *Karamba 3D*, it is important to check the units for each in- and output value. This, since the units differs from the SI-units.

7 Conclusions

The results show that it might be possible to build a 200 m tall timber structure, as long as at least some of the uncertainties falls out in a favourable direction. However, there are several areas stretching today's limits in order to reach this height. The building is not only twice as tall as the current tallest timber building, but it also utilizes larger elements than used in the current largest timber buildings. However, reviewing the history, it is not unusual to break these kinds of records with a significant margin, for example Burj Khalifa was approximately 300 meters taller than its precursor.

Comparing this proposal to the current tallest timber building, Mjöstornet, there is an obvious size difference. Both height-wise and regarding the floor section. This makes a difference in timber mass consumption of almost a factor 15. However, if including the concrete used in Mjöstornet, the mass ratio decreases to a factor of 5. At the same time, the available floor area in *the 200 m timber tower* is 7 times larger than for Mjöstornet. This gives room for discussion whether it is acceptable to build such large buildings or not.

World record buildings are often getting much attention, making it possible to legitimate significant expenses. However, both expenses and the environmental factors related to consumption must be evaluated when determining if a building is justifiable. Despite the bulky construction of *the 200 m timber tower*, it is still approximately 27 times lighter than *Burj Khalifa*. Also, viewing the utilization ratios for the construction, continuous element size optimization could possibly reduce a significant amount of the material, making *the 200 m timber tower* way lighter without loss in performance. Economy is always of major concern when designing buildings, therefore, there are multiple areas that must be considered when determining whether a building is economically justifiable. A few examples of them are the number of joints and joint quality, as mentioned earlier. But also, the cost of making tall buildings, rather than low and wide structures. However, observing the global building stock, there is no questioning in the economic justifiability of a few hundred meters tall buildings, if located in the right area and made with a smart design.

Even though the structural elements of the building are of large sizes, they will not disturb the daylight to a significant extent. As seen in Figure 87, where the real member size is shown, the columns and trusses cover only a fraction of the building facade. A short calculation of the preliminary sized concept shows that approximately 20-30 % of the perimeter is shaded from direct sunlight depending on the storey and the element sizes on the considered floor within the building.

The results show that acceleration at the top of a building is one of the most critical factors for tall timber structures. If sufficient damping cannot be ensured, many of the possible concepts will not fulfill the requirements. The importance of a well-developed building geometry when designing for stiffness has also been highlighted as well as the significant differences in wind loads for a few different building shapes. Therefore, this project has confirmed the hypothesis that major improvements can be made structurally. However, a completed design of a 200 m tall building has not been made.

One could argue that additional time could have allowed for a more detail oriented final proposal. However, even large corporations might spend years on large projects, and it

is therefore unrealistic to strive for a completed building concept within less than half a year. Anyways, additional time is always beneficial since it allows for a deeper investigation and higher attention to details within the project.

Furthermore, several different designs were chosen to be tested, but there are still plenty of other potential options left for future investigations. Early in the process, circular concepts were prioritized over the traditional rectangular shape, which is used in most of the current timber towers. With a longer project period a greater number of concepts could have been evaluated and developed allowing for a further optimized structure. However, in order to design and detail a real tower, the project would demand significantly more work. Also, there are numerous factors affecting the result and it is hard to judge which ones are decisive or not. Maybe seemingly small factors might have such impact on the result that they will ruin the possibilities to build a 200 m tall timber tower.

When building the first 200 m timber tower, inspiration must be taken from the current tallest steel and concrete buildings, or maybe a completely new structural design. With an efficient global geometry, optimized element sizes and topology as well as thoroughly developed buildings, way taller buildings than 85 m are within reach. The potential with additional dampers was never applied in any of the concepts and that could push already well-developed structures to become even taller. It could also mean that most of the analysed alternatives have the possibility to reach 200 meters.

Summarizing this thesis, there is no doubt that it is possible to build way taller than the current 85 m. As soon as the research catches up with the public interest in timber structures and precise models able to predict both strength, stability and dynamics are available, tall timber structures will increase further in popularity. Combining innovative thinking and parametric design with high quality timber products and overall structural optimization, *the 200 m timber tower* is clearly within reach as soon as someone is willing to pay for it.

7.1 Future research

There are two major uncertainties that has affected the results in this investigation, mechanical damping and the element connections in the model. Reviewing the literature, it is clear that there is room for plenty of research regarding the mechanical damping of tall timber structures. Tall buildings in concrete and steel has been around for almost 100 years and are therefore comparably well developed in this regard. However, with the increasing interest in tall timber buildings, the knowledge in the area is surely facing a period of substantial growth. Among all potential research topics, the mechanical damping seems to be one of the critical ones when it comes to reliable modelling of tall timber structures. Actually, in order to increase the production of tall timber structures, more knowledge on the area is a necessity.

There is also a relation between joint slip and mechanical damping for a timber structure. The principle dynamic response to joint slip is illustrated in Figure 88. Since, joint slip affects the global stiffness of a building as well as the mechanical damping, two of the main dynamical properties are impacted when increasing or decreasing the slip. This means that the joint slip introduces additional uncertainties regarding the dynamic behaviour of a tall timber structure. Especially since increased damping is beneficial for the dynamic performance, while reduced stiffness often have a negative contribution to the dynamic performance. This means that the gained damping must be compared to the loss in stiffness, trying to determine whether joint slip actually could be beneficial, or if it is a pure disadvantage. Therefore, in order to determine whether joint slip is an advantage, disadvantage or irrelevant factor for the global dynamical behaviour, further research in the area is needed.

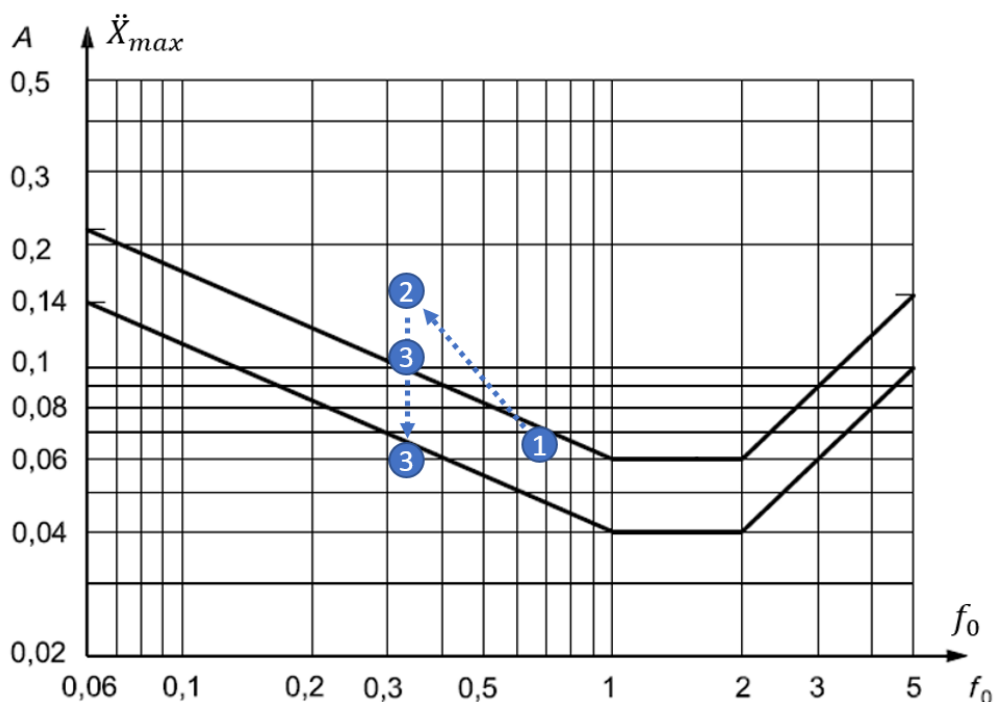


Figure 88: Illustration of the joint slips possible effect on top floor acceleration for a building. 1 indicates a value without joint slip. 2 shows the possible shift due to lower joint stiffness. 3 shows the uncertainty regarding how much damping will be generated as a consequence of joint slip.

8 References

- 14.3.1 *Ledad pelarfot - TräGuiden*. (2017).
<https://www.traguiden.se/konstruktion/limtrakonstruktioner/projektering-av-limtrakonstruktioner/forband-och-anslutningsdetaljer/pelarfot/ledad-pelarfot/>
- 14.3.2 *Fast inspänd pelarfot - TräGuiden*. (2017).
<https://www.traguiden.se/konstruktion/limtrakonstruktioner/projektering-av-limtrakonstruktioner/forband-och-anslutningsdetaljer/pelarfot/fast-inspand-pelarfot/>
- Abrahamsen, R. (2017). *Mjøstårnet - Construction of an 81 m tall timber building*.
<https://www.moelven.com/globalassets/moelven-limtre/mjostarnet/mjostarnet---construction-of-an-81-m-tall-timber-building.pdf>
- Abrahamsen, R. (2018). Mjøstårnet - 18 storey timber building completed. In 24. *Internationales Holzbau-Forum IHF 2018*.
- Alaghmandan, M., Elnimeiri, M., Krawczyk, R. J., & Von Buelow, P. (2016). Modifying Tall Building Form to Reduce the Along-Wind Effect. *CTBUH Journal*, 2, 34–39.
- Ali, M. M. (2001). *Art of the Skyscraper: The Genius of Fazlur Khan*No Title.
- Ali, M. M., & Moon, K. S. (2007). Structural Developments in Tall Buildings: Current Trends and Future Prospects. *Architectural Science Review*, 50(3), 205–223. <https://doi.org/10.3763/asre.2007.5027>
- American Institute of Steel Construction and Skidmore, Owings, & Merrill. (2017). AISC Steel & Timber Research for High-Rise Residential Buildings. In *Skidmore, Owings & Merrill LLP (Accessed 2020-01-22)*.
<https://www.aisc.org/globalassets/why-steel/aisc-steel-and-timber-research-for-high-rise-residential-buildings-final-report.pdf>
- Azumi, Y., Miyake, T., Murakami, M., Kawai, N., Tsuchimoto, T., & Isoda, H. (2018). High-performance connection system for mid-rise CLT buildings in high seismic area. *WCTE 2018 - World Conference on Timber Engineering*.
- Baker, W. F., & Pawlikowski, J. J. (2012). Higher and higher: The Evolution of the Buttressed Core. *Civil Engineering*, 58–65.
<https://doi.org/10.1002/mabi.200800348>
- Boverket. (2011). *Boverkets byggregler (2011:6) – föreskrifter och allmänna råd, BBR. 1(3)*, 1–153.
https://www.boverket.se/contentassets/a9a584aa0e564c8998d079d752f6b76d/ko nsoliderad_bbr_2011-6.pdf
- Boverket. (2019a). *Boverkets konstruktionsregler, EKS11*.
- Boverket. (2019b). *Dagsljus - PBL kunskapsbanken - Boverket*.
<https://www.boverket.se/sv/PBL-kunskapsbanken/regler-om-byggande/boverkets-byggregler/ljus-i-byggnader/dagsljus/>
- CCE - Canadian Consulting Engineer. (2017). *12-storey wood condo, project Origine, in Quebec celebrates capping - Canadian Consulting Engineer*.
<https://www.canadianconsultingengineer.com/buildings/1003405388/1003405388/>
- Cepelka, M. (2017). *Splicing of Large Glued Laminated Timber Elements by Use of Long Threaded Rods*. Norwegian University of Science and Technology.
- Chakraborty, S., Dalui, S. K., & Ahuja, A. K. (2014). Wind load on irregular plan shaped tall building - A case study. *Wind and Structures, An International Journal*, 19(1), 59–73. <https://doi.org/10.12989/was.2014.19.1.059>
- Council on Tall Buildings and Urban Habitat. (n.d.). *Tall, Supertall, and Megatall*

- Buildings*. Retrieved January 31, 2020, from <https://www.ctbuh.org/resource/height>
- Crocetti, R. (2016). *Förband som klarar stora laster - Tidningen Trä*. <https://www.svensktra.se/tidningen-tra/2016-4/kunskap/>
- Crocetti, R., Danielsson, H., Frühwald Hansson, E., Kliger, R., Mårtensson, A., Serrano, E., Johansson, M., Just, A., Piazza, M., & Östman, B. (2016). *Limträhandbok del2*.
- Crocetti, R., Johansson, M., Kliger, R., Lidelöw, H., Mårtensson, A., Norlin, B., & Pousette, A. (2015). *Dimensionering av träkonstruktioner 1*.
- Crocetti, R., Johansson, M., Kliger, R., Lidelöw, H., Mårtensson, A., Norlin, B., & Pousette, A. (2016). *Design of Timber Structures Volume 1*.
- Crocetti, R., Johansson, M., Lidelöw, H., Kliger, R., Mårtensson, A., Norlin, B., & Pousette, A. (2015). *Dimensionering av träkonstruktioner 2*.
- Das Holzhochhaus | HoHo Wien*. (n.d.). Retrieved February 3, 2020, from <http://www.hoho-wien.at/>
- Debney, P. (n.d.). *Hyperboloid Structures in GSA - Oasys*. Retrieved March 27, 2020, from <https://www.oasys-software.com/news/hyperboloid-structures-in-gsa/>
- Development | HoHo Wien*. (n.d.). Retrieved February 3, 2020, from <http://www.hoho-wien.at/Vision/Entwicklung>
- Domone, P., & Illston, J. (2010). *Construction Materials - Their nature and behavior* (4th ed.).
- Edskär, I. (2018). *Modal Analysis, Dynamic Properties and Horizontal Stabilisation of Timber Buildings*.
- Essays, U. (2013). *History Of Timber In Construction Construction Essay*. <https://www.uniassignment.com/essay-samples/construction/history-of-timber-in-construction-construction-essay.php>
- Facts & Figures | HoHo Wien*. (n.d.). Retrieved February 3, 2020, from <http://www.hoho-wien.at/Projekt/Daten-Fakten>
- Gunawardena, T., Fernando, S., Mendis, P., Waduge, B., & Hettiarachchi, D. (2017). Wind Analysis and Design of Tall Buildings , the State of the Art. *8th International Conference on Structural Engineering and Construction Management, December*, 1–10.
- Hayes, J. (2018). *Tall storeys: building super-slender skyscraper homes | E&T Magazine*. <https://eandt.theiet.org/content/articles/2018/10/tall-storeys-building-super-slender-skyscrapers-for-residential-use/>
- HoHo, Vienna Nearing Completion - Timber Architecture*. (n.d.). Retrieved February 3, 2020, from <http://timber-architecture.com/hoho-vienna-nearing-completion/>
- Ibrahim, N., & Hayman, S. (2005). Daylight Design Rules of Thumb. *Conference on Sustainable Building South East Asia, April 2005*, 11–13.
- Introduktion - TräGuiden*. (2017). <https://www.traguiden.se/konstruktion/kl-trakonstruktioner/kl-tra-som-konstruktionsmaterial/1.1-introduktion/introduktion/?previousState=1000000>
- IOS. (1984). *ISO 6897 - Guidelines for the evaluation of the response of occupants of fixed structures, especially buildings and off-shore structures, to low-frequency horizontal motion (0,063 to 1 Hz)*.
- Jendzelovsky, N., Antal, R., & Konecna, L. (2017). Determination of the wind pressure distribution on the facade of the triangularly shaped high-rise building structure. *MATEC Web of Conferences*, 107, 4–9. <https://doi.org/10.1051/mateconf/201710700081>
- Jun, X., Poon, D., & Mass, D. (2010). Shanghai Tower: A Case Study. *CTBUH*

- Journal*, II, 12–18.
- KONE. (n.d.-a). *KONE elevator planner*. Retrieved March 12, 2020, from <https://elevatorplanner.kone.se/spr/Configuration/interface/edit>
- KONE. (n.d.-b). *Turning Torso | Referensprojekt | KONE*. Retrieved March 12, 2020, from <https://www.kone.se/berattelser-och-referenser/referenser/turning-torso.aspx>
- Konstruktionsvirke - TräGuiden*. (2017). <https://www.traguiden.se/om-tra/materialet-tra/trabaserade-produkter/virkestyper-och-kvalitet/konstruktionsvirke/>
- Major Works, Sears Tower (Currently Willis Tower)*. (2011). <http://khan.princeton.edu/khanSears.html>
- Major Works, The John Hancock Center*. (2011). <http://khan.princeton.edu/khanHancock.html>
- Malo, K. A., Abrahamsen, R. B., & Bjertnæs, M. A. (2016). Some structural design issues of the 14-storey timber framed building “Treet” in Norway. *European Journal of Wood and Wood Products*, 74(3), 407–424. <https://doi.org/10.1007/s00107-016-1022-5>
- Medien | HoHo Wien*. (n.d.). Retrieved February 10, 2020, from <http://www.hohowien.at/Company/Medien>
- Moelven. (n.d.). *Trä8 Pelarbalksystemm - Guide for Architect*.
- Origine | Think Wood*. (n.d.). Retrieved February 3, 2020, from <https://www.thinkwood.com/our-projects/origine-tallest-wood-building-in-eastern-north-america>
- Pirinen, M. (2014). Ductility of Wood and Wood Members Connected with Mechanical Fasteners. In *AALTO UNIVERSITY*.
- Platts, M. J. (2014). Strength, Fatigue Strength and Stiffness of High-Tech Bamboo/Epoxy Composites. *Agricultural Sciences*, 5, 1281–1290. <https://doi.org/10.4236/as.2014.513136>
- PLP Architecture - PLP Labs*. (n.d.). Retrieved March 5, 2020, from <https://www.plplabs.com/>
- Pollmeier. (n.d.). *Product overview, tolerances and finishes*.
- Ramage, M., Foster, R., Smith, S., Flanagan, K., & Bakker, R. (2017). Super Tall Timber: design research for the next generation of natural structure. In *Journal of Architecture* (Vol. 22, Issue 1). <https://doi.org/10.1080/13602365.2016.1276094>
- Rodd, P. D., & Leijten, A. J. M. (2003). High-performance dowel-type joints for timber structures. *Progress in Structural Engineering and Materials*, 5(2), 77–89. <https://doi.org/10.1002/pse.144>
- Roszyk, E. (2014). The effect of ultrastructure and moisture content on mechanical parameters of pine wood (*Pinus sylvestris* L.) upon tensile stress along the grains. *Turkish Journal of Agriculture and Forestry*, 38(3), 413–419. <https://doi.org/10.3906/tar-1306-81>
- Sharma, A., Mittal, H., & Gairola, A. (2018). Mitigation of wind load on tall buildings through aerodynamic modifications: Review. *Journal of Building Engineering*, 18(September 2017), 180–194. <https://doi.org/10.1016/j.jobe.2018.03.005>
- Sinovoltaics.com. (2019). *Location Factor for Wind and Solar - Sinovoltaics - Zero Risk Solar™*. <https://sinovoltaics.com/learning-center/basics/location-factor-for-wind-and-solar/>
- SIS. (2003). *SS-EN 1991: Laster på bärverk, snölast*.
- SIS. (2004). *SS-EN 1990: Grundläggande dimensioneringsregler för bärverk*.
- SIS. (2005). *SS-EN 1991: Eurokod 1 Laster på bärverk*. www.sis.se

- SIS. (2008). *SS-ISO 10137:2008 - Bases for design of structures – Serviceability of buildings and walkways against vibration (ISO 10137:2007, IDT)*.
- SIS. (2009). *SS-EN 1995-1-1:2004 - Eurocode 5: Design of timber structures – Part 1-1: General – Common rules and rules for buildings*.
- SIS. (2016). *SS-EN 1998 - Frågor och svar*.
<https://www.sis.se/konstruktionochtillverkning/eurokoder/frgorsvar/ssen1998jor dbvningsresistentkonstruktioner/>
- StoraEnso. (n.d.). *LVL - Wood products* | Stora Enso. Retrieved March 24, 2020, from <https://www.storaenso.com/en/products/wood-products/massive-wood-construction/lvl>
- Svenskt Trä. (2017a). *KL-trähandbok: fakta och projektering av KL-träkonstruktioner*.
- Svenskt Trä. (2017b). *Tillverkning av KL-trä - TräGuiden*.
<https://www.traguiden.se/konstruktion/kl-trakonstruktioner/kl-tra-som-konstruktionsmaterial/1.5-tillverkning-av-kl-tra/tillverkning-av-kl-tra/>
- Technology* | HoHo Wien. (n.d.). Retrieved February 3, 2020, from <http://www.hohowien.at/Projekt/Technologie>
- Träbaserade kompositprodukter av faner - TräGuiden*. (2017).
<https://www.traguiden.se/om-tra/material-1/tra-baserade-produkter/konstruktionselement/tra-baserade-kompositprodukter-av-faner-lvl-laminated-veneer-lumber/>
- Truby, A., Banks, C., Burridge, J., Cammelli, S., A Chiorino, M., Ha, T., Jaeger, J.-M., Keleris, G., Marsh, S., Romo, J., McKechnie, S., Wells, J., Ackerman, C., Sheerin, J., Magee, A., Blundell, S., Mann, A., Lavery, M., & Scott, P. (2014). Tall buildings. In *Engineers Australia*.
https://doi.org/10.4324/9780203404386_chapter_15
- Verhaegh, R., Vola, M., & De Jong, J. (2018). Case study: Haut - A 21-storey tall timber residential building. *WCTE 2018 - World Conference on Timber Engineering*.
- Vikas Kumar Nirmal, A. (2017). Wind and Architecture: Design to the flow. *International Research Journal of Engineering and Technology*, 04(11), 2104–2110. www.irjet.net
- Xie, J. (2014). Aerodynamic optimization of super-tall buildings and its effectiveness assessment. *Journal of Wind Engineering and Industrial Aerodynamics*, 130, 88–98. <https://doi.org/10.1016/j.jweia.2014.04.004>
- Yipintsoi, T. (1976). Single passage extraction and permeability estimation of sodium in normal dog lungs. In *Circulation Research* (Vol. 39, Issue 4).
<https://doi.org/10.1161/01.RES.39.4.523>

Appendix

Appendix I

Structural elements for tall buildings

The elements of a high-rise building are the same as for low-rise buildings, but must fulfill higher demands. Nowadays it is common to use 3D finite element program to gain understanding on how the building will act with different load cases, as well as experience from old cases. It is important to consider loading conditions both during the construction of the building and when the building is finished (Truby et al., 2014).

Slabs

The main purpose of the floors is to transfer applied loads to the vertical elements, such as cores and columns. They can also act as diaphragms to transfer horizontal loads. An optimized floor in a tall building can save a lot of height and weight in total since it is repeated for each level. However, demands such as vibrations, acoustics and deflection must still be fulfilled (Truby et al., 2014).

Prefabricated wooden floor elements in Mjöstornet

Mjöstornet was made with prefabricated floor elements manufactured by *Moelven* (Abrahamsen, 2017). These elements are available in spans up to 8 m with a thickness of 480 mm for the load bearing part and 590 mm for the complete floor. The elements are designed for an imposed load $Q = 2kN/m^2$ (including self-weight of internal walls and installations). Also, the floors are constructed to contain ventilation, electrical installations and plumbing pipes. The self-weight of these slabs is 172 kg/m^3 (Moelven, n.d.).

Composite mass-timber floor

A research project about composite mass-timber floor systems and their appropriacy in high-rise buildings was made at the American Institute of Steel Construction. The lightweight floor was built up by composite CLT with a thin reinforced concrete slab connected with structural screws. The concrete and floor finishes are chosen to solve the problems with acoustics, fire resistance and durability, but also to create a continuity over the beams. The composite floor system consists of approximately 200 mm timber and 70 mm concrete, this means that the total thickness of this floor is larger than a typical concrete floor. The framing of the building used in the project is made in steel to be able to have long spans. The timber parts of the floor are prefabricated and since they are also lightweight, the assembly is fast which saves both time and money (American Institute of Steel Construction and Skidmore et al., 2017).

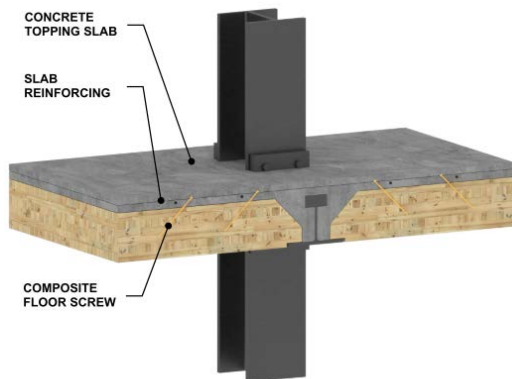


Figure 89: Composite mass-timber floor (American Institute of Steel Construction and Skidmore et al., 2017).

When the composite floor was mounted, the mid span deflection was big, but when the concrete cured the floor system was stiffened up and sufficiently small deflections could be obtained. Self-tapping screws were used to connect the CLT elements to each other giving the floor system a diaphragm-behavior. This action supports the columns, necessary to manage the wind loads during construction. The vibrations in the floor are calculated to be sufficiently small (American Institute of Steel Construction and Skidmore et al., 2017).

This floor system is designed for but not tested regarding fire resistance and it might need some additional gypsum boards to enhance the fire resistance. Regarding the acoustics, the intended use will determine if improvements are necessary. For example, additional gypsum in the ceiling might be a possible improvement to improve the sound properties. The timber parts in moist rooms, such as bathrooms and kitchens, will need special consideration to avoid moisture related issues. Physical tests for both sound and durability might be necessary to check the real performance of the floor system (American Institute of Steel Construction and Skidmore et al., 2017).

Central core

During construction of high-rise buildings, the most important part of the structure is usually the core. With a good planned core, lots of time can be saved during construction. Usually the core transfers around 60 % of the vertical loads when the building is finished and it takes care of most lateral loads. The core can act as a shear wall system and make space for staircases, shafts and elevator shafts for example. It is preferable to have long symmetrical shear walls placed in relation to the centerlines of the finished building. One important aspect for high-rise buildings is all the penetrations in the cores to fit the ducts, this will reduce the stiffness and overall capacity. One way to solve this is to have service shafts next to the core to take care of this (Truby et al., 2014).

Columns

The main intention of columns is to transfer vertical loads from the structure down to the foundation. Sometimes this is done with columns working alongside core walls, which also transfer horizontal loads. When building high-rise buildings, smaller columns are often used higher up in the building, as the loads reduces. Therefore, it is

important to consider eventual eccentricities between the center-points that might cause additional bending moments. Columns are preferably hidden inside the façade, but due to the column sizes in high-rise buildings, this is usually hard to manage. A normal span between columns is 6-10 m, however it is possible to deviate from this range if needed. It is also common for slabs to continue as cantilevers outside of the columns where they connect to the façade. Thereby the façade remains free of interrupting columns, which is favorable (Truby et al., 2014).

Load bearing and stabilizing walls

The main purposes of structural walls in high-rise buildings are to transfer loads vertically and stiffen up the building laterally. If there are large vertical loads in the walls, the lateral loads will have less impact on over-turning the building. The size of the walls usually decreases higher up in high-rise buildings and therefore the offset from the centerline between each wall element must be taken into consideration when designing. The placement of walls is of high importance to reduce the effects of the lateral loads. It is favorable to have symmetry around the center of the building to obtain the same resistance in all directions. For tall buildings it is desirable to obtain similar stress level in the walls and columns on each floor. This will allow for relatively uniform long-term effects. When deciding for opening locations in heavily loaded walls, it is favorable to place the openings near the vertical centerline. This to reduce the strength and stiffness as little as possible (Truby et al., 2014).

When using stabilizing walls, it is critical to design them with the entire structure in mind. Plain wall elements might be incredibly stiff, poor connections and large holes can ruin the behavior of an otherwise thoroughly designed structure. *Haut*, a 21 storey residential building made as a timber concrete composite structure, was initially subject to large losses in global stiffness due to holes in the stabilizing walls (Truby et al., 2014). To manage this, a staggered pattern as shown in Figure 90 were used which allows whole vertical sections to remain intact and therefore provide sufficient global stiffness. However, when designing stabilizing walls, a conservative method is often used (Verhaegh et al., 2018). It assumes that vertical wall portions with holes should be disregarded. For the illustration in Figure 90, this would result in three separate wall elements denoted 1, 2 and 3. Compared to a plain wall element, it is clear that the stiffness for a wall with holes is drastically reduced (Svenskt Trä, 2017a).

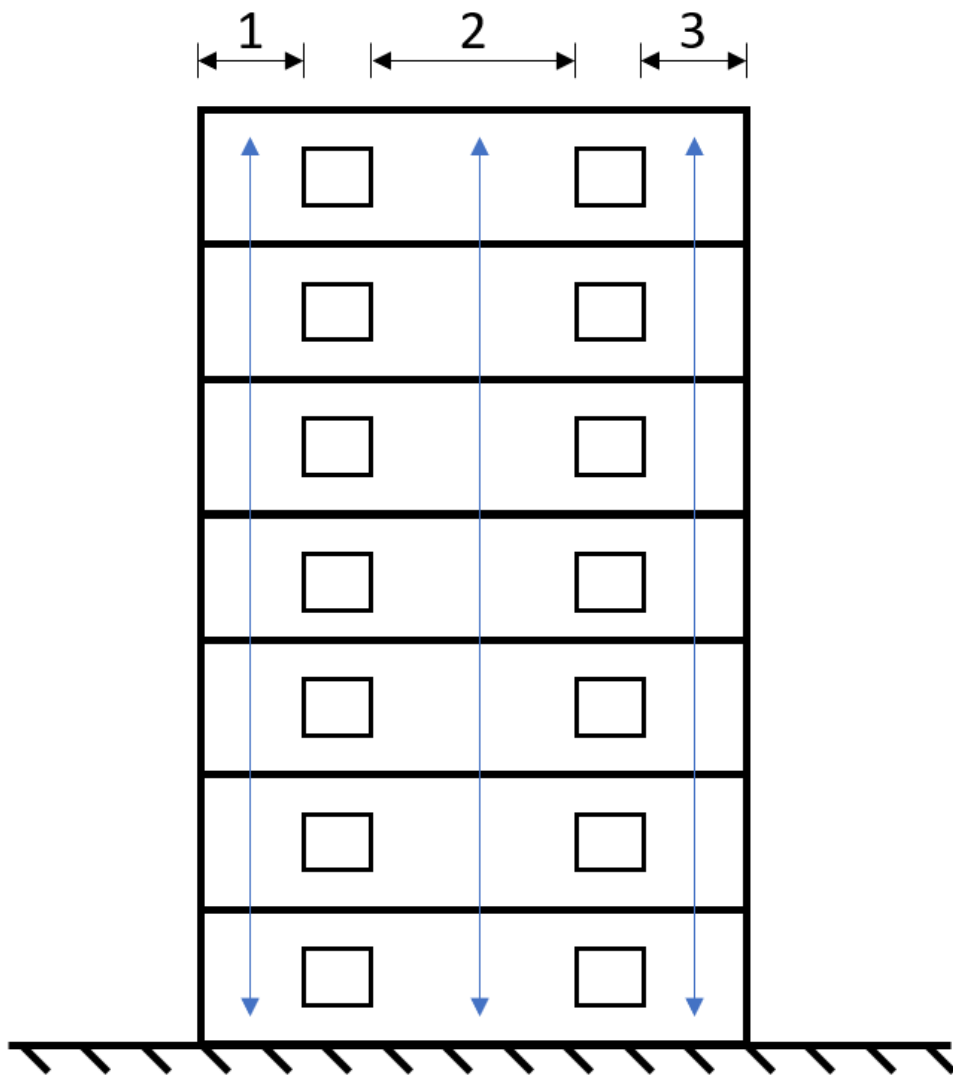


Figure 90: Illustration of a staggered hole pattern for a stabilizing wall. Here with 3 undisrupted vertical sections.

Appendix II

Calculation procedure to determine wind load on a structure or structural component, SS-EN 1991-1-4:2005 and EKS 11.

1. Determine external shape coefficients for the structure. See section 2.13.
2. Characteristic wind velocity pressure.

$$q_p(z) = [1 + 2 k_p I_v(z)] c_r^2(z) c_o^2(z) \frac{1}{2} \rho v_b^2 \quad (1)$$

$q_p(z)$	Characteristic wind velocity pressure.
$k_p(z)$	Peak factor at height z.
$I_v(z)$	Wind turbulence intensity at height z.
$c_r(z)$	Roughness factor.
$c_o(z)$	= 1.0, topography factor.
ρ	= 1.25 kg/m ³ , air density.
v_b	Reference wind speed.

2.1 Peak factor, k_p at height z.

For buildings with considerable dynamic effects:

$$k_p = \sqrt{2 \ln(vT)} + \frac{0.6}{\sqrt{2 \ln(vT)}} \geq 3 \quad (2)$$

For statically governed buildings:

$$k_p = 3$$

$k_p(z)$	Peak factor at height z.
v	Up-crossing frequency.
T	= 600s, averaging time for mean wind velocity.

$$v = n_{1,x} \sqrt{\frac{R^2}{B^2 + R^2}} \geq 0.08 \text{ Hz} \quad (3)$$

v	Up-crossing frequency.
$n_{1,x}$	Estimated lowest eigenfrequency.
B^2	Factor for background response.
R^2	Factor for resonance response.

$$B^2 = e^{\left[-0.05 \left(\frac{h}{h_{ref}} \right) + \left(1 - \frac{b}{h} \right) \left(0.04 + 0.01 \left(\frac{h}{h_{ref}} \right) \right) \right]} \quad (4)$$

B^2	Factor for background response.
h	Building height exposed to wind.
b	Building width exposed to wind.
h_{ref}	= 10m, reference height.

$$R^2 = \frac{2\pi F \Phi_h \Phi_b}{\delta_s + \delta_a + \delta_d} \quad (5)$$

R^2	<i>Factor for resonance response.</i>
F	<i>Karman's wind energy spectrum.</i>
Φ_h	<i>Size factor regarding the building height.</i>
Φ_b	<i>Size factor regarding the building width.</i>
δ_s	<i>Mechanical damping.</i>
δ_a	<i>Aerodynamic damping.</i>
δ_d	<i>Damping due to damping devices.</i>

$$F = \frac{4 y_c}{(1 + 70.8 y_c^2)^{\frac{5}{6}}} \quad (6)$$

F	<i>Karman's wind energy spectrum.</i>
y_c	<i>Unitless factor.</i>

$$y_c = \frac{150 n_{1,x}}{v_m(h)} \quad (7)$$

y_c	<i>Unitless factor.</i>
$n_{1,x}$	<i>Estimated lowest eigenfrequency.</i>
v_m	<i>Mean wind velocity on height h.</i>

$$n_{1,x} = \frac{46}{h} \quad (8)$$

$n_{1,x}$	<i>Estimated lowest eigenfrequency.</i>
h	<i>Building height.</i>

$$v_m(z) = c_r(z) c_o(z) v_b \quad (9)$$

$v_m(z)$	<i>Mean wind velocity on height z.</i>
$c_r(z)$	<i>Roughness factor.</i>
$c_o(z)$	<i>= 1.0, topography factor.</i>
v_b	<i>Reference wind speed.</i>

$$\Phi_h = \frac{1}{1 + \frac{2 n_{1,x} h}{v_m(h)}} \quad (10)$$

Φ_h *Size factor regarding the building height.*
 $n_{1,x}$ *Estimated lowest eigenfrequency.*
 h *Building height.*
 $v_m(h)$ *Mean wind velocity on height h.*

$$\Phi_b = \frac{1}{1 + \frac{3.2 n_{1,x} b}{v_m(h)}} \quad (11)$$

Φ_b *Size factor regarding the building width.*
 $n_{1,x}$ *Estimated lowest eigenfrequency.*
 b *Building width.*
 $v_m(h)$ *Mean wind velocity on height h.*

$$\delta_a = \frac{c_f \rho b v_m(z_s)}{2 n_1 m_e} \quad (12)$$

δ_a *Aerodynamic damping.*
 c_f *Shape factor for the structure, see section 2.13.*
 ρ *= 1.25kg/m³, air density.*
 b *Building width.*
 $v_m(z_s)$ *Mean wind velocity on height z_s.*
 z_s *Reference height when determining the structural factor.*
 n_1 *Estimated lowest eigenfrequency.*
 m_e *Equivalent mass per meter length for the upper third of the building.*

$$z_s = 0.6 h \geq z_{min} \quad (13)$$

z_s *Reference height when determining the structural factor.*
 h *Building height.*
 z_{min} *= 10m, assuming at least 15 % of the surrounding area holds buildings with average height taller than 15 m.*

Table 26: Approximative values for the mechanical damping in a few construction types. Obtained in table F.2 SS-EN 1991-1-4.

Mechanical damping, δ_s	[-]
Timber bridges	0.06-0.12
Concrete bridges	0.04-0.10
Steel bridges	0.02-0.05
Buildings made of reinforced concrete	0.10
Steel buildings	0.05

2.2 Wind turbulence intensity I_v at height z .

$$I_v(z) = \frac{k_l}{c_o(z) \ln\left(\frac{z}{z_0}\right)}, \quad z_{min} \leq z \leq z_{max} \quad (14)$$

$$I_v(z) = \frac{k_l}{c_o(z) \ln\left(\frac{z_{min}}{z_0}\right)}, \quad z \leq z_{min} \quad (15)$$

k_l = 1.0, turbulence factor.
 $c_o(z)$ = 1.0, topography factor.
 z_0 = 1.0, roughness length for terrain category IV.
 z_{min} = 10m, assuming at least 15 % of the surrounding area holds buildings with average height taller than 15 m.

2.3 Roughness factor c_r depending on height z and roughness of the terrain on the windward side of the building:

$$c_r(z) = k_r \ln\left(\frac{z}{z_0}\right), \quad z_{min} \leq z \leq z_{max} \quad (16)$$

$$c_r(z) = k_r \ln\left(\frac{z_{min}}{z_0}\right), \quad z \leq z_{min} \quad (17)$$

z_0 = 1.0, roughness length for terrain category IV.
 k_r Terrain factor as a function of the roughness length.

$$k_r = 0.19 \left(\frac{z_0}{z_{0,II}}\right)^{0.07} \quad (18)$$

$z_{0,II}$ = 0.05m, reference height.
 z_{min} = 10m, assuming at least 15 % of the surrounding area holds buildings with average height taller than 15 m.
 z_{max} = 200m.

3. Wind load on external surfaces.

$$w_e = q_p(z_e) c_{pe} \quad (19)$$

w_e	<i>Wind load on external surface</i>
z_e	<i>Reference height for the surface subject to external wind load.</i>
$q_p(z_e)$	<i>Characteristic wind velocity pressure at height z_e.</i>
c_{pe}	<i>Shape factor for external wind loads.</i>

4. Wind load on internal surfaces.

Since the internal pressure will be of equal magnitude in all directions, it will only affect the wind load on local elements in the façade. The global behavior will be unaffected.

$$w_i = q_p(z_i) c_{pi} \quad (20)$$

w_i	<i>Wind load on internal surface.</i>
z_i	<i>Reference height for internal surface subject to wind load.</i>
$q_p(z_i)$	<i>Characteristic wind velocity pressure at height z_i.</i>
c_{pi}	<i>Shape factor for internal wind loads.</i>

c_{pi} should always be chosen as the most unfavorable value for the particular design situation.

$$c_{pi} = 0.2 \quad \text{if internal pressure is unfavorable.}$$

$$c_{pi} = -0.3 \quad \text{if internal suction is unfavorable.}$$

5. Wind force on a structure or structural element.

For a distinct reference area:

$$F_w = c_s c_d c_f q_p(z_e) A_{ref} \quad (21)$$

For a sub area subject to wind:

$$F_w = c_s c_d \sum_{\text{parts}} c_f q_p(z_e) A_{ref} \quad (22)$$

c_s	<i>Size factor.</i>
c_d	<i>Dynamic factor.</i>
c_f	<i>Shape factor for force on the structure, see section 2.13.1.1.</i>
$q_p(z_e)$	<i>Characteristic wind velocity pressure at height z_e.</i>
A_{ref}	<i>Reference area of the structure or part of the structure.</i>

$$c_s c_d = \frac{1 + 2k_p(z_s) I_v(z_s) \sqrt{B^2 + R^2}}{1 + 6I_v(z_s)} \quad (23)$$

c_s	Size factor.
c_d	Dynamic factor.
$k_p(z_s)$	Peak factor at height z_s .
$I_v(z_s)$	Wind turbulence intensity at height z_s .
B^2	Factor for background response.
R^2	Factor for resonance response.

Shape factor for force on a section with regular polygon shape

The shape factor for a regular polygon shaped building with global geometrical ratios $\frac{\text{height}}{\text{diameter}} > 5$ can according to SS-EN 1991-1-4 be determined as follows:

$$c_f = c_{f,0} \psi_\lambda \quad (24)$$

c_f	Shape factor for force on a regular polygon shaped building.
$c_{f,0}$	Shape factor for force on structure disregarding end effects.
ψ_λ	Reduction factor for force coefficient regarding end effects.

In short, various geometrical properties will have the largest influence on the shape factor. However, the surface finish will also have an impact.

Table 27: Shape coefficients for force for various polygons, disregarding end effect. Based on table 7.11, SS-EN 1991-1-4 (SIS, 2005).

Number of sides	Surface and edge finish	Reynolds number, Re	$c_{f,0}$
5	All	All	1.80
6	All	All	1.60
8	Smooth $\frac{r}{b} < 0.075$	$Re \leq 2.4 \cdot 10^5$	1.45
		$Re \geq 3 \cdot 10^5$	1.30
	Smooth $\frac{r}{b} \geq 0.075$	$Re \leq 2 \cdot 10^5$	1.30
		$Re \geq 7 \cdot 10^5$	1.10
10	All	All	1.30
12	Smooth and rounded corners	$2 \cdot 10^5 < Re < 1.2 \cdot 10^6$	0.90
	All other	$Re < 4 \cdot 10^5$	1.30
		$Re > 4 \cdot 10^5$	1.10
16-18	Smooth and rounded corners	$Re < 2 \cdot 10^5$	As a cylinder
		$2 \cdot 10^5 < Re < 1.2 \cdot 10^6$	0.70

r	Corner radius.
b	Diameter of circle with tangent points in the polygon corners.
Re	Reynolds number.

$$Re = \frac{b v_p(h)}{v} \quad (25)$$

Re Reynolds number.
 b Width of the structure.
 $v_p(h)$ Peak wind velocity at height h .
 h Height of the building.
 $v = 15 \cdot 10^{-6} \text{ m}^2/\text{s}$.

$$v_p(z) = \sqrt{\frac{2 q_p(z)}{\rho}} \quad (26)$$

$v_p(z)$ Peak wind velocity at height z .
 $q_p(z)$ Peak wind pressure at height z . See equation (1) in Appendix II.
 $\rho = 1.25 \text{ kg/m}^3$, air density.

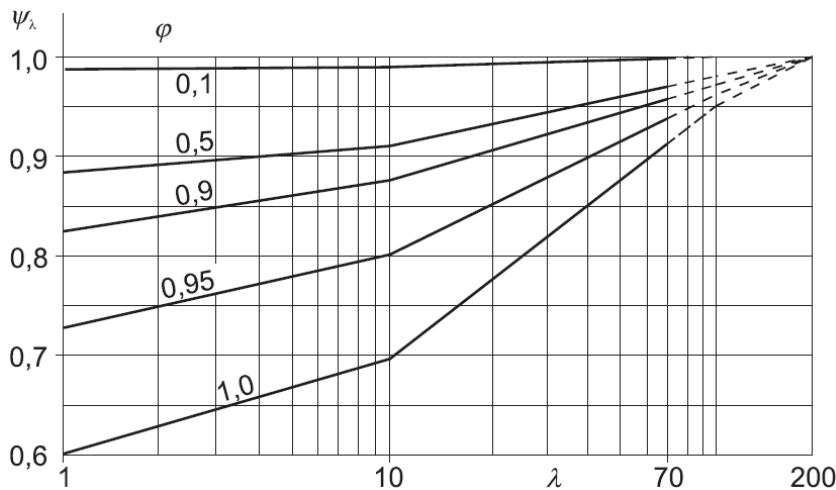


Figure 91: Reduction factor for end effects, figure 7.36 in SS-EN 1991-1-4 (SIS, 2005).

$$\lambda = \frac{l}{b} \quad (27)$$

$$\varphi = \frac{A}{A_c} \quad (28)$$

λ Effective slenderness of the structure.
 l Length of the structure.
 b Width of the structure.
 φ Solidity ratio.
 A Total area of structural parts facing the same direction.
 A_c Gross area of the structure facing the considered direction.

The reference area A_{ref} that should be used with the wind pressure and shape coefficients is case specific. For regular polygon shapes, the reference area should be determined as follows:

$$A_{ref} = l \cdot b \quad (29)$$

l *The building height.*

b *Diameter of the circle which tangents all corners of the polygon.*

Appendix III

Similarly, to hourglass shaped buildings, the available information regarding wind loads on a Y-shaped building is limited. However, there is some available information regarding other shapes which might give an indication of suitable shape coefficients for a Y-shaped building. The Y-shape will mainly be loaded in two different ways as shown in Figure 92. A favourable direction where one of the wings splits the wind load and one unfavourable direction when the wind blows straight into the concavely shaped wall. When making a wind load model, the critical values for these cases must be represented through sufficiently chosen shape coefficients.

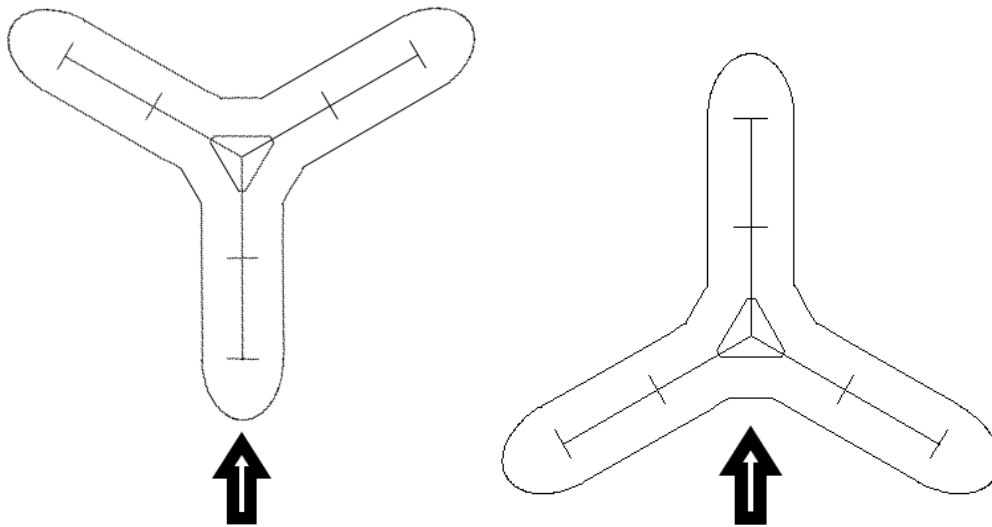


Figure 92: The two main wind load cases for a Y-shape building.

Buildings with equilateral triangular section

As the widespread literature about wind loads on non-conventional structure shapes is limited, these structures cannot be designed purely according to Eurocode. Instead methods such as wind tunnel studies must be used. In 2007 a study was carried out, where an equilateral triangular high-rise building was analysed through both of the mentioned methods whereafter pressure coefficients were determined for both analyses. The analysis is a quite narrow base when regarding the development of widely applicable shape coefficients. Also, the wind tunnel study is only made once, for each of the cases shown in Figure 93, which limits the safety margin when it comes to testing errors and case specific boundary conditions. The authors of the study also conclude that the

pressure coefficients obtained through computational fluid dynamics are slightly higher than the ones obtained by wind tunnel testing (Jendzelovsky et al., 2017).

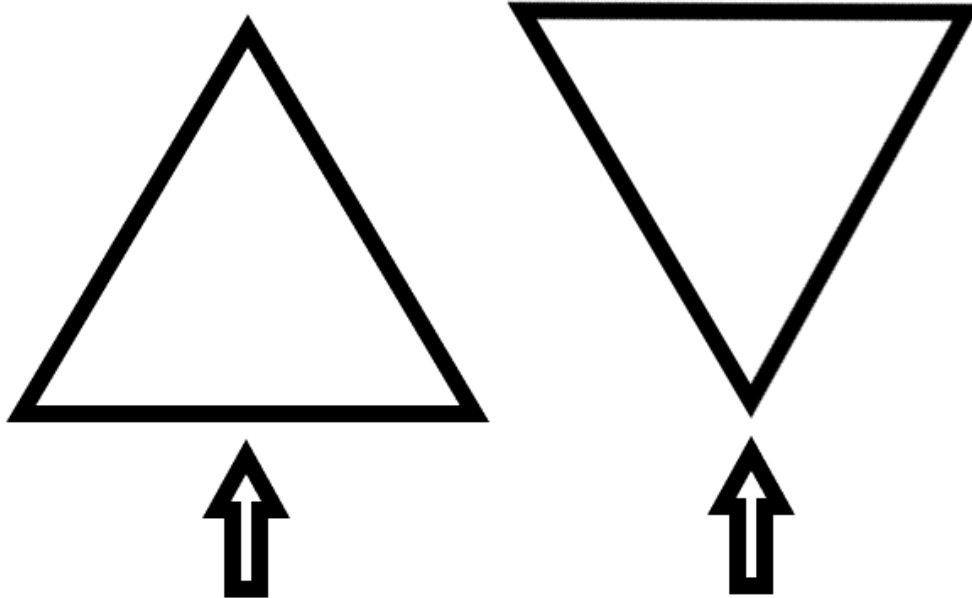


Figure 93: The two main wind directions studied when analyzing wind pressure coefficients on equilateral triangular high-rise structures (Jendzelovsky et al., 2017).

Graphical illustrations of the paper results can be seen in Figure 94 and Figure 95.

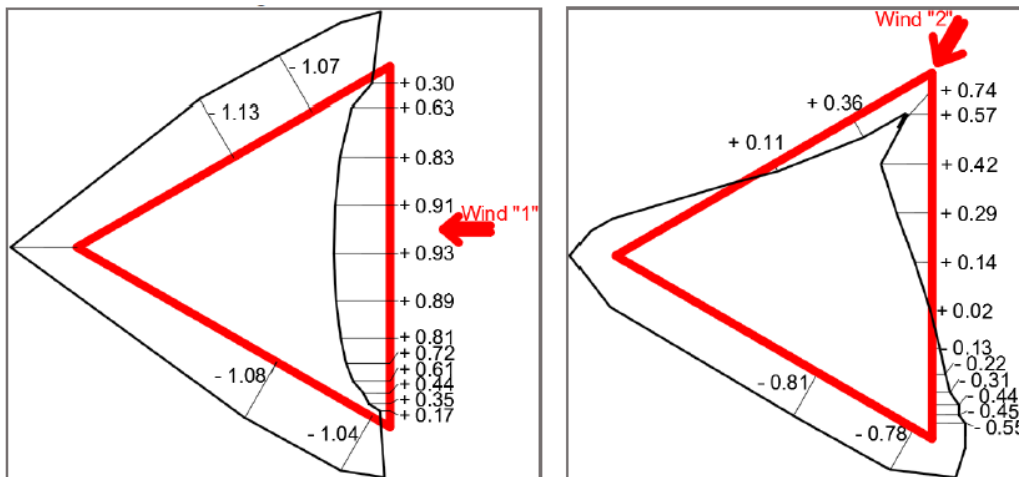


Figure 94: Wind pressure coefficient distribution measured through wind tunnel testing, figure 3 (Jendzelovsky et al., 2017).

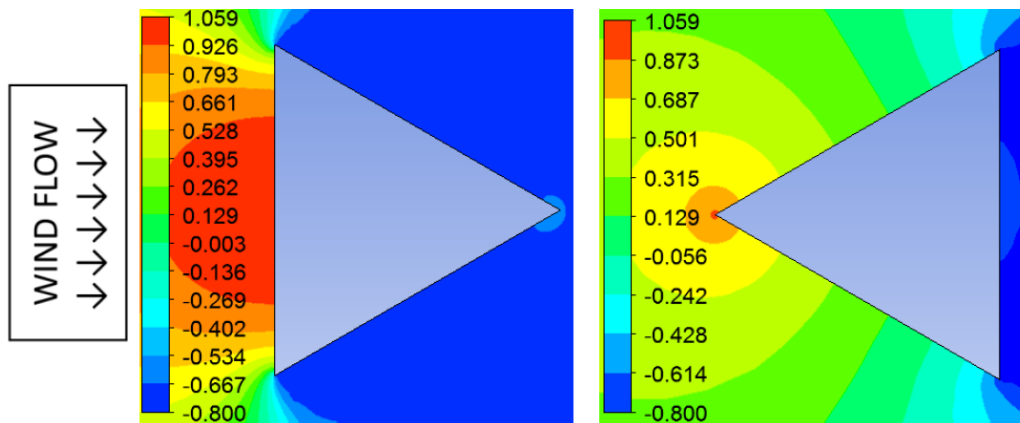


Figure 95: Wind pressure coefficient distribution determined through computational fluid dynamics, figure 6 (Jendzelovsky et al., 2017).

To be able to utilize these results, the critical value for the two cases are compared and simplified into a new summarized wind pressure coefficient model shown in Figure 96.

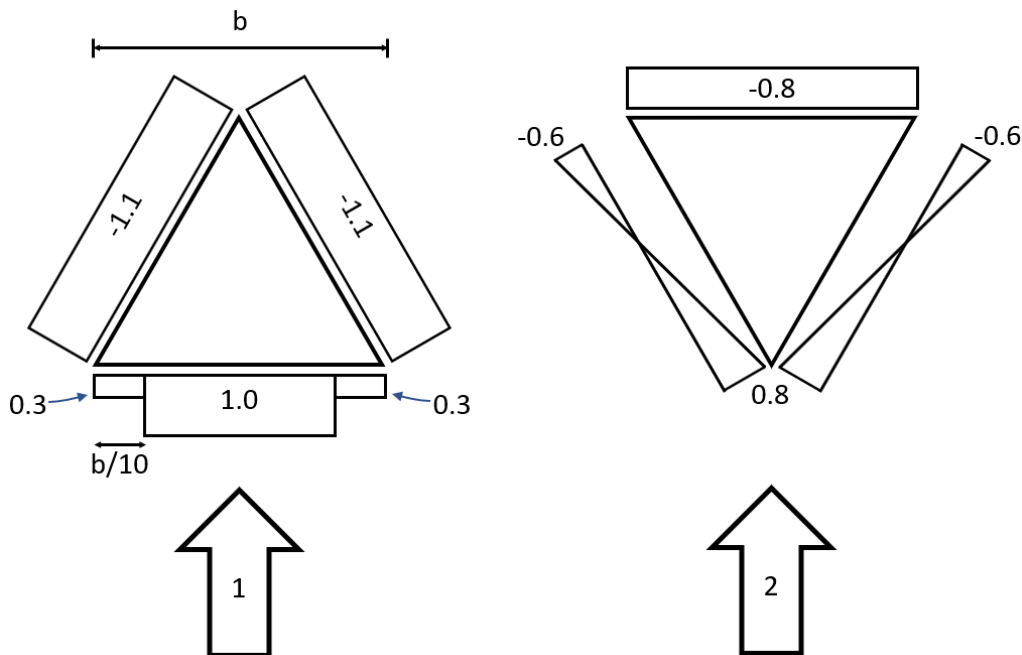


Figure 96: A simplified wind pressure shape coefficient distribution for a building with an equilateral triangular cross-section shape.

Buildings with a plus shaped section

In 2014 a study was completed regarding the wind load and pressure coefficient distribution on a plus shaped cross-section. The study was carried out by a comparison between pressure coefficient results from a wind tunnel test and two different computational fluid dynamics simulations. One simulation according to the *Menter's Shear Stress Transport* turbulence model and one simulation according to the *k-ε* turbulence model. The results are presented comprehensively with contour plots and height dependent mean values for each of the considered building faces. The slenderness of the plus shaped model was 1:2 (Chakraborty et al., 2014).

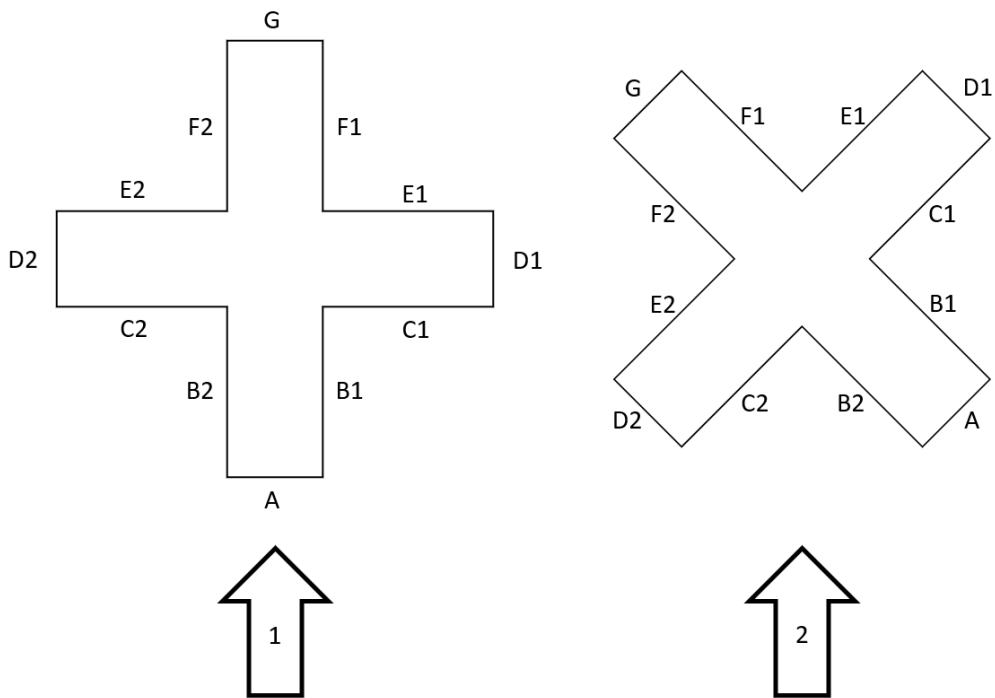


Figure 97: General illustration of the two main wind directions regarded in the study “Wind load on irregular plan shaped tall building”. Faces are numbered A, B1, B2, ..., F1, F2, G.

When applying the wind pressure coefficients, it is beneficial to have them in a simple form. Therefore, initially, the height dependent mean values are of highest interest. An estimated mean of the three analyses for each height is summarized in Table 28 and Table 29 below. Due to symmetry, only pressure coefficients for half of the faces are presented.

Table 28: Table of approximated mean pressure coefficients for the three analyses methods and various elevation of the reference building (Chakraborty et al., 2014). The wind direction is straight towards face A.

Percentage of building height	A	B1	C1	D1	E1	F1	G
0 %	0.40	0.50	0.48	-0.37	-0.50	-0.40	-0.30
20 %	0.43	0.50	0.65	-0.45	-0.50	-0.43	-0.35
40 %	0.45	0.50	0.68	-0.52	-0.50	-0.45	-0.40
60 %	0.50	0.50	0.70	-0.60	-0.50	-0.50	-0.45
80 %	0.52	0.40	0.70	-0.60	-0.50	-0.50	-0.50
100 %	0	0	-0.50	-0.60	-0.50	-0.50	-0.50

Table 29: Table of approximated mean pressure coefficients for the three analyses methods and various elevation of the reference building (Chakraborty et al., 2014). The wind direction is towards the corner between face B2 and face C2.

Percentage of building height	B2	A	B1	C1	D1	E1
0 %	0.90	-0.30	-0.60	-0.65	-0.40	-0.20
20 %	0.90	-0.25	-0.60	-0.65	-0.40	-0.20
40 %	0.93	-0.15	-0.60	-0.60	-0.40	-0.20
60 %	0.95	-0.05	-0.60	-0.60	-0.40	-0.20
80 %	1.00	0	-0.60	-0.60	-0.40	-0.20
100 %	-0.70	0.2	-0.70	-0.45	-0.40	-0.20

Observing the data, many of the faces has an almost constant pressure coefficient distribution along the building height. In those cases where a significant difference can be seen is most often at the upper edge of the building. This is therefore of larger interest when designing details in the structure rather than the global loading and global behaviour. A rough further simplification shown in Table 30 might therefore be applicable when analysing the global structural behaviour.

Table 30: Simplified wind pressure shape coefficients for the different faces of a plus shaped cross-section subject to wind in its two main directions.

Wind direction	A	B1 B2	C1 C2	D1 D2	E1 E2	F1 F2	G
1	0.50	0.50	0.70	-0.60	-0.50	-0.50	-0.45
2	0.95	-0.10	-0.60	-0.60	-0.40	-0.20	

Conclusion on shape coefficients for a Y-shaped building

Even though wind loads are highly case specific, the cases studied earlier in this appendix can to some extent be combined into resulting shape coefficient distributions for a Y-shaped section subject to load. Of course, this will be a rough estimation, but it will be used in preliminary design due to lack of standardized wind load approaches for Y-shaped buildings.

For each of the wind load directions and each of the faces shown in Figure 98, the most relevant wind pressure coefficients will be compared and condensed into an easily usable form and summarized in Table 31. Following is the reasoning behind each choice of pressure coefficient.

Table 31: Table of simplified and summarized shape coefficients for a Y-shaped building.

Wind direction	A	A1	A2	B	B1	B2	C	C1	C2
1	<0.50	<0.50	<0.50	-0.45	-0.50	0.00-1.00	-0.45	0.00-1.00	-0.50
2	-0.35	1.00	-0.70	-0.35	-0.70	1.00	-0.45	-0.50	-0.50

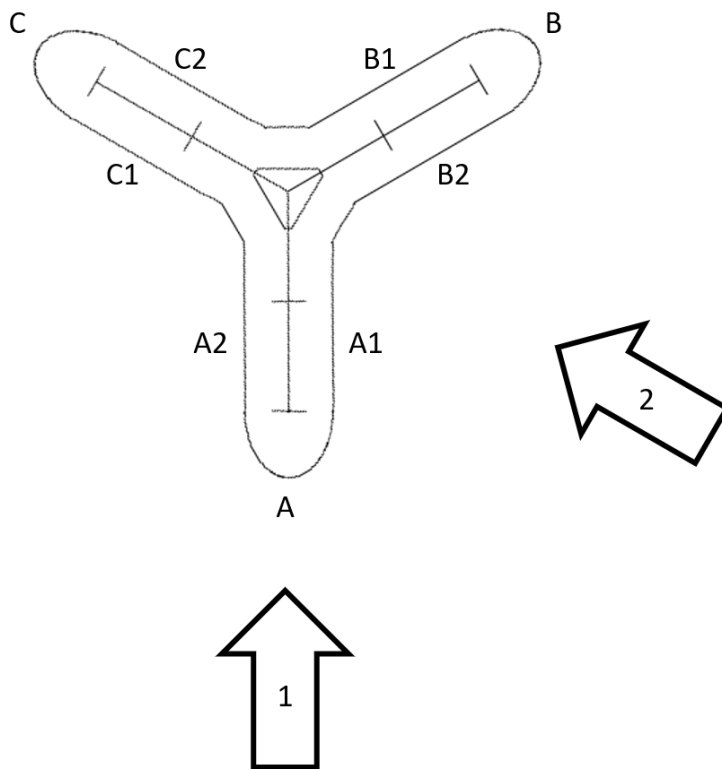


Figure 98: Illustration of the two main wind directions on a Y-shaped section and face notations.

Wind direction 1:

- A: Depends of the face radius, but in the worst reasonable case the face will be flat and therefore similar to *face A* for the plus shaped section with wind load 1.
- A1 and A2: These faces will have a lot in common with *B1 and B2* for the plus shaped section. However, due to the turbulence occurring when wind hits *C1 and C2* the plus shaped section will have somewhat larger wind pressures than the more streamlined Y-shape.
- B2 and C1: A combination between *C1 and C2* for the plus shaped section, wind direction 1 and the windward faces for a triangular section for wind direction 2. Due to the small angle between the wind and the façade the values are shifted in the positive direction.
- B and C: Depends of the face radius. Has similarities with *D1, D2 and G* for the plus shaped section and wind direction 1 but even more with faces *D1 and G* for wind direction 2.
- B1 and C2: A combination between *E1 and E2* for the plus shaped section wind direction 1, *E1 and F1* for the plus shaped section wind direction 2 and the leeward side of a triangular section with wind direction 2.

Wind direction 2:

- A1 and B2: A mix between the windward face of a triangular section with load direction 1 and faces *B2 and C2* for a plus shaped section subject to wind in direction 2.
- A and B: In between faces *A and D2* of a plus shaped section subject to wind in direction 2 and *D1 and D2* with wind direction 1.

- A2 and B1: Has the largest similarities with the leeward sides of a triangular section loaded in direction 1, faces *B1* and *E2* for a plus shaped section loaded in wind direction 2 and faces *E1* and *E2* for the plus shaped section with wind direction 1.
- C1 and C2: Shows large similarities with *F1* and *F2* of a plus shaped section subject to wind in direction 1.
- C: Best approximated by face *G* for the plus shaped section with wind in direction 1.

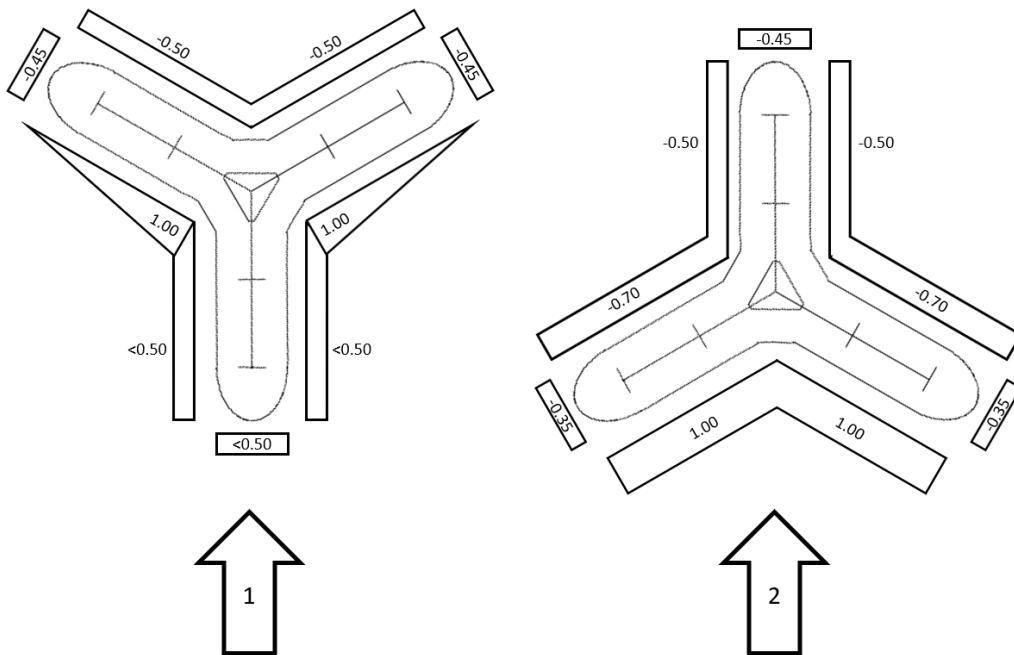


Figure 99: Graphical illustration of the simplified wind pressure shape coefficients for a Y-shaped section subject to wind in the two main directions.

Appendix IV

Design of building components – ULS

Design in any limit state must be made with regard to material properties, time dependent effects, environmental conditions and a variety of design situations (SIS, 2009). The general principle for ULS design is that the design load effect E_d must be smaller than or equal to the design resistance R_d (SIS, 2004).

$$E_d \leq R_d \quad (30)$$

E_d *Design load effect.*
 R_d *Design resistance.*

The design resistance for timber depends on a range of factors including material capacity, load duration, moisture conditions, size effects and a partial coefficient (SIS, 2009). In general, the design resistance can be expressed as:

$$R_d = k_{mod} k_{size} k_{sys} \frac{R_k}{\gamma_M} \quad (31)$$

R_d *Design resistance.*
 k_{mod} *Correction factor accounting for load duration and moisture conditions.*
 k_{size} *Correction factor accounting for size dependent increase in capacity for beam, column and truss elements. Applies to members subject to tension or bending.*
 k_{sys} *Correction factor accounting for system effect on CLT. Applies to CLT elements subject to tension or bending.*
 R_k *Characteristic value for the resistance.*
 γ_M *Partial coefficient for material properties.*

When choosing k_{mod} in Table 34 the probable load duration and climate class must be considered. For examples and indications on what to choose, see Table 32 and Table 33. k_{mod} should be chosen corresponding to the shortest load duration for any of the loads in the considered load combination (SIS, 2009).

Table 32: Load duration classes to consider when determining k_{mod} . Based on table 2.1 and table 2.2 in SS-EN 1995 (SIS, 2009).

Load duration class	Example loads	Load durations
Permanent	Self-weight	>10 years
Long term	Storage	6 months – 10 years
Medium term	Imposed load, snow load	1 week – 6 months
Short term	Snow load, wind load	<1 week
Instantaneous	Wind load, accidental load	

Table 33: Service classes according to section 2.3.1.3 in SS-EN 1995 (SIS, 2009).

Service class	
1	Moisture content corresponding to air temperature of 20°C and relative humidity of the surrounding air exceeds 65 % for a few weeks each year.
2	Moisture content corresponding to air temperature of 20°C and relative humidity of the surrounding air exceeds 85 % for a few weeks each year.
3	Conditions leading to higher moisture content than service class 2.

Table 34: Values of the correction factor k_{mod} accounting for load duration and moisture. Based on table 3.1 in SS-EN 1995 (SIS, 2009) and table 3.3 in KL-trähandboken (Svenskt Trä, 2017a).

Material	Service class	Load duration				
		Permanent	Long term	Medium term	Short term	Instantaneous
Sawn timber	1	0.60	0.70	0.80	0.90	1.10
	2	0.60	0.70	0.80	0.90	1.10
	3	0.50	0.55	0.65	0.70	0.90
Glulam	1	0.60	0.70	0.80	0.90	1.10
	2	0.60	0.70	0.80	0.90	1.10
	3	0.50	0.55	0.65	0.70	0.9
LVL	1	0.60	0.70	0.80	0.90	1.10
	2	0.60	0.70	0.80	0.90	1.10
	3	0.50	0.55	0.65	0.70	0.90
CLT	1	0.6	0.7	0.8	0.9	1.1
	2	0.6	0.7	0.8	0.9	1.1
	3	-	-	-	-	-

Capacity changes due to size effects might be considered when designing for tension and bending. However, this possibility of increased capacity is limited to small sections with low probability of being used in the structural system of a high-rise building (SIS, 2009).

System effects can be seen for CLT elements. In practice, due to the manufacturing process, the likelihood of major defects in a section is small and gets even smaller as the element width increases. The system effect can mainly be seen for elements subject to bending or tension (Svenskt Trä, 2017a).

$$k_{sys} = \min(1 + 0.1 b, 1.15) \quad (32)$$

k_{sys} Correction factor accounting for system effect on CLT.
 b Width of the CLT section contributing with capacity.

The characteristic resistance for a structural member is material dependent. Due to the variety in composition of different timber products, there is a wide range of values available.

The partial coefficient γ_M used to account for material properties and load resistance is also material dependent and should be chosen according to Table 35 (Svenskt Trä, 2017a).

Table 35: Table of partial coefficients γ_M for material properties and resistances. Based on table 2.3 in SS-EN 1995 (SIS, 2009) and table 3.2 in KL-trähandboken (Svenskt Trä, 2017a).

Fundamental combinations:	γ_M
Sawn timber	1.30
Glulam	1.25
LVL	1.20
CLT	1.25
Accidental combinations	1.00

Global design should generally be done assuming linear elastic behaviour. However, if the connection provides enough ductility to allow for load redistribution within the structure, elastic-plastic methods might be used (Svenskt Trä, 2017a).

Capacity verifications of beams, columns and truss elements.

The structural loading of each element depends on factors such as orientation, location in the global structure and support conditions. This means that several capacity checks must be done for each of the structural components. Due to the nature of timber, the structural system of a high-rise timber building must be designed to carry loads in its longitudinal direction to as large extent as possible.

The following sections describes checks that are of main interest for beams, columns and truss elements used in the structure. Relevant stresses are determined through FE analysis in *Grasshopper* and *Karamba 3D* while capacity values are determined according to the following sections.

Tension parallel to the grain

$$\sigma_{t,0,d} \leq f_{t,0,d} \quad (33)$$

$\sigma_{t,0,d}$ *Design value for tensile stress parallel to the grain.*

$f_{t,0,d}$ *Design resistance for tension parallel to the grain.*

Compression parallel to the grain

$$\sigma_{c,0,d} \leq f_{c,0,d} \quad (34)$$

$\sigma_{c,0,d}$ *Design value for compressive stresses parallel to the grain.*

$f_{c,0,d}$ *Design resistance for compression parallel to the grain.*

Also, check for instability as later described in this appendix.

Bending

$$\frac{\sigma_{m,y,d}}{f_{m,y,d}} + k_m \frac{\sigma_{m,z,d}}{f_{m,z,d}} \leq 1 \quad (35)$$

$$k_m \frac{\sigma_{m,y,d}}{f_{m,y,d}} + \frac{\sigma_{m,z,d}}{f_{m,z,d}} \leq 1 \quad (36)$$

$\sigma_{m,y,d}$	<i>Design value for bending stress in the strong direction.</i>
$\sigma_{m,z,d}$	<i>Design value for bending stress in the weak direction.</i>
$f_{m,y,d}$	<i>Design resistance for bending in the strong direction.</i>
$f_{m,z,d}$	<i>Design resistance for bending in the weak direction.</i>
k_m	<i>= 0.7 , factor for stress redistribution due to imperfections in a rectangular cross-section of sawn timber, glulam or LVL.</i>

Provided that lateral torsional stability is ensured, no additional controls are needed with regard to instability.

Combined axial tension and bending

$$\frac{\sigma_{t,0,d}}{f_{t,0,d}} + \frac{\sigma_{m,y,d}}{f_{m,y,d}} + k_m \frac{\sigma_{m,z,d}}{f_{m,z,d}} \leq 1 \quad (37)$$

$$\frac{\sigma_{t,0,d}}{f_{t,0,d}} + k_m \frac{\sigma_{m,y,d}}{f_{m,y,d}} + \frac{\sigma_{m,z,d}}{f_{m,z,d}} \leq 1 \quad (38)$$

$\sigma_{t,0,d}$	<i>Design value for tensile stress parallel to the grain.</i>
$\sigma_{m,y,d}$	<i>Design value for bending stress in the strong direction.</i>
$\sigma_{m,z,d}$	<i>Design value for bending stress in the weak direction.</i>
$f_{t,0,d}$	<i>Design resistance for tension parallel to the grain.</i>
$f_{m,y,d}$	<i>Design resistance for bending in the strong direction.</i>
$f_{m,z,d}$	<i>Design resistance for bending in the weak direction.</i>
k_m	<i>= 0.7 , factor for stress redistribution due to imperfections in a rectangular cross-section of sawn timber, glulam or LVL.</i>

Combined axial compression and bending

$$\left(\frac{\sigma_{c,0,d}}{f_{c,0,d}} \right)^2 + \frac{\sigma_{m,y,d}}{f_{m,y,d}} + k_m \frac{\sigma_{m,z,d}}{f_{m,z,d}} \leq 1 \quad (39)$$

$$\left(\frac{\sigma_{c,0,d}}{f_{c,0,d}} \right)^2 + k_m \frac{\sigma_{m,y,d}}{f_{m,y,d}} + \frac{\sigma_{m,z,d}}{f_{m,z,d}} \leq 1 \quad (40)$$

$\sigma_{c,0,d}$	<i>Design value for compressive stresses parallel to the grain.</i>
$\sigma_{m,y,d}$	<i>Design value for bending stress in the strong direction.</i>
$\sigma_{m,z,d}$	<i>Design value for bending stress in the weak direction.</i>
$f_{c,0,d}$	<i>Design resistance for compression parallel to the grain.</i>
$f_{m,y,d}$	<i>Design resistance for bending in the strong direction.</i>

$f_{m,z,d}$ *Design resistance for bending in the weak direction.*
 k_m $= 0.7$, *factor for stress redistribution due to imperfections in a rectangular cross-section of sawn timber, glulam or LVL.*

Also, check for instability as later described in this appendix.

Shear with zero or one component parallel to the grain

$$\tau_d \leq f_{v,d} \quad (41)$$

τ_d *Design value for shear stress.*
 $f_{v,d}$ *Design resistance for shear.*

Capacity reduction due to cracks must be accounted for. According to SS-EN 1995 an effective width b_{ef} should be used when calculating the shear stresses.

$$b_{ef} = k_{cr} \cdot b \quad (42)$$

b_{ef} *Effective width of the cross-section.*
 k_{cr} *Factor for shear capacity reduction due to cracks in the cross-section.*
 $= 0.67$ *for sawn timber and glulam.*
 $= 1.00$ *for other wood products.*
 b *Physical width of the cross-section.*

However, since the shear stresses are linearly dependent on the section width, utilizing FE analysis to obtain the shear stresses, the factor k_{cr} can be accounted for directly on the determined stress value.

$$\tau_d = \frac{\tau_{FE}}{k_{cr}} \quad (43)$$

τ_d *Design value for shear stress.*
 τ_{FE} *Value for shear stress determined through FE analysis.*
 k_{cr} *Factor for shear capacity reduction due to cracks in the cross-section.*
 $= 0.67$ *for sawn timber and glulam.*
 $= 1.00$ *for other wood products.*

Instability of column, beam or truss elements

If $\lambda_{rel,y}$ and $\lambda_{rel,z}$ are both smaller than or equal to 0.3, no instability check is needed.

$$\lambda_{rel,y} \leq 0.3 \ \& \ \lambda_{rel,z} \leq 0.3$$

For beams or columns loaded in either in pure compression or combined compression and bending.

$$\frac{\sigma_{c,0,d}}{k_{c,y} f_{c,0,d}} + \frac{\sigma_{m,y,d}}{f_{m,y,d}} + k_m \frac{\sigma_{m,z,d}}{f_{m,z,d}} \leq 1 \quad (44)$$

$$\frac{\sigma_{c,0,d}}{k_{c,z} f_{c,0,d}} + k_m \frac{\sigma_{m,y,d}}{f_{m,y,d}} + \frac{\sigma_{m,z,d}}{f_{m,z,d}} \leq 1 \quad (45)$$

$\sigma_{c,0,d}$	<i>Design value for compressive stresses parallel to the grain.</i>
$\sigma_{m,y,d}$	<i>Design value for bending stress in the strong direction.</i>
$\sigma_{m,z,d}$	<i>Design value for bending stress in the weak direction.</i>
$f_{c,0,d}$	<i>Design resistance for compression parallel to the grain.</i>
$f_{m,y,d}$	<i>Design resistance for bending in the strong direction.</i>
$f_{m,z,d}$	<i>Design resistance for bending in the weak direction.</i>
k_m	<i>= 0.7 , factor for stress redistribution due to imperfections in a rectangular cross-section of sawn timber, glulam or LVL.</i>
$k_{c,y}$	<i>Instability factor in the strong direction.</i>
$k_{c,z}$	<i>Instability factor in the weak direction.</i>

$$k_{c,y} = \frac{1}{k_y + \sqrt{k_y^2 - \lambda_{rel,y}^2}} \quad (46)$$

$$k_{c,z} = \frac{1}{k_y + \sqrt{k_y^2 - \lambda_{rel,y}^2}} \quad (47)$$

$k_{c,y}$	<i>Instability factor in the strong direction.</i>
$k_{c,z}$	<i>Instability factor in the weak direction.</i>
k_y	<i>Instability factor in the strong direction.</i>
k_z	<i>Instability factor in the weak direction.</i>
$\lambda_{rel,y}$	<i>Relative slenderness ratio for the strong direction.</i>
$\lambda_{rel,z}$	<i>Relative slenderness ratio for the weak direction.</i>

$$k_y = 0.5(1 + \beta_c (\lambda_{rel,y} - 0.3) + \lambda_{rel,y}^2) \quad (48)$$

$$k_z = 0.5(1 + \beta_c (\lambda_{rel,z} - 0.3) + \lambda_{rel,z}^2) \quad (49)$$

k_y	<i>Instability factor in the strong direction.</i>
k_z	<i>Instability factor in the weak direction.</i>
β_c	<i>Straightness factor.</i>
	<i>= 0.2 for sawn timber</i>
	<i>= 0.1 for glulam and LVL</i>
$\lambda_{rel,y}$	<i>Relative slenderness ratio for the strong direction.</i>
$\lambda_{rel,z}$	<i>Relative slenderness ratio for the weak direction.</i>

$$\lambda_{rel,y} = \frac{\lambda_y}{\pi} \sqrt{\frac{f_{c,0,k}}{E_{0.05}}} \quad (50)$$

$$\lambda_{rel,z} = \frac{\lambda_z}{\pi} \sqrt{\frac{f_{c,0,k}}{E_{0.05}}} \quad (51)$$

$\lambda_{rel,y}$	<i>Relative slenderness ratio for the strong direction.</i>
$\lambda_{rel,z}$	<i>Relative slenderness ratio for the weak direction.</i>
λ_y	<i>Slenderness ratio for the strong direction.</i>
λ_z	<i>Slenderness ratio for the weak direction.</i>
$f_{c,0,k}$	<i>Characteristic compressive strength parallel to the grain.</i>
$E_{0.05}$	<i>Young's modulus parallel to the grain corresponding to the 5 percent fractile.</i>

According to *Limträhandboken del 2*, the slenderness ratios can be determined as follows (Crocetti, Danielsson, et al., 2016):

$$\lambda_y = \frac{\beta L}{i_y} \quad (52)$$

$$\lambda_z = \frac{\beta L}{i_z} \quad (53)$$

λ_y	<i>Slenderness ratio for the strong direction.</i>
λ_z	<i>Slenderness ratio for the weak direction.</i>
β	<i>Buckling coefficient depending on support conditions, see Table 36.</i>
L	<i>Distance between supports.</i>
i_y	<i>Radius of gyration in the strong direction.</i>
i_z	<i>Radius of gyration in the weak direction.</i>

$$i_y = \sqrt{\frac{I_y}{A}} \quad (54)$$

$$i_z = \sqrt{\frac{I_z}{A}} \quad (55)$$

i_y	<i>Radius of gyration in the strong direction.</i>
i_z	<i>Radius of gyration in the weak direction.</i>
I_y	<i>Moment of inertia in the strong direction.</i>
I_z	<i>Moment of inertia in the weak direction.</i>

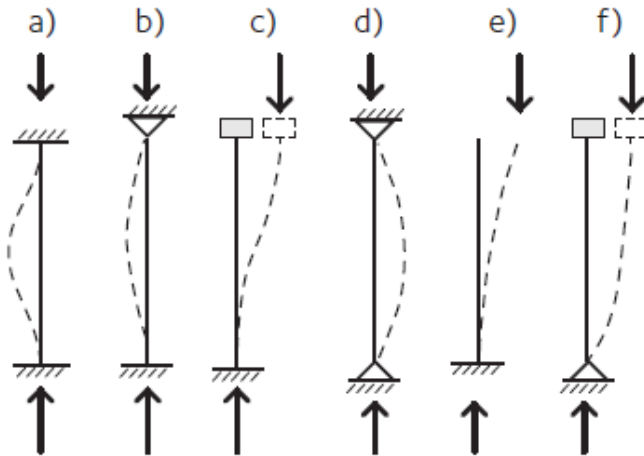


Figure 100: Figure showing potential buckling scenarios for an axially loaded column, beam or truss element. Figure 4.13 in *Limträhandboken del2*, (Crocetti, Danielsson, et al., 2016).

Table 36: Table with buckling coefficients β , for each case shown in Figure 100.

Buckling scenario	a)	b)	c)	d)	e)	f)
Theoretical value	0.50	0.70	1.00	1.00	2.00	2.00
Recommended value	0.70	0.85	1.20	1.00	2.25	2.25

Design of slab and wall elements

As a general assumption when designing CLT elements, only layers loaded parallel to the grain are considered to contribute with load bearing capacity and stiffness (Svenskt Trä, 2017a). Figure 101 show definitions used for the capacity calculations.

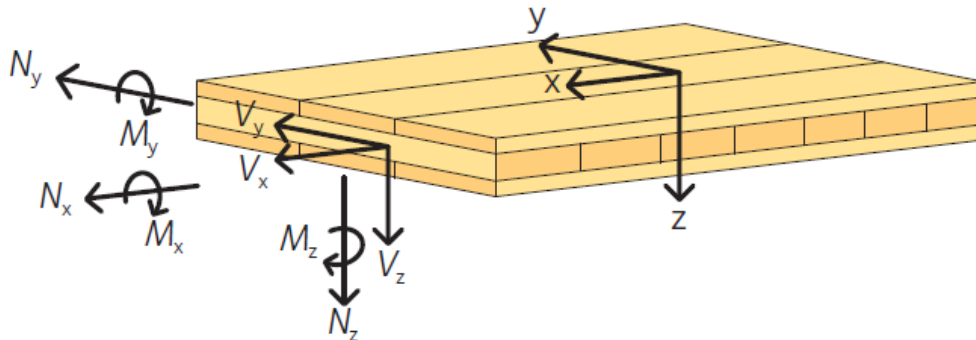


Figure 101: Illustration of axis directions, moment notations and normal force notations. Figure 3.3 in *KL-trähandboken* (Svenskt Trä, 2017a).

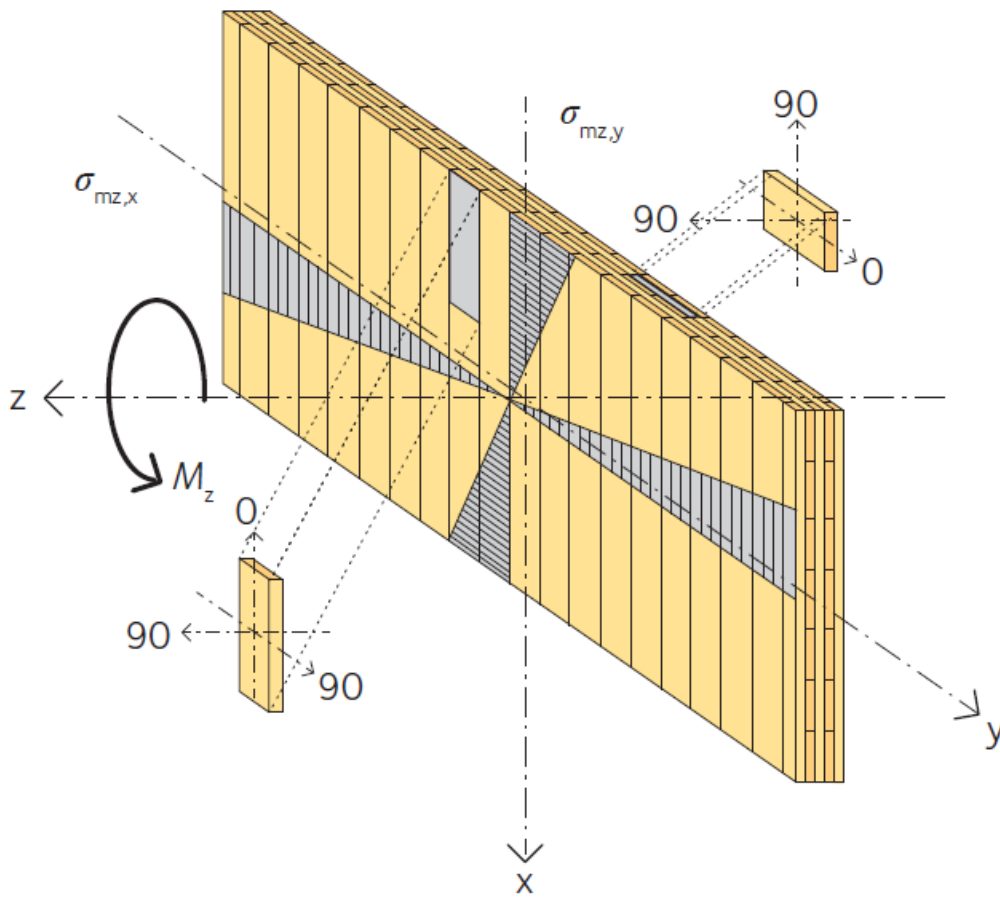


Figure 102: View of a CLT element for global axes and local axes for individual boards. Figure 3.4 in KL-trähandboken (Svenskt Trä, 2017a).

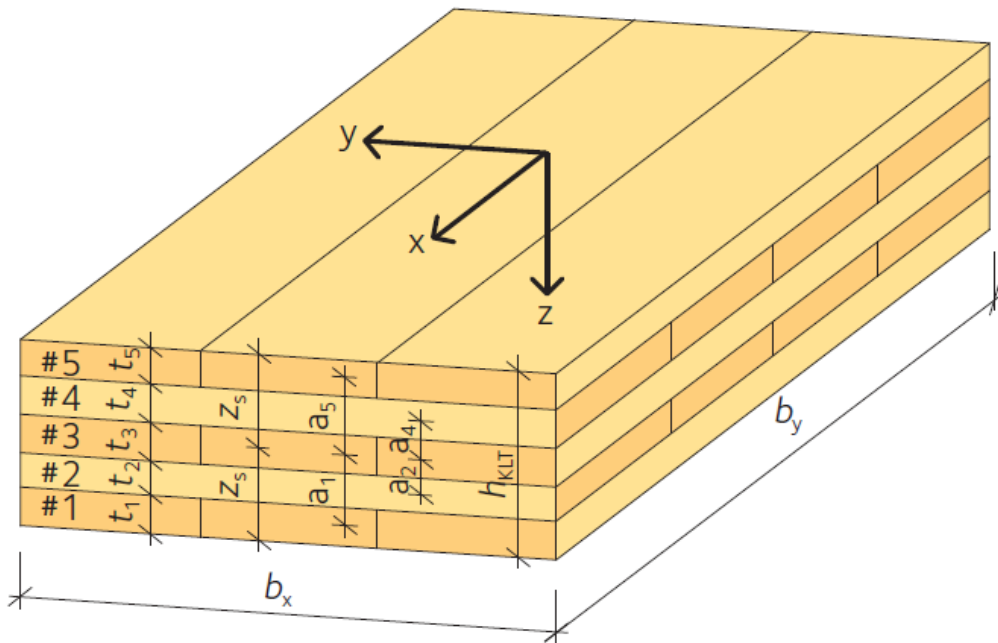


Figure 103: Global axes and notation scheme for layers, thicknesses and distances within a CLT-section. Figure 3.5 in (Svenskt Trä, 2017a).

In-plane tension parallel to the surface grain direction

$$\sigma_{t,x,d} \leq f_{t,0,xlay,d} \quad (56)$$

$\sigma_{t,x,d}$ *Design value for tensile stress parallel to the x-axis.*
 $f_{t,0,xlay,d}$ *Design resistance for tensile stress for the boards with grain direction parallel to the x-axis.*

In-plane tension perpendicular to the surface grain direction

$$\sigma_{t,y,d} \leq f_{t,0,ylay,d} \quad (57)$$

$\sigma_{t,y,d}$ *Design value for tensile stress parallel to the y-axis.*
 $f_{t,0,ylay,d}$ *Design resistance for tensile stress for the boards with grain direction parallel to the y-axis.*

In-plane compression parallel to surface grain direction

$$\sigma_{c,x,d} \leq f_{c,0,xlay,d} \quad (58)$$

$\sigma_{c,x,d}$ *Design value for compressive stress parallel to the x-axis.*
 $f_{c,0,xlay,d}$ *Design resistance for compressive stress for the boards with grain direction parallel to the x-axis.*

If there is a risk of instability, use separate calculation method described below.

In-plane compression perpendicular to the surface grain direction

$$\sigma_{c,y,d} \leq f_{c,0,ylay,d} \quad (59)$$

$\sigma_{c,y,d}$ *Design value for compressive stress parallel to the y-axis.*
 $f_{c,0,ylay,d}$ *Design resistance for compressive stress for the boards with grain direction parallel to the y-axis.*

If there is a risk of instability, use separate calculation method described below.

In-plane bending parallel to the surface grain direction

$$\sigma_{m,z,d} \leq f_{m,xlay,d} \quad (60)$$

$\sigma_{m,z,d}$ *Design value for bending stress parallel to the x-axis.*
 $f_{m,xlay,d}$ *Design resistance for bending stress for the boards with grain direction parallel to the x-axis.*

In-plane shear (panel shear)

$$\tau_{v,xy,d} \leq f_{v,090,xlay,d} \quad (61)$$

$$\tau_{v,yx,d} \leq f_{v,090,ylay,d} \quad (62)$$

$\tau_{v,xy,d}$	<i>Design value for panel shear stress component along the y-axis.</i>
$\tau_{v,yx,d}$	<i>Design value for panel shear stress component along the x-axis.</i>
$f_{v,090,xlay,d}$	<i>Design resistance for panel shear stress component along the y-axis.</i>
$f_{v,090,ylay,d}$	<i>Design resistance for panel shear stress component along the x-axis.</i>

Instability of CLT elements subject to in-plane compression

If $\lambda_{rel,y}$ and $\lambda_{rel,x}$ are both smaller than or equal to 0.3, no instability check is needed.

$$\lambda_{rel,y} \leq 0.3 \ \& \ \lambda_{rel,z} \leq 0.3$$

For CLT elements loaded in pure compression, instability is considered through the following expressions:

$$\frac{\sigma_{c,x,d}}{k_{c,y} f_{c,0,xlay,d}} \leq 1 \quad (63)$$

$$\frac{\sigma_{c,y,d}}{k_{c,x} f_{c,0,ylay,d}} \leq 1 \quad (64)$$

$\sigma_{c,x,d}$	<i>Design value for compressive stress parallel to the x-axis.</i>
$\sigma_{c,y,d}$	<i>Design value for compressive stress parallel to the y-axis.</i>
$f_{c,0,xlay,d}$	<i>Design resistance for compressive stress for the boards with grain direction parallel to the x-axis.</i>
$f_{c,0,ylay,d}$	<i>Design resistance for compressive stress for the boards with grain direction parallel to the y-axis.</i>
$k_{c,y}$	<i>Reduction factor regarding non-linear effects for out-of-plane buckling around the y-axis.</i>
$k_{c,x}$	<i>Reduction factor regarding non-linear effects for out-of-plane buckling around the x-axis.</i>

$$k_{c,y} = \frac{1}{k_y + \sqrt{k_y^2 - \lambda_{rel,y}^2}} \quad (65)$$

$$k_{c,x} = \frac{1}{k_x + \sqrt{k_x^2 - \lambda_{rel,x}^2}} \quad (66)$$

$k_{c,y}$	<i>Reduction factor regarding non-linear effects for out-of-plane buckling around the y-axis.</i>
$k_{c,x}$	<i>Reduction factor regarding non-linear effects for out-of-plane buckling around the x-axis.</i>
k_y	<i>Instability factor for out-of-plane buckling around the y-axis.</i>
k_x	<i>Instability factor for out-of-plane buckling around the x-axis.</i>
$\lambda_{rel,y}$	<i>Relative slenderness ratio for out-of-plane buckling around the y-axis.</i>

$\lambda_{rel,x}$ Relative slenderness ratio for out-of-plane buckling around the x-axis.

$$k_y = 0.5(1 + 0.1(\lambda_{rel,y} - 0.3) + \lambda_{rel,y}^2) \quad (67)$$

$$k_x = 0.5(1 + 0.1(\lambda_{rel,x} - 0.3) + \lambda_{rel,x}^2) \quad (68)$$

k_y Instability factor for out-of-plane buckling around the y-axis.

k_x Instability factor for out-of-plane buckling around the x-axis.

$\lambda_{rel,y}$ Relative slenderness ratio for out-of-plane buckling around the y-axis.

$\lambda_{rel,x}$ Relative slenderness ratio for out-of-plane buckling around the x-axis.

$$\lambda_{rel,y} = \frac{\lambda_y}{\pi} \sqrt{\frac{f_{c,0,xlay,k}}{E_{0,x,05}}} \quad (69)$$

$$\lambda_{rel,x} = \frac{\lambda_x}{\pi} \sqrt{\frac{f_{c,0,ylay,k}}{E_{0,y,05}}} \quad (70)$$

$\lambda_{rel,y}$ Relative slenderness ratio for out-of-plane buckling around the y-axis.

$\lambda_{rel,x}$ Relative slenderness ratio for out-of-plane buckling around the x-axis.

λ_y Slenderness ratio for buckling around the y-axis.

λ_x Slenderness ratio for buckling around the x-axis.

$f_{c,0,xlay,k}$ Characteristic compressive strength parallel to the x-axis.

$f_{c,0,ylay,k}$ Characteristic compressive strength parallel to the y-axis.

$E_{0,x,05}$ Young's modulus parallel to the x-axis corresponding to the 5 percent fractile.

$E_{0,y,05}$ Young's modulus parallel to the y-axis corresponding to the 5 percent fractile.

$$\lambda_y = \frac{0.1 L_x}{i_{x,ef}} \quad (71)$$

$$\lambda_x = \frac{0.1 L_y}{i_{y,ef}} \quad (72)$$

λ_y Slenderness ratio for buckling around the y-axis.

λ_x Slenderness ratio for buckling around the x-axis.

L_x Distance between supports in the x-direction.

L_y Distance between supports in the y-direction.

$i_{y,ef}$ Effective radius of gyration along the y-axis.

$i_{x,ef}$ Effective radius of gyration along the x-axis.

$$i_{y.ef} = \sqrt{\frac{I_{y.ef}}{A_{y,net}}} \quad (73)$$

$$i_{x.ef} = \sqrt{\frac{I_{x.ef}}{A_{x,net}}} \quad (74)$$

$i_{y.ef}$	<i>Effective radius of gyration along the y-axis.</i>
$i_{x.ef}$	<i>Effective radius of gyration along the x-axis.</i>
$I_{y.ef}$	<i>Effective moment of inertia around the y-axis.</i>
$I_{x.ef}$	<i>Effective moment of inertia around the x-axis.</i>
$A_{y,net}$	<i>Effective net section area along the y-axis.</i>
$A_{x,net}$	<i>Effective net section area along the x-axis.</i>

$$E_{0,x,05} = \left(1 - \frac{0.328}{\sqrt{\frac{2 b_x}{0.15} - 1}} \right) E_{0,x,mean} \quad (75)$$

$$E_{0,y,05} = \left(1 - \frac{0.328}{\sqrt{\frac{2 b_y}{0.15} - 1}} \right) E_{0,y,mean} \quad (76)$$

$E_{0,x,05}$	<i>Young's modulus parallel to the x-axis corresponding to the 5 percent fractile.</i>
$E_{0,y,05}$	<i>Young's modulus parallel to the y-axis corresponding to the 5 percent fractile.</i>
$E_{0,x,mean}$	<i>Young's modulus parallel to the x-axis corresponding to the mean value.</i>
$E_{0,y,mean}$	<i>Young's modulus parallel to the y-axis corresponding to the mean value.</i>

Appendix V

SLS design for individual elements

Overall, the verification needed in SLS is that the design load effect E_d must be smaller or equal to the design limit value for the considered service limit state criterion C_d (SIS, 2004).

$$E_d \leq C_d \quad (77)$$

E_d *Design load effect.*
 C_d *Limiting design criterion in service limit state.*

For a structure with components and connections all showing the same creep behaviour and linear load – deflection relation, the following simplified equation can be used for the long-term deformations (SIS, 2009):

$$u_{fin} = u_{fin,G} + u_{fin,Q,1} + \sum u_{fin,Q,i}, \quad i > 1 \quad (78)$$

$$u_{fin,G} = u_{inst,G} (1 + k_{def}) \quad (79)$$

$$u_{fin,Q,1} = u_{inst,Q,1} (1 + \psi_{2,1} k_{def}) \quad (80)$$

$$u_{fin,Q,i} = u_{inst,Q,i} (\psi_{0,i} + \psi_{2,i} k_{def}) \quad (81)$$

u_{fin} *Total long-term deflections.*
 $u_{fin,G}$ *Long-term deflections due to self-weight.*
 $u_{fin,Q,1}$ *Long-term deflections due to the main variable load.*
 $u_{fin,Q,i}$ *Long-term deflections due to secondary variable loads.*
 $u_{inst,G}$ *Instantaneous deflections due to self-weight.*
 $u_{inst,Q,1}$ *Instantaneous deflections due to the main variable load.*
 $u_{inst,Q,i}$ *Instantaneous deflections due to secondary variable loads.*
 k_{def} *Deformation factor accounting for moisture dependency on the creep.*
 $\psi_{2,1}$ *Factor for quasi-permanent value of the main variable load.*
 $\psi_{2,i}$ *Factor for quasi-permanent value of the secondary variable loads.*

Note: If the equations above are used, ψ_2 and $\psi_{2,i}$ should be excluded from the load combination.

The deformation factor k_{def} should be chosen depending on the actual service class according to Table 37.

Table 37: Values for the deformation factor k_{def} . Obtained from table 3.2 in SS-EN 1995 (SIS, 2009) and table 3.4 in KL-trähandboken (Svenskt Trä, 2017a).

Material	Service class		
	1	2	3
Sawn timber	0.60	0.80	2.00
Glulam	0.60	0.80	2.00
LVL	0.60	0.80	2.00
CLT > 7 layers	0.85	1.10	-
CLT ≤ 7 layers	0.80	1.00	-

Table 38: Factors for quasi-permanent value of a variable action. Obtained from table A1.1 in SS-EN 1990 (SIS, 2004).

Load	ψ_2
Imposed load in offices	0.3
Imposed load in commercial areas	0.6
Snow load	0.2
Wind load	0

Beam elements

To fulfill the SLS demands or maintained appearance and human comfort when using the building, the limits shown in Table 39 are stated for beams and beam deflections.

Table 39: Recommended limiting values for beam deflection for various beams. Table 7.2 in SS-EN 1995 (SIS, 2009).

	w_{inst}	$w_{net,fin}$	w_{fin}
Beams with end supports	$\frac{l}{300}$ to $\frac{l}{500}$	$\frac{l}{250}$ to $\frac{l}{350}$	$\frac{l}{150}$ to $\frac{l}{300}$
Cantilever beams	$\frac{l}{150}$ to $\frac{l}{250}$	$\frac{l}{125}$ to $\frac{l}{175}$	$\frac{l}{75}$ to $\frac{l}{150}$

Slab elements

If using pre-fabricated slab elements, the SLS requirements can be assumed as fulfilled.

Appendix VI

Evaluation of wind-induced vibrations – ISO 6897

ISO 6897 is the old standard used to evaluate and assess human response to structural vibrations. It bases the evaluation of the worst 10 consecutive minutes of wind for a 5 years return period (IOS, 1984). When evaluating buildings used for general purposes, curve 1 in Figure 104 should be used. Also, the vibrations considered in this standard are limited to the horizontal plane. This applies to motions induced through both translation and rotation caused by wind.

Wind velocity for a 5 year return period can based on EKS11 be determined as follows:

$$v_{b,5years} = 0.855 v_{b,50years} \quad (82)$$

$v_{b,5year}$ *Reference wind speed with 5 year reoccurrence time.*

$v_{b,50year}$ *Reference wind speed with 50 years reoccurrence time.*

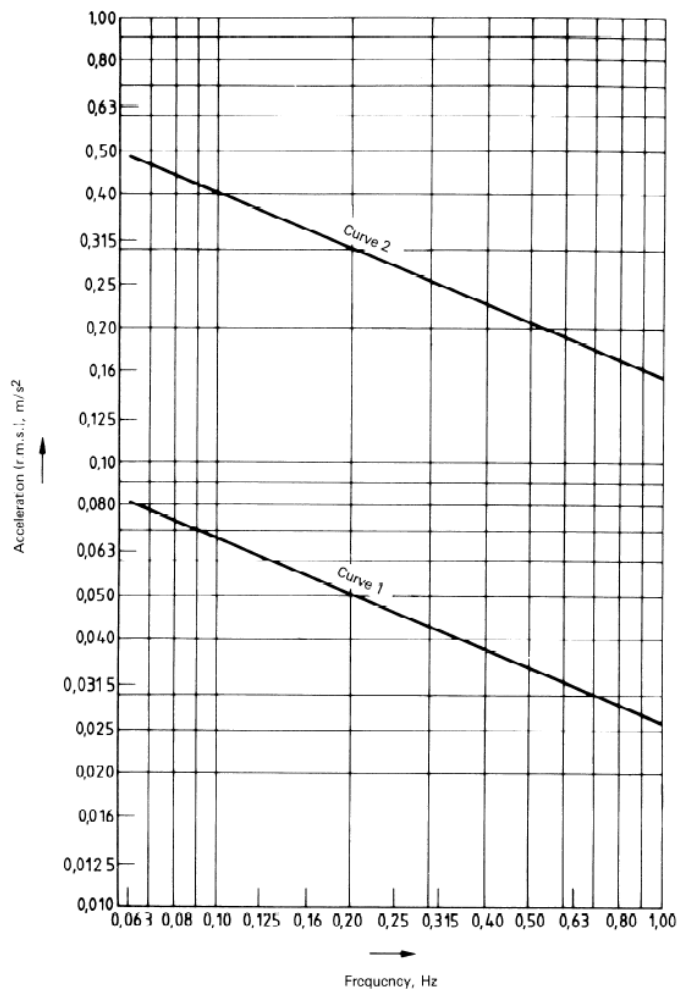


Figure 104: Suggested satisfactory magnitudes of horizontal motion. Curve 1 for general purpose buildings and curve 2 for off-shore fixed structures. Figure 1 in the annex for ISO 6897 (IOS, 1984).

Appendix VII

Verification regarding vortex shedding

To verify the consequence of vortex shedding for the uniformly wide cylindrical structures, the approach shown in the old Swedish national rules BSV97 has been applied as follows:

Determine mean wind speed (SS-EN 1991-1-4)	
Mean wind speed, v_m	31 m/s
Reference wind speed, v_b	25 m/s
Roughness factor, $c_r(200m)$	1.24 -
Terrain factor, k_r	0.23 -
Roughness length, $z_{0,IV}$	1 m
Reference height, $z_{0,II}$	0.05 m
Topography factor, $c_0(200m)$	1 -

Factors (BSV97)	
Kinematic viscosity of air	0.000015 m ² /s
Strouhals number	0.2 -

Critical wind speed (BSV97)	4.5.1 Cylindrical tower with perimeter truss and CLT core	4.5.2 Cylindrical tower with perimeter truss and internal truss	4.5.3 Cylindrical tower with hollow center
Diameter, d [m]	41	41	52
Reynolds tal, Re [-]	8.48E+07	8.48E+07	1.08E+08
Eigenfrequency, f_0	0.30	0.31	0.37
Critical wind speed, v_{cr}	61.5	63.55	96.2
Ratio v_{cr}/v_m	2.0	2.0	3.1

In BSV97, the following is specified:

- If the building height to width ratio is smaller than 1:5, vortex shedding can be neglected.
- If the critical wind speed due to vortex shedding is larger than the characteristic mean wind speed, vortex shedding can be neglected in design.

Since the critical wind speed with regard to vortex shedding is substantially higher than the characteristic wind speed, vortex shedding will not be a problem for any of the considered towers.

Also, if wanting to calculate the equivalent cross-wind wind load due to vortex shedding, the critical wind speed must be used when determining the equivalent wind pressure. Therefore, since the critical wind speed values for these concepts are of such high magnitude, it is not reasonable to use the approach specified in BSV97. It would drastically overestimate the load values.

Appendix VIII

Convergence study

When deciding the mesh size for the core elements, a convergence study was done for the easiest shape. The core structure, with the shape of a 200 m tall H-beam, was modelled with shell elements in *Grasshopper* and analyzed in *Karamba 3D*. The cross-section of the H-beam used for the convergence study consists of a 5.5 m web and two flanges of 6 m, all with the thickness 0.5 m. A point load of 10 kN was applied at the top of the structure and the beam was tested for horizontal deflections in both x- and y-directions. Thereafter, the deformation values for different mesh sizes in horizontal and vertical directions were saved and compared to a simple hand-calculation of a cantilever beam with similar dimensions and load.

The theoretical deformation was determined to 6.39 cm in x-direction and 21.59 cm in y-direction. Since there are different mesh sizes in vertical and horizontal direction, 10 different mesh sizes in each direction was combined with 3 different mesh sizes in the other direction. Result from all meshes from the convergence study can be seen in the graphs below.

To check the model, an even finer mesh was used. For this mesh, the deformation approached 6.29 cm in the x-direction and 21.44 cm in the y-direction. This means deviations of approximately 1.5 % and 0.7 % from the theoretical value. To investigate why the results differed, a 200 m long beam element was modelled with the same dimensions and loads. Even this beam deviated slightly from the theoretical value. The shear modulus for the modelled beam was then chosen to infinity in order to avoid shear deformation. This since shear deformations were not considered in the hand-calculation. A new comparison showed similar deformation values for the modelled beam and hand calculations. Therefore, the difference in the shell element model can be assumed to be due to the shear deformations.

Later, the shear modulus and Young's modulus was chosen close to infinity separately, in order to compare the model results when isolating shear and bending deformations. These results were then compared to hand calculations using the Timoshenko beam theory, which includes shear deformations. But even here the results were deviating. The model deformations were approaching zero while the Timoshenko hand calculations approached a small value. Since the shear and bending contributions are uncoupled the part with realistic stiffness will always remain, while the other part approaches zero.

However, the error between the model and the Timoshenko beam theory calculation remains within 0.5 % when using the real values for Young's modulus and the shear modulus. Therefore, the models can be expected to have a small error when using shell elements.

A small mass error will appear due to overlapping in the corner of the shell elements. Simply due to the way the software extrudes the shell element width outwards from the element center line.

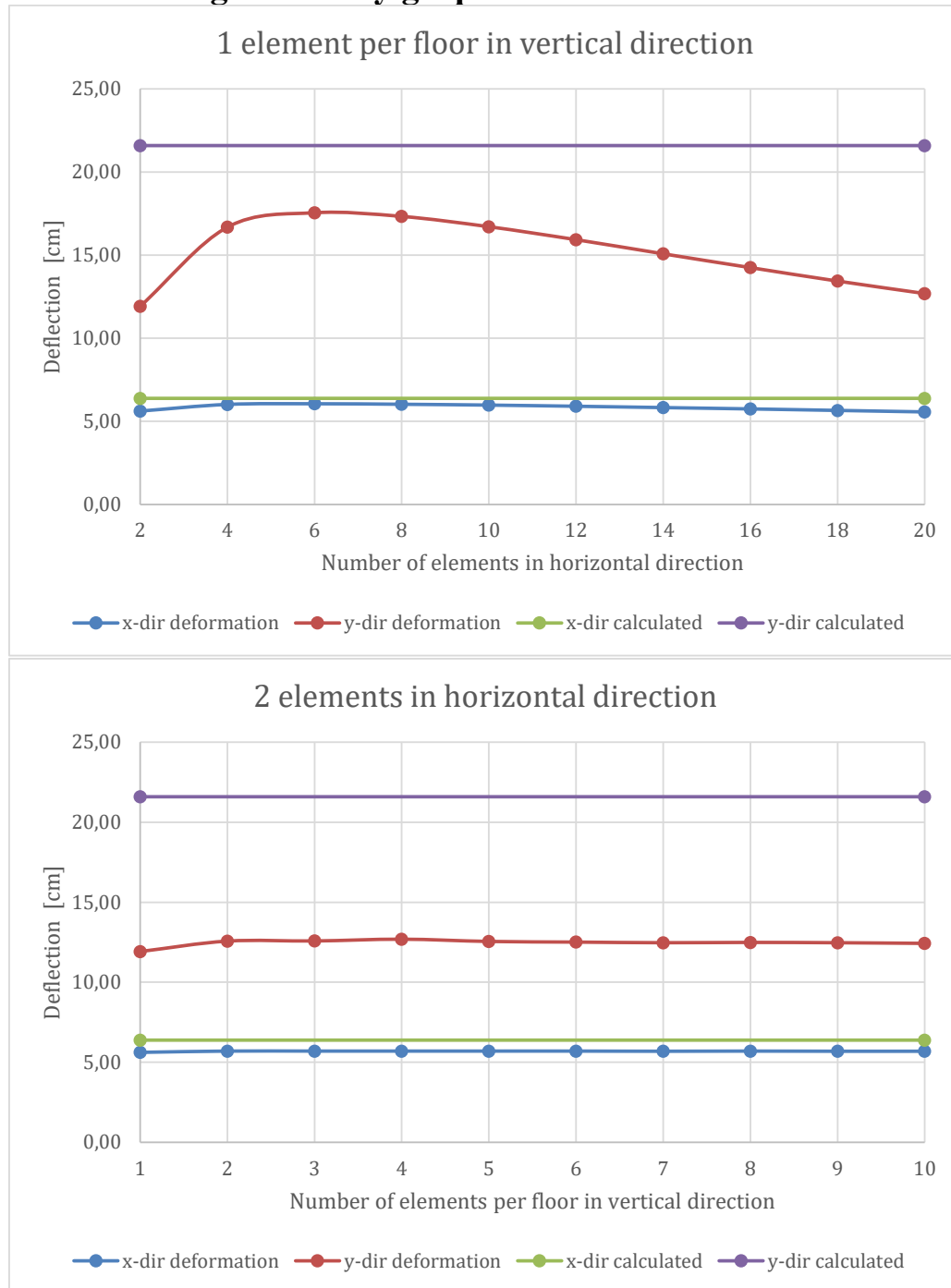
The mesh density of the convergence study was determined as sufficient from 8 elements in the horizontal direction and 10 elements per floor in the vertical direction. This gives an element size of approximately 0.7 x 0.7 m.

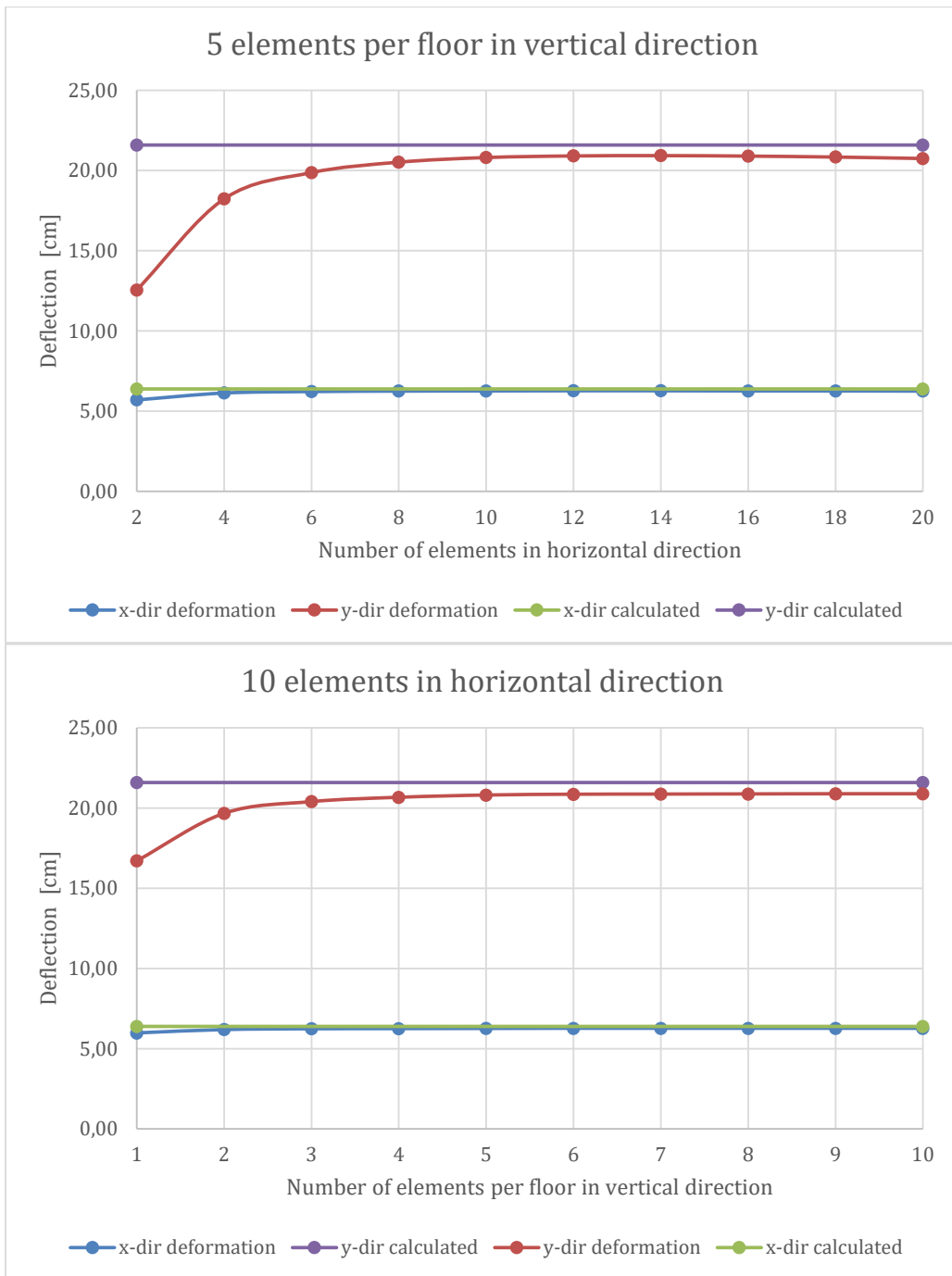
Slenderness ratios lower than 1:5 are chosen for the concepts with uniformly thick proposals, this to avoid problems with vortex shedding. The choice is based Eurocode and EKS11 as follows:

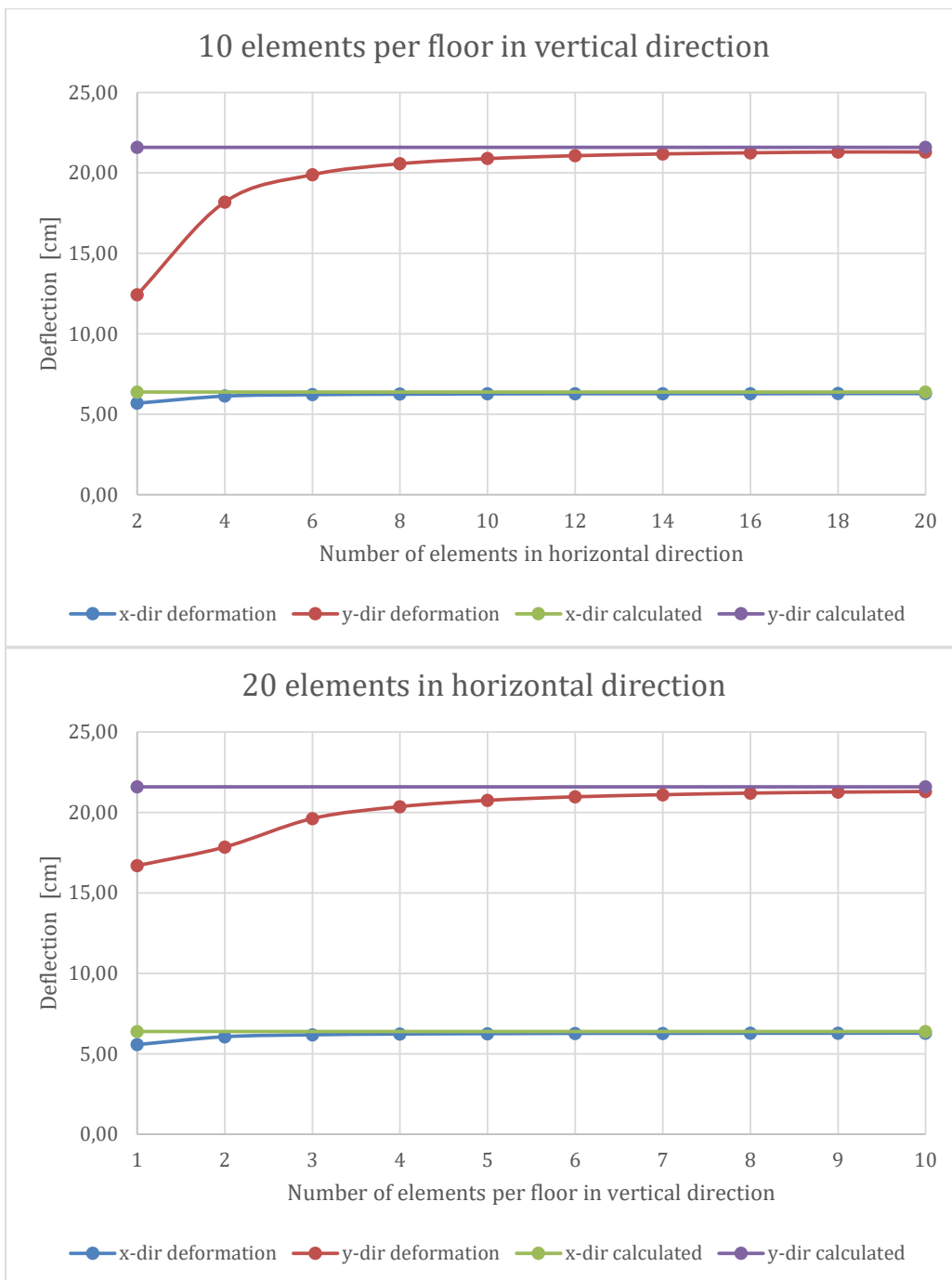
- The informative annex E in SS-EN 1991-1-4 states that vortex shedding is a problem for structures slenderer than 1:6.
- EKS11 refers to the old Swedish calculation procedure in BSV97 which states that buildings slenderer than 1:5 must be controlled for vortex shedding.

However, since the buildings are quite close to the slenderness range when vortex shedding is critical, they have been verified according to BSV97 in Appendix VII.

Mesh convergence study graphs







Appendix IX

High-rise buildings

Since there already are lots of high-rise buildings taller than 200 m, the design of other structures can be used to gain understanding for the topic of tall buildings. Even though different building materials have different advantages and drawbacks, much knowledge can be used independent of the material. Therefore, some of the world's tallest buildings are of great interest.

Burj Khalifa

The current world's tallest building, *Burj Khalifa*, is 828 m high and built based on the buttressed core system. One of the main concerns for this building was to create an efficient structure. Therefore, the aim was to utilize all vertical structural elements when carrying both vertical loads and horizontal loads. When narrowing the cross-section of the building, the shortening was made so that the new façade wall got placed above a cross-wall within the wing. This was the best possible way to manage the gravity loads. Also, the element sizes are relatively constant throughout the building. The accumulated loads are mostly accounted for by the increased number of walls lower down in the structure (Baker & Pawlikowski, 2012).

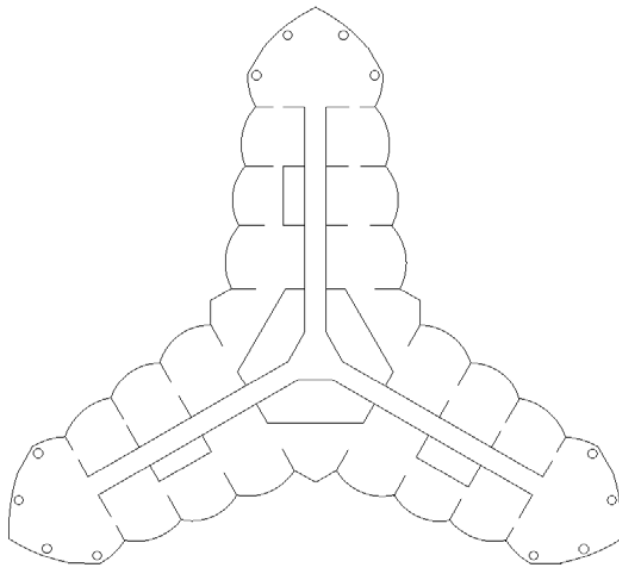


Figure 105: A model of a cross section in *Burj Khalifa*.

When building *Burj Khalifa* extensive wind tunnel testing was done throughout the entire project. From that, critical areas could be detected, and the construction improved. The dynamic response of the building was managed similar to tuning of an instrument, to avoid the aerodynamic harmonics. The set-backs follows a clockwise pattern, opposite to the first intention. But this setup performed better during wind tunnel testing. The building orientation was carefully selected to allow for best possible performance with regard to wind. Also, the setbacks were designed from the wind tunnel studies resulting in a further decrease of the general wind load and vortex shedding (Baker & Pawlikowski, 2012).

To maximize the rigidity of the structure, direct outriggers were used to engage the columns along the parameter of the building (Baker & Pawlikowski, 2012).

Even though *Burj Khalifa* is a thoroughly developed design, there is always room for improvement. In recent years, the responsible architect bureau has worked on a couple of similar buildings. These are however not completed yet, but the development work can give an insight regarding future possibilities when it comes to high-rise buildings (Baker & Pawlikowski, 2012).

Las Vegas Tower was a project with many similarities to *Burj Khalifa*, based on the buttressed core system, but with a few changes which might be of value when building such structures. However, it was never built. One intention with this structure was to create a wind resistant building with a continuous façade without setbacks. The cross-section of the building and the façade was made with a continual change. By doing so and avoiding equally thick sections along major parts of the building wind vortices could be counteracted. Also, stairs at the extremities of each wing makes it possible to continuously form the loadbearing structure to the external façade without the use of setbacks. This staircase placement provides the structure with high inertia. Similar to *Burj Khalifa* the system uses direct outriggers to create interaction between the core and its perimeter columns (Baker & Pawlikowski, 2012).

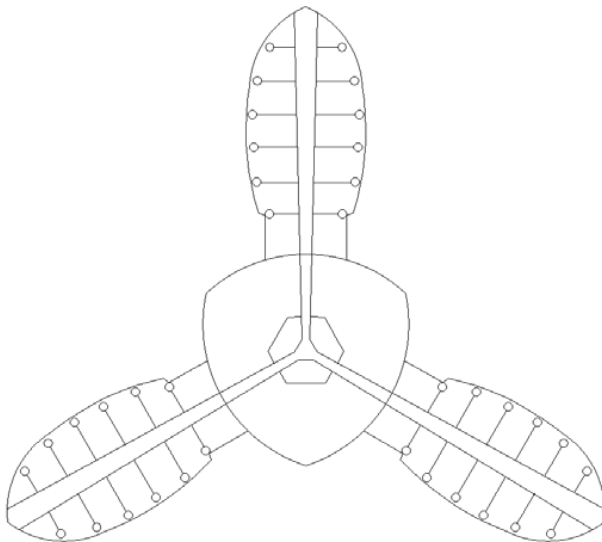


Figure 106: Cross-section (floor plan) of *Las Vegas Tower* in Jeddah.

Kingdom tower in Jeddah, is planned to be the first building taller than 1 000 m. Simply put, it is a further evaluation of the previous towers with the buttressed core system, both with regard to wind response and overall strength. By extensive studying of the wall layout, a new column-free design was developed. Similar to *Las Vegas Tower* it has a staircase at the extremity of each wing, providing the structure with additional capacity and giving the possibility to build without setbacks. The floor elements are cantilevered out from the walls within each of the wings. In practice, simply through optimization, the *Kingdom tower* can reach much higher than *Burj Khalifa* using the same amount of concrete. Its well-developed cross-section also allows for a structure without an outrigger system which is especially favorable when it comes to the building process (Baker & Pawlikowski, 2012).

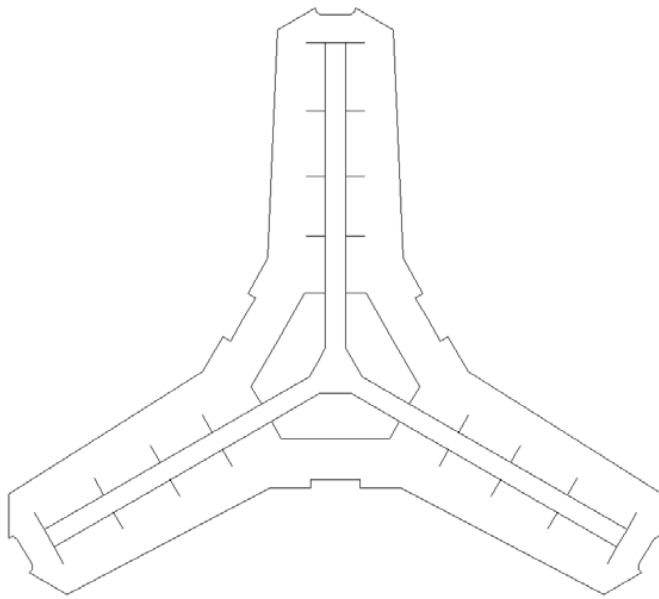


Figure 107: Cross-section (floor plan) of Kingdom Tower in Jeddah.

Shanghai tower

The conditions in *Shanghai* are tough when it comes to high-rise buildings and wind loads of typhoon magnitudes are common. Therefore, three main measures have been utilized in the design, to reduce the wind response. Asymmetric façade, global tapering and rounded corners. To find a balanced and high performing combination of these factors, wind tunnel testing was done during design. The final result was a 24 % reduction in wind load leading to a 5 % reduction in building cost. The occupation of the building ranges from retail stores to restaurants, offices, hotel etc (Jun et al., 2010).

Apart from the challenging wind conditions, *Shanghai tower* is also located in an active earthquake zone. With these environmental factors in mind the structural engineers tried to find a simple structure. This resulted in a system based on a central concrete core coupled with perimetrically placed mega columns coupled together using an outrigger system. The concrete core covers an area of about 30 x 30 m, along each of the sides there are two supercolumns and outside each corner there is also a large column placed parallel to the diagonal of the core. Vertically, the tower is divided into nine main zones spanning over 12 to 15 floors each. At the upper end of each zone, the inner part of the tower steps back resulting in narrowing of the cross-section. The vertical capacity is mainly provided by the inner concrete core while the core, outrigger system and the perimeter columns combined stands the lateral capacity. The outrigger system is made as a steel truss system while the perimeter columns are made as sections of concrete-encased steel (Jun et al., 2010).

As a result of wind management and architectural design, the exterior of the floor plan has a cam shape rotating with elevation. However, the interior loadbearing part with the core, column and outrigger system has a circular shape. This gives the structure two independent wall systems where the load bearing part inside the circular wall is stepwise narrowed while the façade tapers continually with height (Jun et al., 2010).

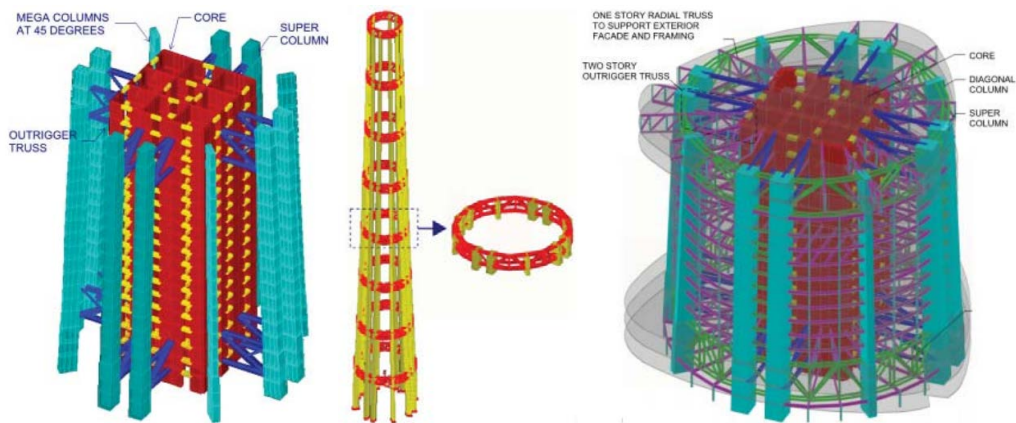


Figure 108: Schematic view of the structure in Shanghai Tower © Council on Tall Buildings and Urban Habitat / Jun Xia; Dennis Poon; Douglas Mass (Jun et al., 2010).

Willis tower

This structure is based on the *Bundled tube* system where a couple of tube structures are coupled together and successively stepped back in order to create a taper in the structure. The individual tubes are connected together, and the interaction provides additional rigidity to the structure on a global level. An advantage with this design over the traditional tubular towers is the increased number of cross-walls and frames within the structure. This gives a higher rigidity than a similar building with the bracing system concentrated to the perimeter of the building. The group effect of the tubes also allows for fewer columns within each of the tubes leaving more room for interior design and flexibility in usage of the building. If wanting to further increase the building height for a structure based on the *bundled tubular system*, additional diagonal bracing elements could be added. There is also a possibility to include an extra rigid core resulting in more of a *tube in tube system*. As each of the tubes can be improved or changed in multiple ways, there is an almost unlimited amount of variations for a *bundled tubular system* (Ali & Moon, 2007).

Observing one single tube within the structure, the size is about 23 x 23 m and it contains 5 columns per side, equally spaced, and with shared corner columns between the sides. At each floor, interaction between the columns is achieved using beams and truss systems within the floor. Also, at a couple of levels, outrigger-like truss structures are used to enhance the global behavior of the building. These, large trusses are also placed and used in a way that allows vertical loads to be distributed to the entire structure below. This is sought due to the setbacks and therefore uneven loading at the upper parts of the structure (*Major Works, Sears Tower (Currently Willis Tower)*, 2011).

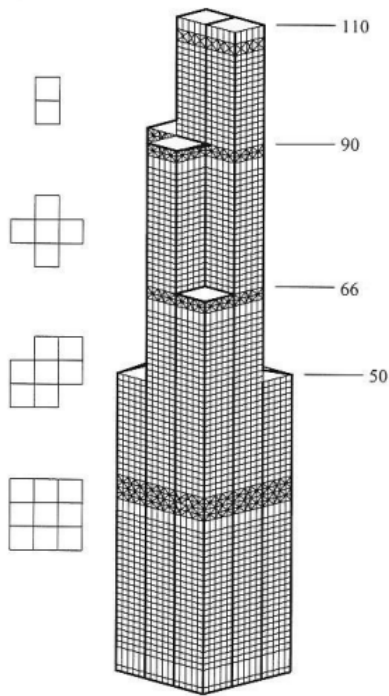


Figure 109: Bundled tube system used in Willis Tower. Credit: (Ali, 2001). Source: *Art of the Skyscraper: The Genius of Fazlur Khan* by Mir M. Ali, Rizzoli Publications, 2001.

The John Hancock Center

Due to the height of the structure, the designers for *The John Hancock Center* found a need to abandon the traditional frame structures and therefore a tube based structure was chosen. In order to reduce the amount of structural steel needed for the structure as well as reducing the overall cost for the project, a further development of the tube system was introduced. Additional trusses spanning over multiple floors provided the structure with the extra rigidity needed for the structure. This system got the name *braced tube system* or *trussed tube system*. These trusses highly improved the structural response due to wind loads and also shifted the global action to a more bending dominant behavior. After the introduction of this system, multiple varieties were composed and used in following buildings. *The John Hancock Center* is approximately 344 m tall (*Major Works, The John Hancock Center*, 2011).



Figure 110: The John Hancock Center (left) and a more recent building with a similar structural system Onterie Center (right) (Major Works, The John Hancock Center, 2011).

Appendix X

Element stresses

In order to get an understanding of how well the structural capacities are utilized for the different proposals, the element stresses were determined for all axially loaded beam elements, i.e. columns and trusses. It showed that the average element stress during ULS loading was way below the material capacity as exemplified in Figure 111. This applies to all buildings investigated, for both columns and trusses. The stress graphs show all the compressive loaded elements. The tensile stresses are not included since they are of similar or lower magnitude and would therefore lower the average stress level.

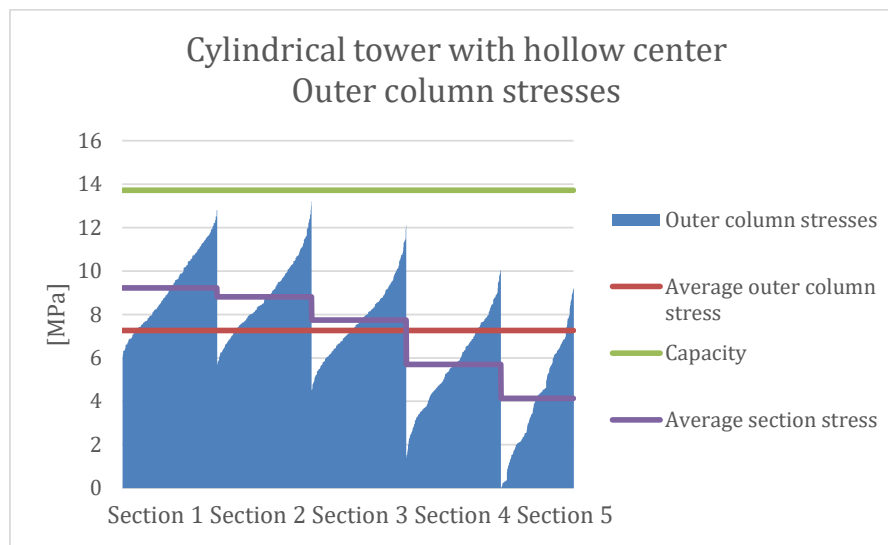


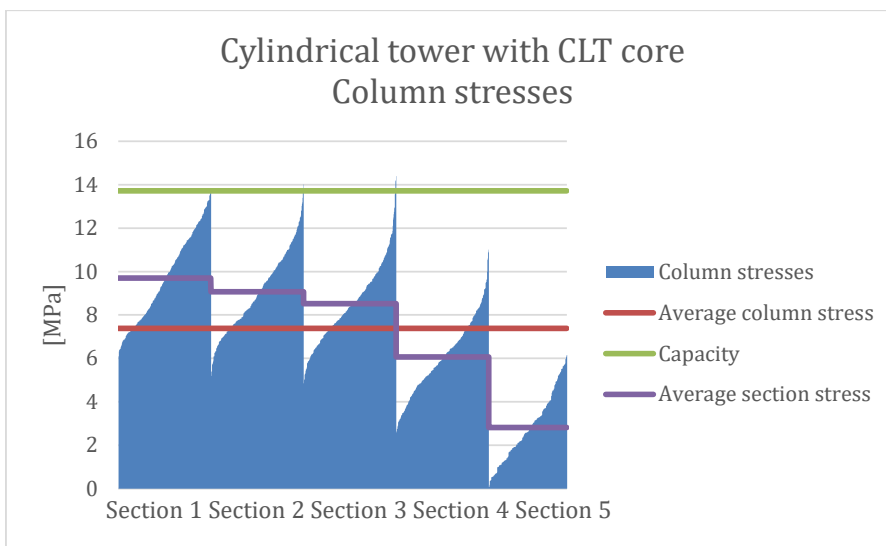
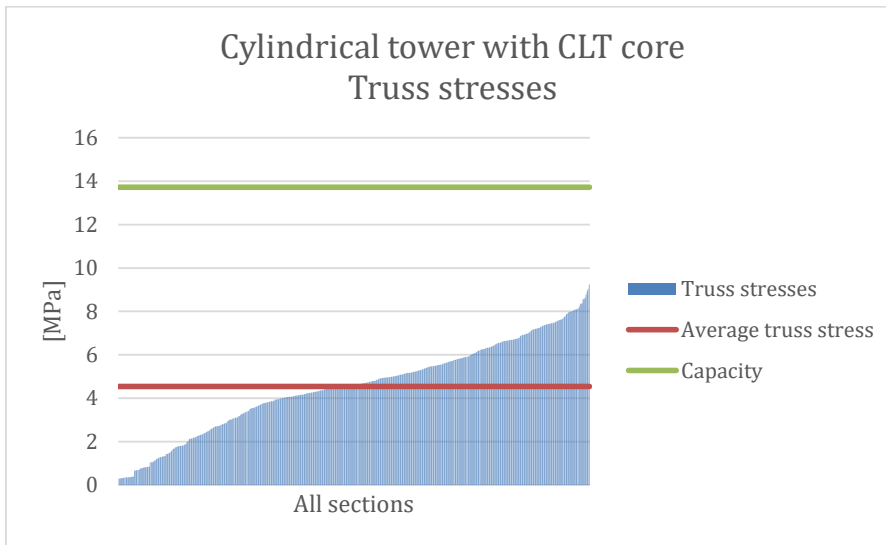
Figure 111: Outer columns stresses for the cylindrical tower with hollow center.

For some cases large elements have been used to redistribute forces within the structures, resulting in low utilization ratios. However, since this difference between average element stress and material capacity can be seen for all structures, it seems to be more of an optimization issue rather than a relevant evaluation criterion suitable for comparing different concepts. Also, these stresses are obtained for one single wind-direction. However, when the wind has another direction, other elements will obtain the higher utilization ratios.

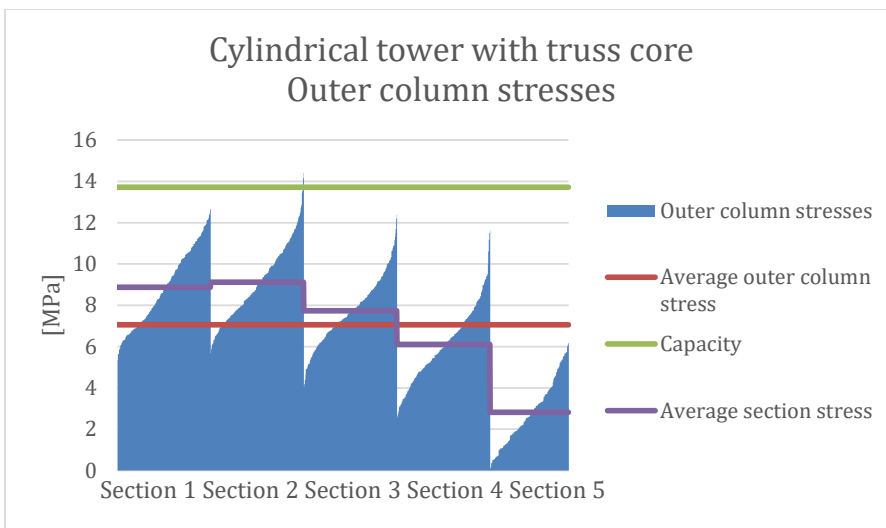
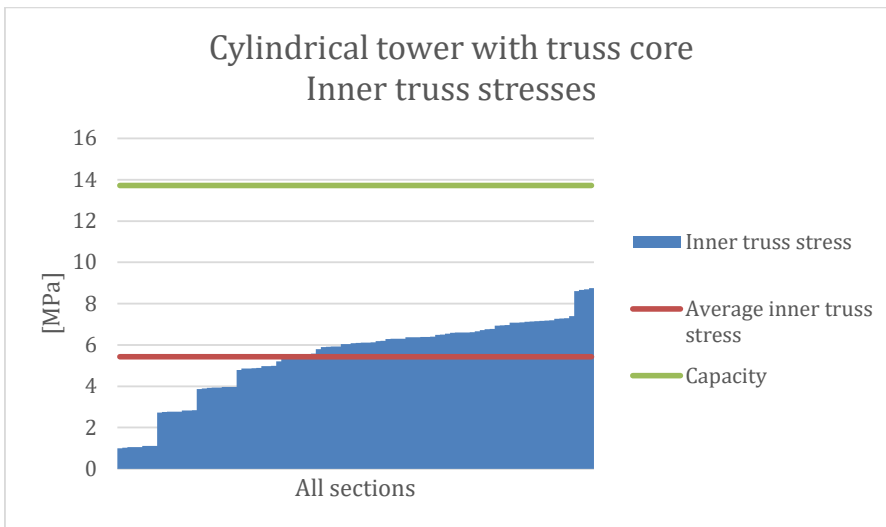
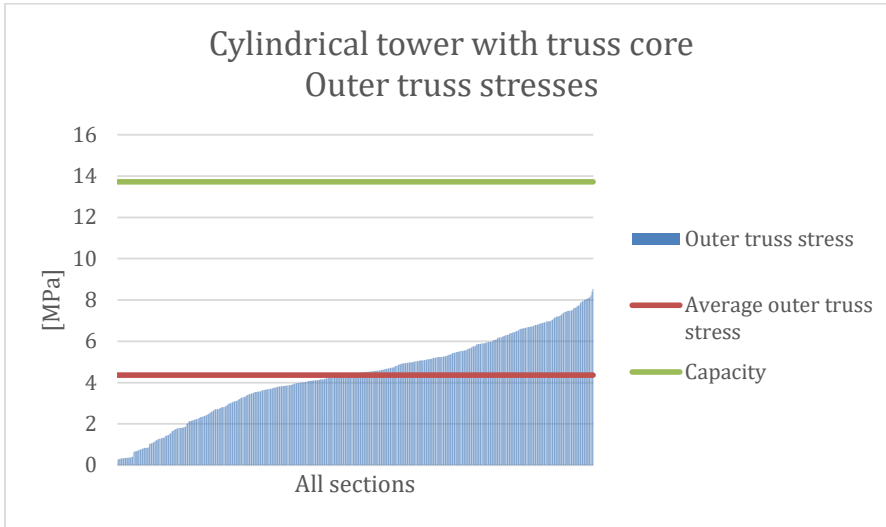
For all graphs of all element stresses for the different proposals, see below.

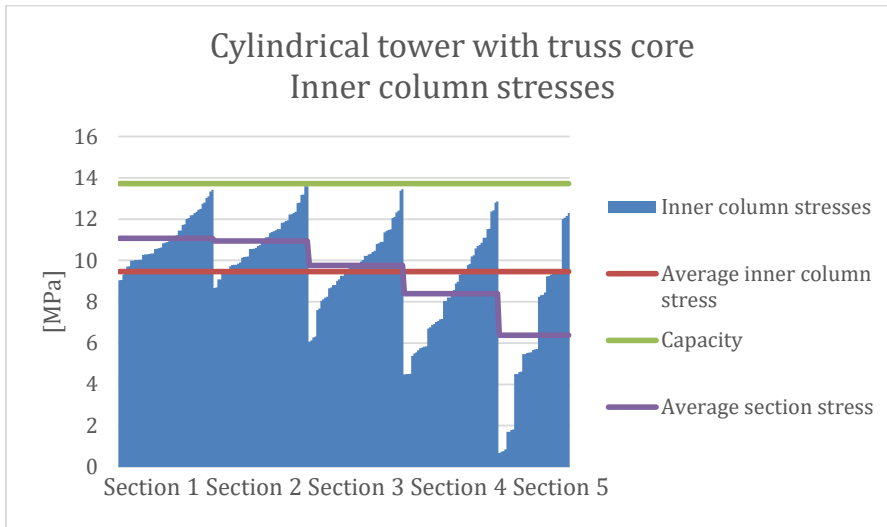
Bar charts showing the stress level for each element. The bars are sorted according to the stress magnitudes. Therefore, the stress distributions for each element type are shown and compared to the average element stress as well as the timber capacity.

Cylindrical tower with CLT core (section 4.5.1)

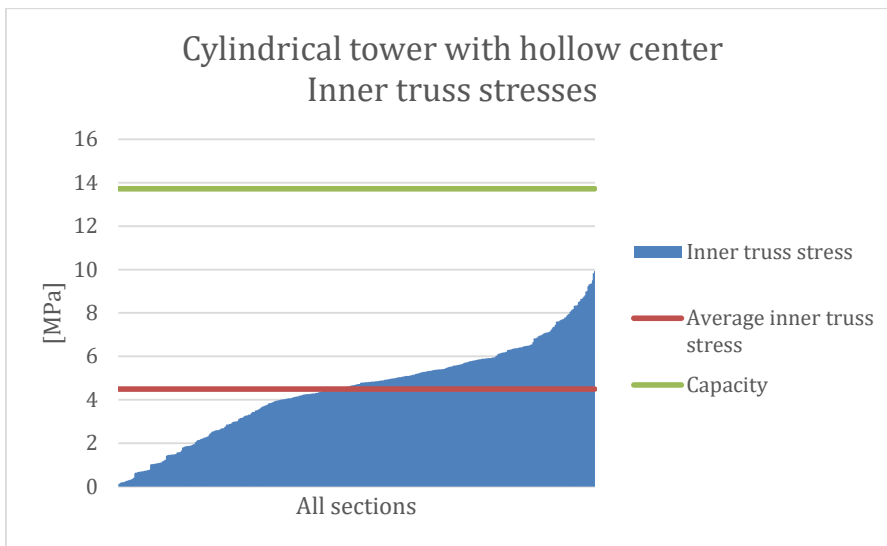
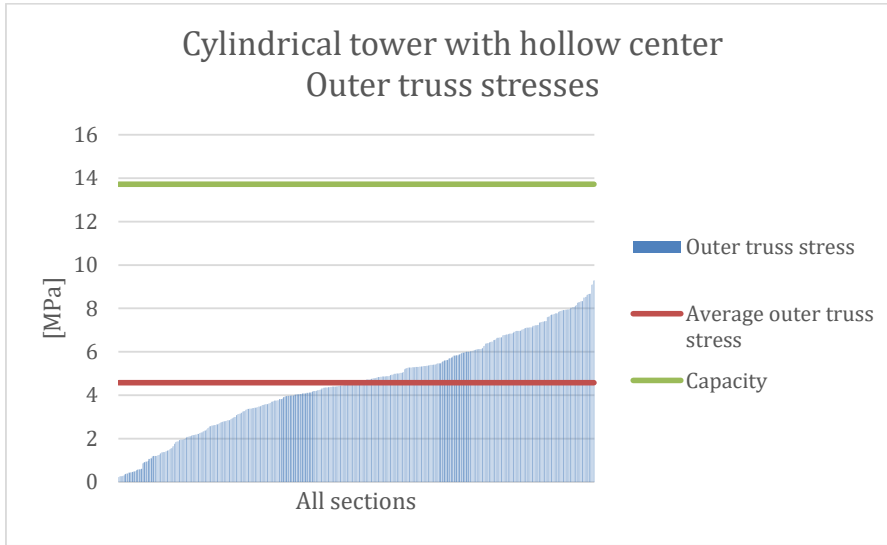


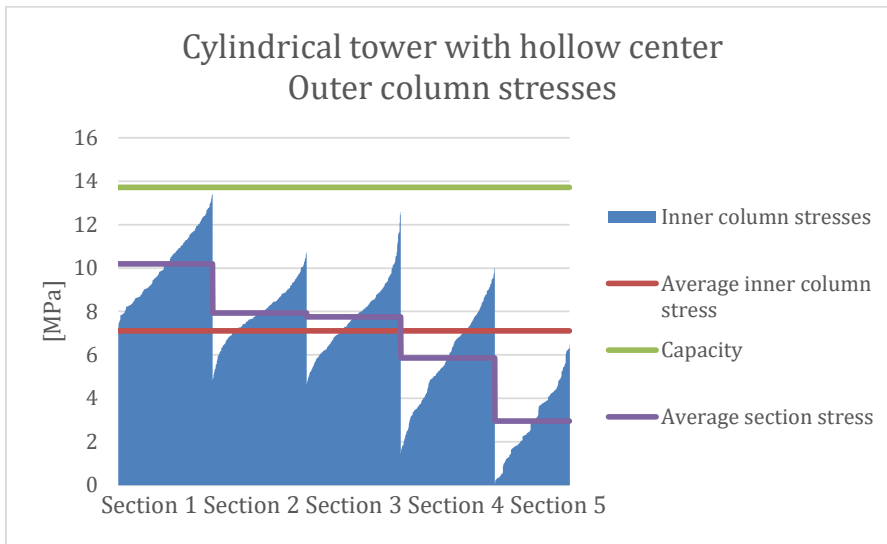
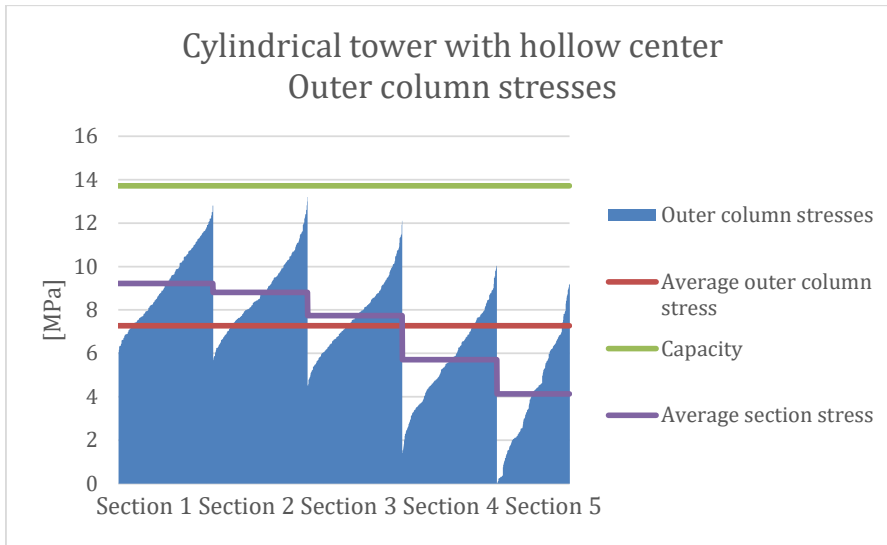
Cylindrical tower with truss core (section 4.5.2)



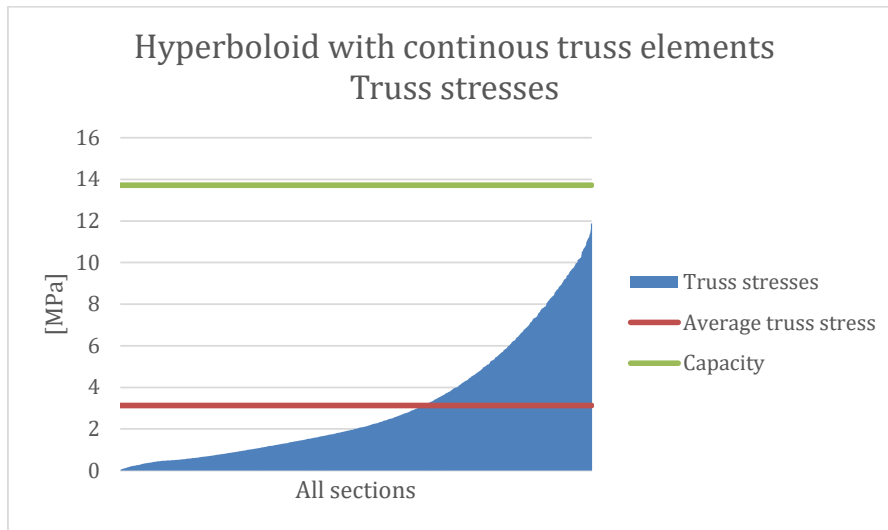


Cylindrical tower with hollow center (section 4.5.3)

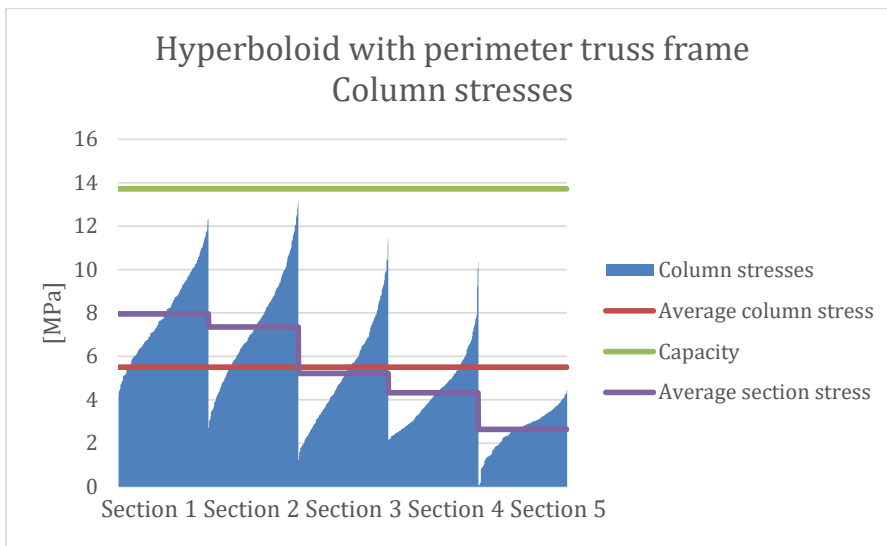
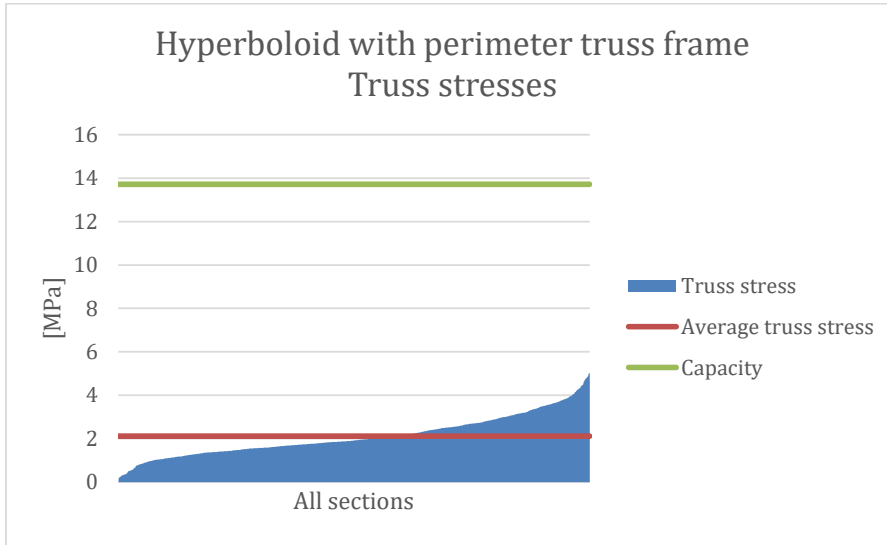




Hyperboloid with continuous truss elements (section 4.5.4)



Hyperboloid with perimeter truss frame (section 4.5.5)



DEPARTMENT OF ARCHITECTURE AND
CIVIL ENGINEERING
CHALMERS UNIVERSITY OF TECHNOLOGY
Gothenburg, Sweden
www.chalmers.se



CHALMERS
UNIVERSITY OF TECHNOLOGY